Title
SPECTROSCOPIC STUDIES OF PHOTOSYNTHESIS

Author
Kuntz, Irwin Douglas

Publication Date
1965-06-01

UCRL-16207

University of California

Ernest O. Lawrence Radiation Laboratory

SPECTROSCOPIC STUDIES OF PHOTOSYNTHESIS

Berkeley, California

DISCLAIMER

Research and Development

UCRL-16207

UNIVERSITY OF CALIFORNIA
Lawrence Radiation Laboratory
Berkeley, California

AEC Contract No. W-7405-eng-48

SPECTROSCOPIC STUDIES OF PHOTOSYNTHESIS

Irwin Douglas Kuntz, Jr.
(Ph. D. Thesis)

June 1965

Spectroscopic Studies of Photosynthesis

ABSTRACT

Sensitive measurements of the visible absorption spectra of photosynthetic materials have revealed that upon illumination conducive to photosynthetic activity the concentrations of various endogenous compounds are reversibly altered. Such measurements require sophisticated averaging techniques to achieve the necessary noise levels of less than 10^{-5} O.D. units and the time resolution of less than 1 millisecond. Suitable instrumentation is described in detail.

A major consideration was the identification of the photo-reactive species on the basis of their absorption spectra. A summary of the available data on the various compounds thought to be involved is presented, and from this evidence it is concluded that chlorophylls, cytochromes, flavins, quinones, carotenoids, and pyridine nucleotides are involved in algal and bacterial photosynthesis. The types of reactions which these molecules might undergo are also discussed.

Our studies included a measurement of the redox properties of bacterial chromatophores which indicated that there are two essential pigments involved; one has a midpoint potential of +0.44 volt and evidence is offered that this pigment is bacteriochlorophyll; the other has a midpoint potential of -0.04 volt. We also undertook several kinetic studies. Some of the intermediates found in the bacterial systems showed different decay kinetics from compound to compound. On such a kinetic basis it was possible to relate the photoproduced absorption band at 433 mμ to the photoproduced electron paramagnetic resonance signal. Kinetic studies in algae indicated by indirect

means that a close correspondence exists between the overall electron flow behavior involved in oxygen evolution and the initial decay rates of the photoproduced intermediates. The restrictions that such observations place on photosynthetic mechanisms are discussed.

A semi-quantitative mathematical analysis of electron flow systems is presented. Relationships between the mathematical models and the experimental observables are emphasized. Analog computer techniques are briefly considered.

ACKNOWLEDGMENTS

The experiments described in this thesis and the conclusions to which they led were generated in large part through the discussions and the assistance of many individuals. Mr. Roland Thompson made major efforts in all stages of the design and development of the instrumentation. The invaluable comments of Dr. M. Klein greatly extended my understanding of the principles and practice of laboratory electronics. Drs. H. Johnston, B. Mahan, R. Powell, and K. Sauer of the Chemistry Department helped explore several aspects of reaction kinetics in complex systems. To my co-workers, Drs. P. Loach, R. Ruby, E. Gould, and R. Hiller, I will always owe a deep debt for the experience and the skills which they shared with me. Most importantly, Dr. M. Calvin as my research director never failed to provide the measure of inspiration and insight which continually renewed my perspective and my enthusiasm for this thesis.

The fellowship support of the National Science Foundation (1961-64) is gratefully acknowledged.

The work described in this thesis was supported, in part, by the United States Atomic Energy Commission.

TABLE OF CONTENTS

		Page
Chapter I.	Introduction to Photosynthesis	1
Chapter II.	Instrumentation	20
Chapter III.	Absorption Spectra of Photosynthetic Intermediates and Review of Photosynthetic Mechanisms	71
Chapter IV.	Results	133
Chapter V.	Kinetic Analysis of Electron Transport Systems	196
Chapter VI.	Conclusions	236

Chapter I INTRODUCTION TO PHOTOSYNTHESIS.

Photosynthesis as it occurs in the algae and higher plants can be summarized by the well known equation:

$$CO_2 \text{ (gas)} + H_2O \text{ (liq)} \xrightarrow{\text{light}} (CH_2O)_x + 1/2\ O_2 \text{ (gas)} \qquad \text{(I-1)}$$

This net reaction is, of course, accomplished by a very large number of intermediate steps. Although each step is important to the overall process, they will not be of equal interest to us. One useful conceptual device is to separate Eqn. I-1 into two stages:

a) the photochemical evolution of O_2 and the concomitant production of a strong reductant and "high energy" phosphate;

b) the enzymatic reduction of carbon dioxide using the reductant and phosphate carrier produced in (a).

These reactions are indicated below.

$$P_i + Y + H_2O + X \xrightarrow[\text{enzymes}]{\text{light}} P\text{-}Y + 1/2\ O_2 + XH_2 \qquad \text{(I-2)}$$

$$3P\text{-}Y + 3XH_2 + CO_2 \xrightarrow{\text{enzymes}} (CH_2O)_x + Y + P_i + X \qquad \text{(I-3)}$$

We shall be most interested in those reactions which involve light directly and those which use the immediate products of the light reactions. The reactions encompassed in Eqn. I-3 have been explored in great detail by Calvin and his colleagues.[1,2] A relatively complete picture of the "carbon-fixation cycle" has emerged from these and related investigations.

It has long been suspected that the tools associated with the study of carbon fixation--radioactive tracers and paper chromatography--would not be suitable for detecting and identifying the intermediates

participating in Eqn. I-2. Techniques were sought that gave rapid, sensitive indications of chemical reaction without requiring the isolation of products. One of the most promising approaches at the time our study began was the use of spectroscopy, in particular the absorption of "visible" and microwave radiation. Our own work has grown more or less directly out of the earlier and continuing efforts in this broad area.* We set out to learn as much as possible about the steps included in Eqn. I-2 by these techniques, hopefully arriving at a fairly detailed set of elementary reactions.

This paper will be divided into six chapters. The rest of this chapter presents a broadly sketched outline of the primary processes of photosynthesis. Chapter 2 contains the details of the instrumentation developed and of some of the routine experimental procedures used. Chapter 3 reviews in detail the specific working hypotheses for the reactions of interest to us. Emphasis is placed on the role that the spectroscopic studies have played in the development of current theories. Some of our results are included in this discussion. Most of our experimental work is described in Chapter 4. Chapter 5 considers a mathematical model for electron transport reactions. Chapter 6 contains the final summary and conclusions.

---

*Specific references will be given in Chapters 3 and 4.

A MODEL FOR PHOTOSYNTHESIS

Eqn. I-2 calls for the photochemical oxidation of water in the presence of an electron acceptor (X) and plant material. Let us divide the elementary reactions involved into three classes:

1) Light absorption, resonance energy transfer.
2) Energy trapping, conversion of electronic energy to chemical potential.
3) Electron transfers from terminal electron donor (water) to terminal electron acceptor (X) with associated production of "high energy" phosphate.

We want to consider these sets of reactions in more detail, including a brief discussion of some of the important evidence for them.

Absorption of Light, Energy Transfer

The photochemical oxidation of water in photosynthesis proceeds efficiently with photons of all visible wavelengths (400-700 m). Figure I-1 shows a typical action spectrum.[3] High efficiency over such a broad spectrum of low energy photons makes this a remarkable photochemical reaction. It becomes even more unique when one realizes that the light being utilized is absorbed by many structurally different compounds (Figure I-2). Furthermore, neither water nor the likely candidates for X* have strong absorption in the active part of

---

*X is probably triphosphopyridine nucleotide (TPN), with the absorption spectrum shown in Figures I-2 and III-27 and the structure shown in Figure III-26.

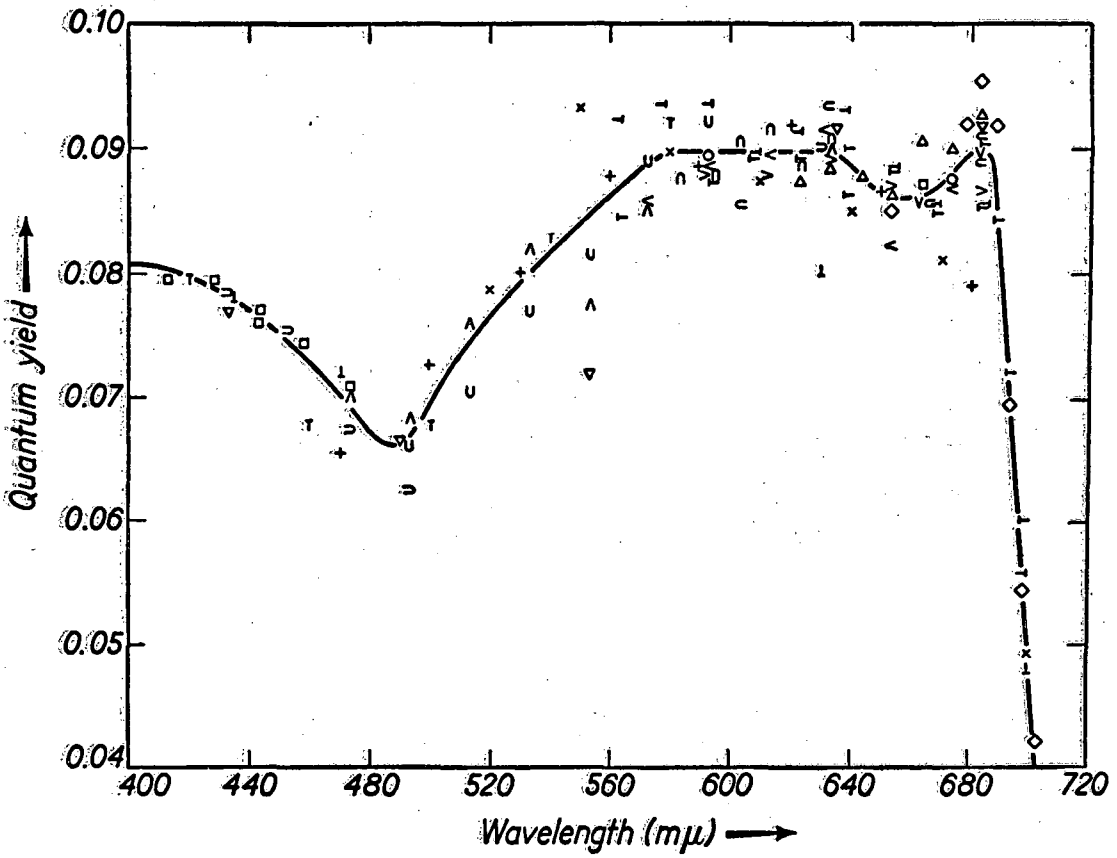

Efficiency of light absorbed by *Chlorella* sp. determined over the range of the visible spectrum. Emerson and Lewis

MUB-6791

Fig. I-1.

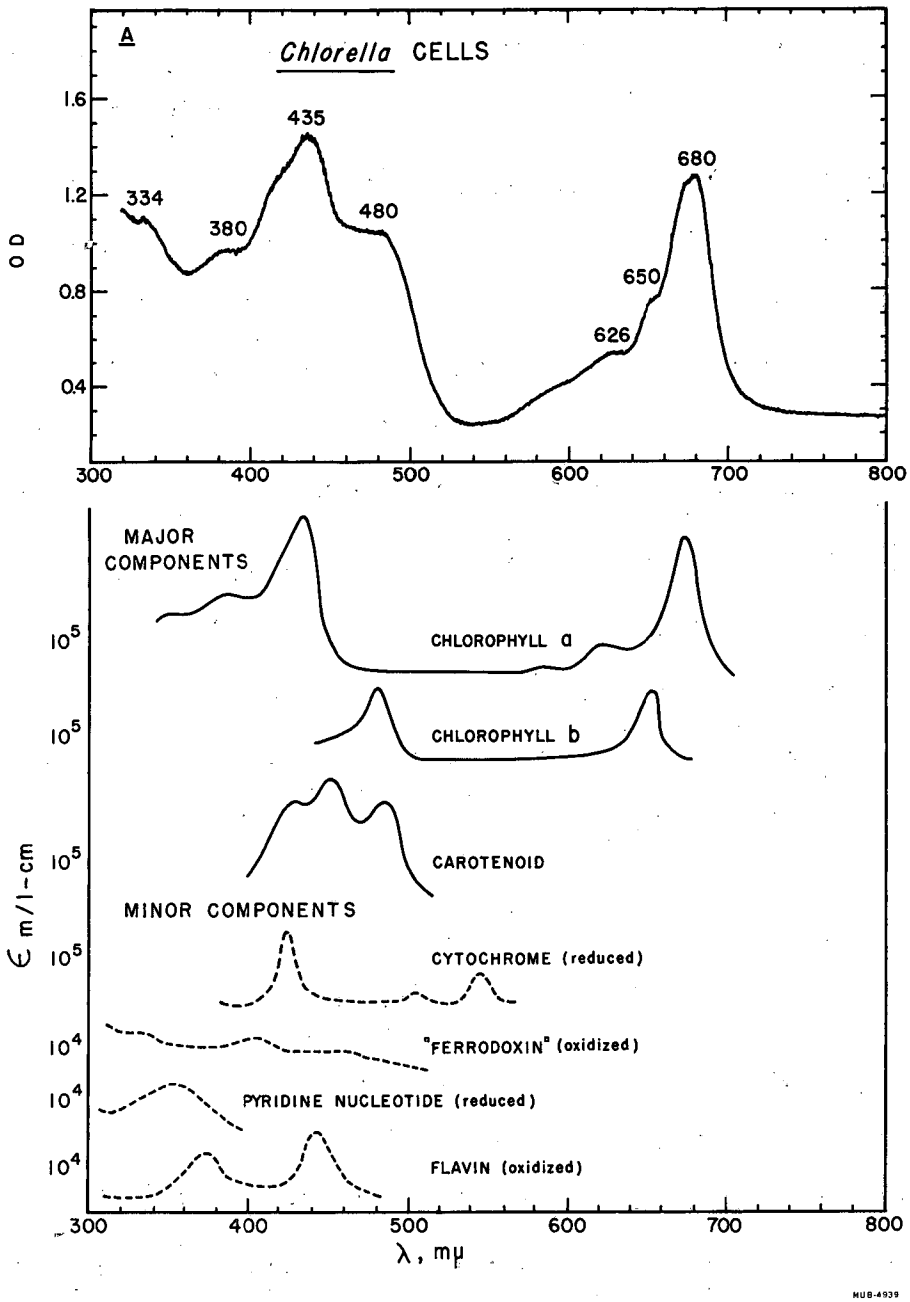

Fig. I-2. Resolved absorption spectra for photosynthetic pigments. These spectra are only approximate. More accurate spectra are presented in Chapter 3.

the spectrum. Hence the overall reaction is formally one of "photo-catalysis" or "photo-sensitization". Thus we must provide a mechanism for transfer of the excitation energy to the reactants.

The pigment molecules shown in Figure I-2 have intense overlapping absorption and emission bands. The molecules are highly concentrated (ca. 0.1 molar) in small volumes within the cellular tissue (Figure I-3).[4,5,6] Direct electronic energy transfer from the high energy levels of one molecular species to the lower lying levels of another molecular species is quite feasible in these systems.[7,8] Such a mechanism is commonly proposed for the very efficient quenching of fluorescence in concentrated solutions of pigment molecules *in vitro*.[9] Let us assume for the moment that chlorophyll *a* molecules lie at or near the end of this energy transfer process (*vide infra*). Then this type of reaction would involve the following steps:

$$P + h\nu = P^* \qquad \text{(I-4)}$$

$$P^* + Q = Q^* + P \qquad \text{(I-5)}$$

$$Q^* + \text{Chl } a = \text{Chl } a^* + Q \qquad \text{(I-6)}$$

where P, Q are any pigments, * indicates the first excited singlet. Good evidence for reactions I-5 and I-6 comes from fluorescence experiments such as that shown in Figure I-4.[10] Only chlorophyll *a* fluorescence is observed in *in vivo* material even though the other common pigments are fluorescent *in vitro*. Also, polarized excitation does not produce polarized fluorescence,[11] indicating a series of "transfer" steps among randomly oriented molecules. These experiments point to one basic photochemical reaction for the photo-oxidation of water rather than parallel pathways for each pigment.

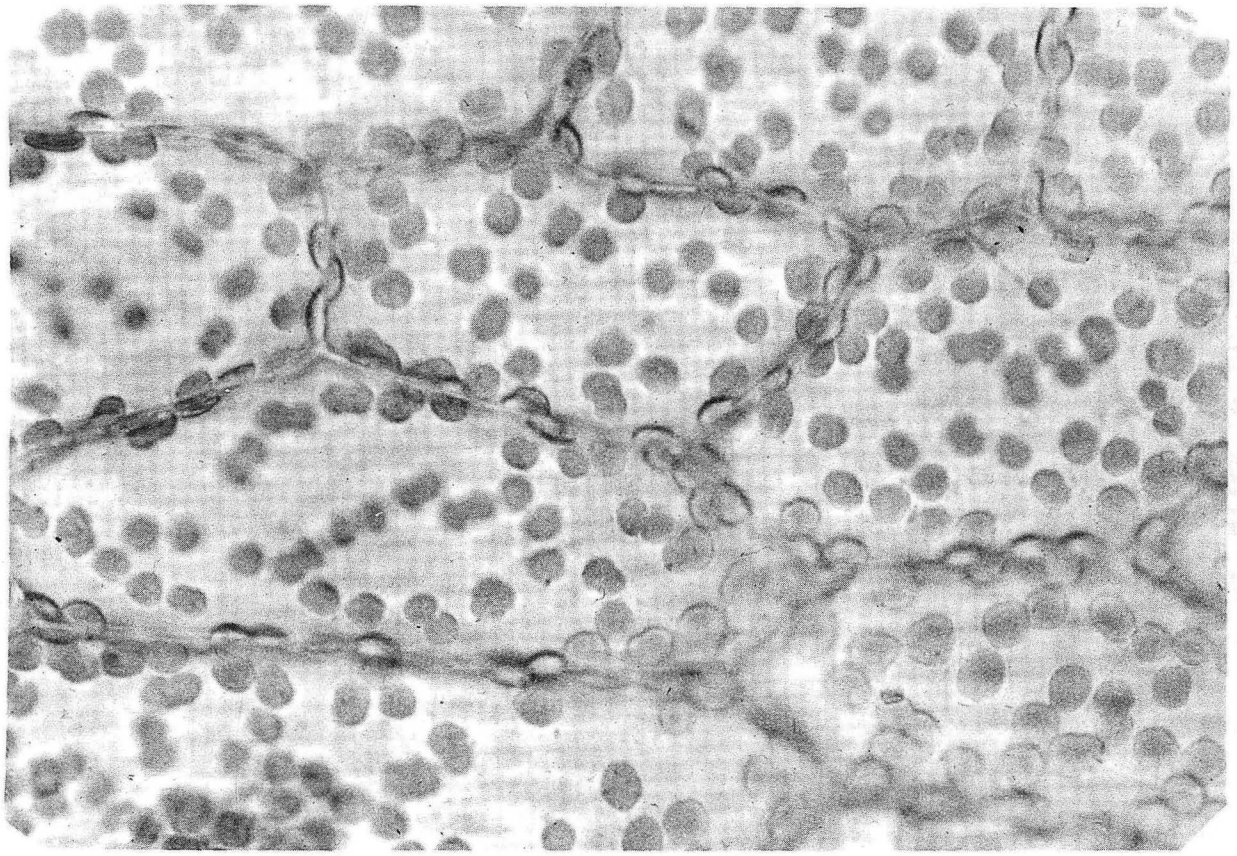

ZN-2673

Fig. I-3. Chloroplasts in Liverwort.

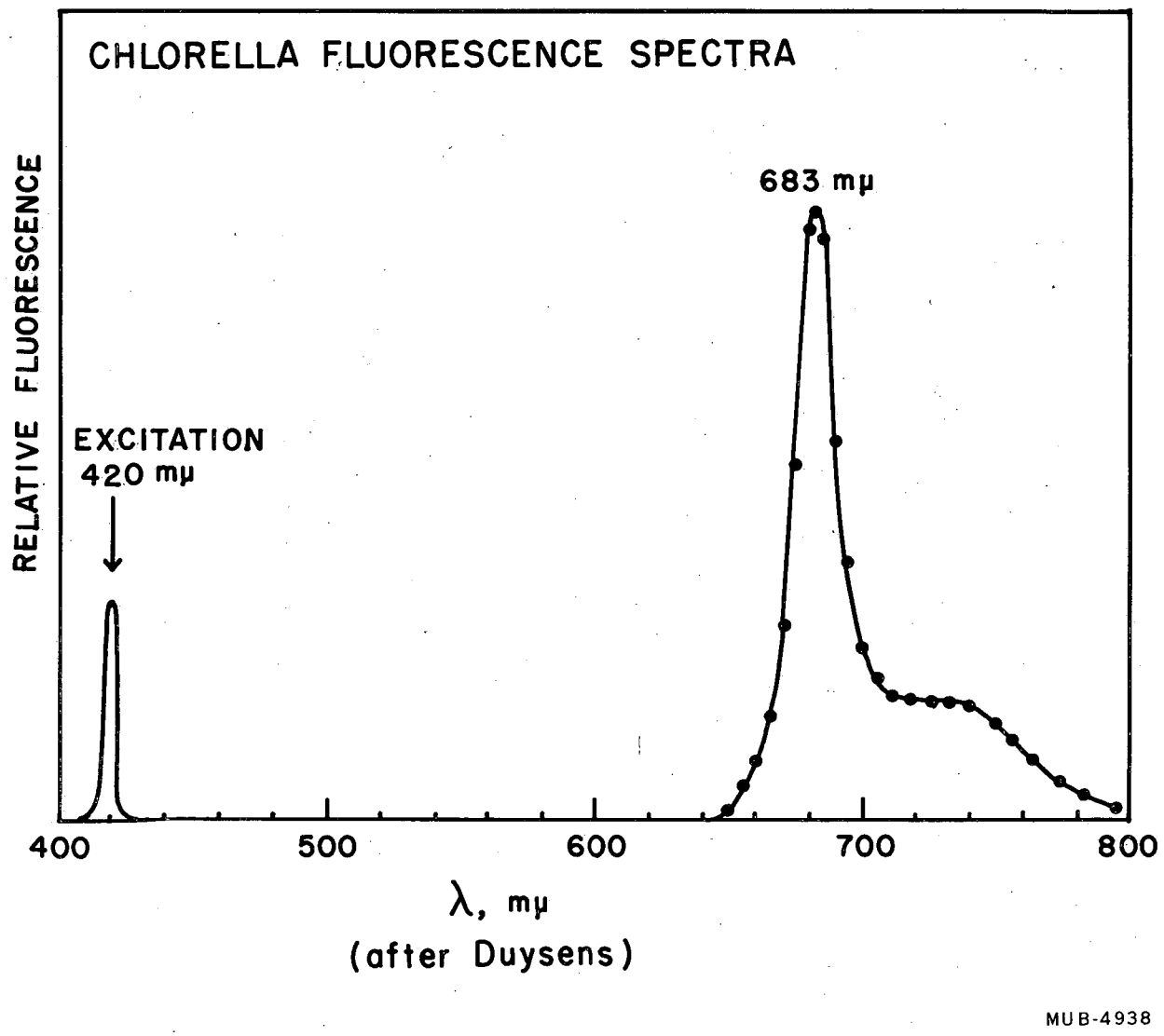

Fig. I-4. Chlorella Fluorescence Spectra.[10]

The free energy storage involved in the overall photosynthetic reaction (Eqn. I-1) can be so high (30-40%)[12] that the quantum yield of the above reactions must be extremely good. Back reactions and losses of various types are then relatively unimportant. These last include chlorophyll a fluorescence (1%),[13,14] long-lived fluorescence or chemilluminescence (0.1%),* phosphorescence (not yet detected), and nonradiative transitions (up to 50% of the input energy, approximately 25% of the input quanta).[18,19]

The relative amounts of energy appearing as fluorescence and as stored chemical potential give some indication of the relative rates of the reactions involved. The radiative lifetimes of the pigments are of the order of 10^{-8} seconds. Since none fluoresce except chlorophyll a, the processes leading to chlorophyll must take a much shorter time, perhaps 10^{-9} to 10^{-11} seconds.**

Energy Trapping, "Quantum Conversion"

Once the absorbed light energy has been transferred to the chlorophyll a molecules (producing excited singlets), it must be "trapped" efficiently. At this point we are primarily interested in the nature of the trap and the type of reaction it undergoes. Impressive but circumstantial evidence suggests that the photosynthetic traps have some unique properties rather than being any randomly selected chlorophyll a

*Ref. 15 quotes this commonly accepted value, but see Refs. 16 and 17 for other views.

**This time scale is supported by the few compounds that do fluoresce in vivo. These compounds, the phycoerthyrins found in red and blue-green algae, have very short radiative lifetimes, ca. 10^{-9} seconds.[20]

molecules. Emerson and Arnold first showed that the active centers, whatever they might be, are much less numerous than the chlorophyll a molecules.[21] Trap concentrations are estimated as 0.1 to 1.0% of the chlorophyll concentration.[6,21,22] Sensitive absorption measurements have indicated a small absorption band at somewhat longer wavelengths than that of the bulk of the chlorophyll a (Figure I-5).[23] The absorption in this region is strongly dichroic, implying that the molecules are aligned relative to one another in an ordered array (Figures I-6 and I-7).[24,25] This array has fixed orientation with respect to the electric moment and the geometry axis of the cells of subcellular units in which they are contained.[26] The concept of an ordered substructure is strengthened by the observation of a polarized fluorescence at somewhat longer wavelengths than the bulk of the chlorophyll fluorescence.[27]

Summarizing this line of argument: approximately 5% of the long-wavelength absorption of in vivo plant tissue belongs to a 690-700 mμ absorption band. The molecules responsible for this absorption are in an organized array. We postulate that one or more molecules within the organized unit are the actual site of photochemical activity. The trap itself is almost certainly a porphyrin-like molecule (from its spectrum), but no structural details are known. Thus it may or may not be chlorophyll a itself.

A trap absorbing at 700 m is a weak one at room temperature (350 cm^{-1} compared to kT of 200 cm^{-1}). Thus its efficient operation must depend upon rapid depopulation through chemical reaction rather than its being a long-lived metastable state. We also know that the

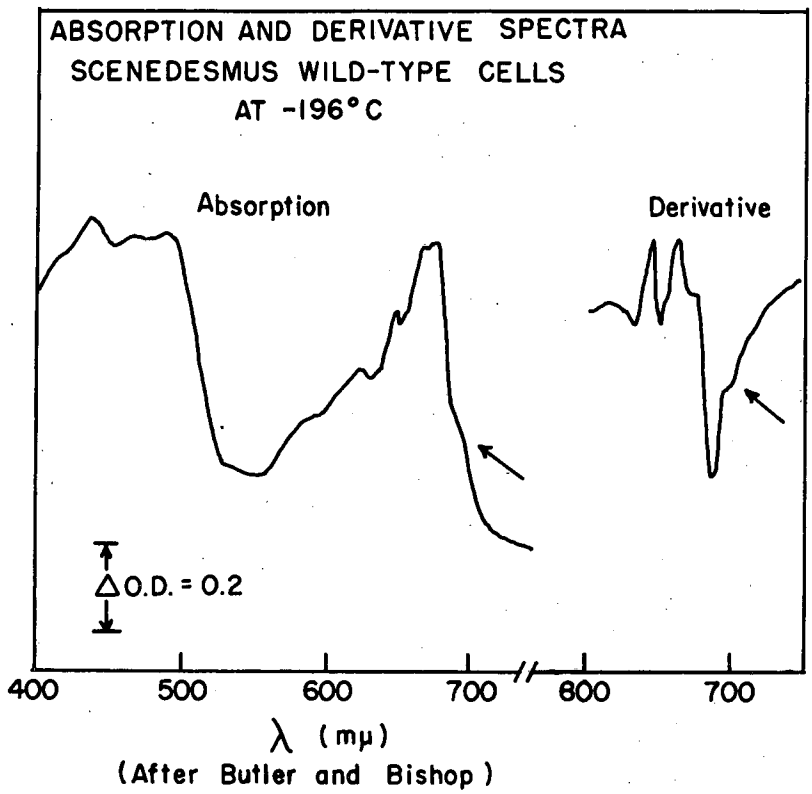

MU-35701

Fig. I-5. Absorption and Derivative spectra of Scenedesmus cells.[23] Shoulder on absorption curve slightly exaggerated.

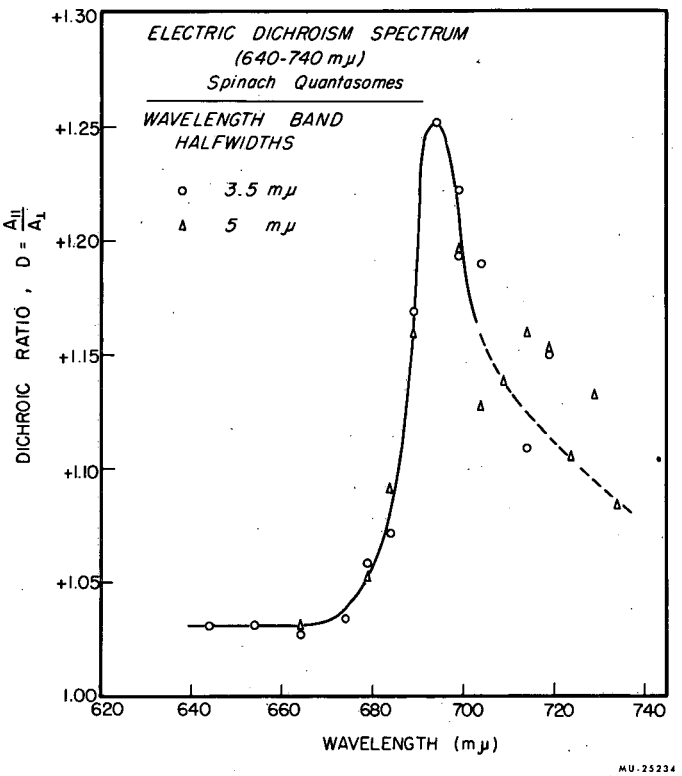

Fig. I-6. Electric Dichroism spectrum of spinach quantasomes. Sauer and Calvin.[24]

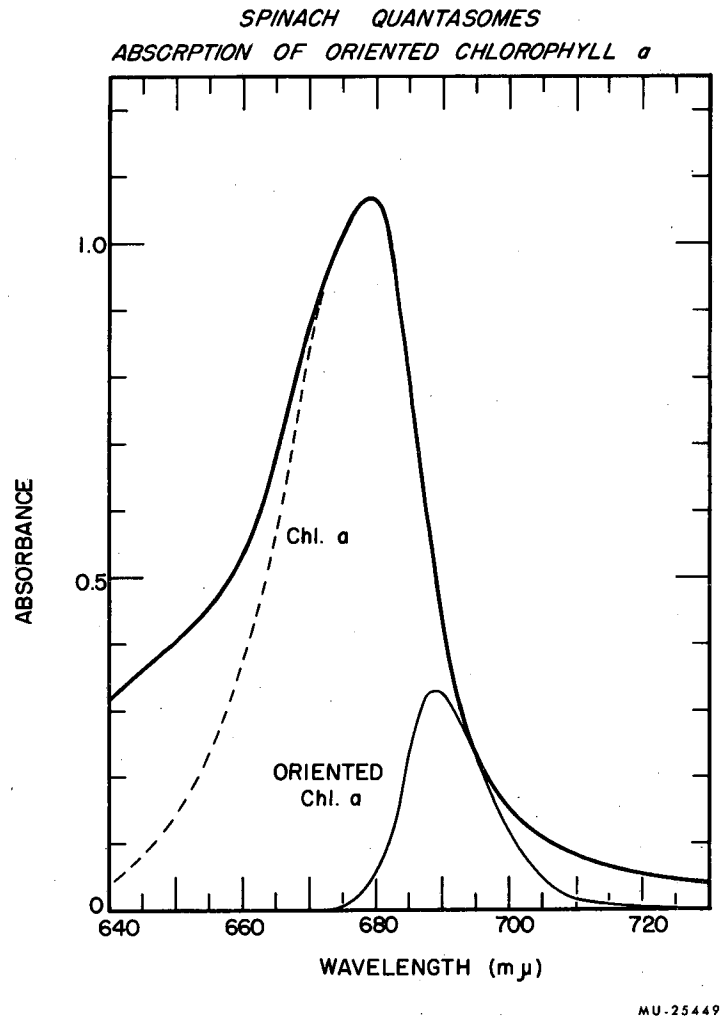

Fig. I-7. Absorption spectrum of oriented and unoriented chlorophyll a. Sauer and Calvin.[24]

reaction

$$\text{Chl } \underline{a}^* + T = T^* + \text{Chl } \underline{a} \qquad \text{(I-7)}$$

must proceed quite rapidly since it provides excellent competition with chlorophyll *a* fluorescence (lifetime ca. 10^{-9} seconds).

Much of the attention of photosynthetic investigations has been focused on the "quantum conversion reaction". By way of definition, the quantum conversion process is that chemical reaction which changes electronically excited species into chemical compounds which are in thermal (but not thermodynamic) equilibrium with the environment.

As we examine the possible mechanisms for this reaction, keep in mind that it must accomplish a large net change in chemical potential (~ 1.4 electron volts) with high efficiency (~ 75%). Four general mechanisms that have been considered are:

Photosensitization

$$T^* + A + B = T + A^+ + B^- \qquad \text{(I-8)}$$

Electron Transfer

$$T^* = T^+ + e^- \qquad \text{(I-9a)}$$

$$\text{or} \quad T^* + A = T^+ + A^- \qquad \text{(I-9b)}$$

$$\text{or} \quad T^* + X = T^- + X^+ \qquad \text{(I-9c)}$$

Proton Transfer

$$TH^* + A = T + AH \qquad \text{(I-10a)}$$

$$\text{or} \quad T^* + XH = TH + X \qquad \text{(I-10b)}$$

Rearrangement

$$T^* = Y \qquad \text{(I-11)}$$

(Y then reacts to give charge separation)

The electron transfer mechanism is the commonly accepted one today. The primary evidence comes from spectroscopic studies such as described in this paper (Chapters 3 and 4). Studies of the effect of changing the redox potential of the environment on the photoproduction of intermediates have made it possible to measure the (dark) reversible oxidation-reduction potential associated with the intermediates. If one can then assume that certain spectroscopic absorption bands are related to the trap itself, it is possible to learn some details of the photochemistry. Results of such experiments point to a one-electron photo-oxidation of the trap molecule (Eqn. I-9b) as the fundamental quantum conversion process.[28-31]

Assignment of the "primary step" in this fashion is quite a difficult task. Of the four reactions mentioned above, none can be rigorously excluded on the basis of present evidence. Reactions I-10 and I-11 would seem to be the most unlikely. The redox studies have generally found no pH dependence of redox potential,[29] indicating an electron transfer. But the complexity of the biological material makes even the simplest interpretation of straightforward pH or isotope studies a risky business. The plausibility of direct nuclear rearrangement is lowered because of the lack of good model reactions. Most photochemical reactions proceed along the thermodynamic gradient. In those cases where the high energy form is favored (such as cis-trans isomerism of conjugated olefins) only a small fraction of the photon energy is actually stored, and the quantum efficiencies of such reactions (i.e., events/quantum) are also low.[32,33]

Somewhat more satisfactory models exist for the electron transfer mechanism (Eqn. I-9). Some photocathodes in photomultiplier tubes show very high quantum efficiencies (up to 75% of the absorbed quanta produce photoelectrons). Chlorophyll can be used as an electron donor or acceptor in reversible photochemical reactions which involve the oxidation of weak reductants (such as ascorbate) or the reduction of weak oxidants (indophenol dyes).[34,35] Energy storage in such reactions cannot be more than a few tenths of an electron volt out of 2.0 ev. Rabinowitch has recently reported the photobleaching of thionine by ferrous ion in a two-phase system. Energy storage here is also 0.3 ev.[36]

Thus our problem appears to be the choice between electron transfer and photosensitization reactions. One basic testable difference is that T^+ or T^- (I-9b,c) should be susceptible to direct spectroscopic study. In the case of photosensitization one must measure the concentration of $\underline{T}^*$, which, at ordinary intensities, is quite likely to have such a low steady-state concentration as to be undetectable by absorption spectroscopy, although it might be observable by means of a characteristic emission.

The postulated identification of an absorption band associated with a trap, if correct, seems to rule out the photosensitization mechanism.

To summarize once more, a good bit of circumstantial evidence points to a discrete, unique "trap" which is the recipient of the electronic excitation energy obtained from the absorption of the photons. The trap molecule then reacts possibly via a direct electron transfer step to produce highly oxidized and reduced moieties.

We will next consider the pathways by which these reactive

intermediates provide or accept electrons to produce the final materials of interest to us (XH_2 and O_2). We will also be interested, in passing, with the mechanism for the formation of ATP.

Electron Transport Reactions

The study and interpretation of the electron transport reactions of photosynthesis have been greatly influenced by a unique and relatively well understood metabolic reaction system: respiration. The overall reaction is strikingly similar to the one we are considering, except that the electron flow is reversed (i.e., electrons move in the direction of spontaneous reaction).[37,38]

$$1/2\ O_2 + (CH_2O)_x = CO_2 + H_2O \qquad \text{(I-12)}$$

We can again subdivide the reaction into parts, with the interesting partial reaction being:

$$1/2\ O_2 + \left[\begin{matrix} TPNH = TPN^+ \\ DPNH = DPN^+ \end{matrix}\right] + H_2O \qquad \text{(I-13)}$$

This reaction is formally exactly the reverse of Eqn. I-2.

The molecular mechanism for respiration is now available in relatively complete form. One simplified scheme is shown in Figure I-8.[39] The major points of interest to us are the molecules involved, the fact that transfer proceeds through 1 and 2 electron redox reactions, and the formation of ATP at suitable potential jumps.

Spectroscopic methods played a vital role in analyzing the role of various compounds in the respiration pathway. If similar reactions are indeed to be found in photosynthesis, then the application of such techniques would hold great promise for mechanistic studies. Because of the very close analogy between the net reactions, much of the current

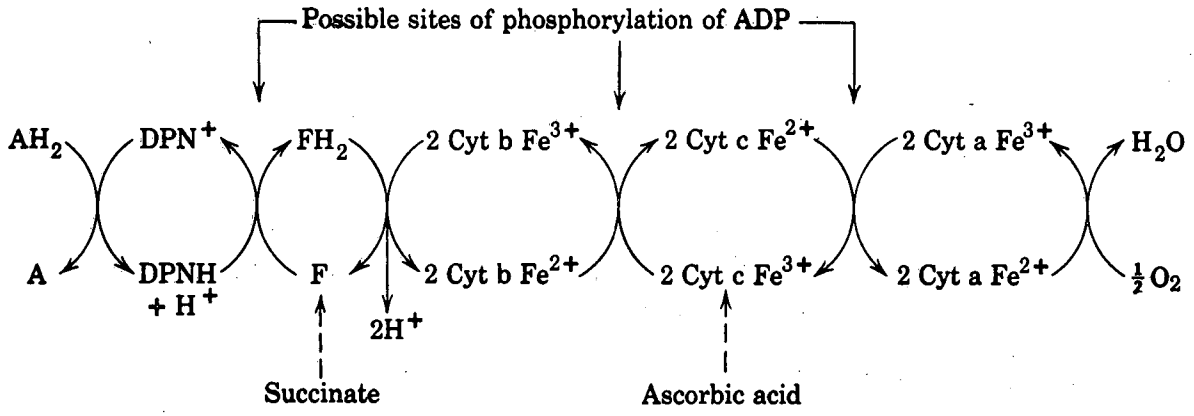

Possible sites of coupling of phosphorylation with electron transport in liver mitochondria. **(Fruton and Simmonds)**

MUB-6795

Fig. I-8.

photosynthetic mechanism is based on analogy with the respiration work. We will treat this model in some detail in a later chapter and hence will defer a more extensive analysis of results and conclusions until that point.

We have seen that the complex reactions making up the overall process of photosynthesis can be broken up into sets of simpler reactions whose mechanisms, for the most part, can be understood in terms of analogous systems. Thus the steps of light absorption, energy transfer, energy trapping, photoionization, and electron transport form a working hypothesis for the photosynthetic mechanism that seems correct in broad outline. We shall assume that a certain number of these steps, presumably involving highly organized molecular and subcellular structures, can provide a satisfactory framework for understanding the studies to be described here.

Chapter II. INSTRUMENTATION

Introduction

The experiments on which this thesis is based are for the most part of a single type. We measured changes in the visible absorption spectrum of photosynthetic systems before, during, and after excitation with strong actinic light. We wished to obtain both spectral and kinetic information from these experiments. The concentrations of photoproduced intermediates were, generally, quite low (ca. 10^{-8} molar), and some lifetimes were less than .01 seconds. One commercially available instrument was useful for some of the larger, slower signals; but more often special equipment had to be constructed to meet the severe sensitivity requirements. Because so much of the work to be described was performed near the limits of sensitivity of visible spectroscopy, it is worthwhile to consider the general features of spectrometers operating in the 350-1000 mμ region.

General Remarks

As with any spectrometer, the basic components are a source, a monochromator, and a detector.

A. Sources. The light source is an extremely important part of a high-sensitivity visible spectrometer because, as we shall see in more detail later, it is the limiting noise source. We required a continuous, high-intensity, high-stability light source.

Tungsten filament projection bulbs served as excellent sources from 320-1000 mμ. Relatively high wattage (500-1000) and color

temperatures (3100-3250°K) were readily available. The outstanding characteristic of tungsten bulbs is their very high stability. Short term fluctuations (1 second) are normally limited by the power supply regulation which can approach 0.01%.

For shorter wavelengths xenon arcs or hydrogen lamps are needed. Relatively little work was done with these sources so their detailed properties will not be discussed.

B. Monochromators. Much of our work was in the visible and near infra-red regions. Here a grating monochromator has some advantages over a prism unit. Resolution was never critical since most of the absorption bands of the molecules of interest proved to be quite broad (5 to 10 mμ half band width). Furthermore, stray light, the major disadvantage of a grating monochromator, never offered serious difficulties. Absorbancies were kept low and color filters were available to remove higher order radiation.

C. Detectors. Photomultiplier tubes (PMT) are now almost universally employed as detectors for radiation of the wavelenghts of interest. There are two basic designs: end-window tubes which permit illumination of the photocathode through a flat window of glass or quartz; and side-illumination tubes where light passes through a curved envelope. The former come in a wider range of cathode materials and generally have more light gathering power, but they are usually less mechanically stable, somewhat more noisy and less compact than their side-illumination counterparts.

Photomultiplier tubes have low intrinsic noise levels. The "dark" noise never proved a limiting factor in these experiments. Photomultipliers

also have very fast intrinsic rise times. All of the common tubes have response times faster than 10^{-8} seconds, the ultimate limit being the transit time of electrons through the tube. Another pleasant feature of these tubes is their linearity, which is in the order of 1-3% at low output currents (well below saturation). The output impedance of such devices falls in the range of 10 K to 1 M ohms, easily compatible with conventional amplifiers. Finally, their dynamic range is very large, approaching one million. Thus one can look for small changes in large signals without much loss in sensitivity.

We routinely used end-window tubes. Our choice was based on two factors: it was easier to obtain good red-sensitive end-window photomultipliers, and their wider collection angle made them more suitable for the high light-scattering associated with cellular and subcellular sized particles.

D. Performance. There are two main areas of interest to us—sensitivity and response time.

Sensitivity. Let us define the sensitivity of a spectrometer as the smallest change in optical density (absorbance) that can be distinguished from the noise. If one is primarily concerned with small signals—that is, small percentage changes in absorbance—the following derivation relates changes in absorbance to the changes in transmitted intensity:

$$A = \log_{10} I_o/I \qquad \text{(II-1)}$$

where A = absorbance, I_o is the intensity of illumination incident on

the sample, $\underline{I}$ is the intensity of illumination transmitted by the sample. Then

$$A \pm \Delta A = \log_{10} \frac{I_o}{I \mp \Delta I} \qquad \text{(II-2)}$$

$\underline{\Delta A}$ is the change of absorbance, $\underline{\Delta I}$ is the corresponding change in the transmitted intensity.

Dividing the argument of the logarithm by I/I and separating the log terms,

$$A \pm \Delta A = \log_{10} I_o/I - \log_{10}(1 \mp \Delta I/I) \qquad \text{(II-3)}$$

or

$$\pm \Delta A = -\log_{10}(1 \mp \Delta I/I) \qquad \text{(II-4)}$$

I $\Delta I/I$ is much less than I we can simplify further:

$$\Delta A = -0.434\ \Delta I/I\ . \qquad \text{(II-5)}$$

For small changes in absorbance we can then consider a simple measurement of $\underline{I}$ and $\underline{\Delta I}$. $\underline{I}$, being much larger, is correspondingly easier to measure, being simply proportional to the voltage from the photomultiplier. Measurements of $\underline{\Delta I}$ are also directly obtained as the changes in the PMT output. However, they may be quite small and, in general, such measurements are limited by shot noise in the light source; pickup, hum, and mechanical vibrations; and control loop noise.

In a well-designed system the shot noise is the most frequent limitation. This noise can best be thought of as random fluctuations in the photon emission from the source. Being a random phenomenon this noise is just proportional to the square root of the total number of photons/sec. which cause ejection of electrons from the photomultiplier cathode. A rough calculation indicates that a 3 mμ bandwidth in the green region of the spectrum, using a tungsten source and a S-20

photocathode and a sample with optical density 1 will have $\sim 10^{12}$ photoemissions/sec. or a signal/noise for a one-second time constant of $\sim$ a million to one. Instruments to be described here can approach this value within a factor of two.*

Pickup and hum can, in principle, be reduced to any desired level by suitable circuit design and shielding. In practice they always give rise to some interference but usually they are not a major problem. Low frequency mechanical noise (vibrations of electron tube components, small movements of the light beam due to building vibrations, etc.) can be a significant problem if long time constant experiments are undertaken. Such noise, being nonrandom, does not average out effectively unless one measures at intervals which are short compared to the major periods of the vibrations.

Most commercial recording spectrophotometers require extensive control circuitry to maintain photometric accuracy in the face of changing lamp properties, photomultiplier drift, and sample absorbances. These circuits frequently contribute significant noise to the total system so that none of the commonly available spectrophotometers really approaches shot-noise limited performance. Figure II-1 illustrates the various types of noise which can be found in electronic systems.

---

*If an instrument is performing near the shot noise limit the only way to increase the signal/noise ratio without increasing the time constant is to increase the photocurrent in the cathode of the PMT. This can be done by improving the quantum yield of photoelectrons, or, more readily, by increasing the light intensity. As indicated above, the signal-to-noise ratio should improve as $I^{1/2}$. This particular route was not open to us because too bright a detecting light would cause appreciable excitation of the material under study.

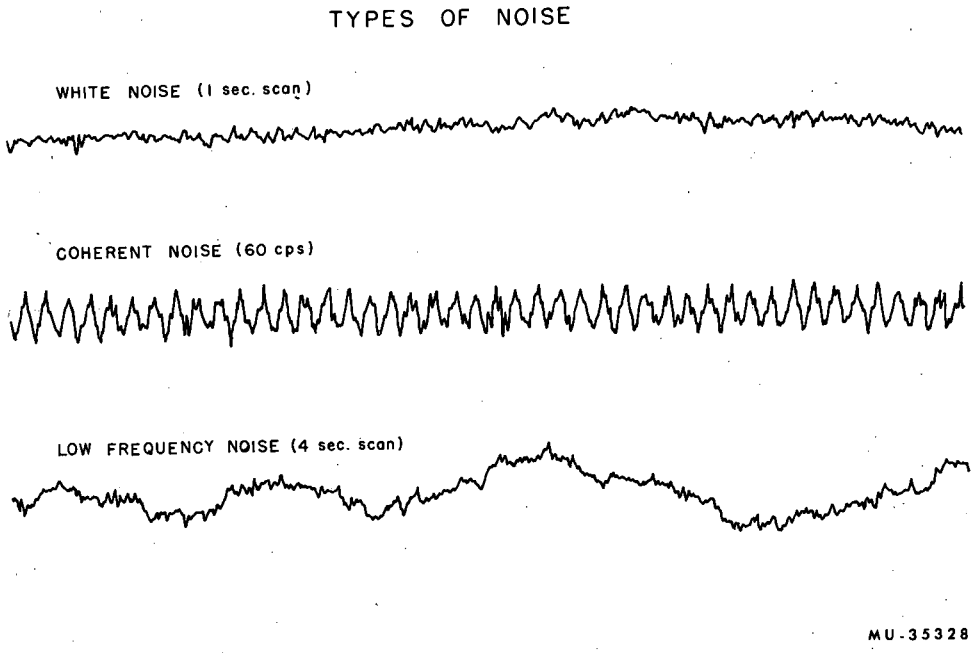

Fig. II-1. Types of electronic noise.

Some well-known problems in other photometric instrumentation are not particularly important in our applications. For example, the thermionic emission ("dark" noise) of PMTs only becomes significant at very low light levels, such as might be present in low-level fluorescence studies. As another example, long-term calibration is fairly easy to maintain because small signal measurements involve linear instead of logarithmic circuits and because changes in PMT sensitivity, monochromator efficiency, or lamp output are automatically corrected since they all enter into both the ΔI and I terms.

Response Time. As indicated earlier, a visible spectrometer using PM circuits has the capability for fast time response. The limits of 10^{-8} seconds are seldom even approached. And commercial equipment is usually limited to a quite slow response of 0.1 seconds. Needless to say, one should select a response time that is faster than that of the phenomenon to be studied but not so much faster as to waste sensitivity.

The relationship between sensitivity and response time is readily available if the noise is random in time and all frequencies are represented by equal amplitudes. For this "white noise" limit

$$V \propto (1/T_r)^{1/2} \qquad \text{(II-6)}$$

where V is the root-mean-square noise voltage and T_r is the response time. This result will apply, for example, to the shot noise described above.

For low frequency measurements (10 cps or less) other forms of noise such as vibrations or line fluctuations become relatively more important. Although these interferences are random in time, they do not exhibit amplitudes that are independent of frequency. In fact, such noise is often termed "1/f" noise because the rms voltage is just

inversely proportional to frequency. Under these conditions no improvement is obtained if the response time of the instrument is reduced. The only effective means of reducing the interference from 1/f noise (aside from improving the instrument itself) is to make measurements for times short compared to the major 1/f components and then average the results. Digital techniques particularly well suited for this approach have been described in the literature[40] and will be discussed in detail below.

We have seen that sensitivity in a well-designed visible spectrometer is limited by the random nature of the photon emission from the light source. As long as this noise is dominant, sensitivity and response-time can be exchanged for one another, sensitivity being inversely proportional to the square root of the response time. However, in all practical circuits 1/f noise becomes important at long times (ca. 1 second). Other means are needed to reduce interference of this type.

Instrumentation

Let us turn from our consideration of the general principles of visible spectrometers to a detailed discussion of the instruments used in our studies.

The Cary Spectrometer

A conventional Cary Model 14M double-beam spectrophotometer (Applied Physics Corp., Monrovia, Calif.) was outfitted with a scattered transmission attachment (Model 1462) (Figure II-2). This unit uses a 2-inch end-window PMT placed within an inch or two of the sample cells. This arrangement collected a large fraction of the light which would ordinarily be scattered out of the monochromator beam by suspensions of

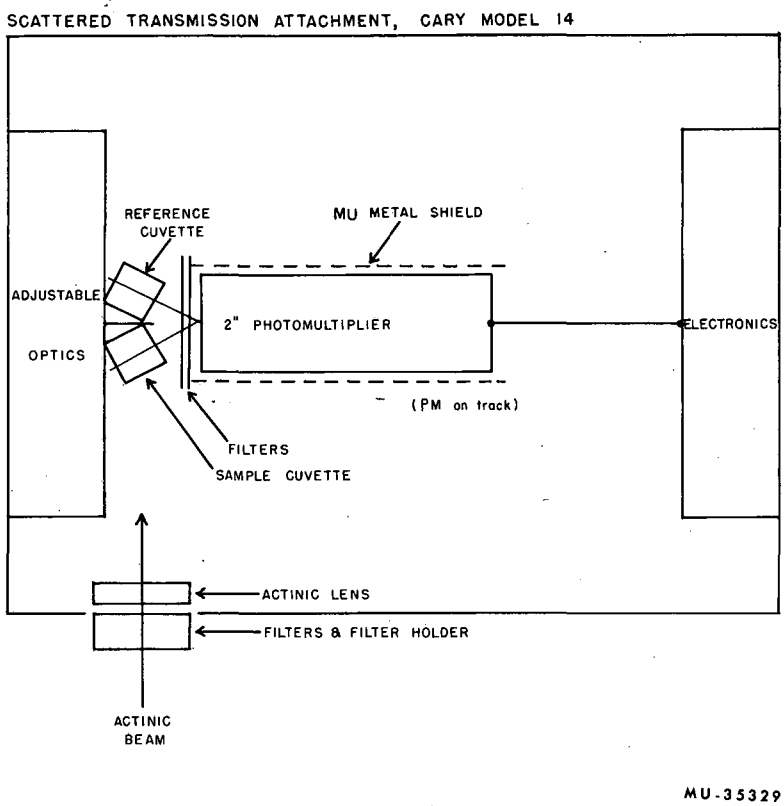

Fig. II-2. Scattered transmission attachment, Cary Model 14 Spectrometer.

algal cells or chloroplasts. The instrument could be used for several experiments involving chemical difference spectra or light-minus-dark spectra. To obtain optimum noise levels we routinely used a 0 to 0.2 O.D. slidewire, low photomultiplier high voltage settings, and minimum gain in the slit servo circuit. The net effect of these adjustments was to produce a noise level of .0005 O.D. units in the blue and .002 O.D. units in the near infra-red. The response time was of the order of 0.1 seconds.

This basic unit was readily modified for photochemical studies. We replaced a side panel with a new panel that permitted illumination of one of the cuvettes at approximately 90° to the measuring beam. A small partition prevented the actinic light from reaching the reference cuvette. If spectra were to be measured while the actinic beam was on, care was taken to exclude the (normally) intense actinic beam from reaching the photomultiplier.* With strongly scattering samples this could only be accomplished by using complementary colored filters in front of the actinic source and the PMT. (See Figure II-2). Those filters had to be changed to examine different regions of the spectrum. A list of those used is given in Chapter IV. In some cases fluorescence from the sample, induced by the actinic beam, interfered with the measurements. Even though this fluorescence is nominally not modulated, a combination of 60 cps ripple (the modulation frequency in the Cary is 30 cps) and the steady bias from this light caused increased noise (fourfold at high actinic intensities) and a baseline shift (.01 O.D. units).

---

*In any case, it is not good practice to illuminate a PMT with very intense light, even with the accelerating voltage turned off. Irreversible damage can occur to the photocathode surface.

The Cary when used as described proved a versatile and powerful tool. Yet it did not meet either the sensitivity or time resolution requirements of many of our experiments, and it proved necessary to construct our own instruments for such studies.

High Sensitivity Fast-response Instruments

Our twin goals of fast response and high sensitivity were mutually exclusive in the standard spectrometer designs available at the time this work was started. Furthermore, the Cary is a well-designed, well-constructed instrument, and it seemed unlikely that a "home-made" copy could proceed in the same direction more successfully. Thus we attempted to approach the problem from a different point of view.

First the sensitivity was improved simply by using constant wide slits (1 mm, 3 mμ bandwidth), thereby delivering as much light as possible to the photomultiplier.* Second, we decided to select for those signals which were produced by the actinic beam. We did this by modulating the actinic light (instead of the normal practice of modulating the detecting beam) at a known frequency and then using frequency and/or phase sensitive detection circuits.

In all, three different instruments were constructed. The primary difference among them was in the detection circuits. These three were all of the single beam type. A double beam instrument is currently under construction. Figure II-3 shows a schematic block diagram which is suitable for all three single beam units. We wished to measure the effect of the actinic light on the absorbance of the sample. If the actinic light is on and off for times which are long compared to the

*Although the detecting beam had to be much weaker than the actinic beam, there was still a large improvement factor available over the Cary which, after all, is programmed for maximum resolution rather than maximum sensitivity.

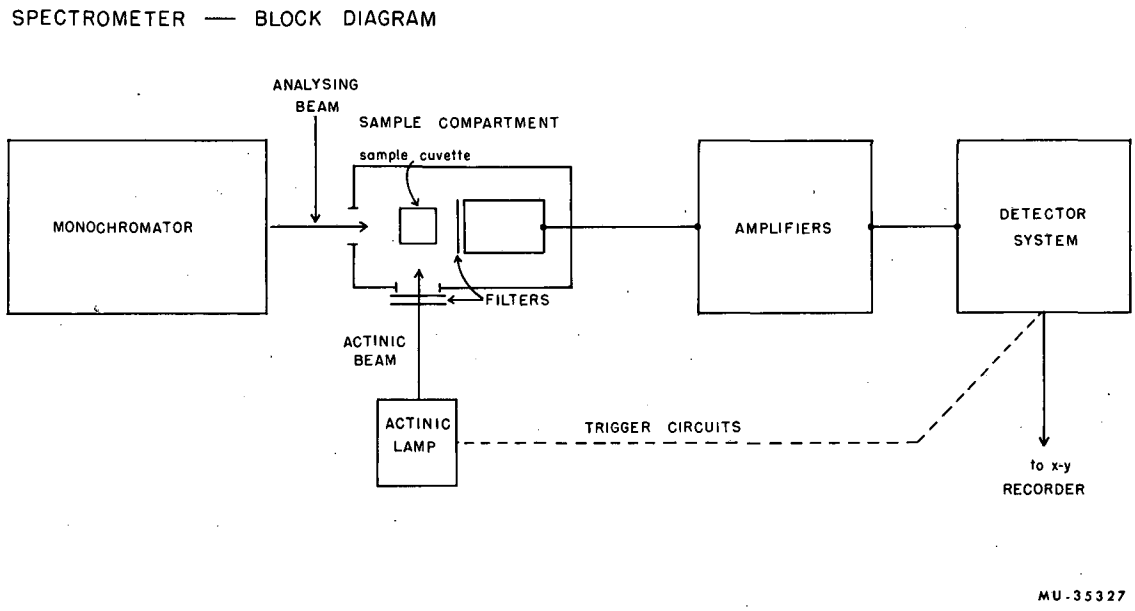

Fig. II-3. Spectrometer — Block Diagram. See text for detailed descriptions.

reaction times, a plot of sample absorbance at one wavelength versus time might look like Figure II-4. Here we have shown a reversible increase in absorbance during the actinic illumination period compared to the absorbance in the dark interval. Note that each transient under these conditions displays the information needed for kinetic analysis: rise and decay curves, as well as steady-state conditions, during both the light and the dark intervals. Note that the baseline is best designated in terms of the dark steady-state level. The figure also attempts to indicate the relatively poor signal/noise ratio present in measurements of this type. However, if all of the repetitions of such transients were essentially identical except for random fluctuations, a suitable averaging device would permit a major enhancement in sensitivity. The instruments described below differ mainly in the way this averaging was performed.

A Tuned Voltmeter

Principle of operation: an actinic light source capable of being modulated over a wide range of frequencies was used. A frequency-sensitive voltmeter was adjusted to the frequency of modulation and the alternating signal at this frequency was recorded. A "dark" reading was obtained with the actinic lamp flashing, but with the actinic beam itself blocked by means of a shutter so that it did not fall on the sample. The dark signal was usually very small in the absence of pickup. The signal produced by the actinic beam was then proportional to the change in transmitted intensity of the sample. A separate measurement of the transmitted intensity was made, and a plot of $\Delta I/I$ as a function of wavelength was prepared. Kinetic information was available from a

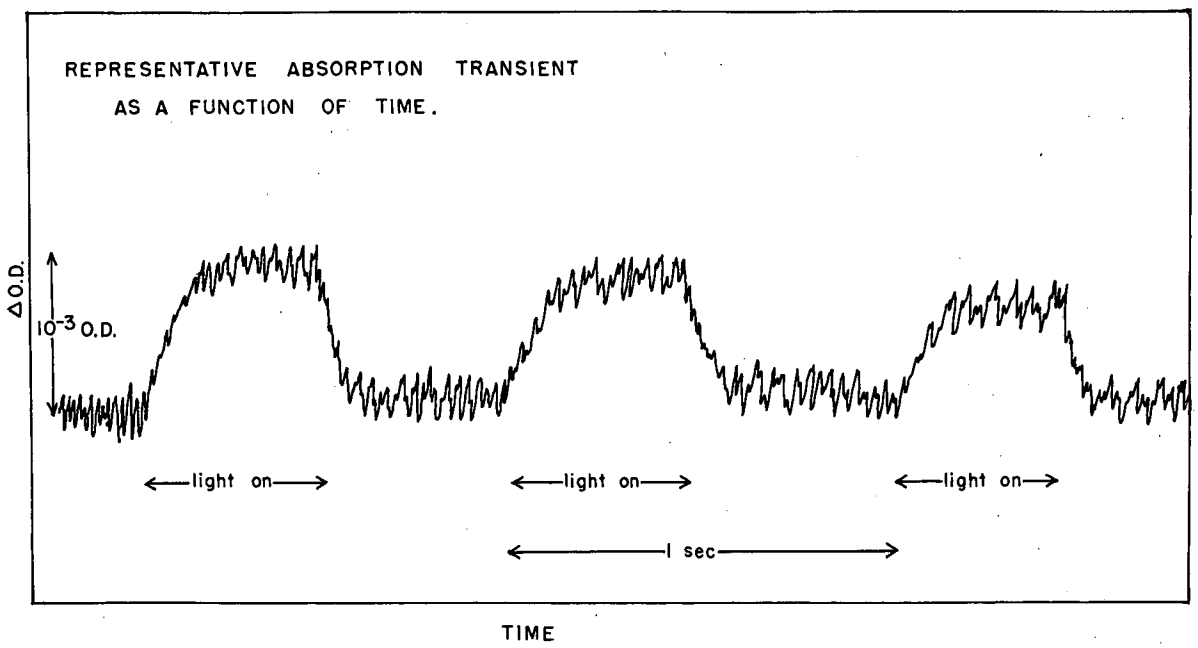

MUB-5951

Fig. II-4. Representative absorption transient as a function of time.

plot of the signal at any one wavelength versus modulation frequency.

A detailed description of the various components in this instrument is given below.

1. Detection monochromator. A 500 mm Bausch and Lomb grating monochromator equipped with a 500 watt tungsten projection bulb (Type CZX) served as a detection source. Monochromator slits of 0.5 to 2.0 mm were routinely employed. The dispersion of the instrument was 3.5 mμ per millimeter of slit width. Checks on various samples showed that 3 mm (11 mμ) slits caused some loss of resolution. Smaller slits were satisfactory for the braod bands usually found in the difference spectra. Direct measurements of the monochromator beam intensity showed it to be less than 1% of the normal actinic beam intensity. Calibrations of the wavelength scale against mercury and neon lines were performed at infrequent intervals. The unit operated for a period of three years within a 1 mμ tolerance. Checks against calibrated narrow-band interference filters were used periodically to insure continued wavelength calibration.

The tungsten source was run from a well-regulated low-ripple Mideastern supply (ST 100-10, Mideastern Electronics, Springfield, N. J.). The lamp was run at 105 volts or less, which greatly increased its life and stability. Ordinarily no ripple was visible if an oscilloscope was connected to the PM output. More sensitive measurements showed considerably less than 0.1% signal at 60 cps and less than 0.01% signal at 120 cps. Most of these signals could be removed by carefully eliminating ground loops.

2. Sample compartment. The final design for the compartment which holds the sample cuvette, the PMT, and the necessary light filters

is shown in Figure II-5. The following features are of interest:

a) metal construction of the entire compartment acted as a Faraday shield.

b) a second PMT was employed to monitor the actinic flashes and/or scattered light.

c) the PMT was mounted on a track so that it could be positioned anywhere along the length of the compartment.

d) the sample cuvette was held on a small removable table. Different tables were constructed for a wide variety of experimental needs. These included provisions for a flow apparatus, low temperature dewars, double beam spectroscopy, and actinic illumination of the cuvette from either the normal 90° angle or, alternatively, co-linear with the detecting beam. Some of these designs are indicated in Figure II-6.

e) a small photodiode (Hoffman Type 120 CG) was mounted on a movable arm so as to be easily swung into position to monitor the intensity of the actinic beam.

3. Photomultiplier tubes. Various tubes were selected depending, of course, on the wavelengths to be studied. Typical relative sensitivity curves are shown in Figure II-7. Secondary considerations were the noise levels and the stability of the tubes. The tubes were all of the end-window type with 10 stages (dynodes). They were all interchangeable. The base circuit we employed is shown in the next figure (Figure II-8). This circuit gave microsecond response times. We normally used a NJE (Model CS-64R40, NJE Corp., Kenilworth, N. J.) high voltage supply. 500-1000 volts proved suitable for most applications.

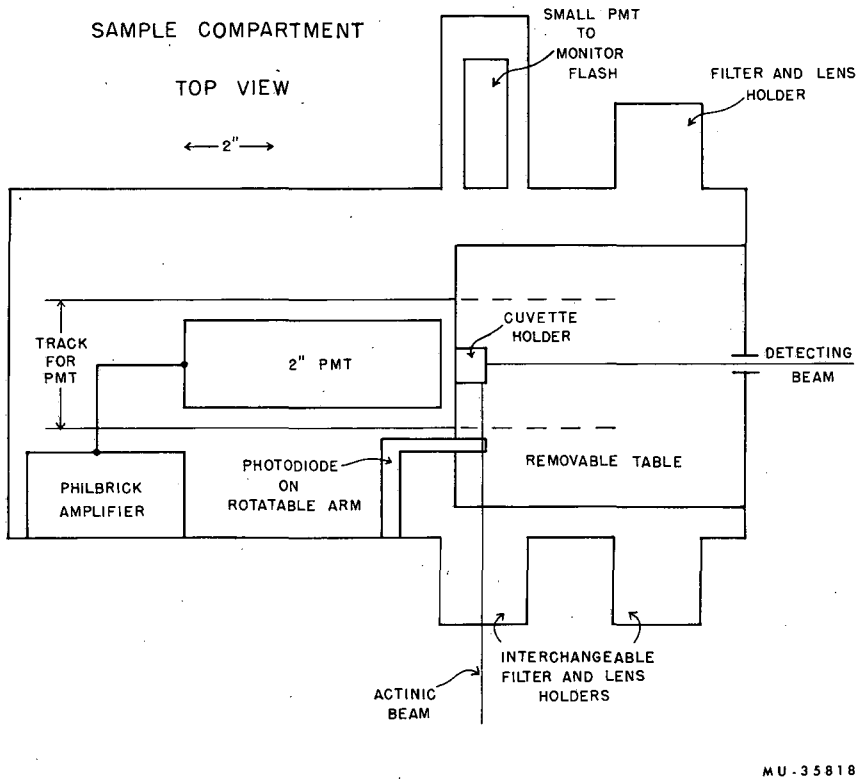

Fig. II-5. Sample Compartment.

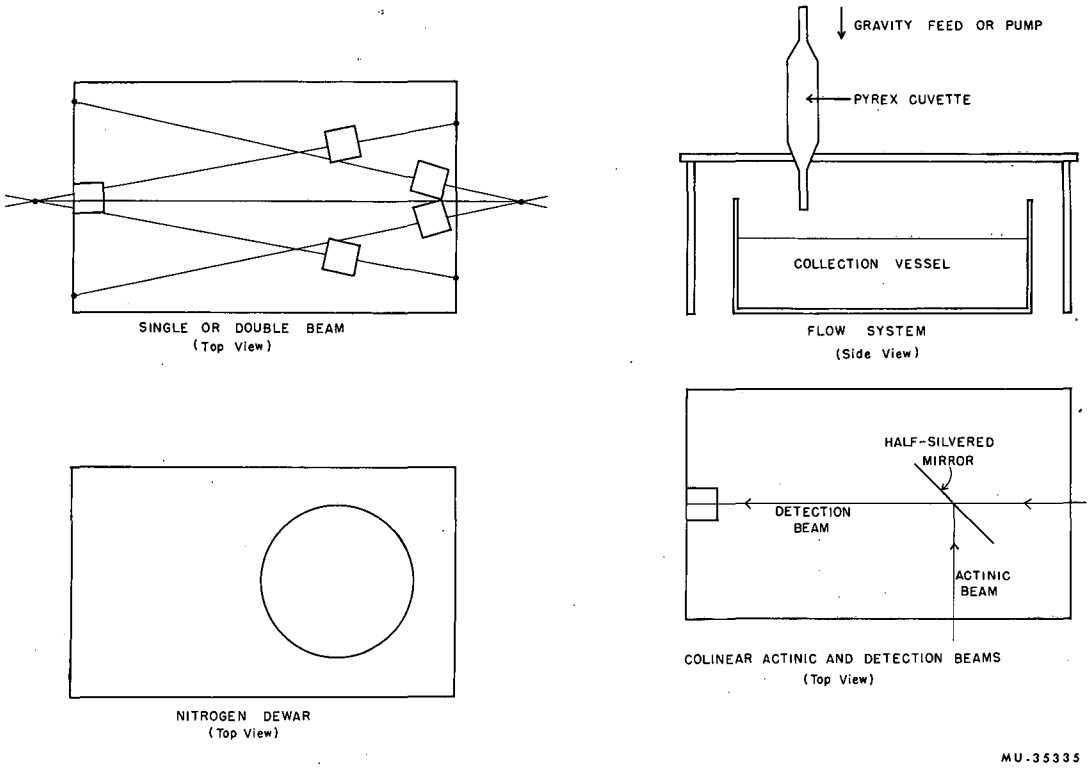

Fig. II-6. Interchangeable tables to be used for special experiments as indicated.

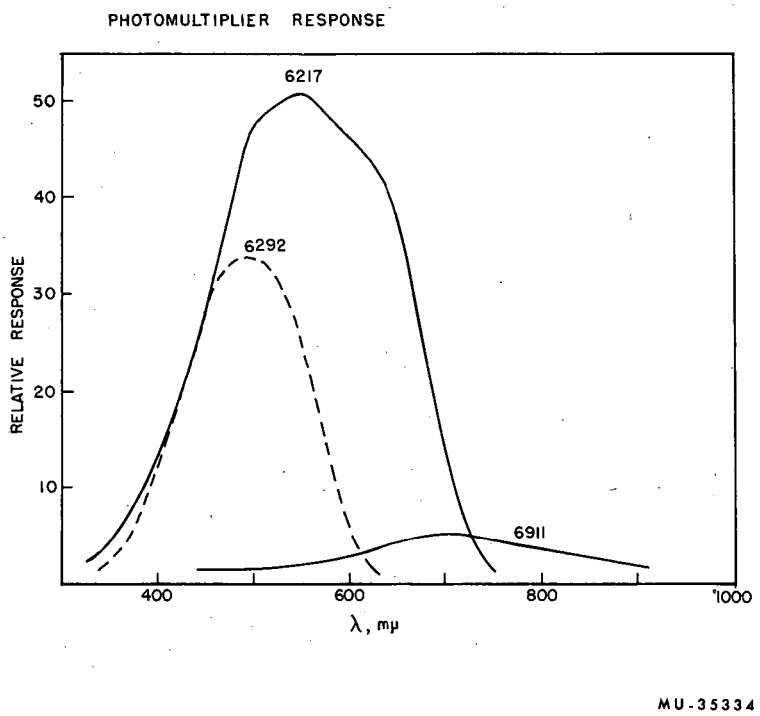

Fig. II-7. Photomultiplier response curves. Only the relative responses at each wavelength are of interest inasmuch as these curves are weighted by the monochromator and lamp characteristics.

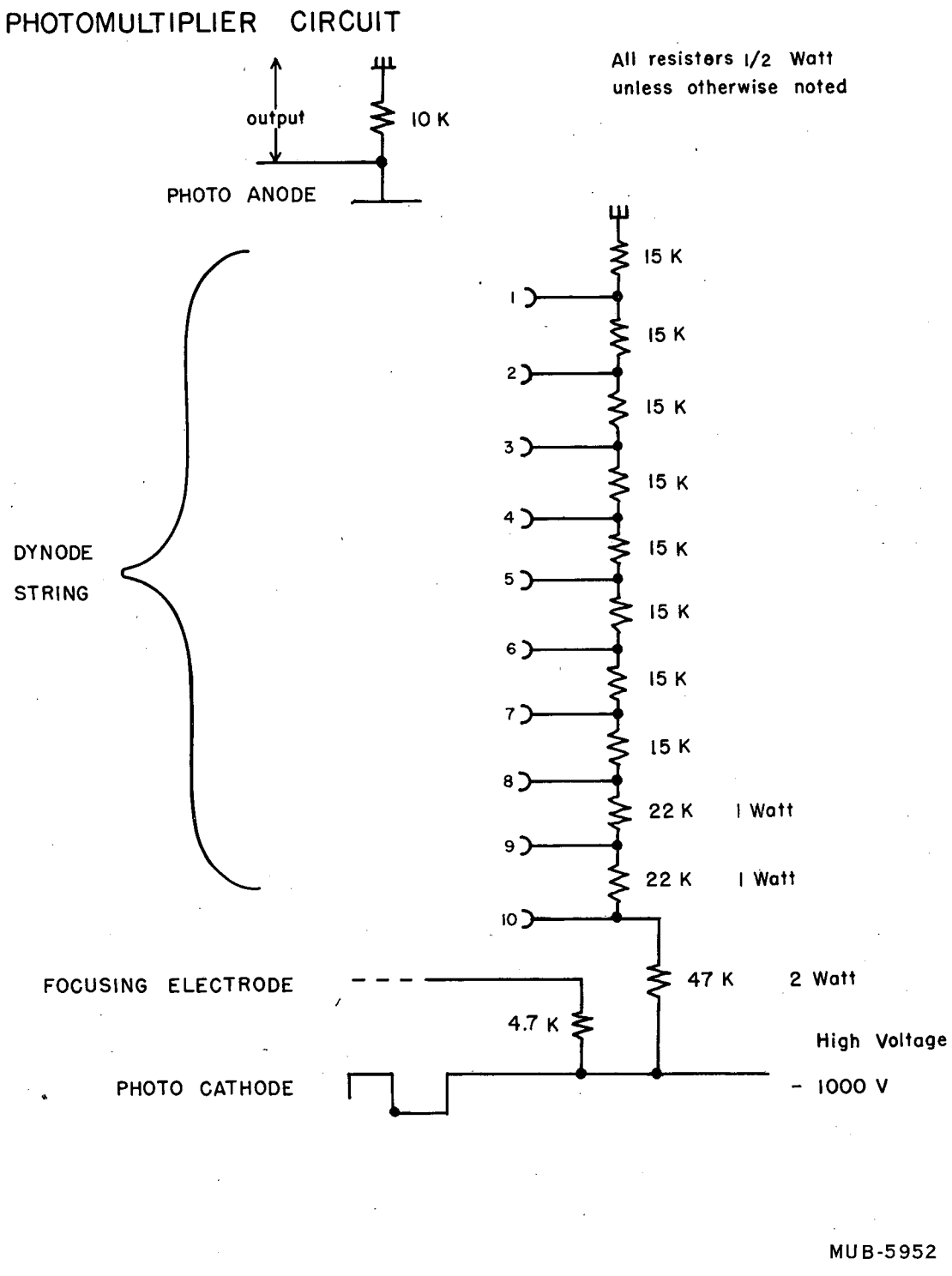

Fig. II-8. Photomultiplier Base Circuit.

Regulation was good (0.01%) and 120 cps ripple was not detectable at the millivolt level. A mμ metal shield protected the PMT from magnetic pickup. The rather close proximity of the actinic beam, the sample, and the PMT frequently required that we tape the detecting beam filters directly to the front of the mμ metal shield to minimize light leaks.

4. Actinic source. The actinic lamp for these experiments was a 40 watt electrodeless neon arc, driven by a 10 megacycle oscillator. The lamp could be turned completely on and off at frequencies of 0.1 cycles per sec to 10,000 cycles per sec by the simple expedient of gating off the driving oscillator on and off. The lamp design and a working model were kindly lent to us by Dr. L. Piette of Varian Associates.

The spectral output consists of the usual neon line spectrum, with most of the energy between 500-750 mμ (Figure II-9). Light output was approximately 10^{16} quanta/sec/cm^2. Rise and decay times were in the order of 10-20 microseconds. Appreciable jitter in the rise time occurred if the lamp was run at very low frequencies (0.1 cps). Up to 50 microseconds of jitter was observed under these conditions. Forced cooling helped the stability. Amplitude fluctuations were very small (1% or less).

Bulbs were constructed in the following manner. Ten 1-cm diameter bulbs (quartz or pyrex) were blown on capillary tubing. The tubing was connected to a vacuum line in the usual fashion, provision being made for connections to a flask of neon (Linde, high purity) and a McLeod gauge. The bulbs were outgassed for several hours, sparked with a Tessler coil, and heated in an attempt to remove most of the adsorbed oxygen. Neon was added to a pressure of 2 mm. Sparking was resumed,

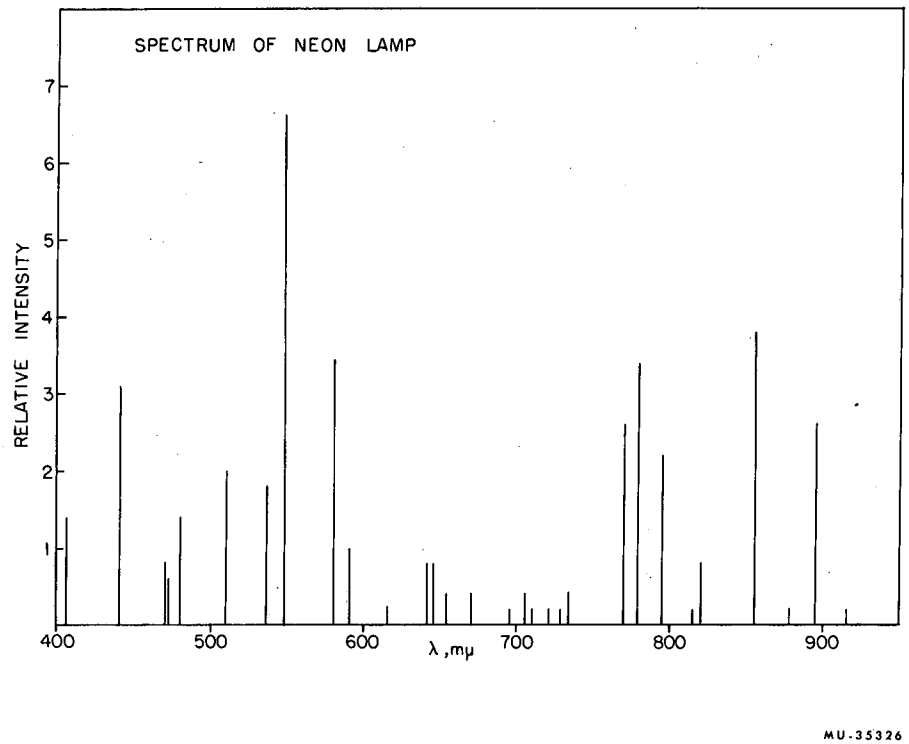

Fig. II-9. Output of Neon Lamp, corrected to relative numbers of quanta at each wavelength.

and the system was degassed once more. Then neon was readmitted at the same pressure. The neon pressure was a very critical factor in obtaining high intensity discharges. Only 10-20% of the bulbs ran satisfactorily. However, bulb life was very long (greater than 1 year), and the low yield was not a serious difficulty.

Mercury arcs could be readily obtained by cooling the lamps to liquid nitrogen temperatures while they were still on the vacuum system. A small amount of mercury would then distill over from the McLeod gauge. Essentially all the emission would be found in the normal lines of a low pressure mercury arc. Modulation performance was similar to that described for the neon arc, but the very high frequency performance was inferior. The quartz bulbs produced appreciable light at 1850 Å and 2547 Å, and the usual care required for UV sources had to be exercised.

In operation these lamps showed two major disadvantages: relatively low intensity and lack of emission at many wavelengths of interest. However, the ease of modulation over a wide range of frequencies made them useful actinic sources for our early studies.

5. Detection system. The PMT output was connected to the input of a wave analyzer (Hewlett-Packard Model 302A, Palo Alto, Calif.). This unit served as both a highly sensitive amplifier (1 microvolt gave a meaningful scale deflection) and a tuned voltmeter operating with a 3 cps bandwidth at frequencies from 10 to 50,000 cps. We improved the sensitivity of this unit still further by connecting its output to a slow-response electrometer voltmeter (Keithley Model 220, Keithley Instruments, Inc., Cleveland, Ohio). This permitted the detection of one part per million change in absorbance under normal operating conditions. The system response time was limited by the time constant of

the voltmeter to 5 seconds.*

Evaluation of performance: As indicated above, noise levels with this apparatus were of the order of 10^{-6} optical density units. Transients with frequency components up to 50,000 cps (corresponding to a time constant of 3 microseconds) could be detected. The averaging time constant was approximately 5 seconds. This apparatus was useful for both wavelength dependence and kinetic response studies. However, there were several basic difficulties. First, and most important, to obtain a true "time course" from frequency information would require taking a complete frequency spectrum and then obtaining the Fourier transforms. We lacked both the very low frequency data and the means to easily record and manipulate the data into a form suitable for computer processing. So instead of performing these calculations we measured the frequency response of the photochemical system. Figure II-10 shows the results of such a measurement on the phosphorescence

*Notice that for the study of repetitive signals a measuring system contains two different types of time constants. The first is what might be called the transient response time. This is the shortest interval that would contain meaningful information about the repetitive signal. In the experiments we are discussing this time would be associated with frequency components of 50,000 cps. But we cannot learn of non-repetitive changes in this system at anything like this rate. At best, the wave analyzer would respond in a time commensurate with its 3 cps bandwidth, and we had also placed a 5 second filter in the circuit. This second time constant we could call the averaging response time. An implicit assumption in all of our experiments of this type is that the sample properties are constant over the averaging time period. This separation of time constants is not normally found in most chemical experiments because there are few chances for rapid repetition of experiments. Photochemistry and the relaxation techniques now used for rapid reaction studies are the major exceptions. Thus it was essentially the reversible nature of the signals we obtained that permitted a repetitive experiment to be set up. This in turn permitted us to learn "high-frequency" information without sacrificing sensitivity.

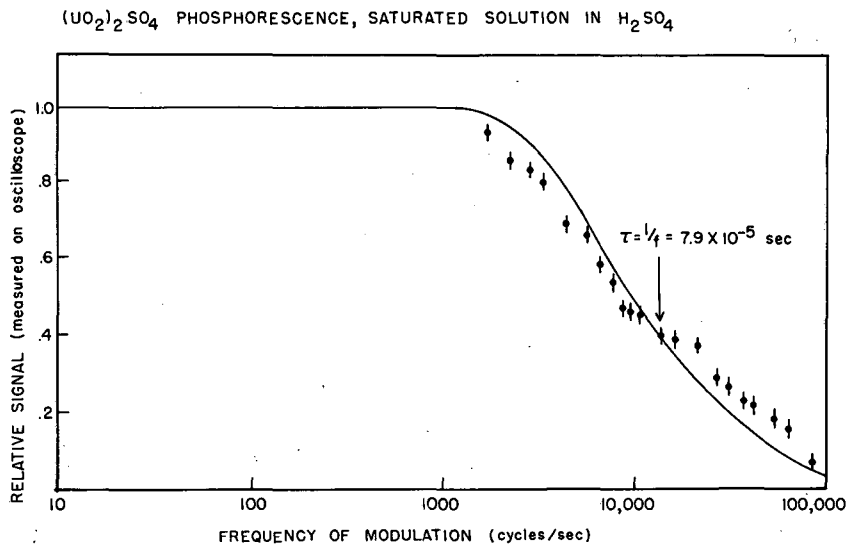

Fig. II-10. Uranyl Sulfate Phosphorescence Lifetime. The alternating signal induced by the flash is plotted against the frequency of modulation.

of uranyl sulfate. The plot of alternating phosphorescence signal as a function of frequency of modulation shows a smooth decline at high frequencies. For such a case we can determine that we are dealing with a single first-order decay rate constant. The experimental value of 7.9×10^{-5} sec compares well with the literature value of 9×10^{-5} sec.[41] Some of the other problems with the wave analyzer unit included: 1) sample fluorescence and scattered light could only be corrected for by a rather uncertain control experiment; 2) this method of detection was not sensitive to signal polarity (one could not tell readily whether a given deflection represented an increase or decrease in absorbance).*

Examples of the results we obtained with this apparatus are shown in Figures II-11 and II-12.

The Boxcar Integrator

Principle of operation: to meet the difficulties just discussed we adopted a time sampling technique (instead of a frequency sampling one). The circuit we employed was a well-known one, developed for NMR spin echo studies. In essence it measures the signal occurring during a very small portion of the repetition period. This information is accumulated for many repetitions. Then a second small interval is investigated. This principle, now used for sampling oscilloscopes, results in a faithful representation of a repetitive transient with considerable improvement in signal-to-noise ratios.

---

* One method we used to determine signal polarity was to mix in, deliberately, a small amount of scattered light. This light must always simulate a decrease in absorbance. Thus, if the signal plus the scattered light gave a deflection that was the sum of the two separately, both must have the same sign (the signal was an absorbance decrease). If the combination gave one of the algebraic differences, the signal and the scattered light had opposite signs (signal was an absorbance increase).

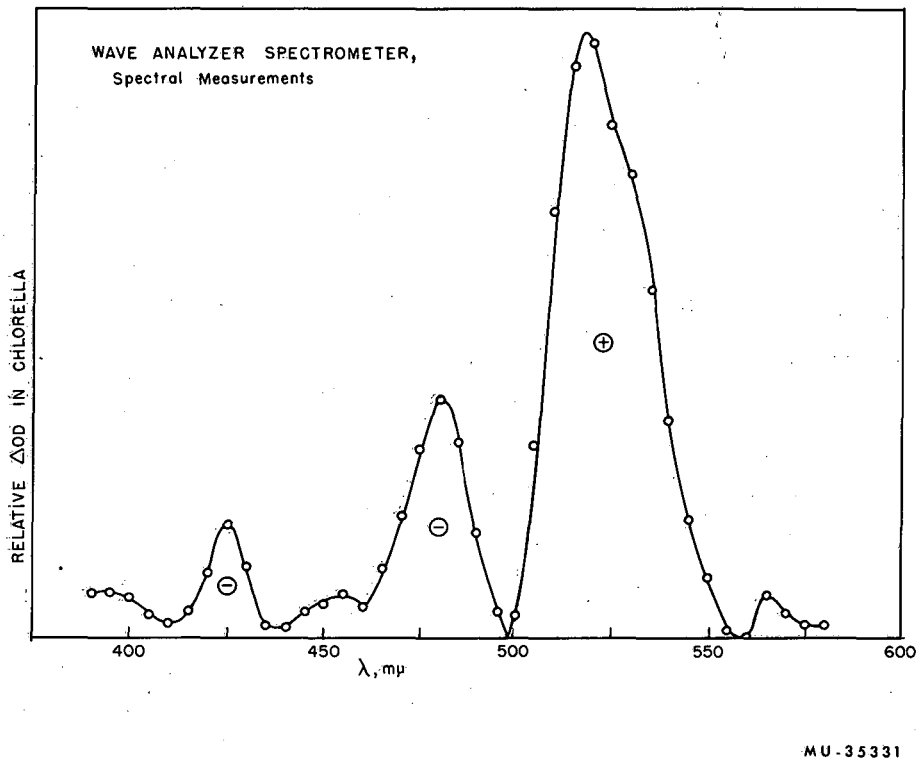

Fig. II-11. Light-dark spectrum of Chlorella cells using wave analyzer. Neon lamp modulated at 20 cps. Polarity of signals determined as described in the text.

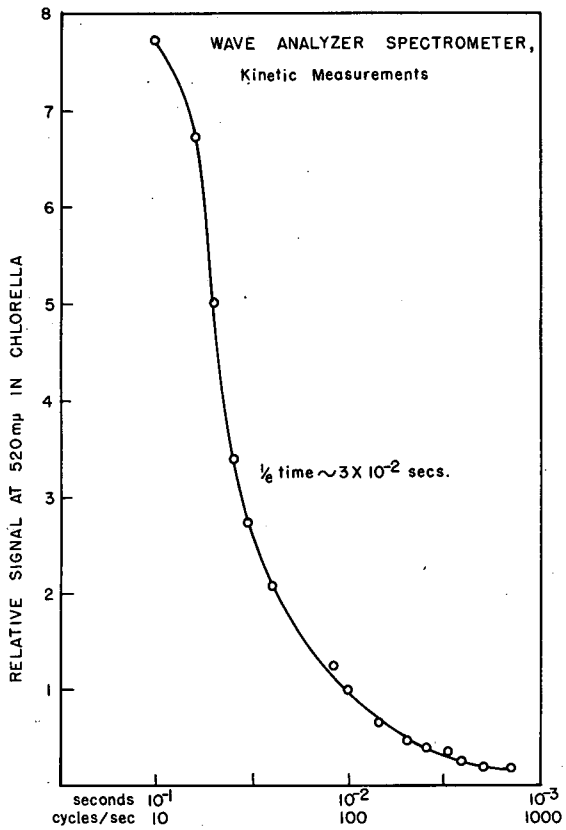

Fig. II-12. Kinetic measurements of the 520 mμ band in Chlorella, using the wave analyzer. The alternating signal is plotted against the frequency of modulation.

The monochromator, sample compartment, and PMTs were not altered from the previous instrument.

A. Actinic Lamps. Most experiments did use the neon and mercury lamps previously described. However, it proved possible to use a conventional tungsten source chopped with a sector wheel. The wheel was adjusted to provide a dark period of 27.7 milliseconds and a light period of 5.6 milliseconds, corresponding to a repetition rate of 30 times per second. The intensity was adjusted by means of a Variac, the wavelengths could be selected by interference filters and color glasses.

B. Detection Circuit. A block diagram of the spectrometer is given in Figure II-13. In brief, the spectrometer operates as follows: The light from the monochromator passes through the sample and then falls on a photomultiplier. A modulated actinic beam also illuminates the sample. Changes in the absorption of light by the sample thus appear as a modulation on the transmitted intensity. The photomultiplier output, then, consists of a dc signal (transmitted intensity) and a small ac signal (repetitive absorption change). The ac signal is amplified further while the dc level is stripped off by ac coupling or dc suppression. The amplified signal now consists of a pulse train whose voltages represent the periodic fluctuations in the absorbance of the sample. The pulses are fed into a sampling circuit—the so-called "boxcar integrator". The boxcar integrator is turned on for a very short time at the pulse repetition frequency. It is held in a fixed (but adjustable) phase relation to the incoming signal and acts as a rectifier. Thus a dc signal related to the average input voltage during the short sampling

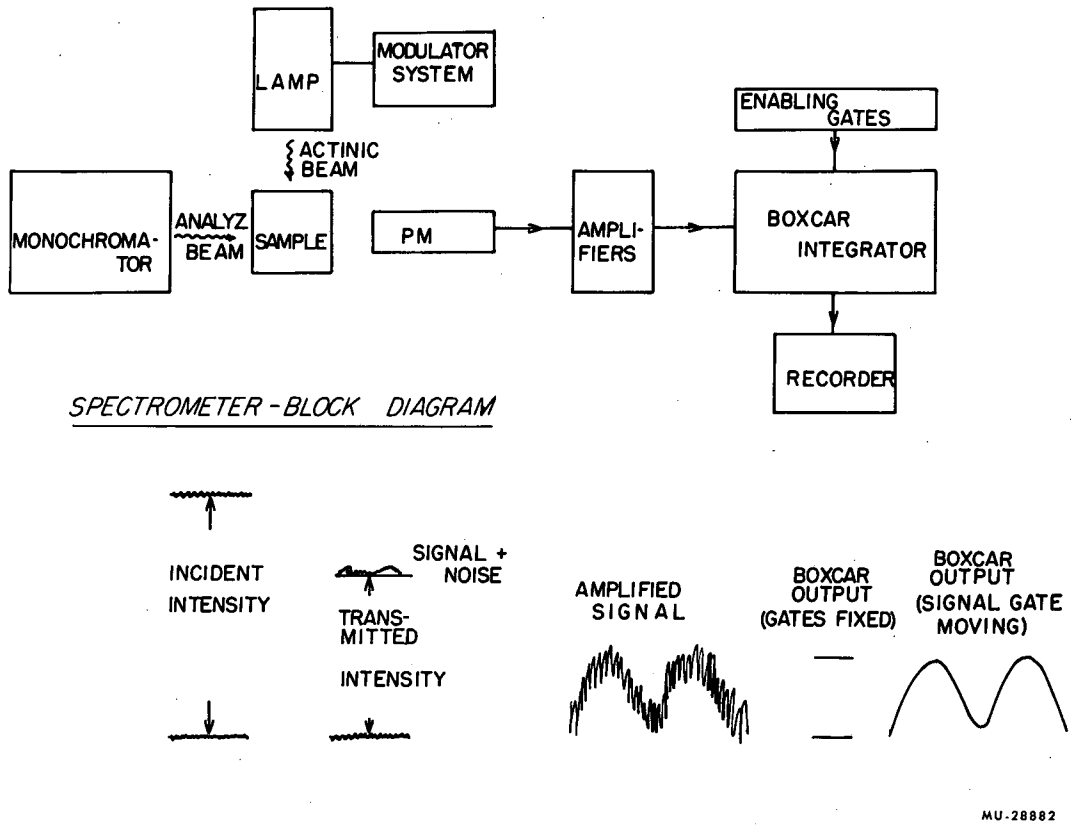

Fig. II-13. Block diagram of spectrometer and signals present.

interval is available to charge an RC circuit. The noise level on the output depends on the value of the integrating time of this filter circuit. However, the time resolution depends only on the small time interval that the boxcar circuitry is on. Thus we have achieved our goal of the independence of sensitivity and transient response time. The filtered output drives the Y axis of an X-Y recorder. Appropriate motor drives permit an automatic readout proportional to the changes induced in the sample by the actinic light. Figure II-13 also shows the waveforms in various parts of the spectrometer.

Voltage amplification of 100 to 10,000 is used to boost the initial signal above the internal noise in the detection circuit. We have employed Tektronix plug-in preamplifiers with limited success. Since these units were designed for oscilloscope use, they do not have long-term stability of very low noise levels. For various applications we have used the Type D, Z, and E plug-ins, powered from a Type 127 power supply.

The boxcar integrator was constructed locally from a circuit due to Blume.[42] Figure II-14 shows the circuit we used. It differs only in minor details from that described by Blume. The unit can be thought of as an electronic switch and a storage circuit. The four diodes (VI-4) are normally back-biased and nonconducting until an enabling gate is supplied. The average incoming potential during the gate interval is impressed across the capacitance (C1). If the RC charging time (often called the "learning time") is short compared to the gate duration, the voltage across C1 is equal to the average input voltage. After the enabling gate is turned off, this potential remains unchanged

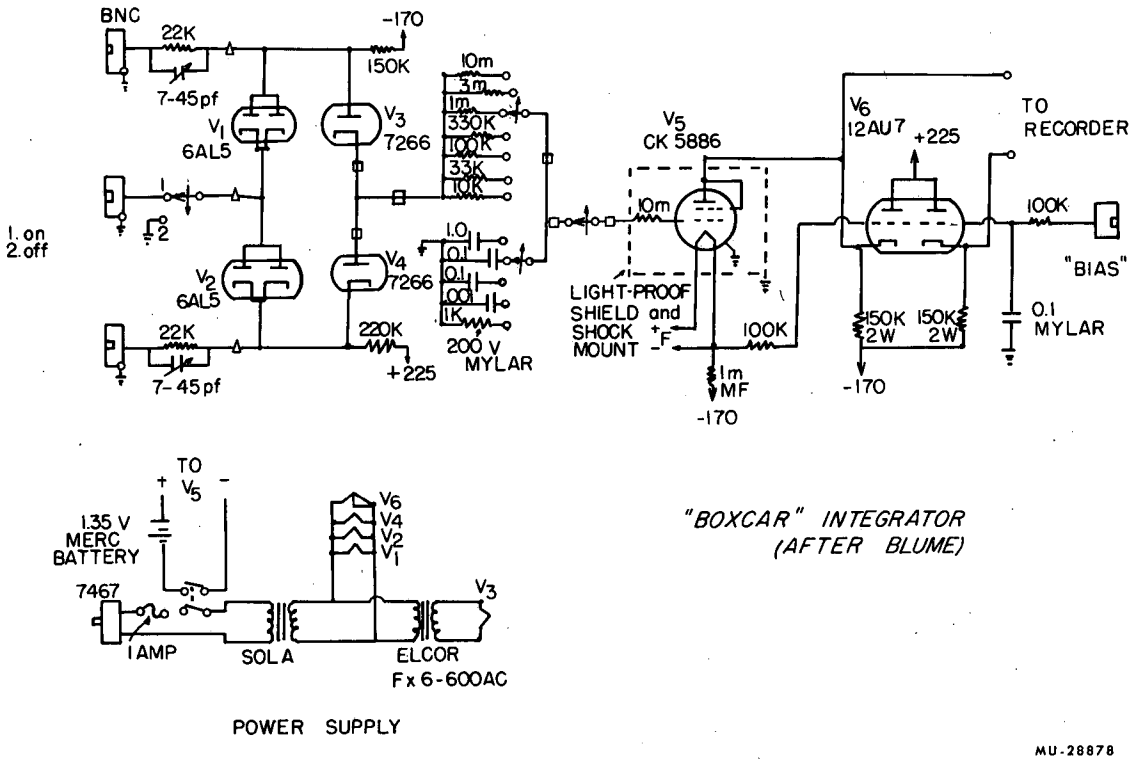

Fig. II-14. Boxcar circuit (after Blume[42]).

except for leakage paths to ground. Since the back resistance through the ceramic diodes (V3,4) is about 10^{13} ohms, the discharge time (or "holding time") is very long, on the order of thousands of seconds. Note that if one gate interval is not of sufficient length to charge the capacitance to the full input voltage, successive pulses will also contribute to the potential across the condensor. Thus one can average many samples of the same signal, allowing a signal-to-noise improvement.

The proper phasing of the enabling gates with the incoming signal is essential. We use a four-trace preamplifier (Tektronix Type M) in conjunction with a Tektronix 535A oscilloscope. Also, we use two separate boxcar channels, one to give us a reference signal. The two enabling gates, the amplifier output, and the signal from a photomultiplier which monitors the flash lamp are all presented simultaneously. Figure II-15 shows a block diagram of the required trigger circuits. Figure II-16 presents the phase relationship of the spectrometer waveforms. Figure II-17 shows the boxcar output obtained by slowly changing the phase of the "signal gate", allowing the boxcar to trace out a rapid electronic transient. The boxcar output is compared to that obtained when a low-pass filter is used to reduce the noise in a conventional circuit. For comparable noise levels the latter would greatly distort the transient shape.

For construction details the reader is referred to Blume's paper.[42] Considerable care must be taken because of the very high resistance required for successful operation. For instance, ordinary shielded cables represent virtual short circuits. Teflon-insulated wire is required in the vicinity of the storage circuit and the diodes. The high

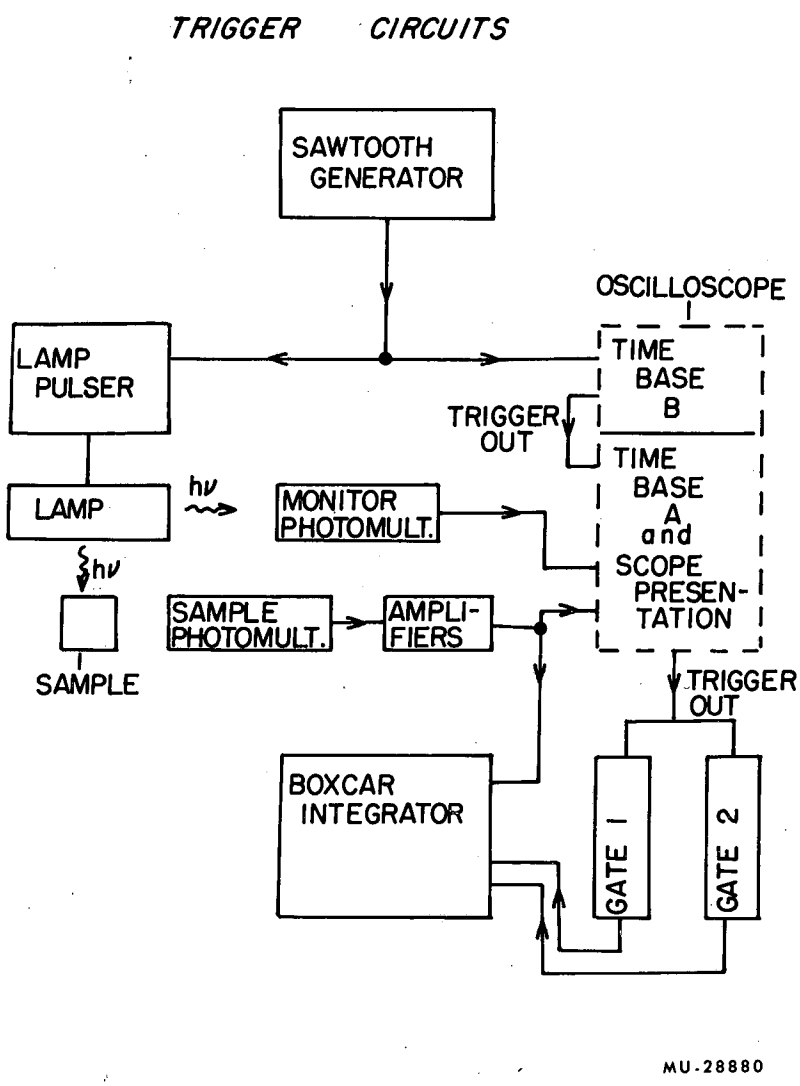

Fig. II-15. Boxcar Trigger Circuits.

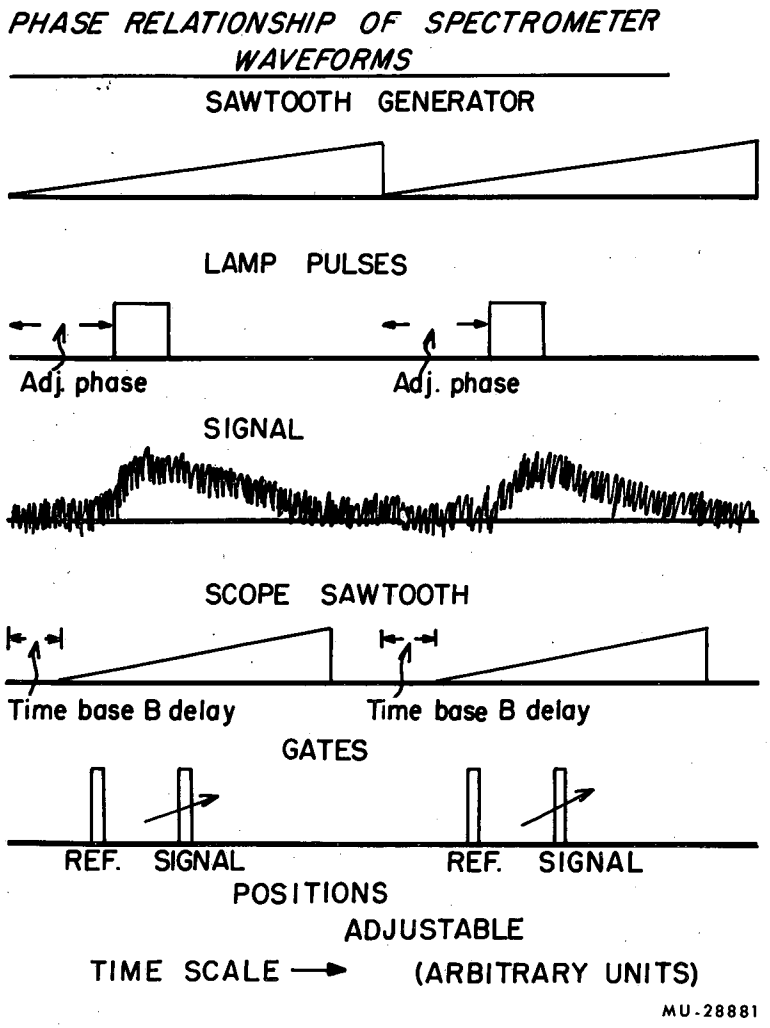

Fig. II-16. Phase relationship in boxcar spectrometer.

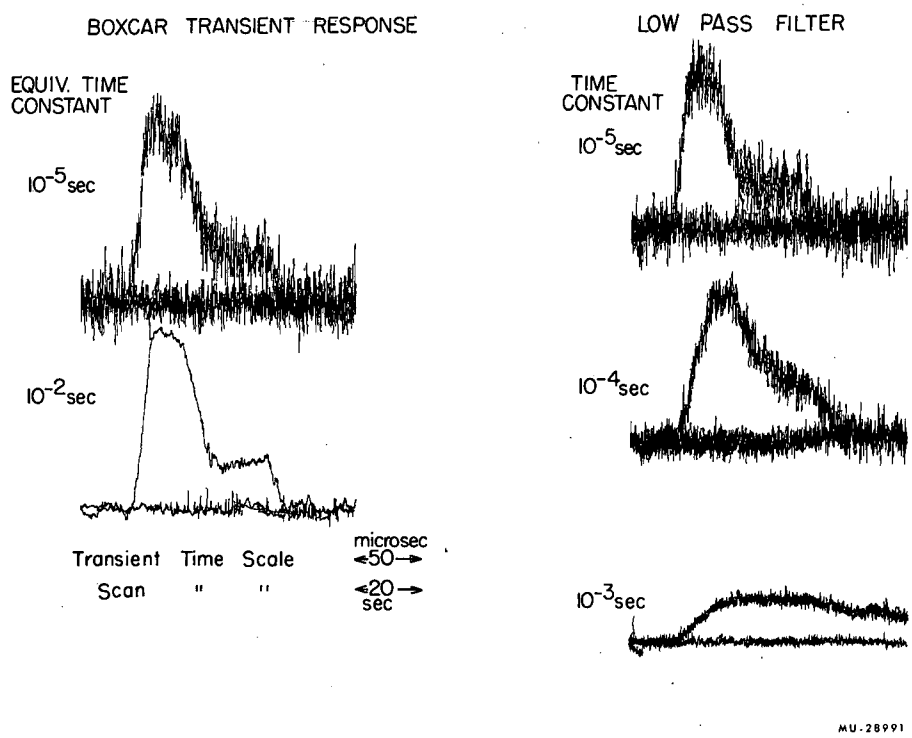

Fig. II-17. Comparison of the transient response of boxcar and low-pass filter. The signal is due to electrical pickup and is not a biological signal.

resistances also require the use of the electrometer tube. Trying to read the potential on the condenser with an oscilloscope or an ordinary vacuum tube voltmeter rapidly discharges the circuit.

The performance of the boxcar integrator has been quite satisfactory. Typical operating conditions are 10-μsec to 10-msec gate durations, 1 to 10 cps repetition rates, and storage times of 0.01 to 1 sec. Internal noise under these conditions is less than 1 mV. The peak-to-peak noise level from the incoming signal is 5 to 50 mV (with amplifier gains of 200) and corresponds to a change in absorbance of 5 to 50 ppm. The center of the noise (the signal detectability) can be read as closely as 1 ppm under optimum conditions.

C. Automatic Gain Control Circuit. It will be remembered that a small change in absorbance is determined by two measurements: the change in transmitted intensity and the absolute value of the transmitted intensity. If some means were available to maintain, automatically, a constant value of the transmitted intensity, then measurements of ΔI would lead directly to ΔA.

It proved much more convenient to manipulate the PMT output rather than the actual transmitted intensity, but this has no effect on the argument given above. A feedback circuit to maintain constant PMT output is shown in Figure II-18. The amplifier (tube 6DJ8) acts as a variable resistor. When the PMT signal tries to go more negative (greater transmission) the grid of the passing tube is forced negative and the tube conducts poorly, acting as a large dropping resistance which decreases the actual high voltage developed across the PMT. If the absorbance were to increase, the PMT tries to swing more positive, because of the gain the grid of the passing tube does go more positive,

AUTOMATIC GAIN CONTROL CIRCUIT

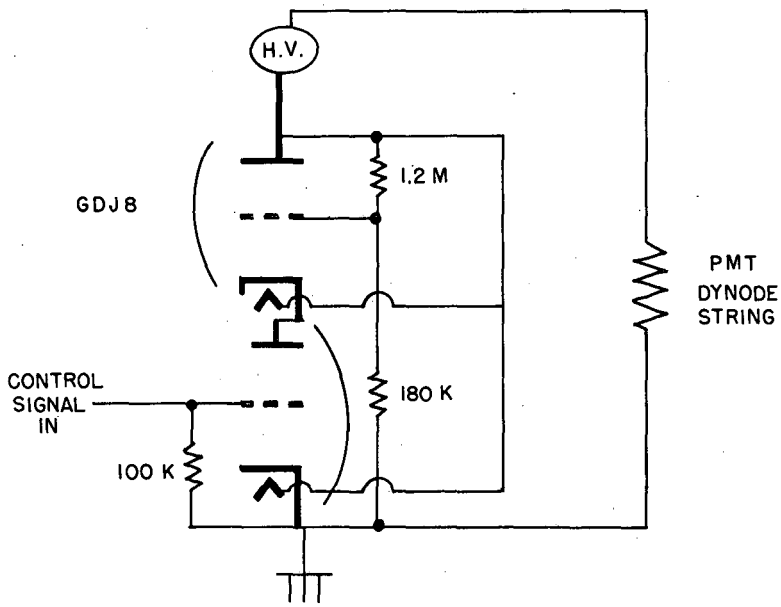

MU-35899

Fig. 18

which permits a higher voltage to be applied to the PMT. Such a circuit permits a constant PMT output (± 2%) for very wide changes in incident light and PMT sensitivity (factors of a thousand or more, depending on the gain in the feedback circuit). A low frequency cutoff filter can be used to prevent the feedback from suppressing fast signals.

The automatic gain control circuit worked satisfactorily for whole cell studies which normally involved fast response (about 0.01 seconds) photo signals. Our normal operating conditions did increase the noise in the spectrometer, probably from a low level, low frequency oscillation. However, the convenience involved in using the circuit far outweighed this loss of signal/noise ratio. Figure II-19 shows a spectrum run in 5 minutes with the automatic gain control circuit; compare it with Figure III-1, where the spectrum was taken in a point-by-point manner and took approximately 4 hours. To the best of our knowledge, the use of the AGC loop with the boxcar detection unit provides the first continually scanning spectrometer working at these sensitivity levels.

The expected advantages of the boxcar detection unit over the tuned voltmeter were in fact achieved. The following performance figures were normally available:

Transient response:	10^{-5} seconds (10^{-6} seconds with alternate pulse generators)
Averaging time constant:	10^{-4} seconds to 10 seconds (longer times were limited by drift in the apparatus)
Noise level (not scanning):	10^{-5} optical density units for a 1 second averaging time

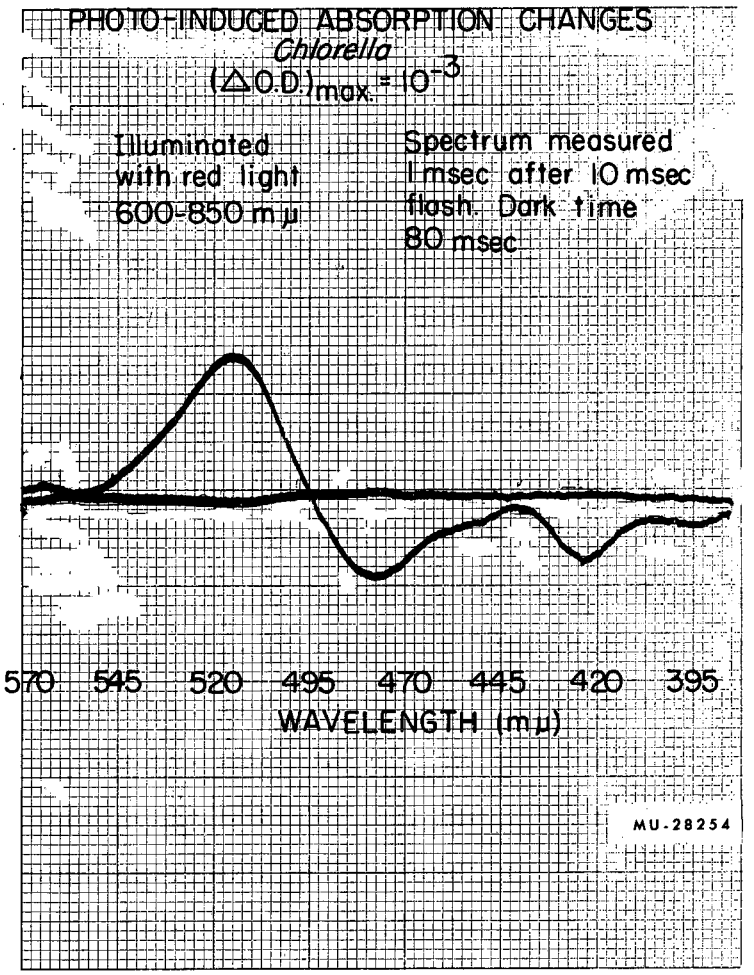

Fig. II-19. Light-dark spectrum, Chlorella cells, using boxcar circuit and AGC loop.

Noise level (scanning):	5×10^{-5} optical density units for a 0.3 second averaging time
Spectral scan rates:	1 mμ/second
AGC frequency response:	signals slower than 0.5 cps would be attenuated 50%

Of course the problem of signal polarity did not develop with this circuitry, which is directly coupled. Some success was achieved in separating fluorescence and scattered light from the signals of interest just by placing the sample gate 1 millisecond after the light went off, because the former had much faster response times. However, this technique was only useful for relatively small amounts of fluorescence (10 times the signal magnitudes or less). Larger amounts upset the control loop.

The major disadvantages in this instrument were: 1) it was relatively inefficient for obtaining kinetics because only one small interval of each signal was examined on a single repetition; 2) as mentioned above, the feedback control was only satisfactory for rapidly reversible signals. Many of the cell-free preparations had too slow a response time to permit use of the scan unit. Examples of the kinetic data obtained with this unit are shown in Figure II-20.

Digital Memory Instrument

A third detection system was set up to provide greater efficiency in obtaining kinetic information. We employed a digital memory and associated logic circuitry to provide on-line averaging. A few additional changes in the spectrometer assembly are also discussed below.

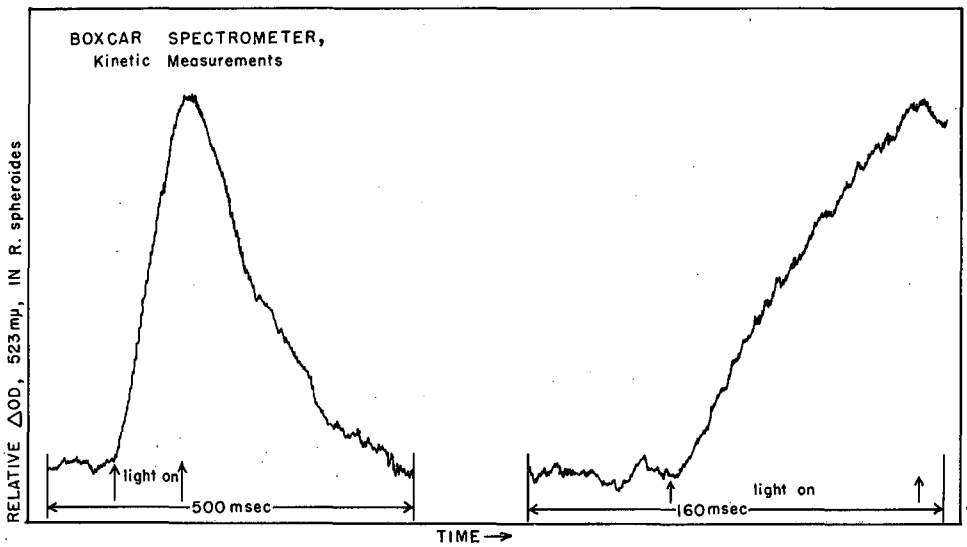

Fig. II-20. Rise and decay curves for the 523 mμ band in R. spheroides cells. Boxcar spectrometer with automatic scan.

A. Actinic lamp. After some experience with the biological materials of interest it became apparent that the intensity and wavelengths of the actinic light were just as important variables as the rise and decay times of the flash. Thus we looked into methods which would permit the modulation of conventional continuous sources. There are many types of light shutters but most had various problems associated with adaptation to our particular needs. Sector wheels were far too inflexible to meet the range of on and off times we needed. They also failed to provide a fast rise or decay time when used for slow transients. Kerr cells and pocket cells are not well suited to long flashes of light (0.1 to 10 seconds). Also, these units are not "fast" optically, requiring a fair degree of colimation, and, of course, two polarizers. Camera shutters had far too short a lifetime in our experimental situation.

Our solution to this problem was to adapt a stepping motor to act as a light shutter, following a suggestion of Dr. R. Ruby of our laboratory.

We modulated actinic light by means of a shutter (phosphor bronze) driven by a commercial stepping motor (Cedar Engineering, Minneapolis, Minn., Model SS-1100). This motor moves in 45° steps on application of a suitable trigger pulse. Transit times are 3 msec. The circuitry was arranged so that successive trigger pulses drove the motor alternately clockwise and counterclockwise. Thus the shutter first blocked the actinic light beam and then, on a trigger, it moved rapidly to an "open" position. A second trigger pulse restored the shutter to its

original closed position. Commercial pulse generators were used (Models 161 and 162, Tektronic, Beaverton, Oregon).

The shutter had 0.5-2.0 msec rise or decay times (depending on beam geometry and the driving current supplied to the motor). Jitter is less than 1 msec. The "light on" and "light off" times can be independently adjusted to have durations from a few milliseconds to indefinitely long. Because it has a small number of moving parts, the stepping motor should have a long life. It has been used for many thousands of operations without noticeable change in performance. The drive circuit is shown in Figure II-21. It was constructed locally, closely following the manufacturer's suggested circuit.

B. Detection system. Two new amplifiers gave additional gain and stability. The Philbrick (P65AH, Philbrick Research, Boston, Mass.) amplifier provides a gain of 10 and a dc bias control (Figure II-22). It is located within the sample compartment to minimize pickup problems. The Kintel amplifier provides additional gain (10 to 1000).

We used a commercially available multiscaler, the Computer of Average Transients, manufactured by Technical Measurements Corp., Pearl River, N. Y. The theory and operation of these instruments have been discussed in detail elsewhere.[40] They can record information of moderate frequencies (0-10 Kcps) with a very high dynamic range. For some applications they provide a convenient and powerful method of improving signal/noise ratios. The trigger circuits needed to synchronize the 400 channels of computer memory with the flashes of actinic light are shown in the next figure (II-23).

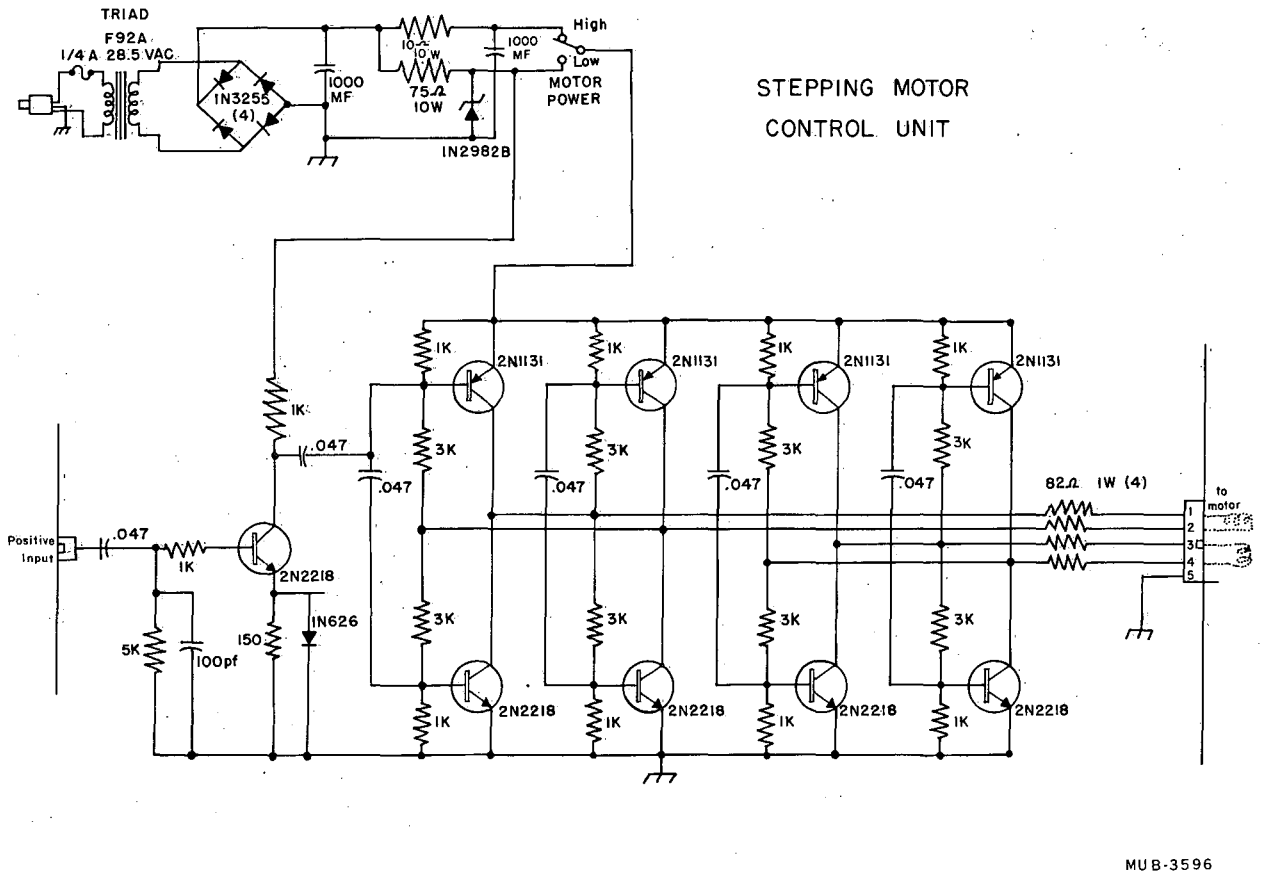

Fig. II-21. Stepping Motor Drive Circuit.

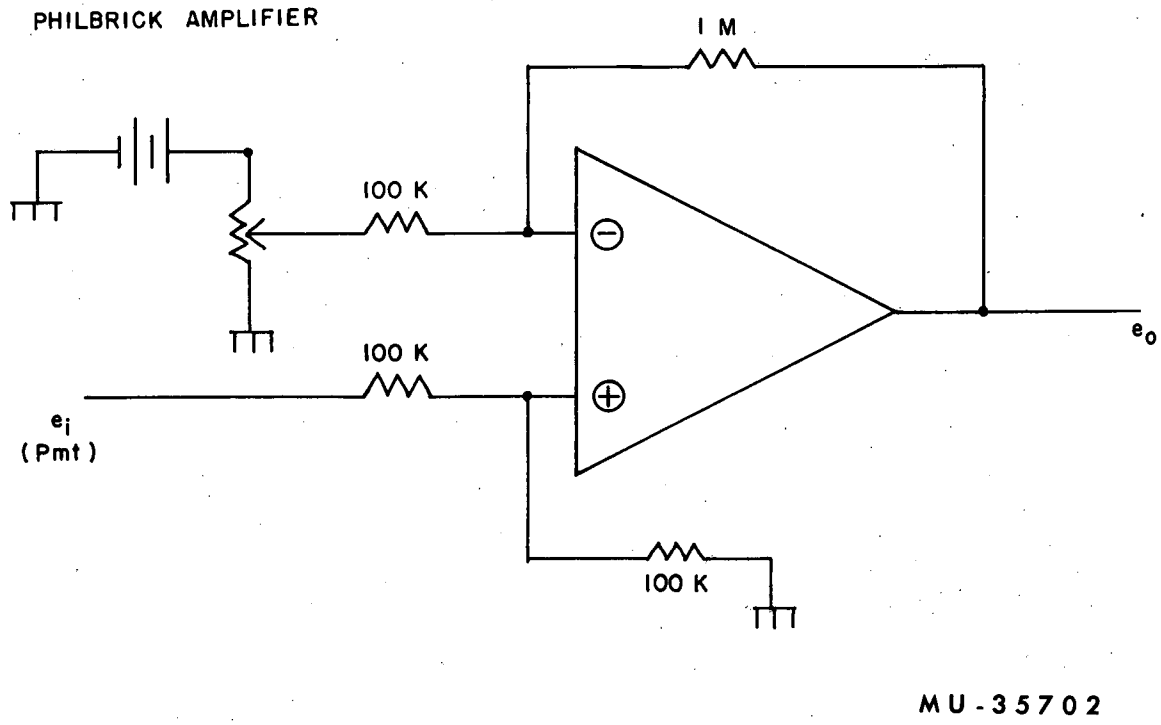

Fig. II-22. Philbrick amplifier and dc suppression circuit.

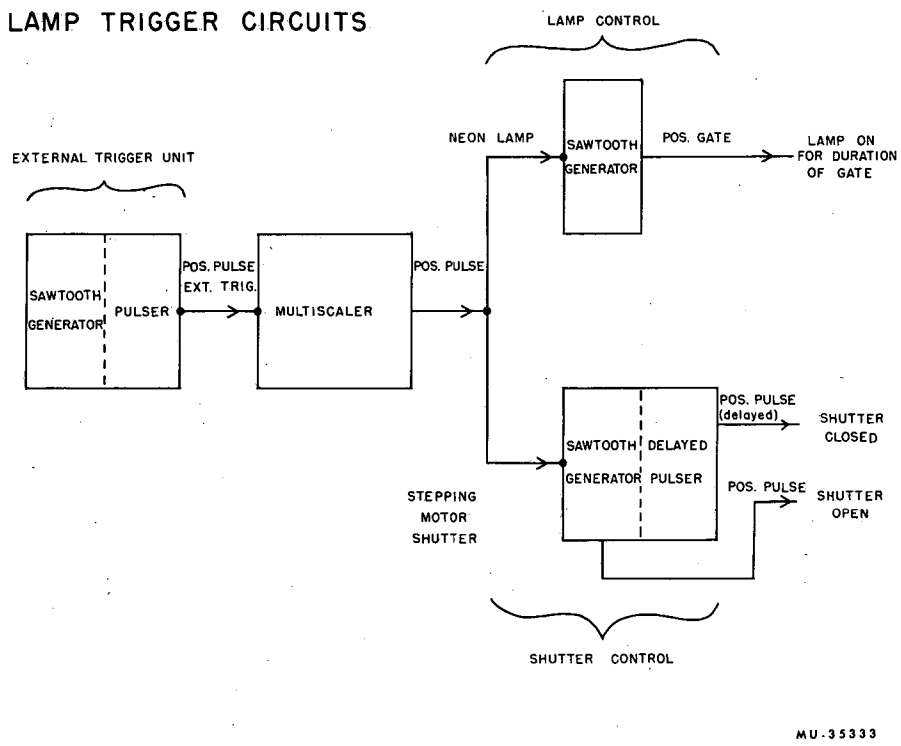

Fig. II-23. Lamp Trigger Circuits. The block diagram shows alternate paths for use of the neon lamp on the stepping motor shutter.

Performance

Transient response time:	10^{-4} seconds (but flash rise time only 10^{-3} seconds)
Averaging time:	up to a few thousand seconds, limited by the stability of the biological material
Noise level:	less than 10^{-5} optical density units for a 100 second real-time experiment. The theoretical factor of $(10)^{1/2}$ could be obtained for each power of ten increase in averaging time

Instrumentation in Other Laboratories

Several other laboratories have developed roughly equivalent instrumentation. The various types of instruments will be briefly discussed in this section.

1) Duysens and his associates have constructed a single-beam spectrometer. It follows the usual commercial design, chopping the detecting beam and then detecting the modulated signal with a tuned amplifier. The actinic beam is not modulated, but, of course, causes changes in the amount of modulated light transmitted by the sample when the photochemical reactions occur. The detecting beam can also be sent through a reference position which can be used to compensate for photomultiplier drift. Noise levels of 10^{-4} optical density units for 0.1 second response times are achieved. Conventional actinic sources and shutters are used.[10]

2) Chance has developed a similar instrument.[43] One important and unique feature of Chance's spectrometer is that two separate monochromators are used to provide two detecting beams of different wavelengths to monitor the absorbance of a single cuvette. One wavelength is selected as a "reference" wavelength. A tuned difference amplifier measures the changes in absorbance at the two different wavelengths. Although there are occasions when a stable reference wavelength is difficult to establish, this double-beam feature provides a simple and efficient method of compensating for both instrumental and sample "drifts". Response times up to 0.03 seconds are possible. The sensitivity is comparable to that of Duysens, 10^{-4} optical density units. A version of this instrument is now available commercially through Aminco (Cat. No. 4-8450, American Instrument Co., Silver Spring, Md.).

Witt and coworkers have utilized the flash photolysis approach. A single unmodulated monitor beam of relatively high intensity passes through the sample. A high intensity flash tube provides the actinic light (approximately 10^{22} quanta/second, duration 10^{-5} seconds). Absorbance signals are amplified and displayed on an oscilloscope. A frequently employed averaging technique is to take a multiple exposure of the results of several flashes. Instrument response time is faster than 10^{-5} seconds. The noise level is somewhat higher than most of the other instruments discussed, but it approaches 10^{-4} optical density units under favorable conditions.[44]

Kok's instrument is actually the closest to the one built at Berkeley. A sector wheel modulates the actinic source. Another rotating shutter blocks the monitor beam when the actinic light is on.

This eliminates interference from fluorescence and scattered light. After the actinic light is extinguished the monitor beam is restored and measurements can be performed within a millisecond after the flash. A tuned amplifier, adjustable RC filter, and a gating network are used to permit examination of different portions of the decay curve. Sensitivity is somewhat better than 10^{-4} optical density units, response time is as fast as 1 millisecond. Averaging times were 0.1-1.0 seconds.[45]

Recently Ke[46] has described a digital memory device used in conjunction with a Witt-type spectrometer. The specifications of such a unit are identical to the digital instrument we have built, except that Ke[47] has reported a somewhat higher noise level (2 to 5 times 10^{-5} optical density units for a 100 second experiment).

Summary

We have considered at some length a variety of high-sensitivity, low-resolution, rapid-response spectrometers. Most operate at the limit of performance as determined by the intensity of the detection beam and the quantum efficiency of the PMT. The only way to improve performance, when operating at these limits, is through some form of averaging procedure. We have discussed three averaging techniques: RC filters, digital memories, and multiple exposure photographs. There are many other methods such as magnetic tape, hand calculations, and computer calculations. Generally speaking, the digital method has two advantages over the other common techniques. First, it has a very wide dynamic range; second, it permits the reduction of 1/f noise. Its major disadvantage with respect to capacitors or photographic film is the limited

response time currently available. For most of the experiments described here the digital equipment has proved a superior approach. It has provided a 2 to 20-fold gain in sensitivity over that obtained in other laboratories. This margin of performance has made possible many of the kinetic measurements to be described.

Chapter III. ABSORPTION SPECTRA OF PHOTOSYNTHETIC INTERMEDIATES AND REVIEW OF PHOTOSYNTHETIC MECHANISMS

The purpose of our experiments was to study and hopefully elucidate the mechanism of the quantum conversion and electron transport reactions of photosynthesis. Needless to say, a large body of experiments and theories have been published in this field. No attempt will be made to review this work in its entirety. Instead we will consider those points which appear to be most directly pertinent to the experiments conducted in this laboratory.

Theories usually start from a central core of fact, and the facts at the heart of the presently accepted theories of photosynthesis are a collection of light-minus-dark difference spectra which are thought to show the reactive intermediates in the quantum conversion and electron transport processes. In this chapter we will first examine these spectra and discuss the identification of the various absorption bands. Then we shall consider the reactions in which these compounds might participate.

Figures III-1 to III-14 are a representative collection of difference spectra of photosynthetic organisms and subcellular preparations. Where possible absorption spectra are presented as well. Table I serves as an index to these figures.

Table I

Figure No.	Organism	State	Type of Organism	Reference for difference spectrum
III-1	*Chlorella*	cells	green alga	48
III-2	*Scenedesmus*	cells	green alga	50
III-3	*Porphyridium*	cells	red alga	48
III-4	*Anacystis*	cells	blue-green alga	51
III-5	*Ochromonas*	cells	brown alga	52
III-6	*Nitzchia*	cells	diatom	50
III-7	*Spinacea*	chloroplasts	higher plant	50,53a
III-8	*R. rubrum*	chromatophores	bacterium	31
III-9	*R. rubrum*	cells	bacterium	53,10
III-10	*R. spheroides*	chromatophores	bacterium	31
III-11	*R. spheroides*	cells	bacterium	53,54
III-12	*R. spheroides* carotenoid-less mutant	chromatophores	bacterium	30
III-13	*Chromatium*	chromatophores	bacterium	31
III-14	*R. vaneii*	cells	bacterium	55

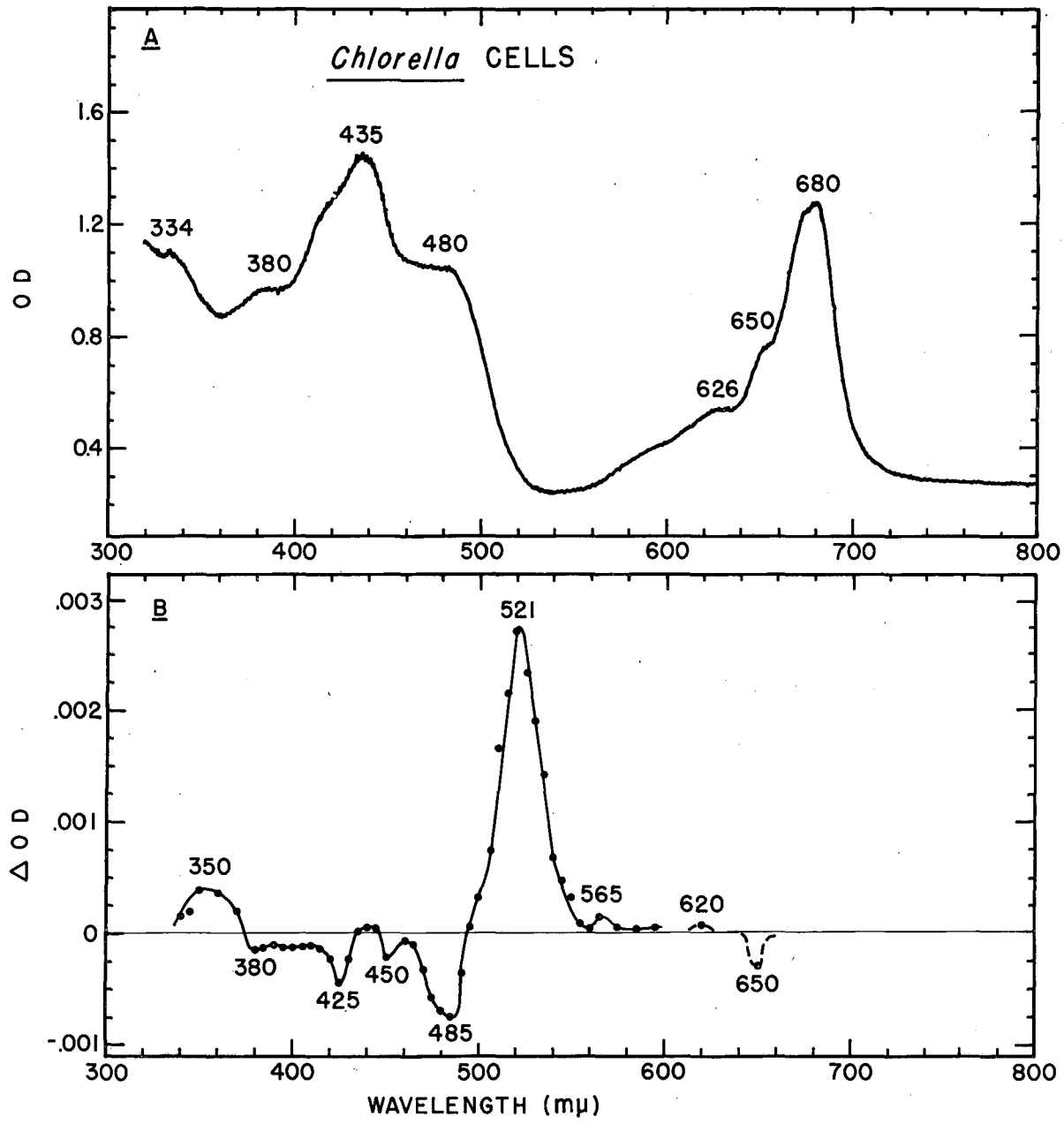

Fig. III-1. Absorption and light-minus-dark difference spectra for Chlorella.

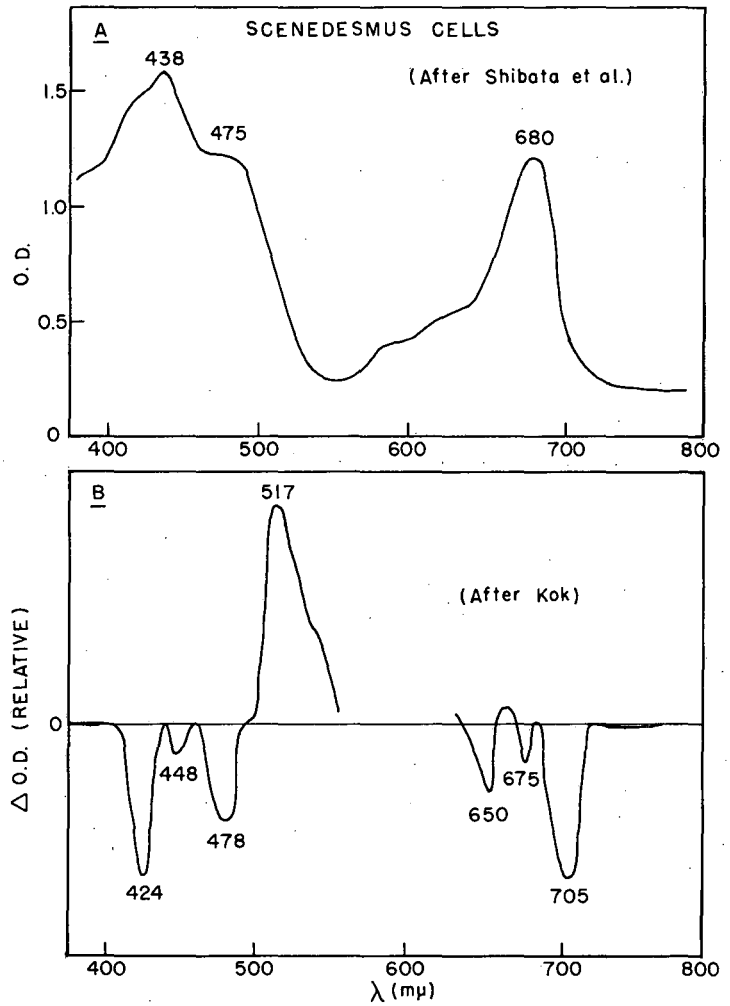

Fig. III-2. Absorption and light-minus-dark difference spectra for Scenedesmus.

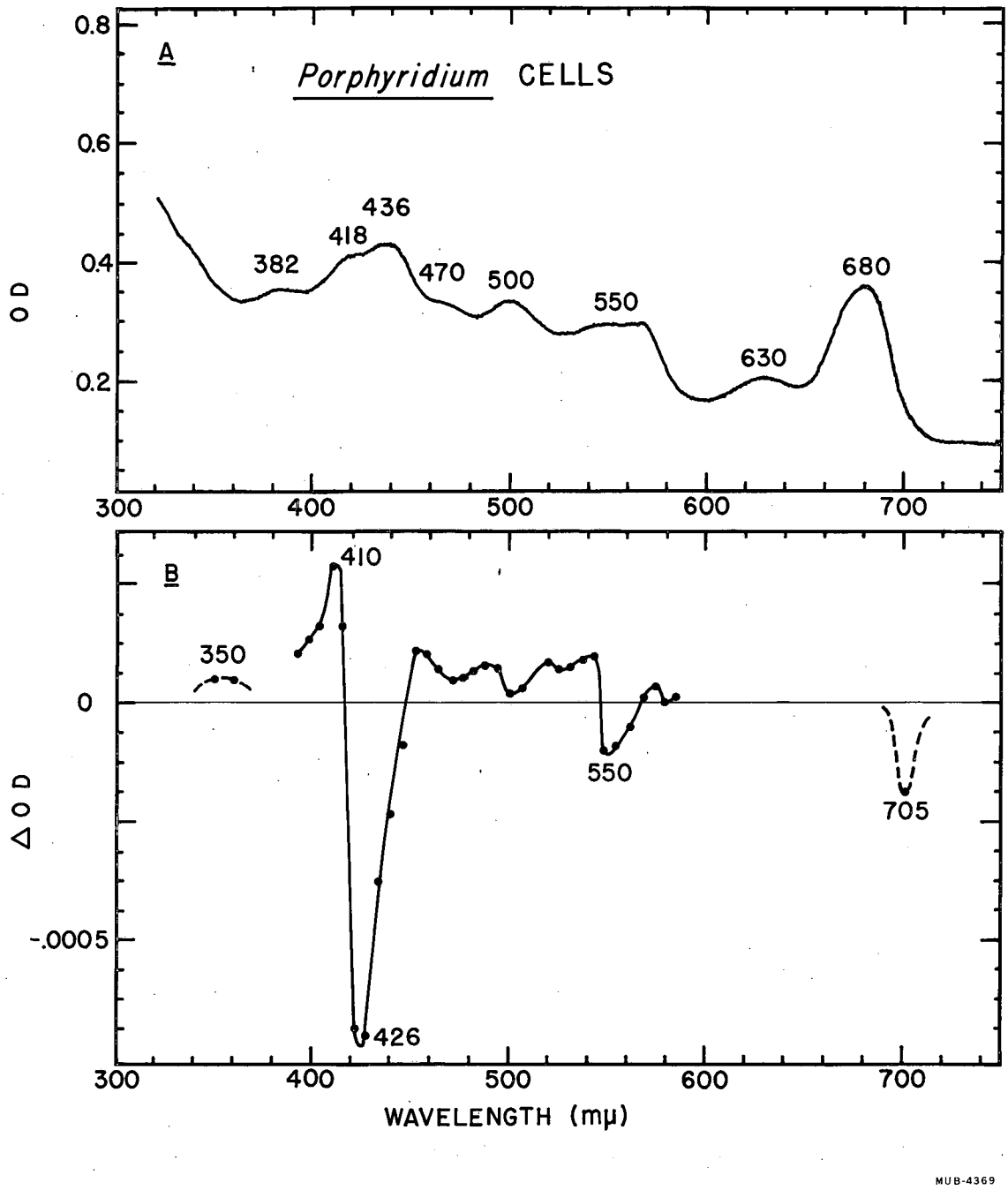

Fig. III-3. Absorption and light-minus-dark difference spectra for Porphyridium cruentum.

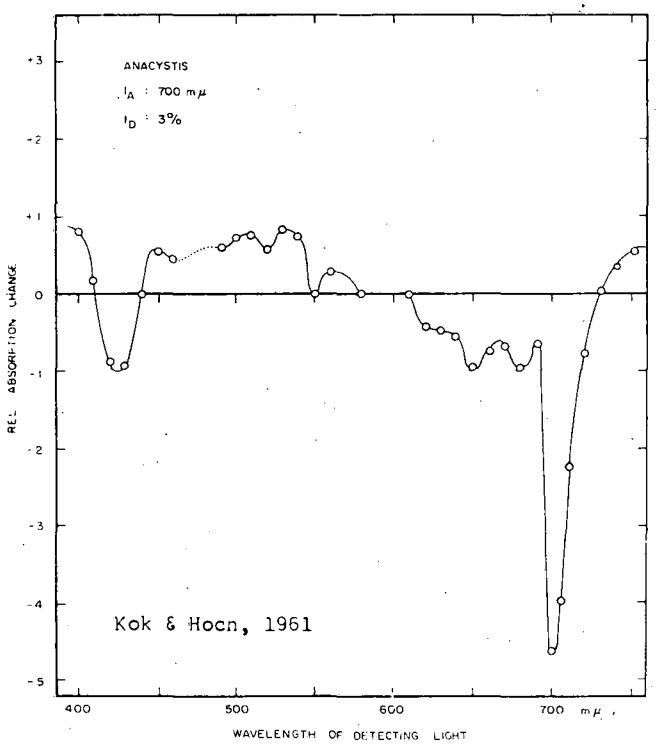

MU-28353

Fig. III-4. Light-minus-dark difference spectrum for Anacystis.

450 500 550

λ (mμ)

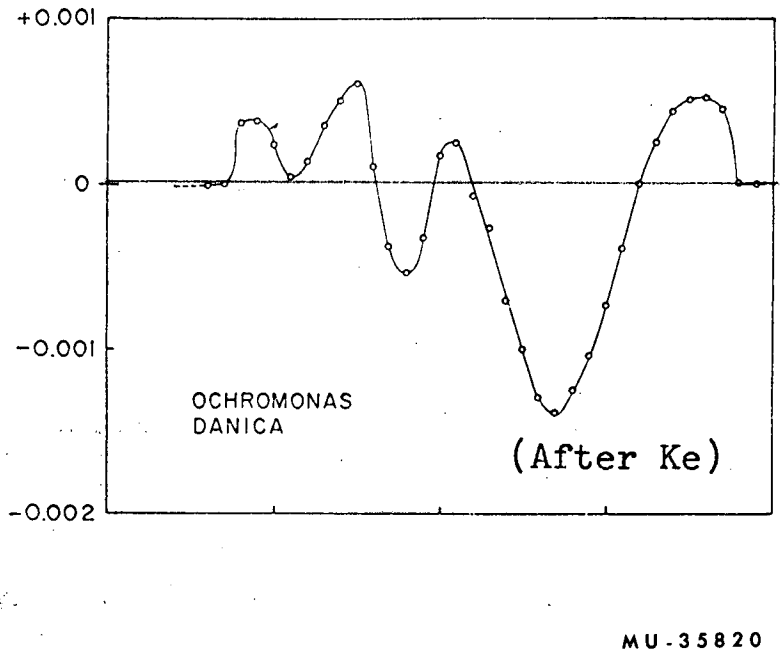

Fig. III-5. Light-minus-dark difference spectrum for Ochromonas danica.

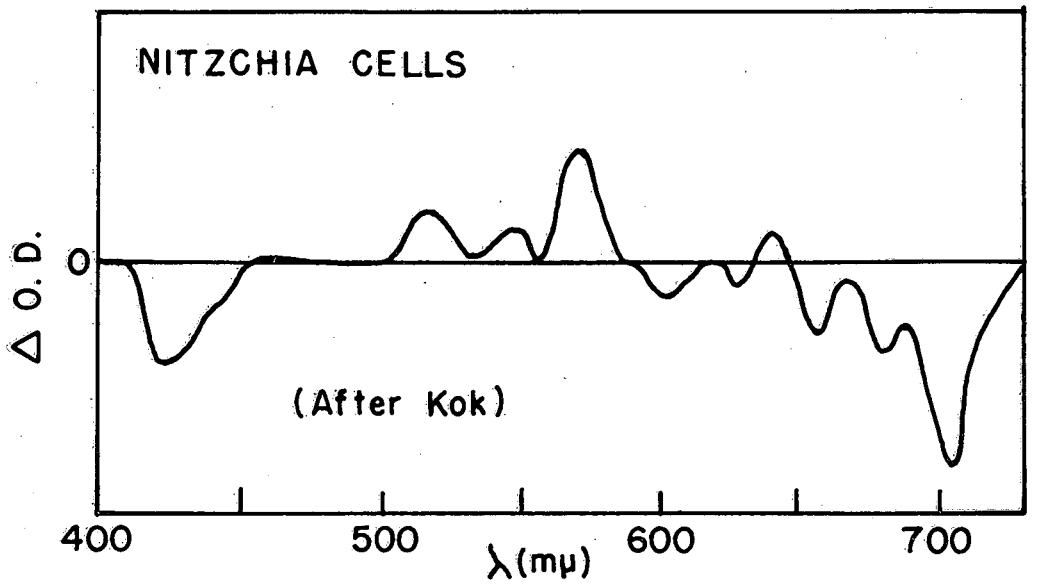

MU-35805

Fig. III-6. Light-minus-dark difference spectrum for Nitzchia.

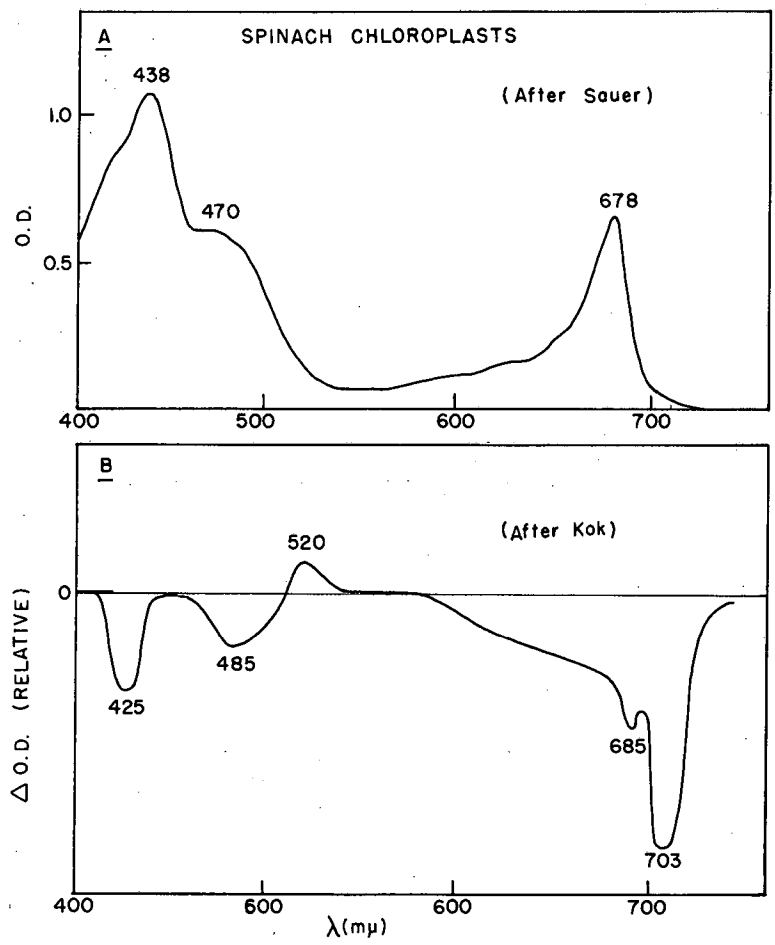

MU-35763

Fig. III-7. Absorption and light-minus-dark difference spectra for spinach chloroplasts. The difference spectra for chloroplasts are extremely sensitive to pretreatment.[50]

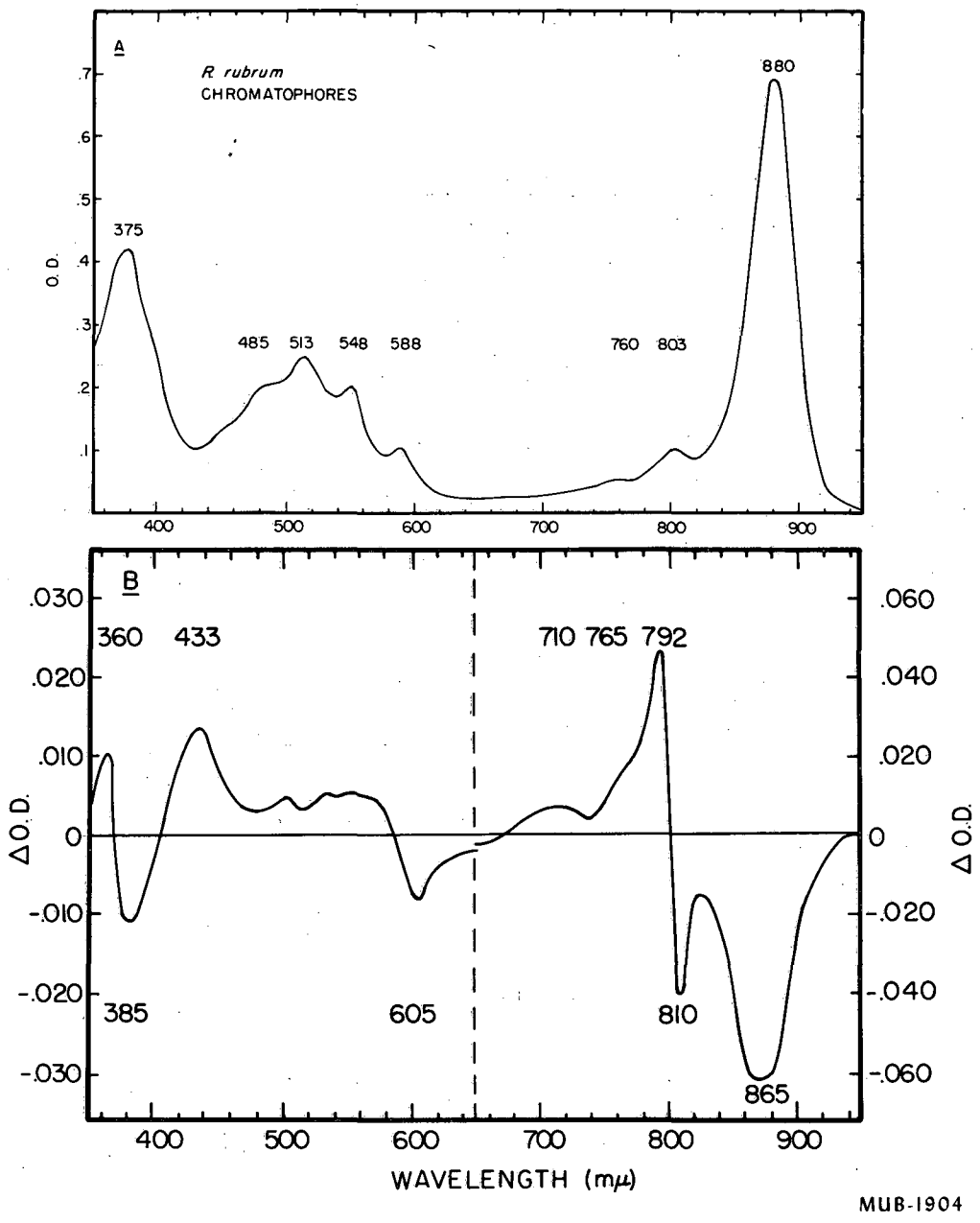

Fig. III-8. Absorption and light-minus-dark difference spectra for R. rubrum chromatophores.

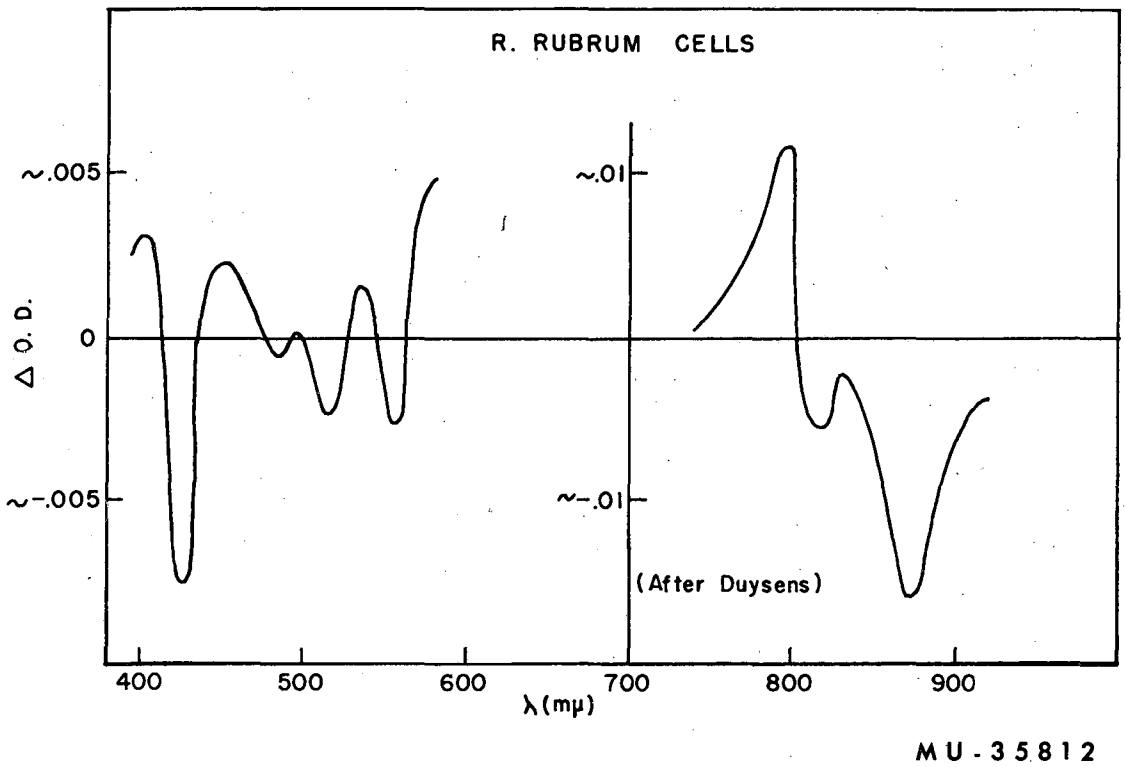

Fig. III-9. Light-minus-dark difference spectrum for R. rubrum cells. The absorption spectrum would be essentially the same as that of III-8A.

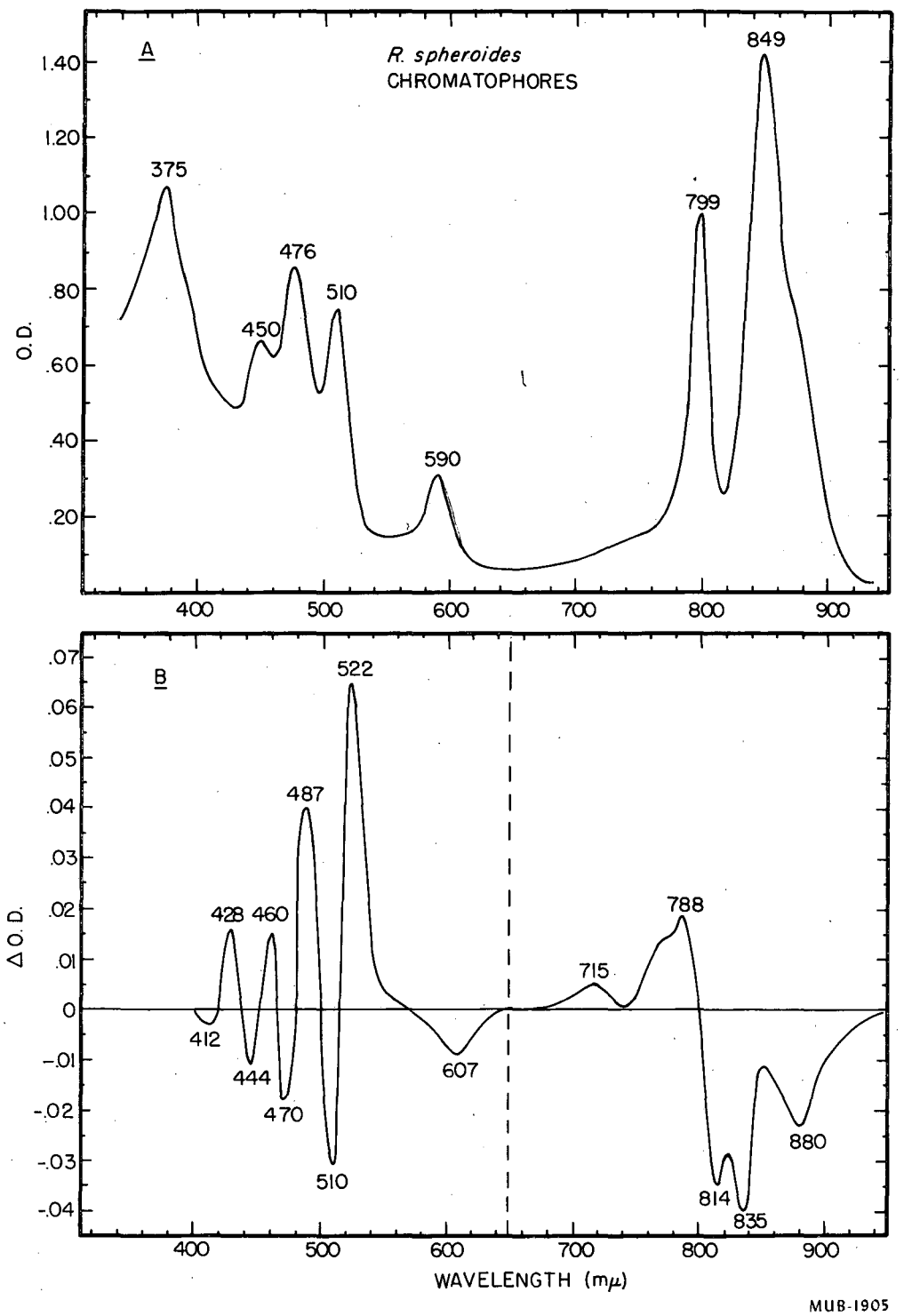

Fig. III-10. Absorption and light-minus-dark difference spectra for R. spheroides chromatophores.

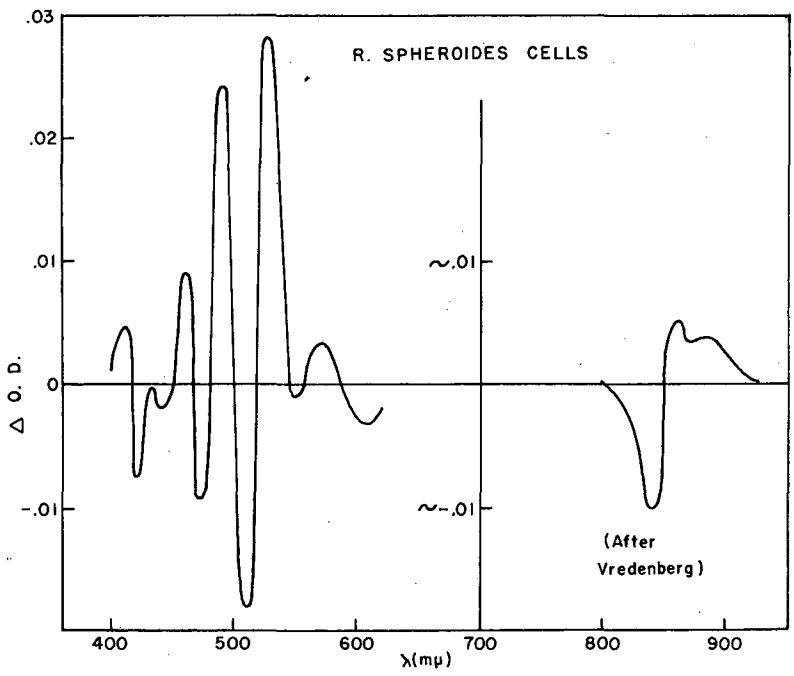

Fig. III-11. Light-minus-dark difference spectrum for R. spheroides cells. The absorption spectrum would be essentially the same as that of III-10A.

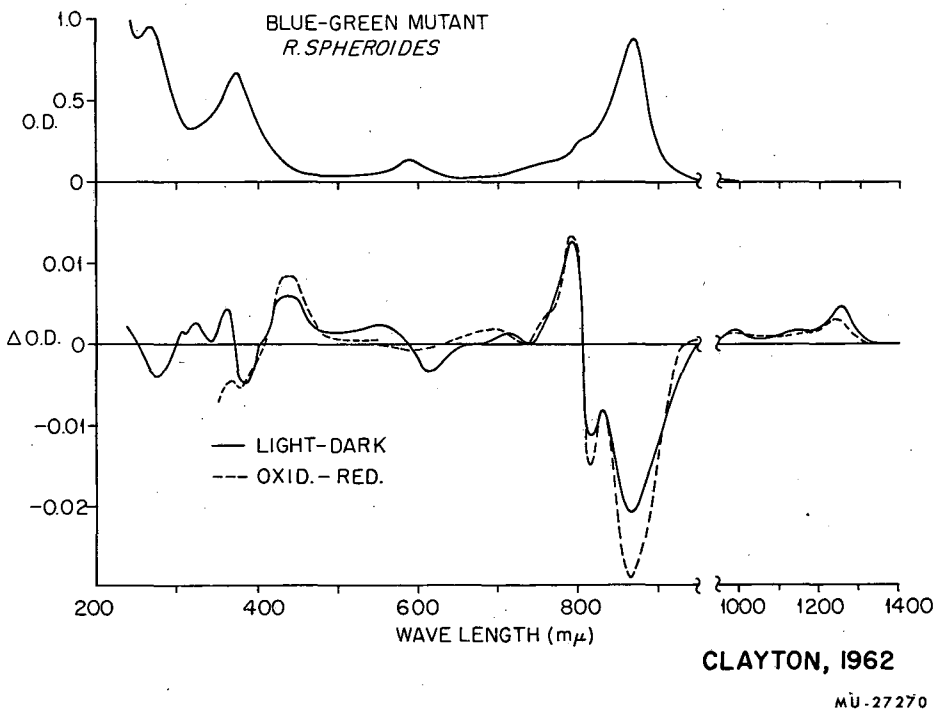

Fig. III-12. Absorption and light-minus-dark difference spectra for the chromatophores of the blue-green mutant of R. spheroides.

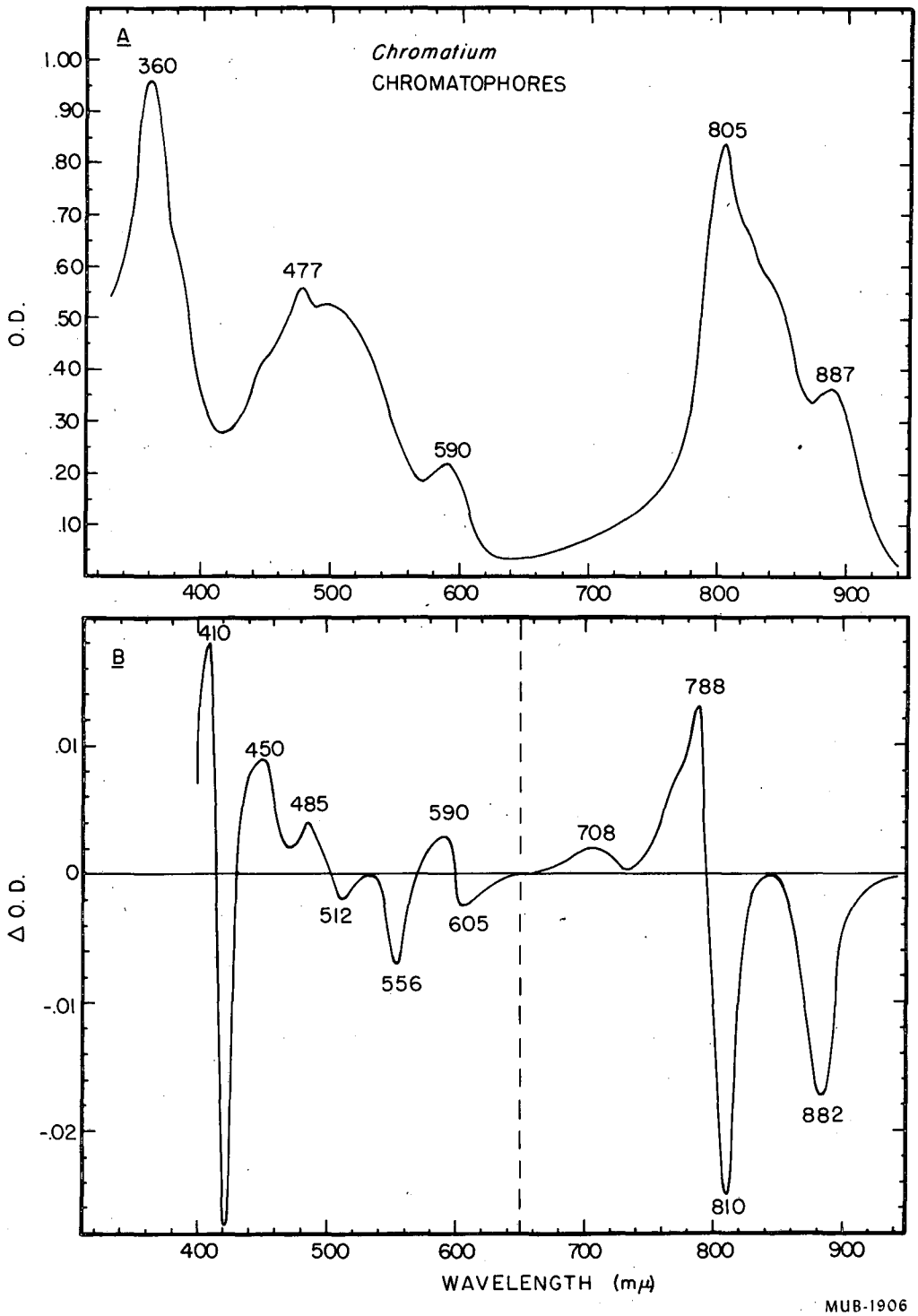

Fig. III-13. Absorption and light-minus-dark difference spectra for Chromatium chromatophores.

400 500 600

λ (mμ)

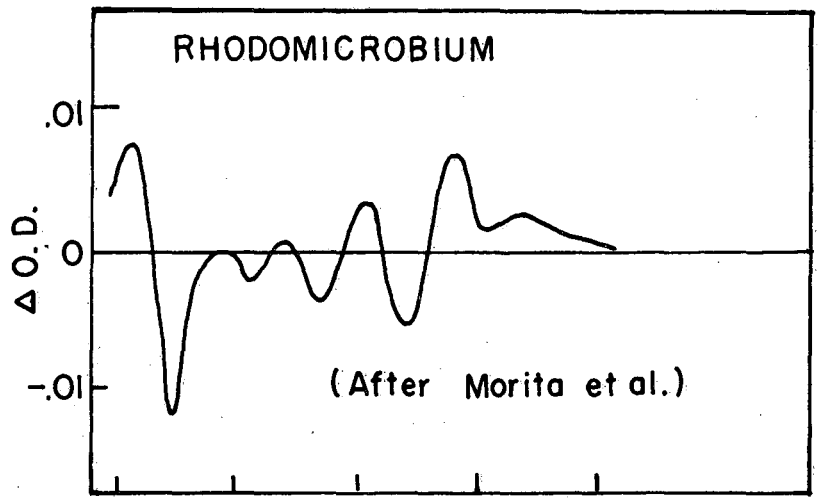

MU-35822

Fig. III-14. Light-dark difference spectra for Rhodomicrobium vaneii.

The most striking feature of the spectra just presented is their diversity. Some use can be made of this wealth of spectral information. The usual assumption one must make is that the in vivo spectra can be related in a reasonably straightforward fashion to the in vitro spectra of isolated chromophores. An implicit and more subtle assumption is that the very small amounts of the photoactive pigments have the same molecular structures as the spectroscopically similar compounds which are actually isolatable from the living material. Of course, assumptions of this type are not rigorously correct. The most common difficulties occur when the in vivo spectra are strongly perturbed from the "model" spectra, as, for example, by the binding of chromophore to a protein molecule. The question of small structural differences is also difficult to settle by spectra alone. Bacteriochlorophyll provides good examples of both of these problems. A quick glance at the large number of peaks in the 750-1000 mμ region of the bacterial spectra shows no close correspondence with the spectrum for bacteriochlorophyll in solution (Figures III-8A, 10A, 12A, compared to Figure III-20). And even if a small photoactive band were observed in this region, one can only speculate that the active chromophore is indeed structurally identical bacteriochlorophyll. Clearly, the assignments suggested by the difference spectra must be confirmed by other types of experiment.

With these difficulties in mind, we can proceed to the assignments of the compounds involved in the light-minus-dark spectra. Our interest will be a critical but not exhaustive survey of the proposed identities of the light-dark bands. Heavy emphasis will be placed on observations made in this laboratory, but strongly dissenting opinions or evidence

will certainly be noted. The following outline will be used for the various compounds of interest:

1) Structural formulas of the chromophore; 2) *in vitro* spectra of the isolated chromophore, or, if possible, of an isolated and purified protein-chromophore complex; 3) *in vivo* spectra; 4) spectra of pertinent chemically or photochemically produced derivatives; and 5) interpretations and conclusions.

Cytochrome-type Molecules

The structure of the heme portion of cytochrome c and its binding to the protein moiety are known (Figure III-15).[56] A wide variety of cytochrome spectra are available. The "pure" protein-chromophore complexes of some cytochromes are commercially obtainable. Figure III-16 shows the visible and UV spectrum of cytochrome c.[57] Spectra of the protein complexes are in good agreement with the *in vivo* spectra obtained from relatively unpigmented materials such as mitochondria and etiolated plant leaves.[58,59] Cytochromes readily undergo one-electron redox reactions with the iron atom commonly changing between +2 and +3. Oxidized-minus-reduced difference spectra have been measured and ordinarily show a characteristic four-line spectrum in the visible region (Figure III-17).[60] This distinctive pattern plus the high molar extinction coefficients make possible the detection and identification of cytochrome-type molecules. A more difficult question is to determine which type of cytochrome is involved. This can be answered from both spectral and redox considerations. The two most common cytochromes known to be present in photosynthetic tissue are a "b" type with absorption maxima

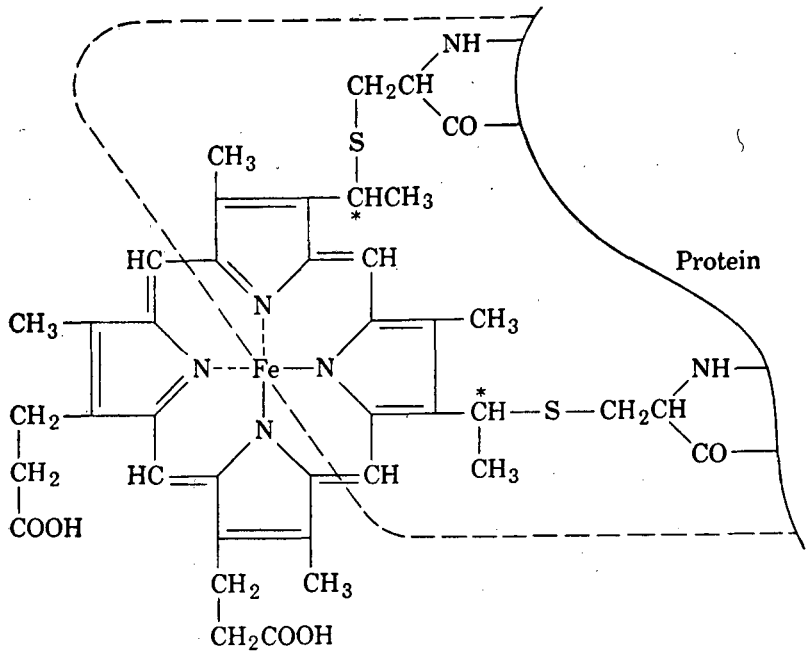

Cytochrome c

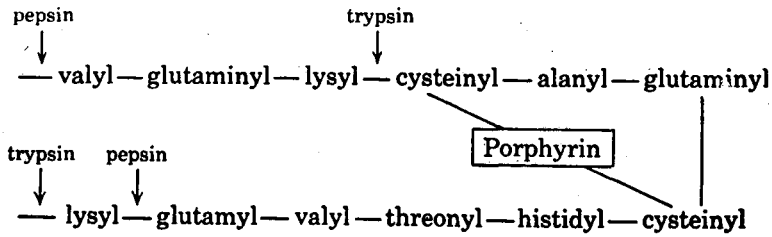

Probable amino acid sequence in beef cytochrome c **(Fruton and Simmonds)**

MUB-6794

Fig. III-15. Structure of heme group and the probable binding of the heme to the protein moiety for cytochrome c.

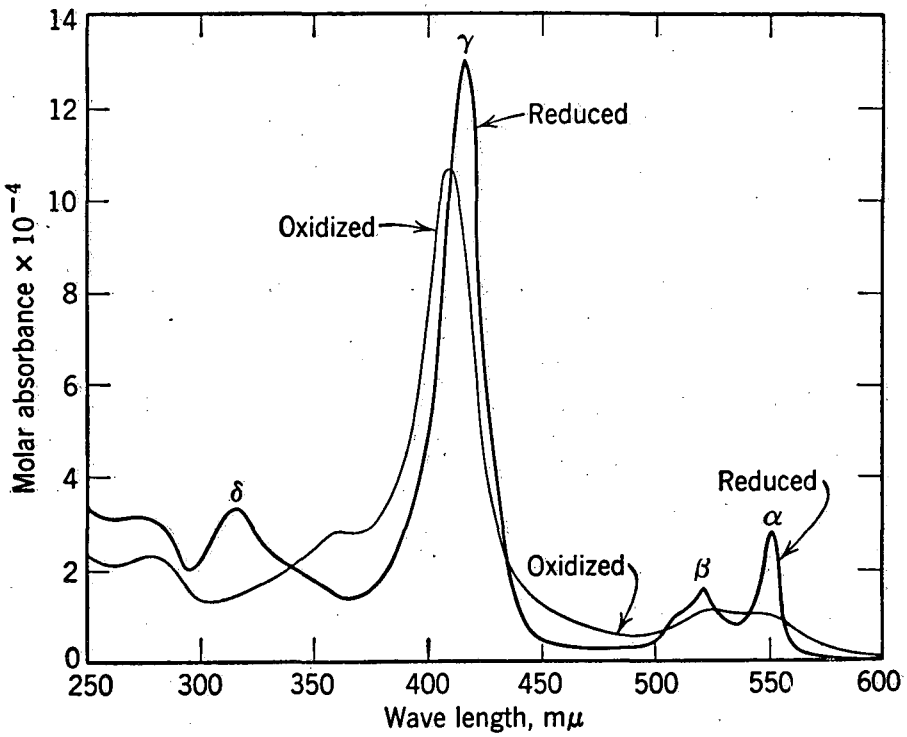

Absorption spectra of oxidized and of reduced cytochrome c from horse heart; this preparation contained 0.45 per cent iron. [From D. Keilin and E. C. Slater, *Brit. Med. Bull.*, **9**, 89 (1953).]

MUB-6793

Fig. 16

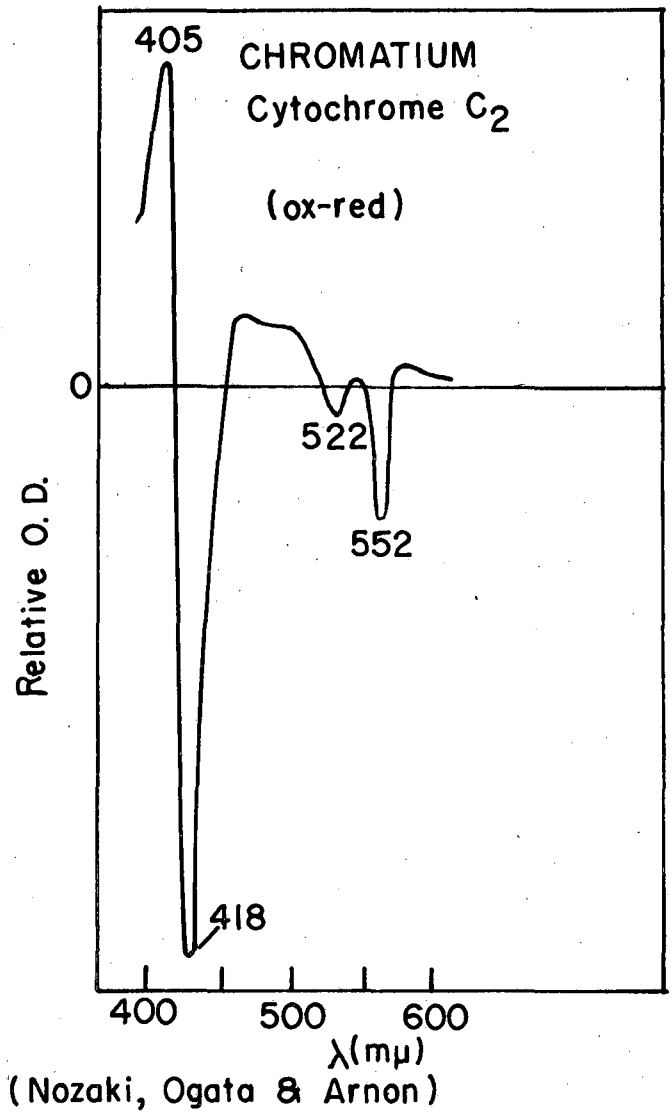

Fig. III-17. Difference spectrum for oxidized-minus-reduced cytochrome c.

at 420-425, 525-530, and 555-565 mμ, and a midpoint potential of approximately 0.00 volts and a "c" or "f" type which absorbs at 415-425, 520-525, and 550-555 mμ, and has a high potential (ca. 0.4 volts). A summary of typical cytochrome absorption bands is given in Table II.

Participation of cytochrome molecules in the light-dark difference spectra is easily detected in Figures III-3, 4, 9, 13, 14. The close correspondence strongly suggests that the cytochromes are undergoing reversible photo-oxidation. Two sidelights of the role of cytochromes in photosynthesis are pertinent here. Kamen has frequently proposed a "ferryl" form of cytochrome with the iron in a +4 oxidation state.[64,65] The spectrum of such a compound is not readily available.

Some isolated cases of cytochrome photoreduction have been reported,[66,67] although there is no clear-cut indication of this type of reaction in the spectra we have collected.

Chlorophyll-type Molecules

The structures of chlorophyll a, chlorophyll b, and bacteriochlorophyll are shown in Figures III-18 and 19. The spectra of the various chlorophylls in organic solvents are shown in Figure III-20.[68] The visible transitions are quite solvent sensitive.[69] Chlorophyll-protein complexes have been prepared, and their spectra show considerably perturbed, red-shifted maxima.[70] The long-wavelength transition is particularly sensitive. The maximum of the red band in acetone is 20 mμ from that in living tissue. The bacteriochlorophyll transition is shifted over 100 mμ. The chlorophyll-protein complex appears to afford a good model for *in vivo* absorbances. Other data comes from the "carotenoidless" mutants of various algae and bacteria. In fact, the chlorophyll a

Table II

Cytochrome Bands

Type	Oxidized bands			Reduced bands			Ref.
	Soret	β	α	Soret	β	α	
a	422-3	540	597	443.5	517	603	62
b	418	545		429	532	562	63
b*	412	530	560	421	525	556	61
b_6**				429	537	563	58
c*	410	530		416	522	552	61
f**				422	524	563	58

*Euglena **Higher plants

Table III

Approximate Chlorophyll Absorption *in vivo*

Chl a	390(sh)	434		625(sh)		678
Chl b		(480)?				650
EChl		375	590	800	850(sh)	880-890

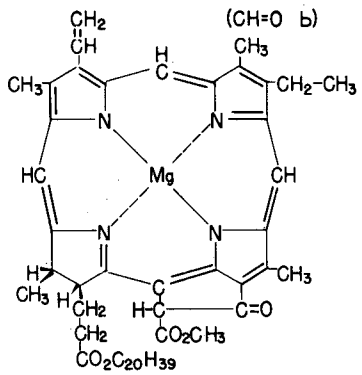

CHLOROPHYLL a (b)

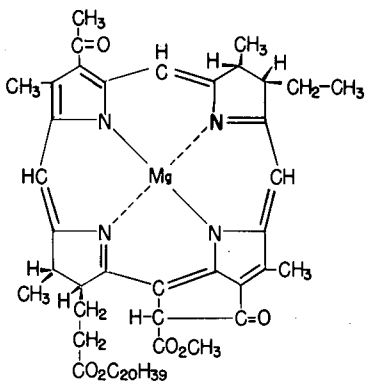

BACTERIOCHLOROPHYLL

MU-35767

Fig. III-18. Structures of Chlorophyll a, Chlorophyll b, and bacteriochlorophyll.

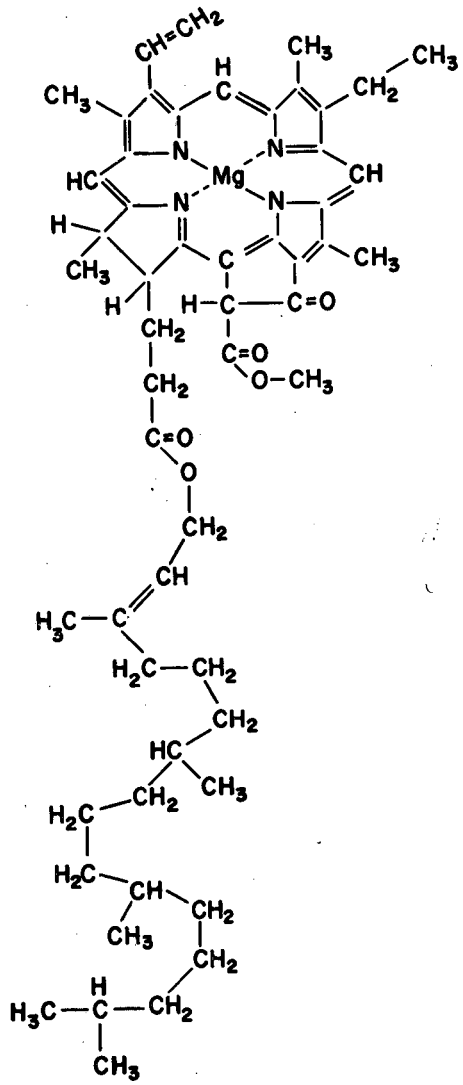

Fig. III-19. Structure of Chlorophyll a showing the extended phytol chain.

CHLOROPHYLL AND PHEOPHYTIN SPECTRA

(Smith and Benitez)

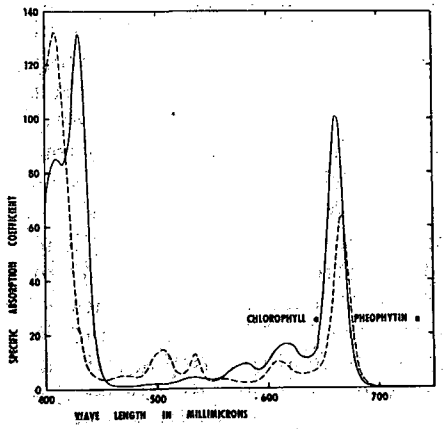

Absorption spectra of chlorophyll *a* and pheophytin *a* in ether.

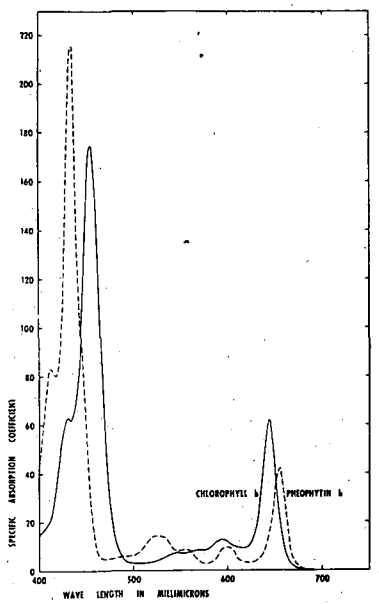

The absorption spectra of chlorophyll *b* and pheophytin *b* in ether.

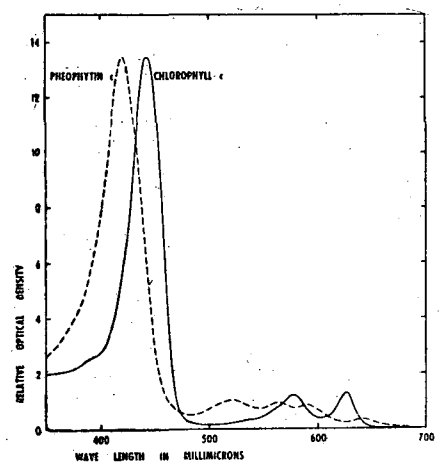

The absorption spectra of chlorophyll *c* and pheophytin *c* in ether.

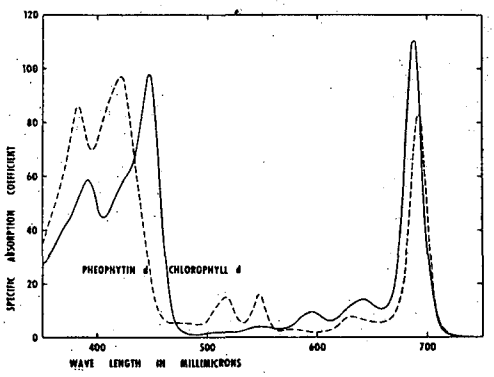

The absorption spectra of chlorophyll *d* and pheophytin *d* in ether. (Molecular weight assumed for chlorophyll *d*, 893.48.)

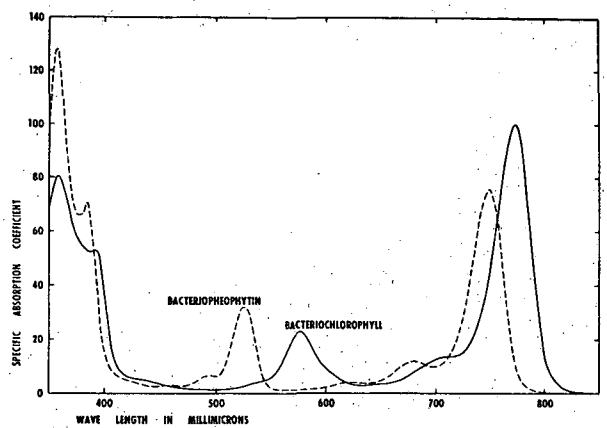

The absorption spectra of bacteriochlorophyll and bacteriopheophytin in ether.

Fig. III-20. Absorption spectra of various chlorophylls in ether. The spectra of the respective pheophytins (Mg^{++} removed) are also shown.

absorption is so intense that it even dominates the spectrum on normally pigmented cells in the 430 and red regions. Thus, assignment of most of the *in vivo* absorption maxima can be done with some confidence (Table III).

A considerable body of data is now available on the oxidation and reduction properties of chlorophyll in organic solvents. Also the absorption of the lowest triplet has been measured. Representative spectra are given in Figure III-21.[9,71,72] Figure III-22 contains the calculated difference spectra for these reactions if they proceed from the normal chlorophyll ground state absorption as a starting point. Of course the prediction of *in vivo* spectral features from these figures is a highly speculative business.

Inspection of the light-dark spectra shows, in each case, loss of absorption in the major red and blue chlorophyll absorption bands of bacteriochlorophyll and chlorophyll *a*. Speaking broadly, there have been no conclusive identifications of *increases* in absorbance which have been shown to be related to these absorption decreases. (However, see Ref. 30.) Whether the positive bands for the triplet or reduced forms would be seen is a difficult question. That the 430 and 700 mμ bands are due to a singlet → triplet conversion is normally discounted because the lifetime observed for it in chlorophyll solutions is much shorter (10^{-4} to 10^{-5} seconds)[9] than that observed for the absorbance transients (10^{-2} seconds). The choice between chlorophyll oxidation or chlorophyll reduction has been based on redox experiments, some of which were performed in this laboratory. They will be described in detail in a later chapter. The strongest conclusion we draw from the spectral evidence above is that chlorophyll *a* and bacteriochlorophyll

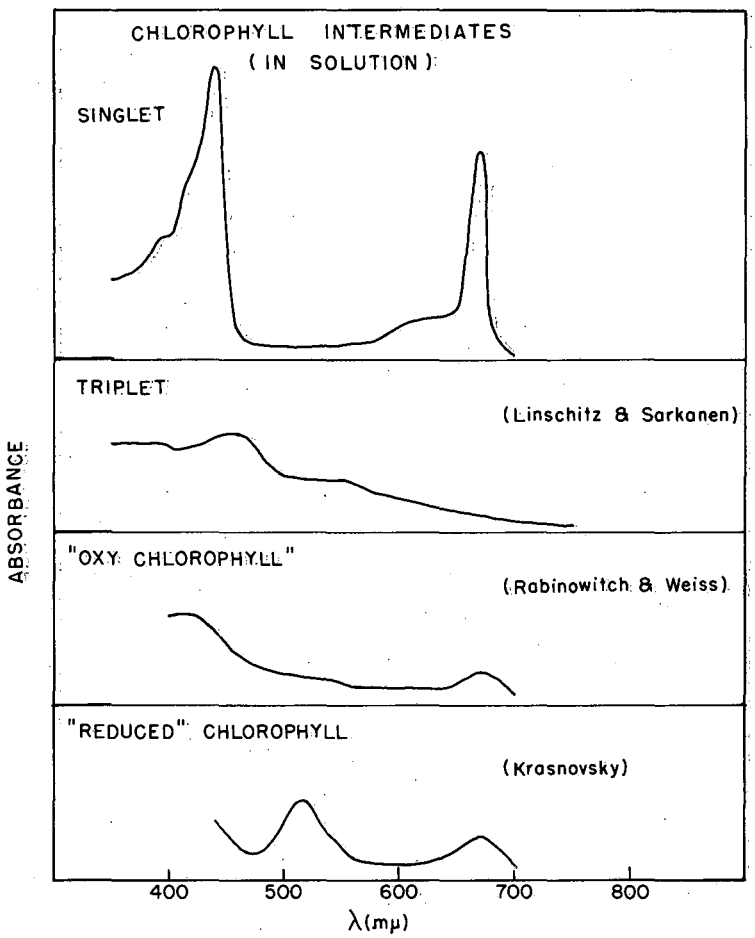

Fig. III-21. Absorption spectra of chlorophyll derivatives of interest. The "oxy chlorophyll" and "reduced" chlorophyll are not well-characterized compounds.

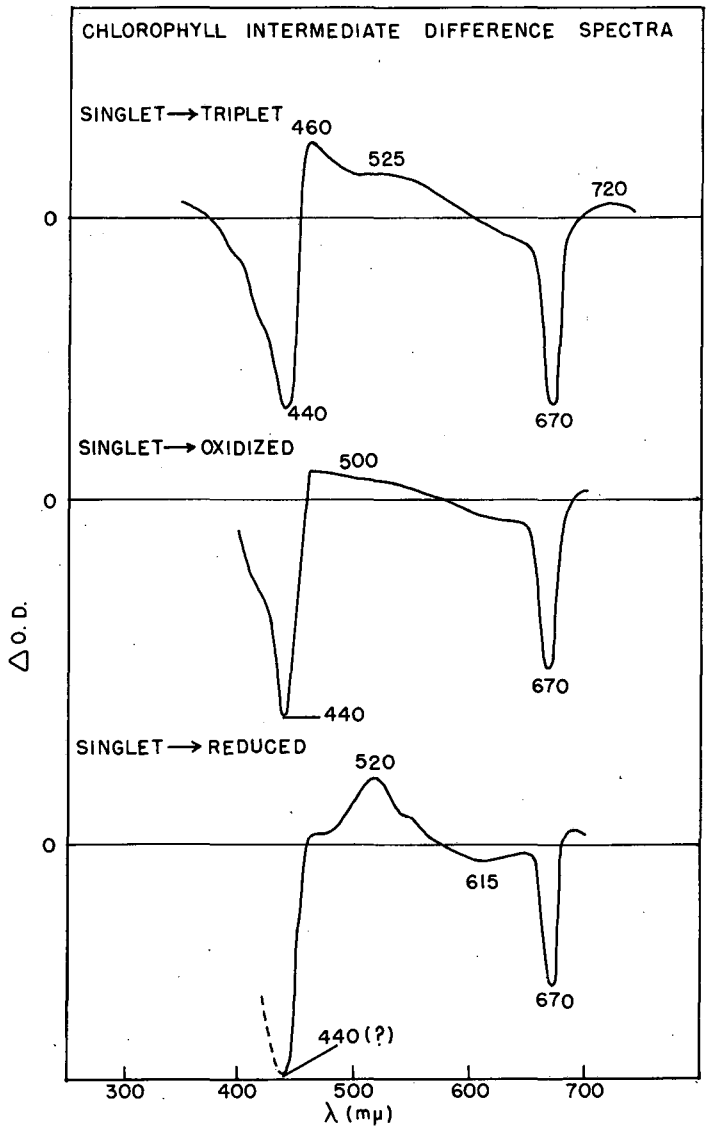

Fig. III-22. Difference spectra for "Intermediate" minus chlorophyll ground state. Calculated from data in Fig. III-21.

are photochemically active and are transformed by light into a weakly absorbing form.

"Minor" Chlorophyll Reactions

Several bands in the bacterial systems and a few in the green systems can also be tentatively ascribed to chlorophyll reactions. In particular, the bands at 260, 605, 765, 792 and 810 mμ, in Figures II-8, 10, 13, and at 380, 620, and 650 mμ, in Figures II-1 or 2, probably arise from some reactions of bacteriochlorophyll and chlorophyll a or chlorophyll b respectively. Notice that many of these bands show a characteristic positive, negative pattern (increased absorbance at the shorter wavelength) which suggests a slight blue shift of the absorption bands. This suggestion is supported by direct absorption measurements in the 800 mμ region for R. rubrum chromatophores.[73]

The interpretation of these shifts is not easy. Let us assume that these difference bands do arise from chlorophyll.* It is thought that the multiplicity of absorption bands in the near infrared (Figures II-8, 10, 12, 13) are due to bacteriochlorophyll bound to a variety of protein environments.** In green systems both protein-binding and vibrational bands probably contribute to the in vivo absorbance spectrum.

The simplest interpretation of the light-induced changes in absorbance would be that illumination produces a small, reversible perturbation on the binding of the chlorophyll molecules to their supporting protein. This perturbation shifts the electronic transitions

---

*Extraction and chromatographic studies have only detected one form of chlorophyll in each of these systems, except that both chlorophyll a and chlorophyll b are present in green algae.

**Relative magnitudes are sensitive to pH and to growth conditions, ruling out vibrational splittings as the explanation of these bands.[74]

slightly and affects any vibrational splittings a small amount. Such an interpretation would consider these biphasic signals as arising from a different phenomenon than a light-induced electron transfer reaction, although the shifts might well be a reflection of such an electron transfer step occurring "nearby".

Carotenoids

The structure of a common carotene and that of its hydroxylated derivative are presented in Figure III-23. The visible absorption spectrum consists characteristically of three closely spaced maxima (Figure III-24). The splittings are assumed to be vibrational fine structure. There are indications that the carotenoid absorption *in vivo* is not greatly different. Notice for instance Figures III-8, 10, where the carotenoid bands are relatively free of interferences. A typical carotenoid spectrum was also found by a difference spectrum technique using spinach quantasomes which had been partially irreversibly photo-oxidized.[75]

Carotenoids are known to undergo two photo-reactions, a general irreversible photo-oxidation, and a cis-trans conversion. Both of these reactions produce large blue shifts in the absorption spectrum.

The 400-500 mμ region of the light-minus-dark spectra is a most complex one. The only clear-cut assignment of bands to a carotenoid molecule can be made in the *R. spheroides* spectrum. As shown in detail in Figure III-25, the minima in the difference spectra match the carotenoid maxima, and the maxima in the difference spectrum are uniformly red-shifted by approximately 15 mμ. A carotenoid-less mutant of *R. spheroides* that can live photosynthetically does not show any of these

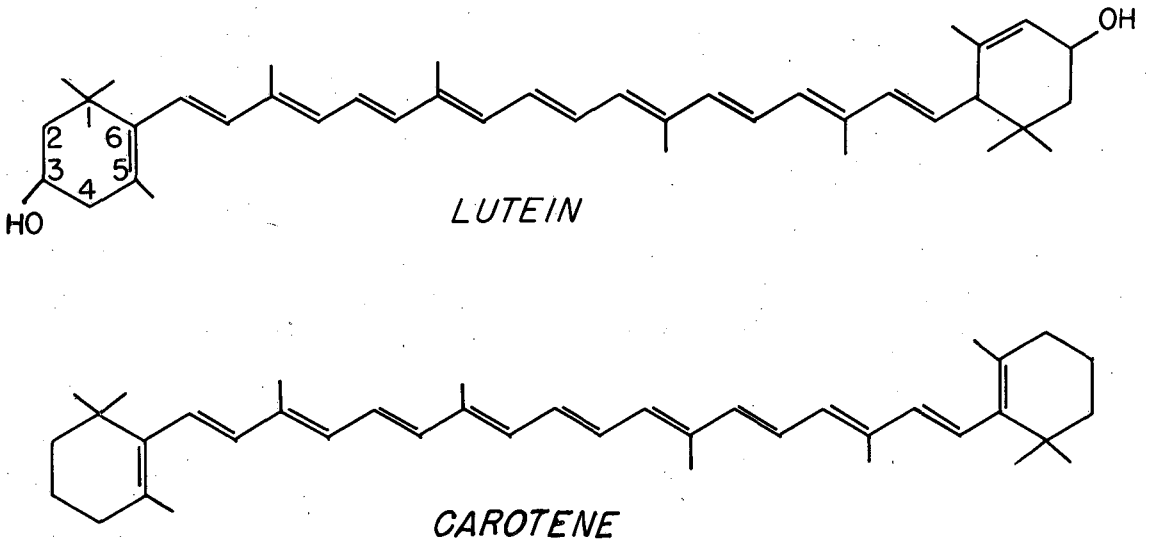

Fig. III-23. Structures of representative carotenoids.

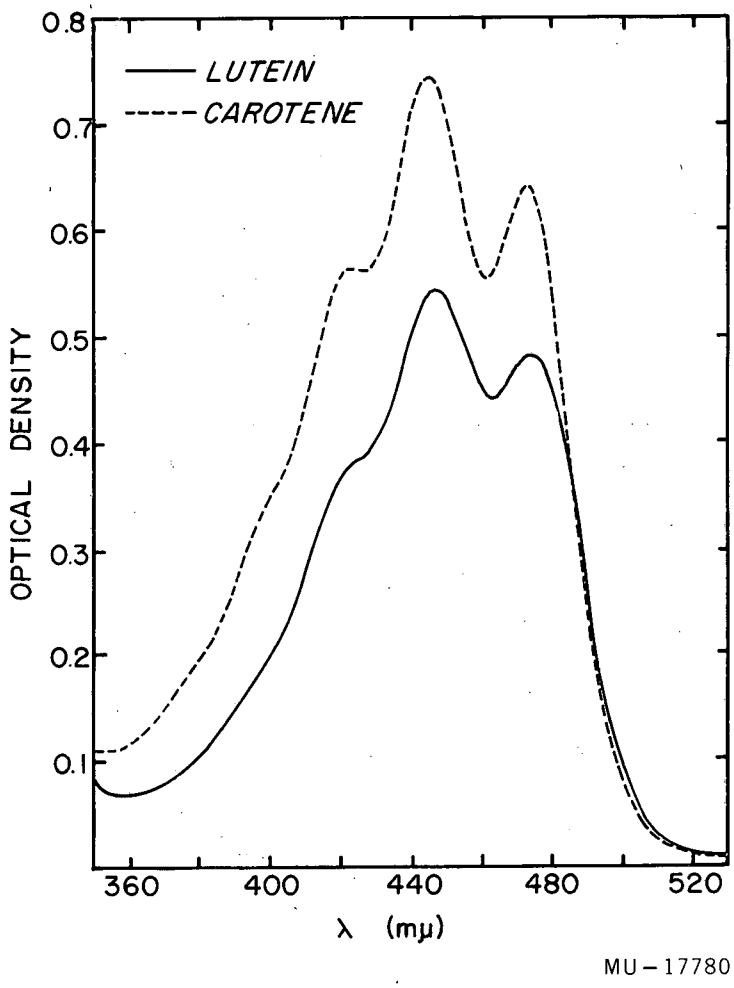

Fig. III-24. Absorption spectra of carotenoids.

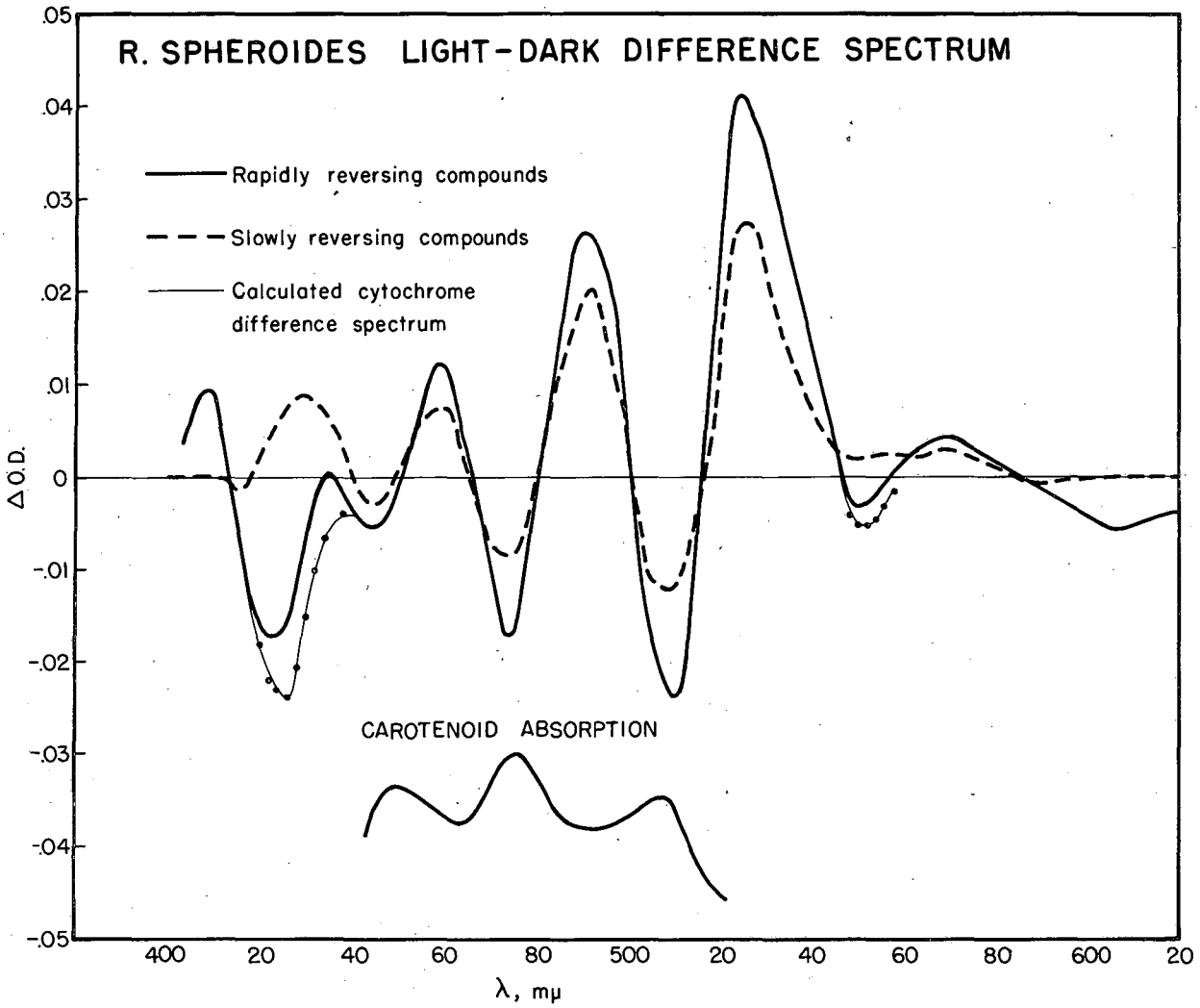

Fig. III-25. A detail of the light-minus-dark difference spectrum of R. spheroides cells. "Rapidly reversing" reactions have a half time ≤ 5 seconds. "Slowly reversing" reactions have a half time of ≥ 30 seconds. The calculated cytochrome spectrum was computed on the assumption that a positive-going signal of the same shape as that shown for the slow spectrum but only 50% as large was present in the rapid spectrum.

bands (Figure III-12). In other bacterial samples there are no distinct light-induced changes of this type, although the small amount of structure at 500-585 mμ in R. rubrum and ca. 485 mμ in Chromatium might arise from carotenoid effects.

In general, algae and spinach preparations also do not show a six-line spectrum such as that of R. spheroides. The one exception is the spectrum of Ochromonas (a brown alga), recently reported by Ke[52] and shown earlier in Figure III-5. However, experiments done some years ago by Chance on a carotenoid-less mutant of Chlamydamonas (a green alga) suggest that the pronounced difference bands at 480 and 520 mμ that are normally seen in green alga might be directly or indirectly produced by the presence of carotenoid pigments since these bands were missing in the mutant.[76] Assignments made in this fashion are, admittedly, extremely tenuous, and there exist a wide range of other proposals for the identity of the 480-520 mμ bands.*

None of the above observations are in keeping with the large blue shifts to be expected from carotenoid photochemistry. Thus we would again propose that the light-dark differences be understood as small chemical or structural changes which do not directly alter the carotenoid molecules. Instead, these changes affect the binding of the carotenoids to some other species. This interpretation has focused on "binding". Other weak interactions could produce these effects. Some possibilities include a change in the local dielectric constant or electric field strength, a small bending or rotation of one or more

---

*Chlorophyll reduction;[77] chlorophyll triplet;[78] complex with plastoquinone;[79] chlorophyll b.[80]

of the carbon-carbon bonds, a small change in electron density due to a shift in nearby hydrogen bonds or "charge-transfer" complexes. These suggestions are meant to emphasize the relatively weak nature of the postulated interaction and also to point up the fact that there are many physically reasonable sources for such changes.

The logical consequences of this interpretation include the important idea that the "carotenoid" difference spectra need not show identical physical, chemical, or kinetic properties to those intermediates which lie directly along the electron transport pathway.

Pyridine Nucleotides

The structural formulas for TPN^+ and TPNH are given in Figure III-26. In vitro spectra are available for both the oxidized and reduced forms of the pyridine nucleotides (Figure III-27).[81] The oxidized-minus-reduced spectrum looks very much like the oxidized spectrum at wavelengths longer than 320 mμ. In vivo spectra have only been obtained indirectly. There is some evidence for a moderate red shift of the oxidized absorption maximum out to 350 mμ (TPNH) or 360 mμ (DPNH).[82] Additional confirmation of the activity of pyridine nucleotides in living cells comes from fluorescence measurements.[82,83] A sizable fraction of the compounds in cellular systems is not closely bound to protein moieties, and this pool shows a moderately strong blue-green fluorescence when excited at 340 mμ.

Both the absorbance and fluorescence data indicate that pyridine nucleotides are reduced during illumination of whole cells. The broken cell systems do not show similar effects because the pyridine nucleotides

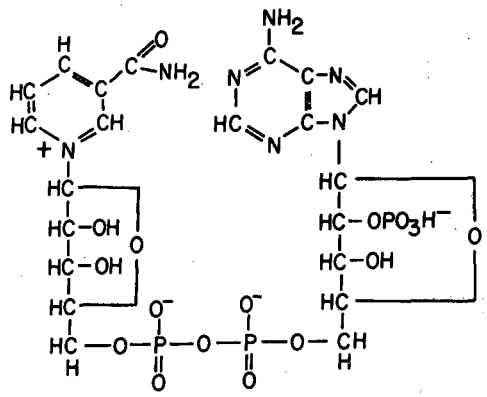

TRIPHOSPHOPYRIDINE NUCLEOTIDE
(OXIDIZED FORM) (TPN^+)

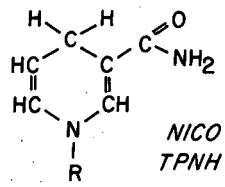

NICOTINAMIDE PORTION OF
TPNH (REDUCED TPN^+)

MU-35703

Fig. III-26. Structures of oxidized and reduced triphosphopyridine

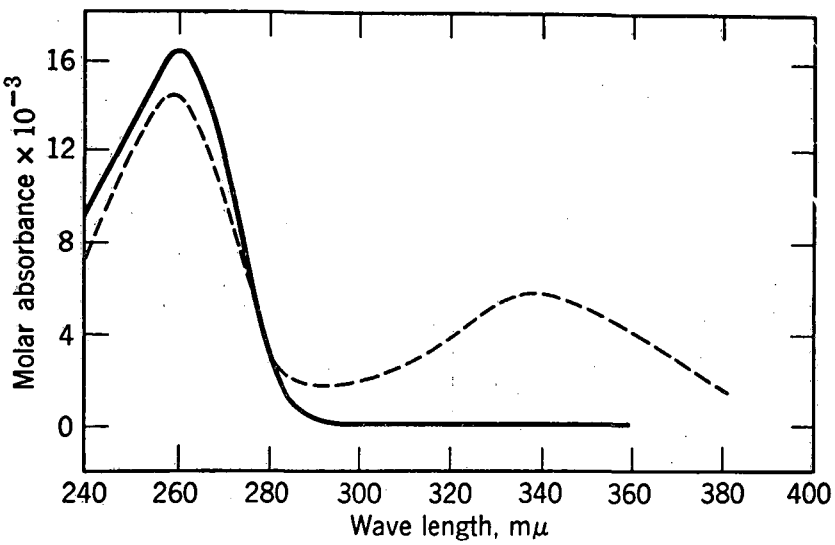

Absorption spectra of triphosphopyridine nucleotide (solid line) and of reduced triphosphopyridine nucleotide (dash line). (Fruton and Simmonds)

MUB-6792

have been removed during the preparative procedure.*

Flavins and Flavoproteins

The structures of some common flavins are given in Figure III-28. Spectra for the oxidized and reduced forms as well as an oxidized-minus-reduced spectrum and a schematic representation of the semiquinone spectrum are collected in Figures III-29, III-30,[84] and III-31.[85]

An examination of the light-dark spectra for an indication of some of the difference spectrum shown in Figure III-30 must take into consideration the relatively low molar extinction coefficient of the flavin chromophore. A small but definite loss of absorption at 450 mμ is particularly noticeable in the green algae (Figures III-1, 2). There are some kinetic indications that the broad negative band centered at 400 mμ contains a component that corresponds to 450 mμ components.[86] Careful examination of other difference spectra also indicates small negative bands in the 450 mμ region.

On the assumption that this band is a flavoprotein, the loss in absorption would indicate a light-driven reduction.

Other Compounds

Two compounds have been reported by other workers that have not been studied in this laboratory.

A quinone, perhaps plastoquinone (structure, Figure III-32; spectrum, Figure III-33)[87] is thought to be responsible for the loss in absorption in the 260 mμ region (Figures III-12, 33). If we base our interpretations

*Pyridine nucleotides and appropriate enzymes can be restored to such a system and on illumination a high rate of PN reduction can be observed.

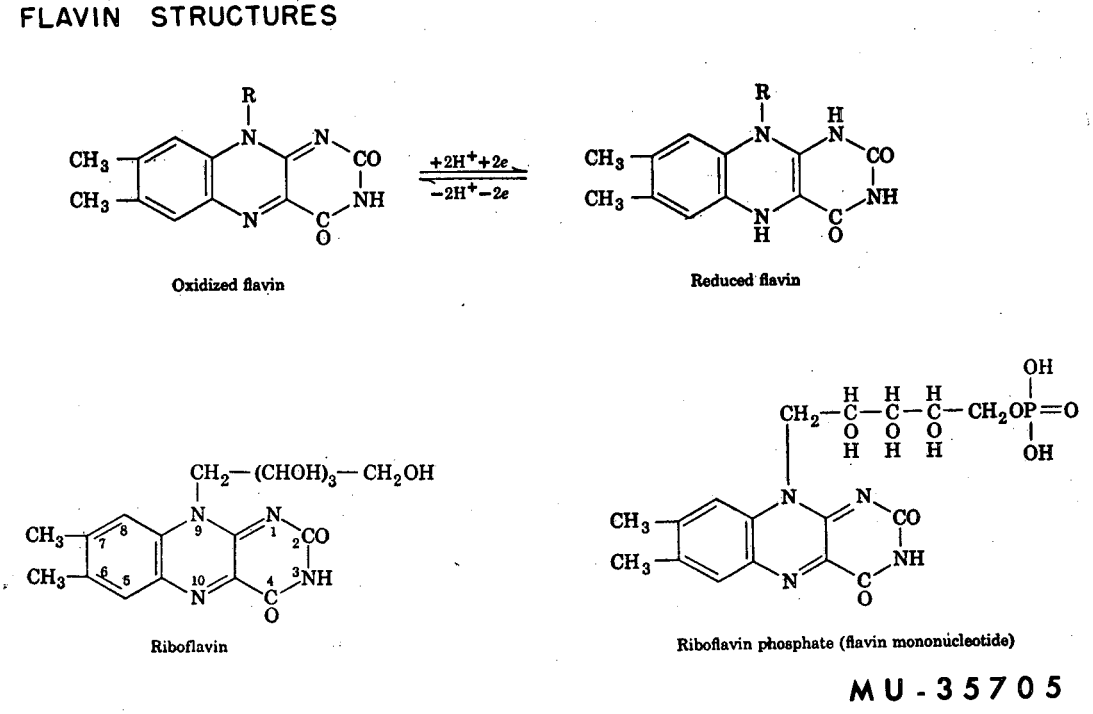

Fig. III-28. Structures of oxidized and reduced flavin and flavin derivatives.

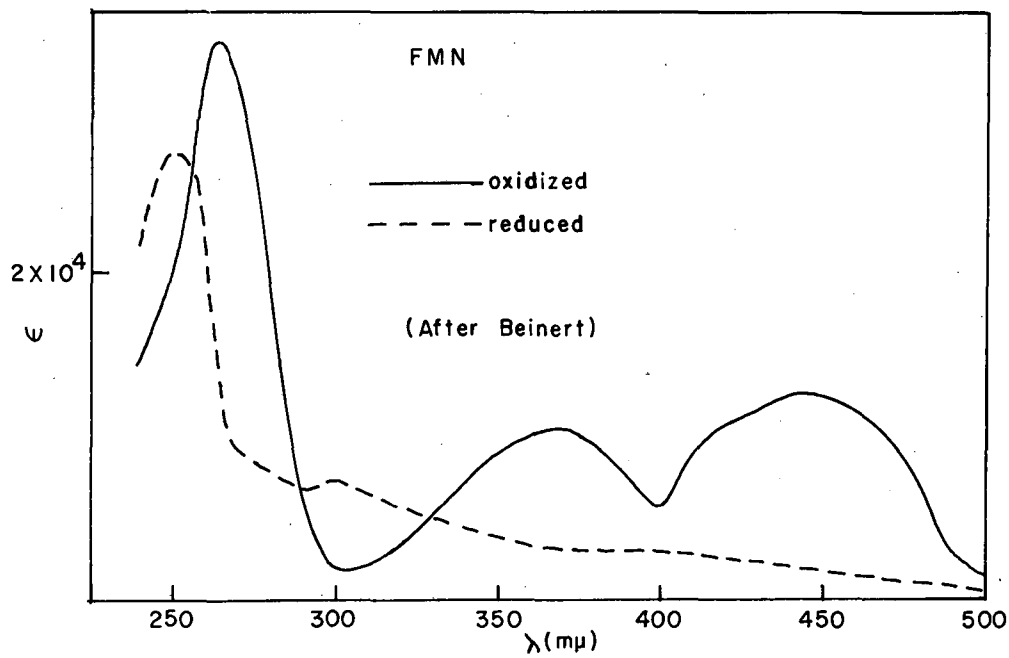

Fig. III-29. Spectrum of oxidized and reduced flavin mononucleotide (FMN).[84]

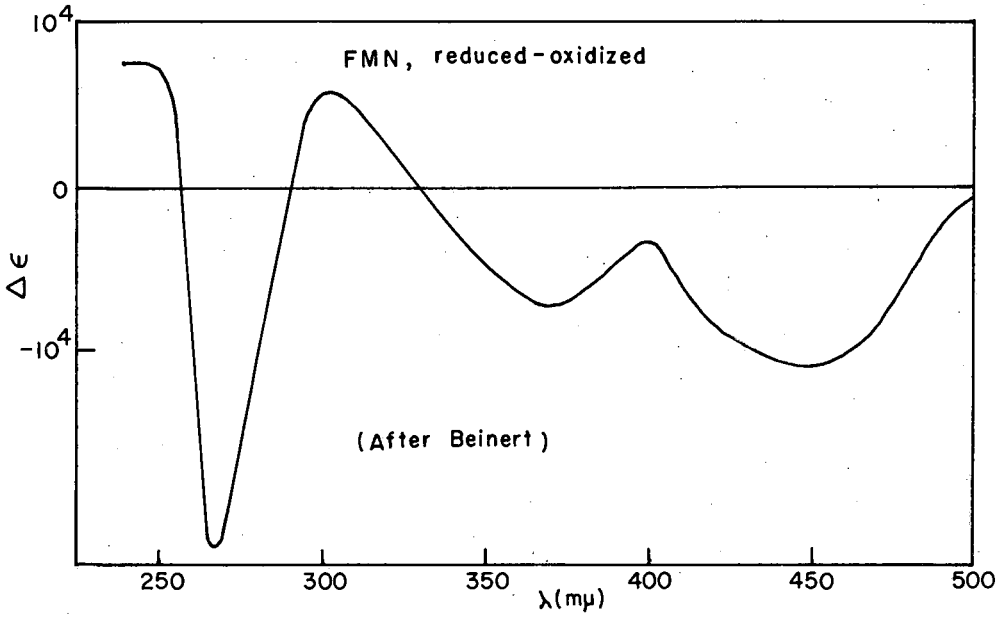

MU-35823

Fig. III-30. Reduced-oxidized difference spectrum for FMN, calculated from the data of Beinert.[84]

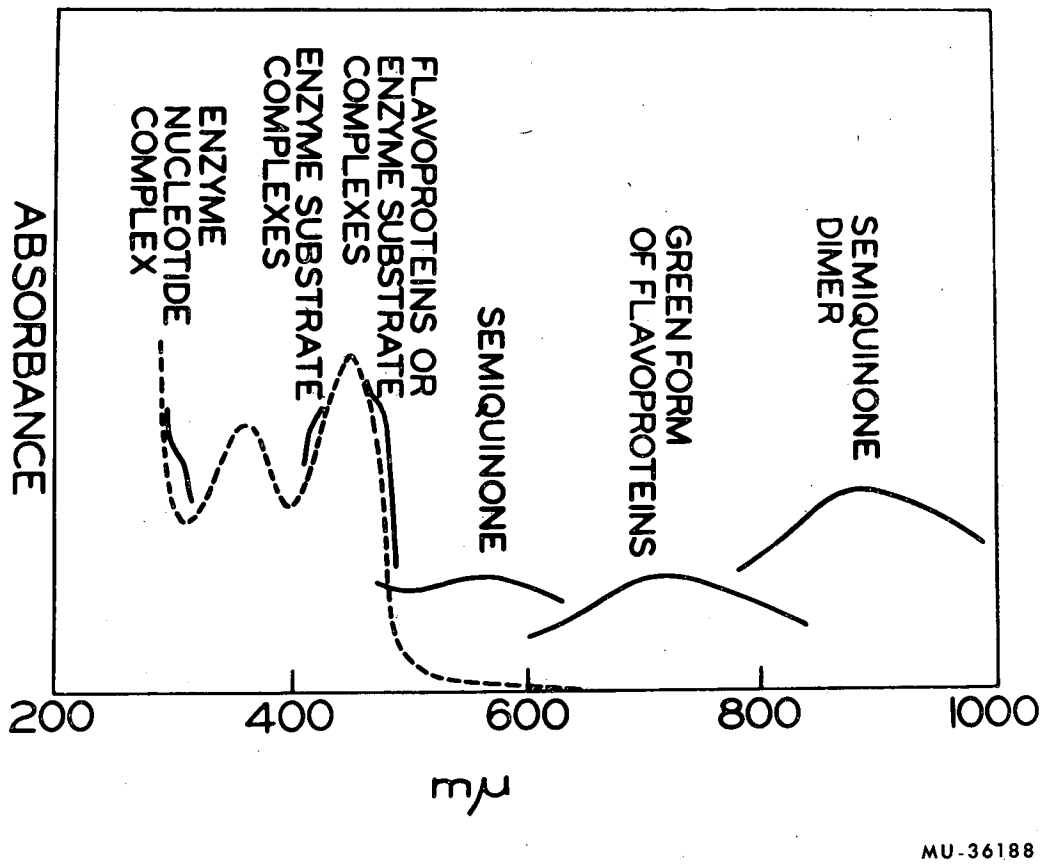
ABSORBANCE
ENZYME NUCLEOTIDE COMPLEX
ENZYME SUBSTRATE COMPLEXES
FLAVOPROTEINS OR ENZYME SUBSTRATE COMPLEXES
SEMIQUINONE
GREEN FORM OF FLAVOPROTEINS
SEMIQUINONE DIMER
200
400
600
800
1000
mμ
MU-36188

Fig. III-31

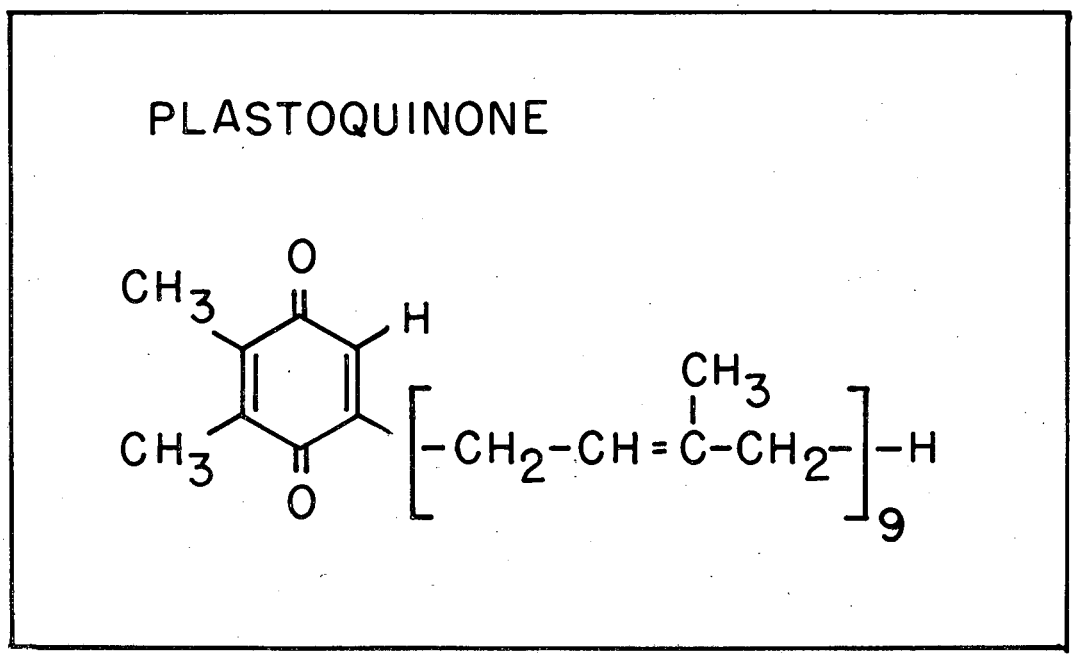

Fig. III-32. Structure of Plastoquinone.

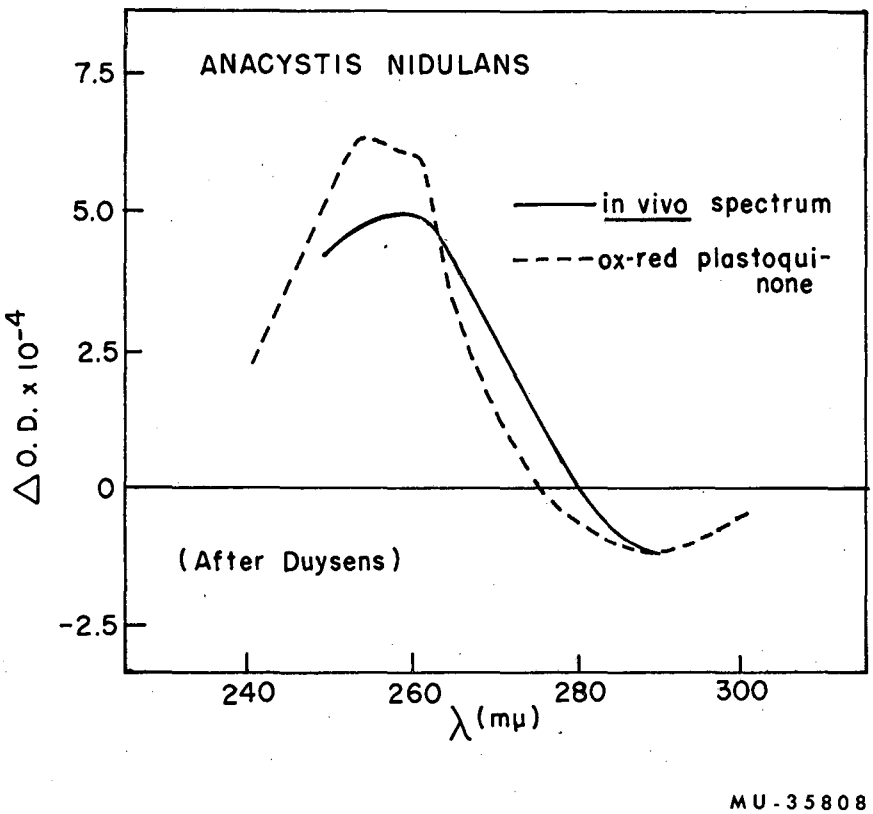

Fig. III-33. Spectrum for oxidized-reduced plastoquinone (dotted line) compared to the observed light-dark difference of Anacystis nidulans (solid line).[89]

upon the *in vitro* spectra, both light-driven reductions and light-driven oxidations have been reported.[88,89,90]

Plastocyanin has been studied in some detail by de Kouchousky and Fork.[91] They interpret the 597 mμ band prominent in some marine algae as a photo-oxidation of this copper containing pigment. A spectrum of purified plastocyanin is shown in Figure III-34.[92]

Finally, there are some absorption changes which have not been related to any known compounds. Particular note should be taken of the 433 mμ band in bacterial chromatophores (Figures III-8, 9, 25) and the small 555 mμ band in green algae (Figures III-1, 2).

In summary, it has been possible to identify most of the bands in the light-dark difference spectra as either the compounds known to be present in unilluminated photosynthetic tissue or as photoproducts, particularly oxidized or reduced forms, of the compounds present in the dark.

These identifications were made by means of analogy with *in vitro* spectra and obviously require much supporting evidence. The specific assignments made in this section should be regarded, for the most part, as simple working assumptions. Much of the work to be discussed in later chapters can be thought of as tests of some of these assumptions. We turn next to the presently accepted theory which attempts to correlate the spectra with the general considerations outlined in the first chapter.

Current Theories

Although photosynthesis in plants and bacteria shows many differences, it is commonly thought that some essential features are very similar.[93,94,95]

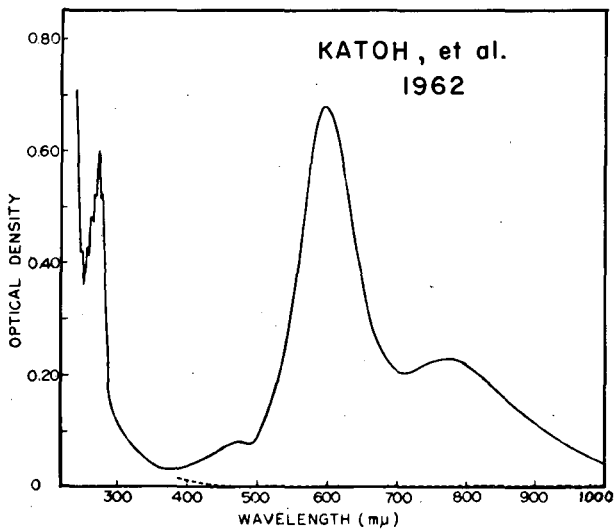

Absorption spectra of the oxidized and reduced spinach plastocyanin. Solid line, oxidized form; broken line, reduced form.

MU-28438

Fig. III-34.

It is known, though, that oxygen production is on the whole a more complex process. We shall first describe the "green plant" mechanism. Then we shall consider those parts of the mechanism which appear to be directly applicable to the photosynthetic bacteria.

Photosynthesis in Oxygen Evolving Systems

Considerable evidence indicates that oxygen production involves two light-driven reactions. The most universally accepted scheme, shown in greatly simplified form in Figure III-35, was proposed by Hill and Bendall.[96] The figure clearly indicates three essential features: 1) two quanta are needed to transport one electron from H_2O to TPN^+; 2) the two photo-steps are separated by a set of dark reactions which move electrons along the potential gradient from about zero to +0.4 volts; 3) two more sets of dark reactions, one at either end, connect the photoproduced oxidant and the photoproduced reductant to water or pyridine nucleotide respectively.

The mechanism, even in this simple form, makes three powerful predictions. First, the quantum requirements for steady-state oxygen evolution should be not less than 8. Second, the color of the actinic light might have a large effect on photosynthesis, depending, of course, on the wavelengths of light that are effective in driving the two photochemical steps. Third, with suitable chemical or biological (i.e., mutants) means it should be possible to "split" photosynthesis into two independent halves: the oxidation of water and reduction of added electron acceptor by "$h\nu_2$"; and the reduction of pyridine nucleotide and oxidation of some added electron donor by "$h\nu_1$".

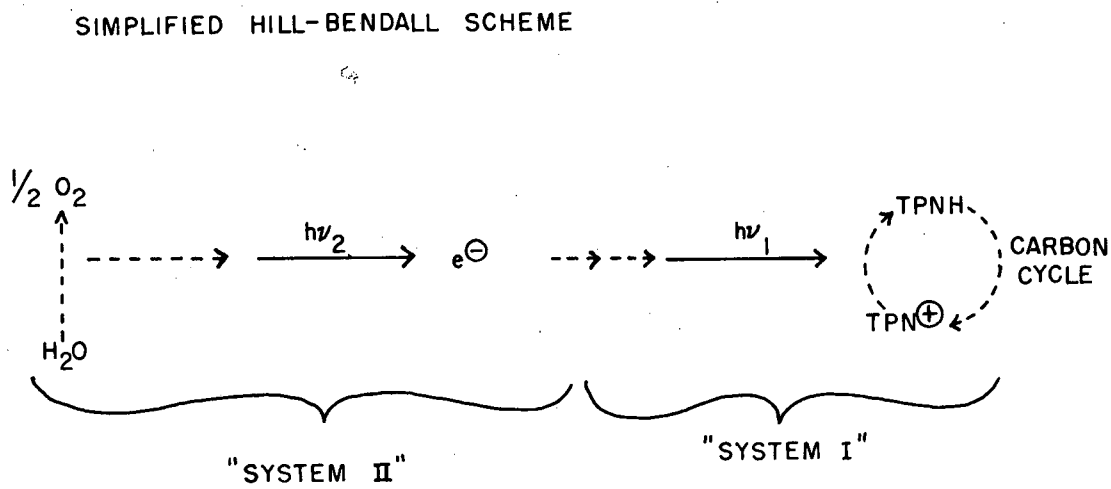

Fig. III-35. Simplified Hill-Bendall mechanism for photosynthesis.

All of these predictions have been borne out to some degree as we shall now see.

Quantum yields. This basic measurement turns out to be a very difficult one because of the problems of determining the true absorption spectrum of the biological materials. Light scattering is severe, and the pigment molecules are contained within inhomogenous structures which might produce large internal changes in the index of refraction. Furthermore, few techniques are sensitive enough to permit working at low absorbances, thus most experiments must deal with a fairly steep light intensity gradient across the sample. Finally, there are not very satisfactory chemical actinometers in the 600-900 mμ range, a region of crucial interest to photosynthetic studies. Of course, these technical problems are superimposed on the vagaries of biological materials. All of these difficulties are clearly reflected in the wide range of quantum yields that have been reported.[97] For the classical case of the oxygen evolution values of the quantum requirement per mole of oxygen range from 3 to 12 or more. The generally accepted value is approximately 8, which does fit the picture of 2 quanta/electron. However, some quite reliable work has consistently given values of 6 to 7 for long-term quantum requirements (i.e., a several-hour experiment).*[98]

Dependence on wavelengths of actinic light. Figure III-36 indicates the results obtained in a typical experiment where the quantum yield of oxygen evolution is determined as a function of the color of

---

*Even if this finding were correct, it would not automatically rule out two light reactions arranged in series since one of these steps could transport theoretically two electrons per quantum.

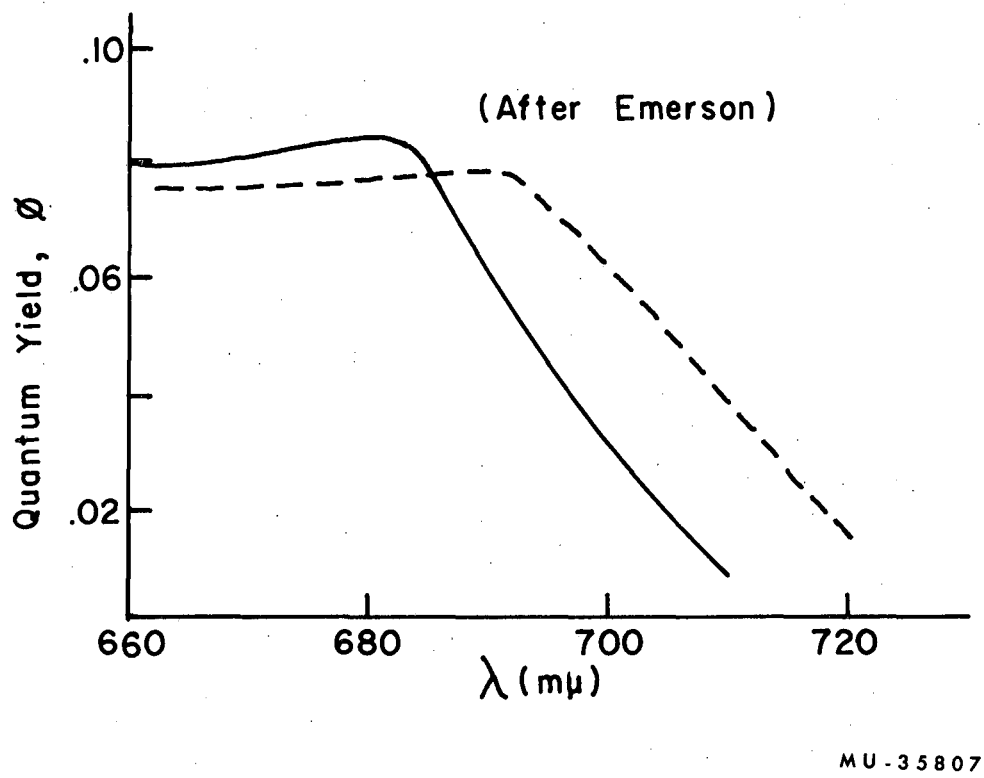

Fig. III-36. Quantum yield of O_2 production as a function of actinic wavelength. Solid curve: no supplemental light, "red-drop" experiment. Dotted curve: with short wave- length supplemental light, "enhancement" experiment.

the actinic light.[99] Notice the pronounced drop in quantum efficiencies on the long wavelength side of the chlorophyll maximum. As a separate experiment, the figure also shows the results when two light beams are simultaneously shown on the sample. It is found that the rate of oxygen is now higher than the sum of that produced when the two lights are applied independently. If the entire "excess" oxygen production is ascribed to the increased efficiency of the long wavelength light, one obtains the quantum yields shown.

These experiments certainly form an integral part of the theory we are discussing. They supplement the material already presented by indicating that the two light reactions have overlapping "photon collection systems" from 600-800 mμ. Only beyond 700 mμ are the light collection systems sufficiently separated for the overall process of oxygen evolution to be strongly affected. The actual quantum step associated with each photochemical reaction is difficult to ascertain. The $h\nu_1$ quantum would seem to have a longer wavelength than 700 mμ. The $h\nu_2$ quantum might lie between 650-680 mμ.

The interactions that obviously occur between the two reaction systems, as indicated by the "enhancement" experiment described above, is a subject of great current interest. Notice that the Hill-Bendall picture shows the photochemical steps coupled by a set of dark reactions. This is consistent with recent findings that relatively little interaction occurs at the level of direct excitation energy transfer.[100]

Separation of partial reactions. Two well-known chloroplast reactions are thought to be the two partial reactions predicted by the Hill-Bendall mechanism. The first is the "Hill reaction": oxygen evolution with the

reduction of an exogenous electron acceptor such as ferricyanide, benzoquinone, or indophenol dyes. Second, if oxygen evolution is poisoned with DCMU (dichlorophenyl dimethyl urea) photoreductive capacity can be demonstrated if an external electron donor is used. Ascorbate can, for instance, be used to reduce pyridine nucleotide. These two reactions show different action spectra, different quantum yields, different limiting rates, different stabilities to aging or detergents, and they can be shown to proceed in certain mutants in which the complete reaction from H_2O to CO_2 does not occur.

Thus, considerable evidence is available to support the hypothesis of two quite different photochemical reaction pathways that are present in the photosynthetic material derived from algae and plants. Furthermore, these reactions tie in well with the partial steps postulated by Hill and Bendall. However, in spite of this impressive circumstantial evidence, the actual nature of the relationships between the two processes is still a matter of speculation.

Reaction sequences in the Hill-Bendall mechanism. Hill and Bendall placed reaction intermediates at various points along a "potential" diagram. These sequences were largely determined by redox potentials and by analogy to the respiration electron transport reactions. This general approach has been considerably extended so that all of the spectral bands which have been assigned can be associated with various steps in the scheme (Figure III-37). In this section we will discuss the current state of development of the theory as well as discussing some of the supporting evidence.

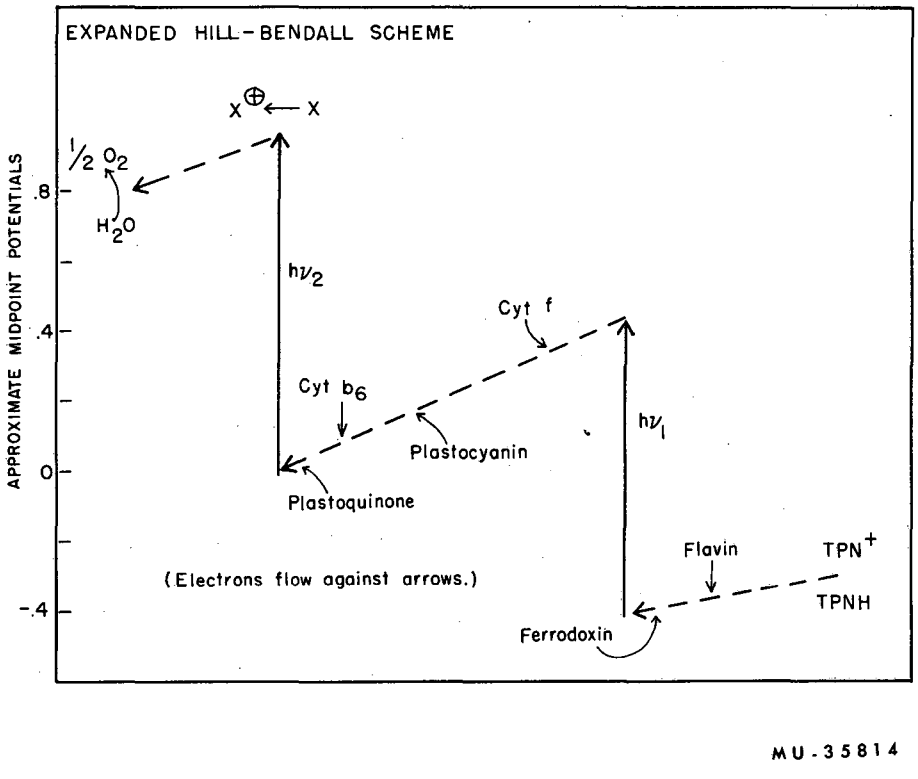

Fig. III-37. Expanded Hill-Bendall mechanism.

a) Photochemical Reaction 1

The small fraction of chlorophyll a which appears to be responsible for the losses in absorption at 430 and 700 mμ is thought to be the primary reactant, undergoing the reaction:

$$\text{Chl } a \text{ (700 m}\mu \text{ form)} + h\nu_1 = \text{Chl } a^+ + (e^-) \; * \qquad \text{(III-1)}$$

A redox potential of +.45 volts has been reported for the chlorophyll a - chlorophyll a^+ couple.[51]** Thus, this reaction would be incapable of providing oxygen directly.

The path of the electron produced in Eqn. III-1 is fairly clearly marked. An iron protein, ferrodoxin,*** has been isolated from photosynthetic tissue[101] and has been shown to be a highly stimulatory reagent for the photoreduction of added pyridine nucleotides by cell-free materials.[102] The in vivo potential for ferrodoxin is estimated to be -0.4 volts. Recently Chance, et al., have shown that substrate amounts of ferrodoxin can also be reduced in such systems, indicating that the electron is generated by a strong reductant.[103] Ferrodoxin undergoes univalent electron transfer reactions. The only major argument against assigning an important role to ferrodoxin is that it has not yet been detected, or at least identified, by in vivo absorbance studies. However, as Figure III-38[104] indicates, the extinction coefficients are low and, further, the bands occur in the region of chlorophyll and cytochrome spectral transients (see also Figure III-39). Thus, the failure to observe the postulated ferrodoxin reactions in vivo is presently ascribed to a masking effect of the other intermediates.

---

*This is a partial reaction. The electron is certainly not "free".

**The experimental procedures used will be discussed in the next chapter.

***When associated with a flavoprotein moiety the name "photosynthetic pyridine nucleotide reductase" (PPNR) is applied to this material.

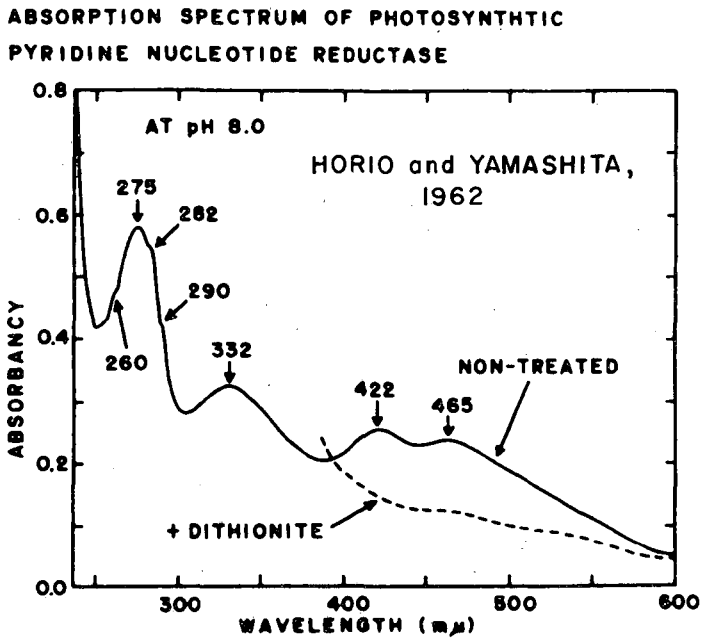

Fig. III-38. Oxidized and reduced spectra for PPNR.[104]

$\varepsilon_{max} \cong 1.0 \times 10^3$.

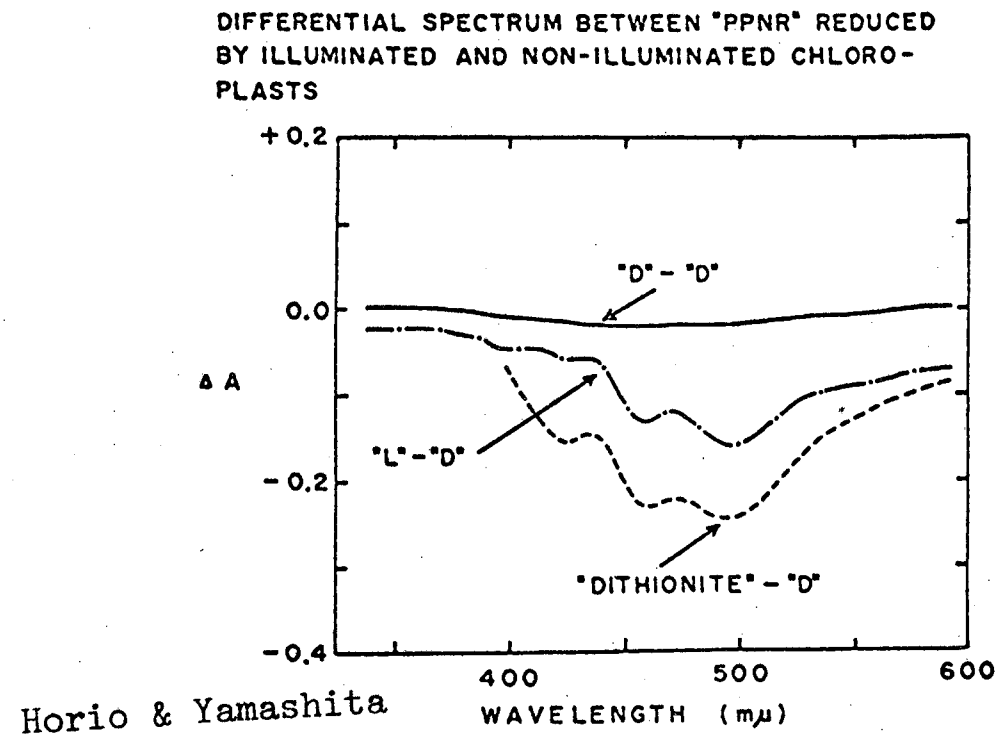

Fig. III-39. Light-dark and reduced-oxidized spectra for PPNR.[104]

As mentioned earlier, ferrodoxin is isolated in close association with a flavoprotein. Both components are required for efficient reaction with substrate amounts of electron acceptors. The redox potential and the detailed structure of the flavoprotein are not known, but the potential can be estimated as falling in the -.4 to -.2 volt range. The 450 mμ band present as a distinct minimum in the difference spectra of the green algae might be indicative of the photoreduction of this compound. The two reactions described above are:

$$e^- + \text{Ferrodoxin } (Fe^{+3}) = \text{Ferrodoxin } (Fe^{+2} \qquad \text{(III-2)}$$

$$2 \text{ Ferrodoxin } (Fe^{+2}) + \text{Flavoprotein (ox)} = 2 \text{ Ferrodoxin } (Fe^{+3}) + \text{Flavoprotein (reduced)} \qquad \text{(III-3)}$$

Pyridine nucleotides, particularly TPN^+, have long been associated with electron transfer reactions. They are likely candidates to form the bridge between the very low potential, relatively unstable, reductants formed from the photochemical reactions and the normal biochemical reactions of carbon dioxide fixation and respiration. The midpoint potential of the TPN^+-TPNH couple is estimated as -0.3 volts. The absorbance increase centered at 350 mμ probably arises from the photoproduction of TPNH.

$$\text{Flavoprotein (red)} + TPN^+ = \text{Flavoprotein (ox)} + TPNH \qquad \text{(III-4)}$$

$$H_2O + 2TPNH + CO_2 \xrightarrow[ATP]{\text{Enzymes}} (CH_2O) + 2TPN^+ + 2OH^- \qquad \text{(III-5)}$$

Having envisioned the path of the electron from chlorophyll to CO_2, let us turn our attention to the fate of the positive hole left behind as Chl $\underline{a}^+$. As noted earlier, the pool of photoreactable chlorophyll is not large enough to maintain steady-state photosynthesis for any appreciable time. Thus we are seeking a pathway to a suitable electron source. The first reducing agent on this path is not known. One popular candidate

is the "f" type cytochrome:

$$\text{Cyt f } (Fe^{+2}) + Chl^{+} = \text{Cyt f } (Fe^{+3}) + Chl \qquad \text{(III-6)}$$

These cytochromes have appropriate characteristics: $E_h \sim +0.3$ volts and univalent transfer reactions. Also they are concentrated in the chloroplast tissue. The major piece of direct evidence comes from low temperature spectroscopy (77° K). At these temperatures, in oxygen-evolving systems, photo-oxidation of chlorophyll and cytochromes can be observed, but these processes are no longer reversible. No other absorption changes are noted at these temperatures.[29,105] There are several objections to this role for cytochrome f.* However, no other compound can fit all the data any better.

If we assume that some reaction of the type of Eqn. III-6 is involved, we can write a summary reaction for the first photochemical step:

$$H_2O + TPN^{+} + 2 \text{ Cyt f } (Fe^{+2}) \xrightarrow[\text{Chl } \underline{a}]{h\nu_1} 2 \text{ Cyt f } (Fe^{+3}) + TPNH + OH^{-} \qquad \text{(III-7)}$$

b) Photochemical Reaction 2

The next series of reactions serve to oxidize water, transferring the electrons thus produced to cytochrome f or its equivalent. If we

---

*These include: no steady-state cytochrome signal is observable in green plants or green algae under "normal" conditions. The cytochromes are there and can be photo-oxidized but only in the presence of far-red light, DCMU, or low temperatures is a detectable steady-state obtained. Furthermore, one must postulate a light-induced electron transfer from cytochrome to chlorophyll to explain the oxidation of cytochrome and the absence of a back reaction. But this would lead to a very low steady-state level of reactive chlorophyll, much smaller than is, in fact, observed. Finally, as Chance has shown,[105] there is no evidence of an induction period in the rise time of Cyt^{+}, making it unlikely that Eqn. III-6 is strictly correct.

start again with the photochemical reaction,

$$X + h\nu_2 = X^+ + e^- \qquad \text{(III-8)}$$

where X is an unknown high energy oxidant (E_h greater than +0.8 volts at pH 7 and probably even higher since oxygen is evolved efficiently at pH 4). No absorbance signal has been unambiguously assigned to X. Witt feels that chlorophyll b serves this role in the green algae and plants.[80] Almost all the workers in the field feel that some form of a chlorophyll-type molecule is involved. Similarly, the reactions whereby X^+ produces O_2 are not known. In the absence of information let us make the simplest assumption:

$$4X^+ + 2H_2O \longrightarrow 4X + O_2 + 4H^+ \qquad \text{(III-9)}$$

The electrons generated in the oxidation of water are thought to follow the sequence of steps given below before being available for the reduction of cytochrome:

$$2\ e + \text{plastoquinone (ox)} = \text{PQ (reduced)} \qquad \text{(III-10a)}$$

$$\text{PQ (red)} + 2\ \text{Cyt } b_6(Fe^{+3}) = \text{PQ (ox)} + 2\ \text{Cyt } b_6(Fe^{+2}) \qquad \text{(III-10b)}$$

$$\text{or PQ (red)} + 2\ \text{plastocyanin} = 2\ \text{plastocyanin (red)} + \text{PQ} \qquad \text{(III-10c)}$$

$$\text{plastocyanin} + \text{Cyt f}(Fe^{+3}) = \text{plastocyanin (ox)} + \text{Cyt f}(Fe^{+2}) \qquad \text{(III-10d)}$$

These steps have been formulated primarily on the basis of the appropriate redox potentials (for spontaneous reactions). The presence of appropriate steady-state absorbance changes for these intermediates is not, unfortunately, universally found. However, such a sequence as shown in Eqn. III-10 is probably a good working model, even if the exact components vary from one organism to another.

In summary, we have discussed at length the currently accepted detailed mechanism for electron flow in photosynthesis. In broad

outline it ties in well with the major qualitative experiments. However, many of the explicit reactions are rather tenuously supported by the spectroscopic studies.

Bacterial Photosynthesis

Bacterial photosynthesis is generally considered to be a simpler process than that of the higher plants because no one has been able to show the presence of two light reactions.[106] Action spectra do not indicate any compounds which have low photosynthetic efficiencies THAT CAN BE "ENHANCED" by other wavelengths of actinic light. Nor has it been possible to separate the bacterial electron transport system into two or more partial reactions.

A simple starting assumption is that the mechanism of bacterial photosynthesis involves only the mild oxidant, strong reductant step we have called photoreaction 1 (Eqn. III-7). Certainly pyridine nucleotides are reduced and, as we shall see, evidence points to the presence of an oxidized bacteriochlorophyll with a redox potential of +0.4 volts (Chapter 4). Ferrodoxin is also present in whole cells of bacteria, though it is washed out of the chromatophore preparations.

Thus, we shall tentatively postulate a single photochemical process analogous to photoreaction 1 where now an electron-donating substrate (such as malate or succinate) serves in the role of the cytochrome.

$$\text{Substrate} + TPN^{+} \xrightarrow[\text{enzymes}]{\text{light}} TPNH + \text{oxidized substrate} \qquad \text{(III-11)}$$

An interesting extension of this hypothesis would simply require that the substrate interacted with the bacterial electron transport chain

at the level of, say, the quinone in Eqn. III-10. Then the mechanism of bacterial photosynthesis might be even more analogous to that just described for the higher plants. Such an extension is quite in keeping with the spectroscopic data which indicates that both cytochromes and quinones are active intermediates in bacterial reactions.

Chapter IV. RESULTS: REDOX AND KINETIC EXPERIMENTS

A mechanism as complicated as the Hill-Bendall proposal can be tested in many ways. One could, for example, study the specific interactions that are proposed: chlorophyll-cytochrome, ferrodoxin-TPNH, etc. This is the approach most frequently pursued by workers in this field. Or one could examine the overall behavior of the set of reactions under a variety of conditions. Our rationale was (and is) that the basic qualitative features of the total electron transport system should be developed as rapidly as possible. Although specific steps are extremely important, it is precisely the coupling of several relatively unsurprising reactions that produces the unique efficiency of photosynthesis. Whichever point of view is adopted, studies of the specific steps and studies of coordinated sets of reactions are both necessary for a complete understanding. The previous chapter was primarily concerned with a discussion of specific reactions. In the next two chapters we shall emphasize the "systems" aspect of photosynthesis.

Two different kinds of experiments are discussed in this chapter. The response of suitable cell-free materials to alteration of the external redox potential seemed a logical starting point since the primary motivation for the development of the Hill-Bendall theory was the redox properties of the intermediates. Second, the most positive tests of reaction sequences and overall system response can normally be made through kinetic measurements. The first section of this chapter discusses the redox properties of bacterial chromatophores with

respect to their photochemical reactions. The second section presents a wide range of kinetic studies involving chromatophores, whole-cell bacteria, and whole-cell and cell-free materials from oxygen-evolving plants.

A. REDOX EXPERIMENTS*

Since oxidized and reduced moieties are formed very early in the energy conversion process, a careful systematic study of the redox dependence of light-induced changes might result in the identification of the participating pigments and indicate how they interact with one another.

If some or all of the redox couples composing the photosynthetic apparatus equilibrate with the potential established in the external medium by a suitable redox buffer, the effects of light might be expected to be seen as transient departures from the redox equilibrium. For those systems in which the equilibrium oxidation-reduction ratio is essentially completely in favor of that oxidation state toward which light drives it, the light could not produce a noticeable change.

Cell-free materials were obviously required for these studies since cell walls greatly restrict the rate of equilibration of cell contents with the external medium. We shall assume that the results obtained are directly applicable to the photochemical aspects of photosynthetic mechanism. We choose bacterial preparations for two purely pragmatic reasons: the signals involved were ten times as large as

---

*Work in this section was done in collaboration with Dr. P. Loach (present address: Department of Chemistry, Northwestern University, Evanston, Illinois). Much of this material has been published in Ref. 31.

those from corresponding preparations of algae or plants; and the bacterial mechanism is thought to be the simpler one.

Experimental*

Materials. Chemicals, special reagents, and the preparation of chromatophores from Rhodospirillum rubrum, Rhodopseudomonas spheroides, and Chromatium used in these studies have been described elsewhere.[107]

Methods. All redox experiments reported in detail have been conducted in the presence of a 10- to 1000-fold molar excess of the external redox couple over the estimated concentration of the photoactive pigments. Values of potential are measured at 22 ± 2° C and pH 7.4. With these large excesses of redox "buffers" the electrodes responded immediately to small changes in potential (0.5 mv), and adjustments to desired values were made quite easily.

For interpretation of the data obtained it has been assumed that the relatively high concentrations of redox buffers do not complex with the pigments being investigated to such an extent that the pigment properties are changed. Where possible a number of redox couples have been used to cover the same range of potential, and experiments were carried out to determine the effect of reagent concentration and the effects of light on the couples.

Measurements in the absence of air, used apparatus and techniques patterned after those designed by Harbury.[108] A rectangular, four-sides-clear quartz cuvette was cemented (de Khotinsky's cement) to pyrex tubing, as illustrated in Figure IV-1. From standard taper 2

*For ease in reading, some of the experimental details are presented in conjunction with the experiments rather than in the instrumentation chapter.

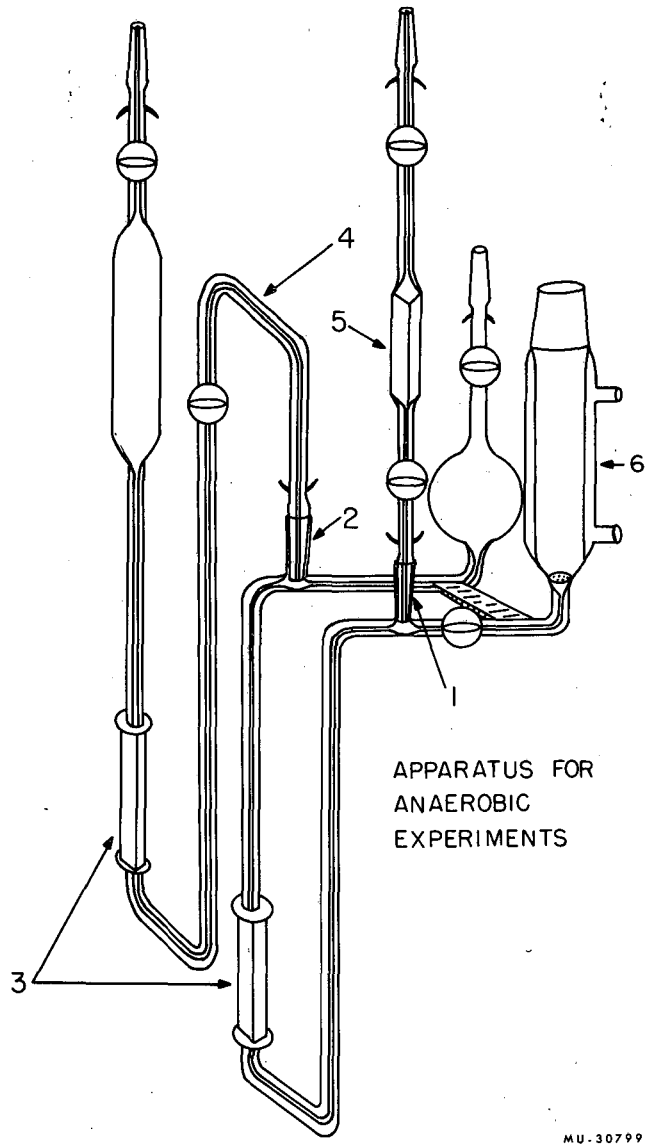

Fig. IV-1. Apparatus for anaerobic redox experiments. (1) 10/30 standard taper for sample cell (5) or microburette; (2) 10/30 standard taper for connection to reference cell or for microburette; (3) four-sides-clear rectangular quartz cuvettes; (4) bridge to reference cell; (6) main titration vessel with water jacket.

a bridge was connected to a second cuvette which resided in front of the reference beam of a Cary spectrophotometer. The two cuvettes were separated, when placed in the spectrophotometer compartment, by means of a black metal septum. With this apparatus both the reference and the sample material could be adjusted under identical conditions and light-minus-dark spectra observed. Chemical difference spectra could also be obtained with a minimum of manipulation of the sample. Also shown in Figure IV-1 is a cell in standard taper 1 which could be deaerated and filled with a sample of the material being investigated. The contents of this cell could then be examined with the rapid-response spectrometers described in Chapter II.

Instrumental. The light-dark difference spectra and the spectral changes attendant to chemical titrations were measured on the Cary Model 14M spectrophotometer, also described in Chapter II. The excitation source was a 500-watt tungsten projection bulb. Appropriate filters prevented the exciting beam from reaching the photomultiplier. Table IV shows the filter and photomultiplier combinations employed for different regions of the spectrum.

Table IV

Filters and Photomultipliers Used in the Cary Spectrometer

Detecting wavelengths (mμ)	Exciting wavelengths (mμ)	Photomultiplier	Detecting beam filters*,#	beam filters#,**
650-1100	400-500	Dumont 6911	2403	4600, 9782
380-620	650-900	RCA 6217	9782	2403
260-420	750-900	Dumont 7664	9863	2600

*Placed in front of photomultiplier
#All numbers refer to Corning color glasses
**Cary experiments included a 5 cm water filter in the exciting beam

The peak-to-peak noise under normal operating conditions was 0.0005 O.D. unit when using the blue-sensitive photomultipliers. An increase in the noise (0.002 to 0.003 O.D. unit) and a base line shift (0.001 to 0.010 O.D. unit) occurred as the exciting light was turned on for measurements above 650 mμ. These effects were not observed at low light intensities and probably resulted from infrared fluorescence or scattering of the actinic light. Since the base line shift is independent of wavelength, it was easily corrected for by selecting a wavelength at which no absorption change occurs. The precision of these experiments was consistent with the noise levels described.

Results

Magnitude of reversible photoabsorption changes as a function of redox potential

1. High potential. Samples of the deaerated chromatophores were treated with mixtures of $K_4Fe(CN)_6$ and $K_4Fe(CN)_6$ to cover the potential range of +0.30 to +0.55 v.* Representative absorption spectra and light-dark difference spectra for control samples (E_h = +0.35 v)** were shown in Figures III-8, 10, 13. These results are in relatively good agreement with those of other workers.[10,30,110]

The oxidized-minus-reduced and the light-minus-dark signals at 792, 810 and 865 mμ were measured at each potential. As shown in Figure IV-2 and Table V, raising the potential through the region of +0.4 v removes

*In the absence of externally added redox couples a well-defined oxidation-reduction potential of each sample could be measured and the system seemed to be somewhat buffered at the measured value, but the couple(s) equilibrating with the electrode is unknown.

**The symbols E_h and E_m are used as suggested by Clark.[109]

Fig. IV-2. Variation with "high" potential of the light-induced absorption changes at 865, 810 and 792 mμ in chromatophores from R. rubrum. 0.05 M phosphate buffer, pH 7.4. Absorption at 880 mμ was 2.0. Total concentration of ferricyanide and ferrocyanide varied from 5×10^{-6} M to 2×10^{-4} M. Reducing agent, 0.01 M $Na_2S_2O_4$. After removal of oxygen, enough $K_4Fe(CN)_6$ was added to make it 5×10^{-6} M. ○, △, □, experimental points taken at 865, 810, and 792 mμ after increasing $K_3Fe(CN)_6$ concentration to increase potential. ●, ▲, ■, experimental points taken at 865, 810, and 792 mμ upon addition of increasing amounts of $Na_2S_2O_4$ to lower the potential, beginning after all $K_3Fe(CN)_6$ had been added. The solid and dashed lines were obtained by use of the equation $E_h = E_m + RT/nF \ln(\text{m.s.} - \text{l.s.})/\text{l.s.}$ with n = 1 and 2, respectively, and E_m = +0.439 v, m.s. = maximum light-induced signal, observed between +0.35 to +0.30 v, l.s. = light-induced signal observed at potential reported.

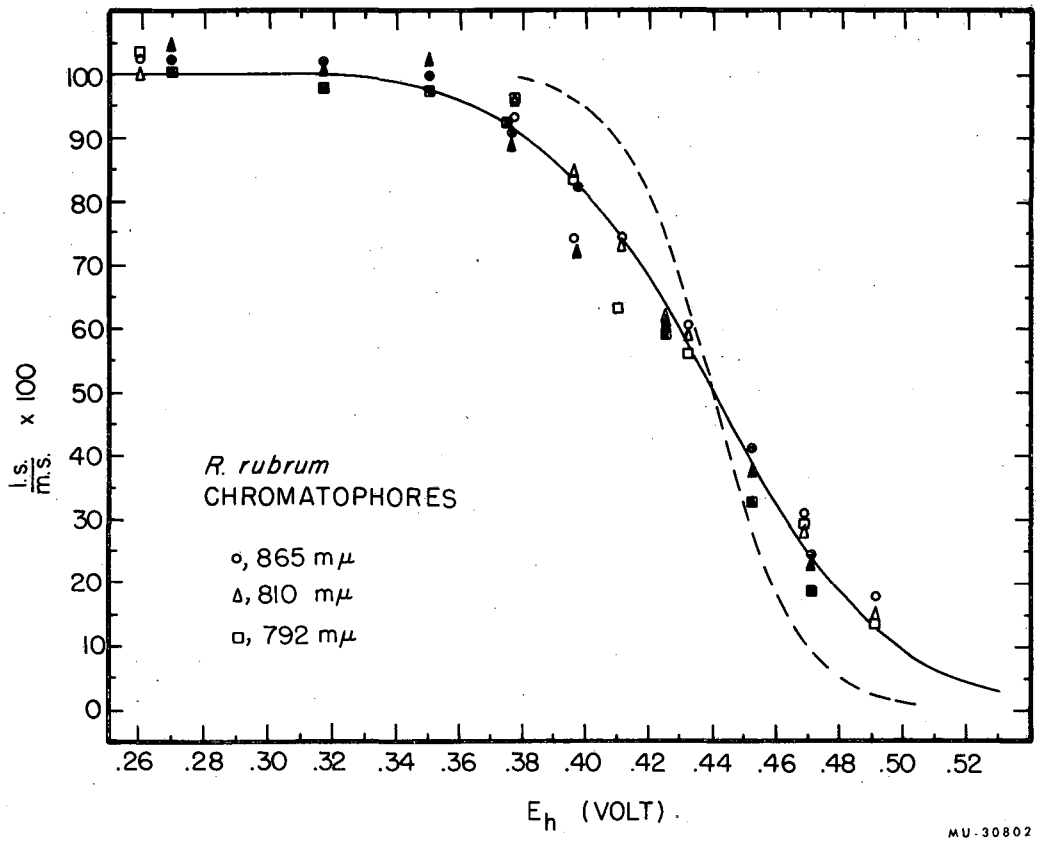
100
90
80
70
60
50
40
30
20
10
0
i.s./m.s. x 100
R. rubrum
CHROMATOPHORES
o, 865 mμ
Δ, 810 mμ
□, 792 mμ
.26 .28 .30 .32 .34 .36 .38 .40 .42 .44 .46 .48 .50 .52
E_h (VOLT)
MU-30802

Table V

Quantitative Comparison of Light-dark and Chemically-induced Spectral Changes*

	$\Delta OD_{792} + \Delta OD_{810}$			ΔOD_{865}		
E_h	Photo-oxidizable	Chemically oxidized	Total active pigment	Photo-oxidizable	Chemically oxidized	Total active pigment
0.37_7	0.051	0.005**	0.056	0.041	0.004**	0.045
0.39_6	0.043	0.014	0.057	0.032	0.009	0.041
0.41_1	0.036	0.019	0.055	0.032	0.016	0.048
0.43_2	0.032	0.026	0.058	0.026	0.022	0.048
0.46_9	0.016	0.039	0.055	0.015	0.036	0.051
0.49_1	0.008	0.045	0.053	0.008	0.036	0.044

*Data not corrected for irreversible selective or general bleaching
**Arbitrary zero assigned on basis of 90 percent light changes at 0.38 v

the light-dark signals, replacing them with the same bands in the oxidized-reduced spectra. The samples were then reduced in a stepwise fashion with sodium dithionite to demonstrate the reversibility of the effects. The midpoint of both the disappearance of the photochanges and the chemical titrations for each wavelength studied was +0.439 v. Figure IV-2 also shows the theoretical curves for one- and two-electron transitions with E_m = +0.439 v. The data are consistent with a one-electron transition occurring in a key pigment(s) with a midpoint of +0.439 v. Within the limits of the experiment there is quantitative agreement between the amount of material available for reversible photochemistry and that available for reversible oxidation (Table IV, columns 4 and 7).

In the above experiment potassium iridic chloride could replace potassium ferricyanide as oxidant, and potassium ferrocyanide could replace sodium dithionite as reducing agent. Results to be described below show that changes in the kinetics are not responsible for the loss of signal.

2. Intermediate potential. Experiments conducted through the range of potential from +0.05 to +0.35 v showed no variation in the absorbance change spectra.

3. Low potential. The reversible light-induced absorbance changes in R. rubrum chromatophores are not observed if the redox level of the solution is below -0.15 v. Figure IV-3 shows the effect of lowering the potential through the region of +0.02 v to -0.1 v. The oxidized forms of indigo tetra- and trisulfonic acid were present at 2×10^{-5} M as "buffers" in the potential ranges +0.02 to -0.06 and -0.06 to -0.10 v,

Fig. IV-3. Variation with "low" potential in the light-induced absorption changes at 810 and 792 mμ in R. rubrum chromatophores. 0.05 M phosphate buffer, pH 7.4. Absorption at 880 mμ was 1.22. Total concentration of reductant used varied from 5×10^{-6} M to 6×10^{-5} M. Reducing agent, reduced indigodisulfonic acid. The dyes indigotetrasulfonic acid and indigotrisulfonic acid were present at approximately 2×10^{-5} M concentrations to act as redox buffers. , experimental points obtained from the sum of Δ OD at 792 and 810 mμ as recorded by the Cary spectrophotometer using very high light intensity; points were recorded sequentially as the potential was lowered. , experimental point obtained as circles except $K_3Fe(CN)_6$ was added to -0.12 v sample. , experimental points taken from a separate experiment in which indigotetrasulfonic acid (1×10^{-5} M) was the only dye present. , experimental points obtained from steady-state values at 792 mμ using the kinetic spectrometer; these data have been corrected for changes in decay rate over this potential range (Figure IV-12) as noted in the text. The solid and dashed lines were obtained by use of the equation $E_h = E_m + RT/nF \ln l.s./(m.s.-l.s.)$ with $E_m = -0.044$ v and n = 1 and 2 respectively. As in Figure IV-2, m.s. = maximum signal observed between +0.35 and +0.30 v and l.s. = the light-induced signal observed at the potential reported. Anaerobic conditions.

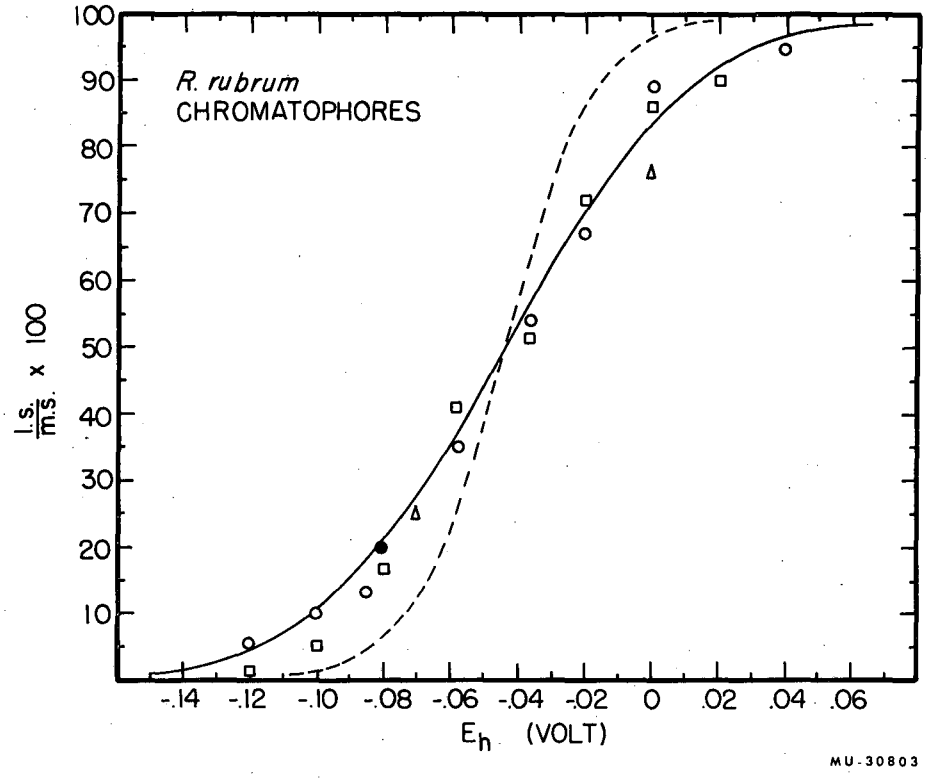
R. rubrum
CHROMATOPHORES
100
90
80
70
60
50
40
30
20
10
I.S./M.S. x 100
-.14
-.12
-.10
-.08
-.06
-.04
-.02
0
.02
.04
.06
Eh (VOLT)
MU-30803

respectively. The potential was lowered slowly by the addition of reducing agent, reduced indigodisulfonic acid, prepared separately by 95 percent reduction with sodium dithionite. The absorbance changes at 792 and 865 mμ disappeared in the same relative proportions as the potential was lowered. Unlike the ferricyanide treatment, this reduction does not replace the light-induced signals with chemically-produced counterparts. The only pronounced change in the visible or near infrared spectrum is the reduction of an iron porphyrin complex (probably the Rhodospirillum heme protein of Kamen and Bartsch.[111] The low potential data are also compared with theoretical curves representing one- and two-electron transitions in Figure IV-3. The data are consistent with a one-electron change with a midpoint of -0.044 v. Again, results to be described below show that changes in the kinetics are not alone responsible for the loss of signal.

The effects of 10^{-5} M concentrations of other strong reducing agents (sodium dithionite, semiquinone of methylviologen, and reduced phenosafranine) were each examined on separate samples of well deaerated R. rubrum chromatophores. In each case no light-induced signals could be observed in the presence of these reducing agents.

Discussion

The observation that we can duplicate in a quantitative manner the action of light by use of a moderate oxidant (ferricyanide) is not surprising in terms of the theories so far discussed. We would predict for bacterial systems that that a chlorophyll-type molecule would undergo photo-oxidation if the analogy with the Hill-Bendall picture did hold. The experiments just considered indicate a one-electron photo-oxidation, characterizing the reacting pigment as having a redox potential of

+0.44 v. In earlier discussions of the difference spectra (page 97) evidence was summarized that indicated that this pigment has a reduced band in the 865-880 mμ region, in vivo, making a porphyrin-type pigment a likely candidate.

The titration of absorption changes at low potential can also be derived from our working hypothesis if a few more details are added to the mechanism. Thus, the proposed reaction with light is:

$$BChl(865) \xrightarrow{h\nu} BChl^{+} + e^{-} \qquad (IV\text{-}1)$$

There is no evidence for a "pool" of "free" or solvated electrons in these systems, so we must, in fact, have a very rapid reaction with an electron acceptor. Now the normal terminal acceptors such as ferrodoxin or pyridine nucleotides have been removed during preparation. Furthermore, no substrate has been added. The reversible signals that we observe must then constitute a closed cycle. Thus a better representation of the elementary reactions which takes both of these observations into account is given by:

$$\begin{aligned} BChl + X &\overset{h\nu}{\rightleftharpoons} BChl^{+} + X^{-} \\ X^{-} + Y &\rightleftharpoons Y^{-} + X \\ Y^{-} + BChl^{+} &\rightleftharpoons BChl + Y \end{aligned} \qquad (IV\text{-}2)$$

In such a mechanism a strong, externally added, reducing agent can interact in several ways. First, any of the compounds, BChl, X^{-}, or Y^{-}, might be reducible to another nonreactive state. Second, X or Y or both might be reduced completely, leaving no readily available electron acceptor. Thus the realization that the photochemistry requires a cyclic process in these cell-free preparations offers various explanations for the observation that too low a potential

will stop the entire sequence. The picture of a photo-induced electron transfer from a high potential donor ($E_m \geq +0.44$ v) to a low potential acceptor ($E_m \leq -0.04$ v) is quite consistent with the mechanisms so far considered. The electron acceptor should be susceptible to spectroscopic study though it may absorb well into the UV. In addition, we have seen some evidence that a BChl-type molecule is intimately involved in the photo-oxidation. Tentatively, we assign this molecular species the role of the "trapping site" at which quantum conversion takes place in bacterial photosynthesis.

New and interesting information pertinent to the nature of the photo-active species and their interaction(s) with their environment was obtained by treating chromatophores with very strong oxidants. This work is described below.

Separation of photoactive pigments from bulk pigments by use of strong oxidants

Irreversible oxidation of large amounts of the long wavelength absorbing pigments in the presence of an excess of strong oxidant[107] leaves a material which still has, on reduction, absorption changes of the same magnitude as the original samples. Figures IV-4, 5, 6 compare the light-dark changes and absorption spectra of K_2IrCl_6-treated chromatophores prepared from R. rubrum, R. spheroides, and Chromatium. The similarity of the absorbance of these materials in the near infrared is as striking as the dissimilarity among the absorbance of the original chromatophores. Note also the loss of the light-dark carotenoid change in R. spheroides (compare changes at 444, 460, 470, 487, 510, and 522 mμ in Figures IV-5 and III-10), and the participation of what is probably an iron porphyrin complex in the light-induced changes

of [illegible].

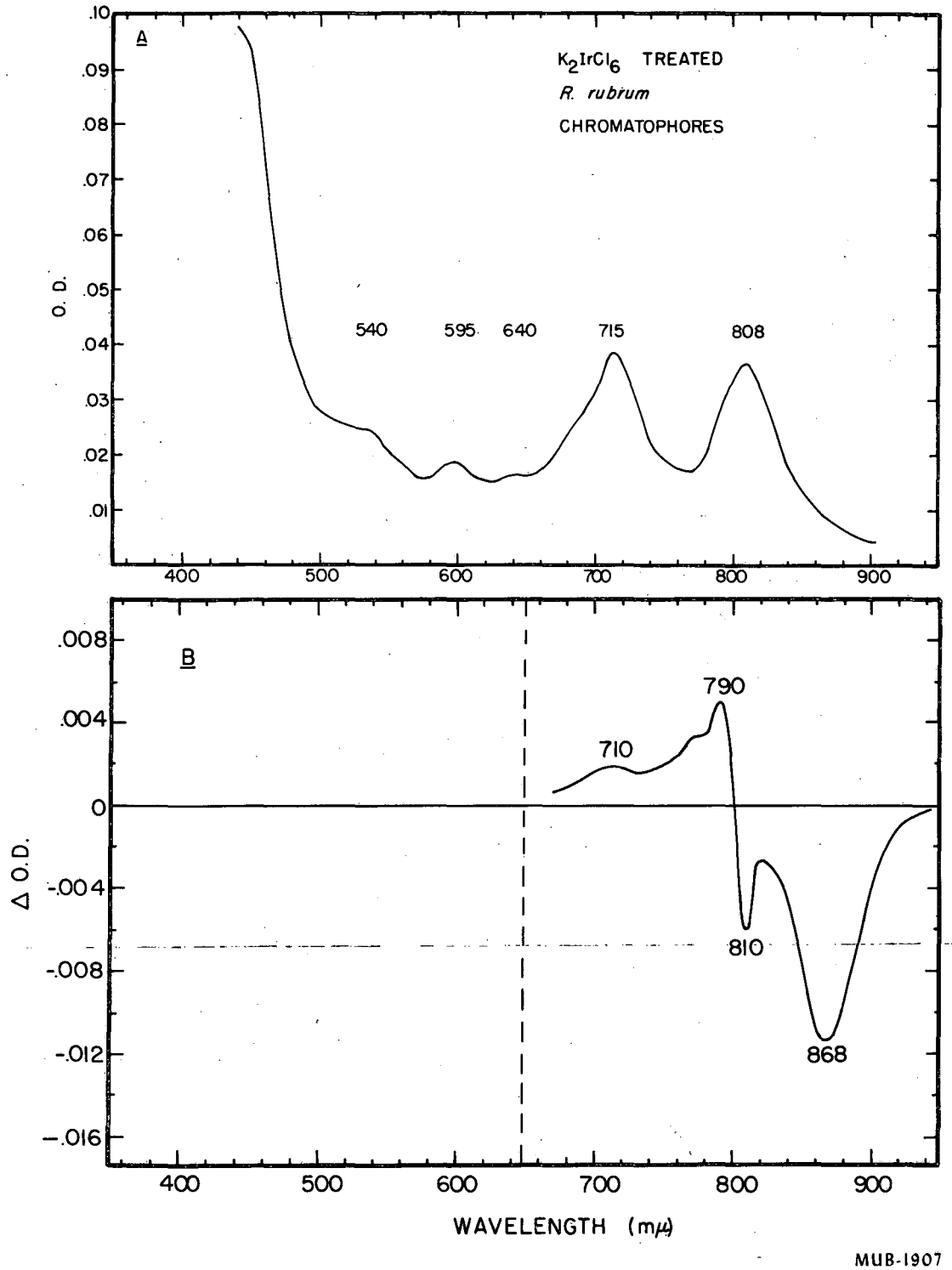

Fig. IV-4A. Absorption spectrum of K_2IrCl_6-treated R. rubrum chromatophores suspended in 0.05 M phosphate buffer, pH 7.4; 1 cm cuvette.

Fig. IV-4B. Light-induced absorption changes in the sample whose absorbance is given above; 1 cm cuvettes.

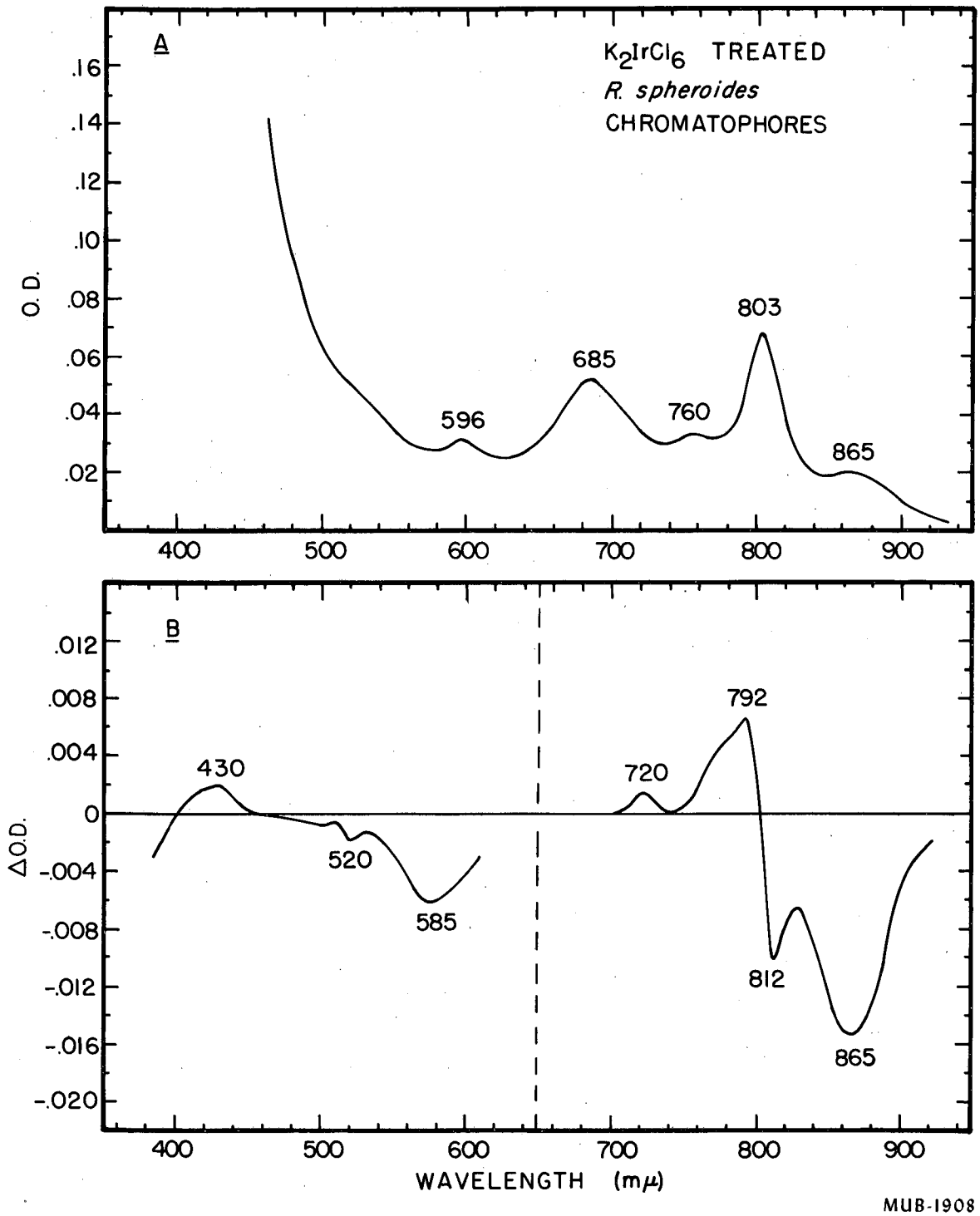

Fig. IV-5A. Absorption spectrum of K_2IrCl_6-treated R. spheroides chromatophores suspended in 0.05 M phosphate buffer, pH 7.4. Excess $K_4Fe(CN)_6$ present (approx. 0.05 M); 1 cm cuvette.

Fig. IV-5B. Light-induced absorption changes in the sample whose absorbance is given above; 1 cm cuvettes.

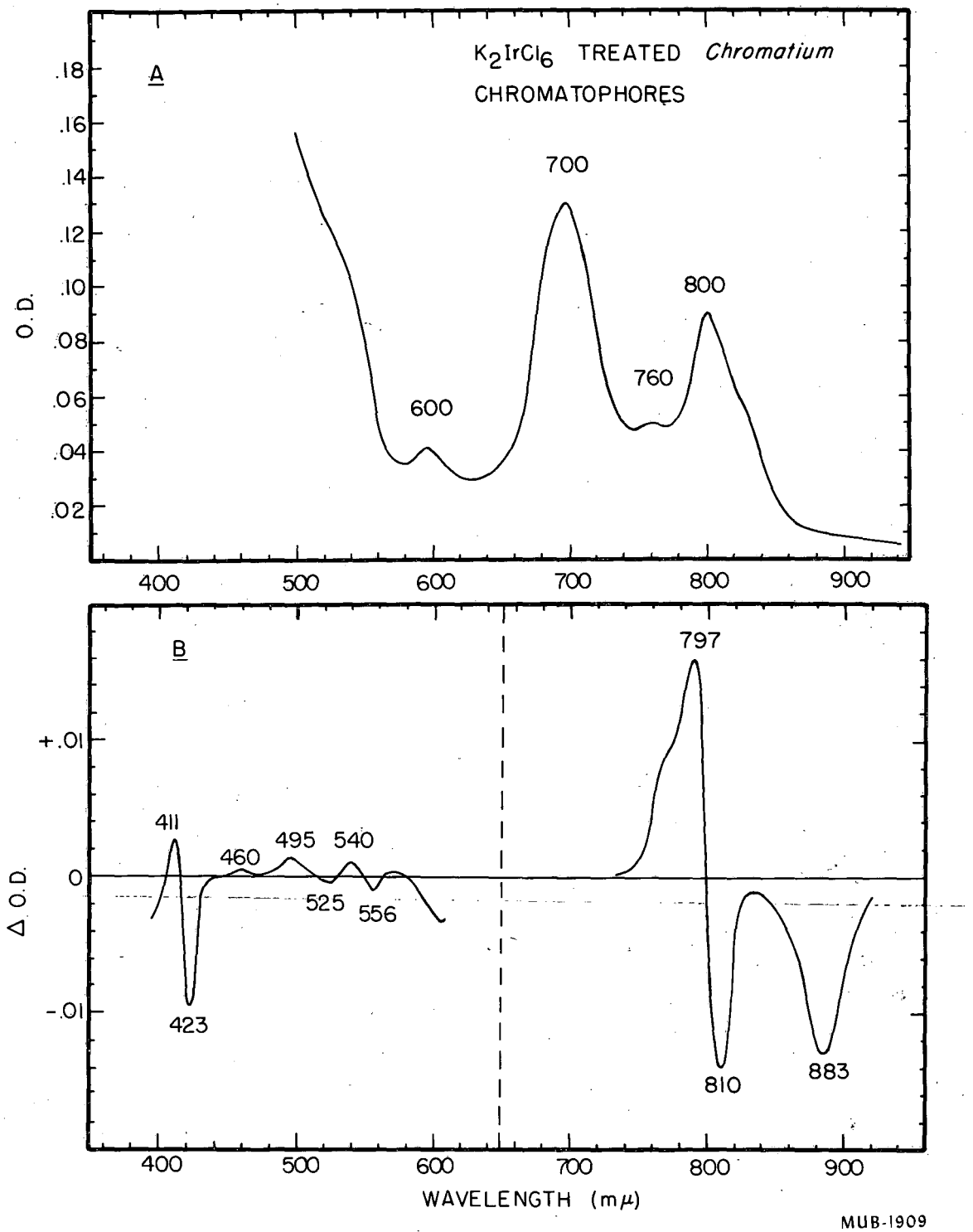

Fig. IV-6A. Absorption spectrum of K_2IrCl_6-treated Chromatium chromatophores suspended in 0.05 M phosphate buffer, pH 7.4. Excess $K_4Fe(CN)_6$ present (approx. 0.05 M); 1 cm cuvette.

Fig. IV-6B. Light-induced absorption changes in the sample whose absorbance is given above; 1 cm cuvettes.

of Chromatium (compare similarities at wavelengths 410, 423, and 556 mμ in Figures IV-6 and III-13. Higher incident light intensity is required to produce the same size absorption change in these K_2IrCl_6-treated systems as in the unmodified material; this seems to reflect the loss in absorption rather than a major change in quantum efficiency.

If the K_2IrCl_6-treated material from R. rubrum is reduced with ferrocyanide, dialyzed, and then is chemically titrated in the dark with ferricyanide, absorbance changes identical to those obtained by the action of light can be observed. Thus, it appears that the bulk pigments are not essential components in either the light-produced absorption changes or the chemically-induced changes.

One very exciting aspect of the K_2IrCl_6-treated preparations was that it had a much higher ratio of active to bulk pigments. At best the relative concentration of active pigment was increased 10- to 20-fold, which left it at the level of 10% of the total IR absorption. However, this was a sufficient enhancement so that it was thought profitable to explore spectroscopic and chromatographic means to attempt a more positive identification of the active components. These experiments were performed in collaboration with Dr. E. Gould.* The experimental details have been reported elsewhere.[112] The important findings for our present purposes were that only bacteriochlorophyll and its oxidation products could be obtained from acetone extracts of the oxidized chromatophores. Thus we will continue to adopt the hypothesis that bacteriochlorophyll is the active site. The unique resistance of the "trap" towards irreversible oxidation is ascribed to some feature of the protein environment of certain of the bacteriochlorophyll molecules.

---

*Present address: Stanford Research Institute, Menlo Park, California.

In summary, the removal of the bulk pigment absorption produces only small changes in the IR spectra of the photosignals and does not change their magnitude. It thus appears that the 880 mμ pigment in R. rubrum, the 850 mμ and part of the 800 mμ pigment in R. spheroides, and the 880 and 800 mμ pigments in Chromatium, which can be irreversibly removed by chemical oxidation, are not essential components in either the light-produced absorption changes or the light-produced ESR signals,[107] both of which may be produced qualitatively and quantitatively in the same fashion in their absence as in their presence. Thus, the bulk pigments can only act as energy-gathering and energy-transferring systems which may supply the photoactive unit. This clean-cut separation of the active and bulk pigments offers considerable support to the concept of a "photosynthetic unit".[10,21,30,110]

B. KINETICS

Kinetic measurements have a long and productive history as the "method of choice" in mechanistic studies. It would be profitable at this time to outline the types of information one can expect when such measurements are performed on complex systems such as the ones of interest to us. These ideas will be developed in a more quantitative fashion in the next chapter.

Assume for the present purposes that the photosynthetic reactions are of the general forms:

$$a)\quad Z + A = Z^- + A^+, \text{ "Light" reaction} \qquad (IV\text{-}3)$$

$$b)\quad Z^- + X = Z + X^-, \text{ "Dark" reaction} \qquad (IV\text{-}4)$$

Assume that in the whole cell reactions these electron transfer steps form a reaction sequence from an ultimate electron donor to a terminal electron acceptor. In cell-free systems the reaction chain may involve various added substrates or redox reagents or the reactions may proceed by a cyclic path involving no net electron transfer to or from the environment. In the dark the concentrations of the various redox couples are determined by their effective potentials and their participation in the reactions associated with the normal cell metabolism. When light is applied the concentrations of the intermediates shift from the steady-state values. Figure IV-7 shows, schematically, some of the time courses that might be seen for light-induced absorbance increases.

A indicates the pattern that might be expected for a typical "intermediate" somewhere in the middle of the reaction chain. Some time is required after the light is turned on before reaction begins. This lag time or induction period is associated with the time required for precursors to respond to the light. Similarly, when the light is turned off, preceding intermediates do not return to their dark steady-state concentrations "instantaneously", and the time required for a substantial change in the precursor concentrations may also create a "light off" induction period. These induction periods are functions of light intensity, the various rate constants, and the initial concentrations along the chain so that their magnitudes cannot be predicted without considerable additional information. Also indicated in Figure A are the times for half-rise and half-decay, the maximal rise and decay rates, and the steady-state level of the signal, which are all useful parameters with which to characterize the reaction chain.

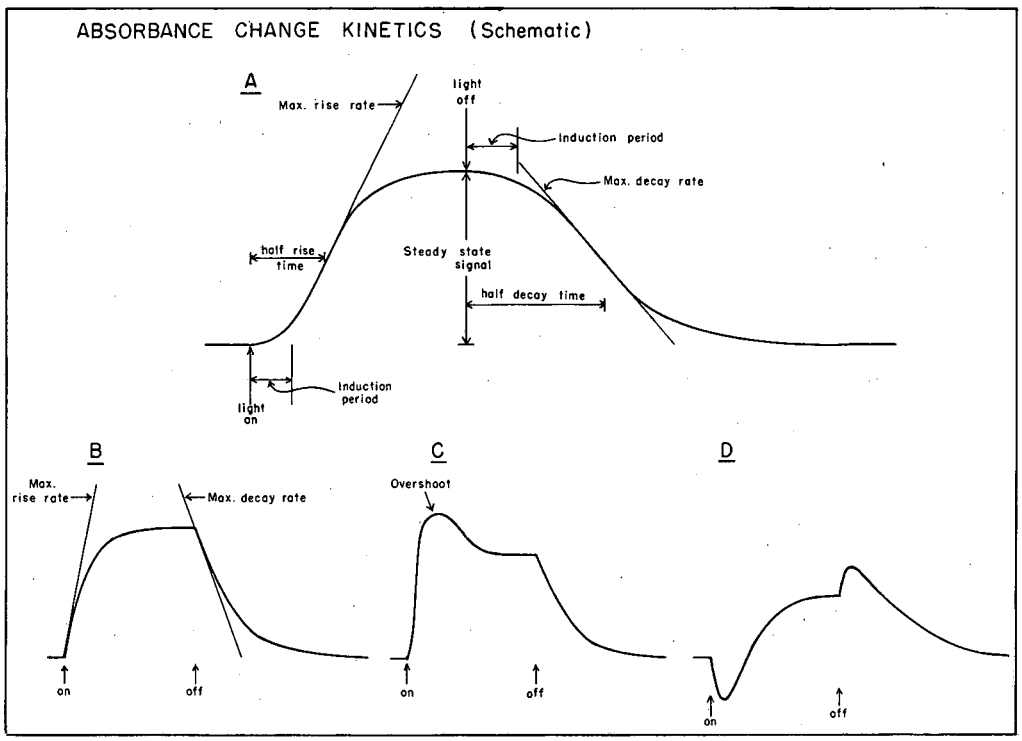

Fig. IV-7. Schematic absorbance change kinetics: see text for details.

Signal B has no observable induction periods. Such a signal is expected for the primary quantum conversion steps and for any fast "follow" reactions. The data in signal B is more readily translated into other useful information because of the lack of induction periods. The initial rise rate, which is now the maximum rise rate, can be related to the maximum quantum yield of the intermediate reaction.* The initial decay rate is useful as a measure of the steady-state rate of electrons flowing through the intermediate. This rate can also be converted to the "steady-state" quantum yields.*

Signals C and D illustrate some of the complicated "over-shoot" and "under-shoot" transients that may be seen in a cyclic or straight-chain system with appropriate time constants. Further complications could arise from interactions of the two different photochemical reactions postulated for "green plant" photosynthesis. And any of the kinetic patterns could be added together by having two (or more) different compounds absorbing at the same wavelength.

There are several obvious differences between this type of study and photochemical or thermal reactions of less complex systems. One is normally interested, in these latter cases, in relating the rate of production of products to the concentration of reactants. One ordinarily formulates a hypothesis based in large part on the concentration dependence of the reaction rate. The biological system involves three major differences. First, the reactions are, under many conditions, zero order with respect to substrate concentration, being limited by rates along the chain itself. Thus, our problem needs to be redefined.

---

*For absolute calculations one would need extinction coefficients.

We will usually wish to express reaction rates in terms of intermediate concentrations. Second, we will normally not be able to exercise any direct control over the internal reactant concentrations and thus must resort to various indirect procedures to test and even to develop the rate laws of interest. Third, increasing amounts of evidence, some of which we examined in the last section, point to independent photoactive units which may contain a very small number of reactive molecules. The rate laws displayed by a collection of a large number of such small units will not, in general, be the rate laws exhibited by similar reaction mechanisms occurring in normal solution chemistry.

As mentioned earlier, all of these qualitative observations will be dealt with in a more quantitative fashion in the next chapter. They should be kept in mind as we examine the kinetic studies described below.

I. Absorption Change Kinetics in Bacterial Chromatophores*

Experimental. The multiscaler detection system was used. All of the work described here was done with the neon discharge lamp (previously described) as the actinic source. The filters and photomultipliers needed for the various spectral regions are given in Table VI. Note that the same excitation wavelengths were used for most of the detecting wavelengths. Chromatophores were prepared and redox adjustments were performed as with the titration experiments described earlier. An anaerobic cell for the kinetic spectrometer which could be used to remove samples form the major redox control equipment was shown in Figure IV-1.

*This work is part of the redox study done with Dr. Loach.

Table VI

Filters and Photomultipliers Used in the Kinetic Spectrophotometer

Detecting wavelengths (mμ)	Exciting wavelengths (mμ)	Photomultiplier	Detecting beam filters*,**	Exciting beam filters**
750-1100	580-700	Dumont 6911	5031 (2)	3480 4600 (2), IF#
350-500	580-700	Dumont 6292	5031 (2)	3480 4600 (2) IF#
607	650-700	Dumont 6292	IF##	IF# 2030

*Placed in front of photomultiplier

**All numbers refer to Corning color glasses

#Baird-atomic broad band interference filter (transmits 580-720 mμ)

##Baird-atomic narrow band interference filter (transmits 607 ± 6 mμ)

Kinetics

Rise and decay times were studied as a function of wavelength, light intensity, and potential.

Variation of kinetics with wavelength. Typical rise and decay curves at 433, 792, 810, and 865 mμ for deaerated samples ($E_h \simeq +0.35$ v) are shown in Figures IV-8 and IV-9. The rise times were all inversely related to the absorbed intensity from the actinic source. Hence, different sources, high optical densities, or the presence of colored reagents could change the rise constants. The decay constants were not particularly sensitive to these effects. Although the time for half-rise was nearly the same for each band measured, significant differences

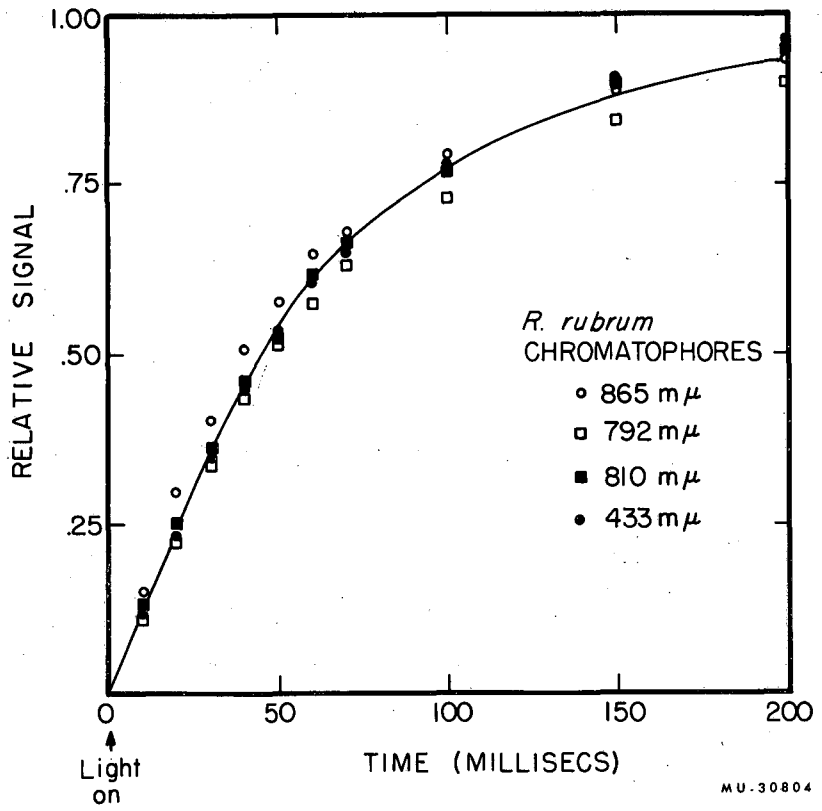

Fig. IV-8. Variation with wavelength in the rise kinetics of the light-induced absorption changes in R. rubrum chromatophores at 433, 792, 810, and 865 mμ. For purposes of comparison signal heights are normalized and all signals are shown as positive. The actinic lamp was on for 0.4 sec. and off for 3.6 sec. Anaerobic conditions; 10^{-4} M $K_4Fe(CN)_6$ present to keep E_h = +0.35 v; 1 cm cuvette; 0.01 M phosphate buffer, pH 7.4; OD at 880 mμ, 0.70.

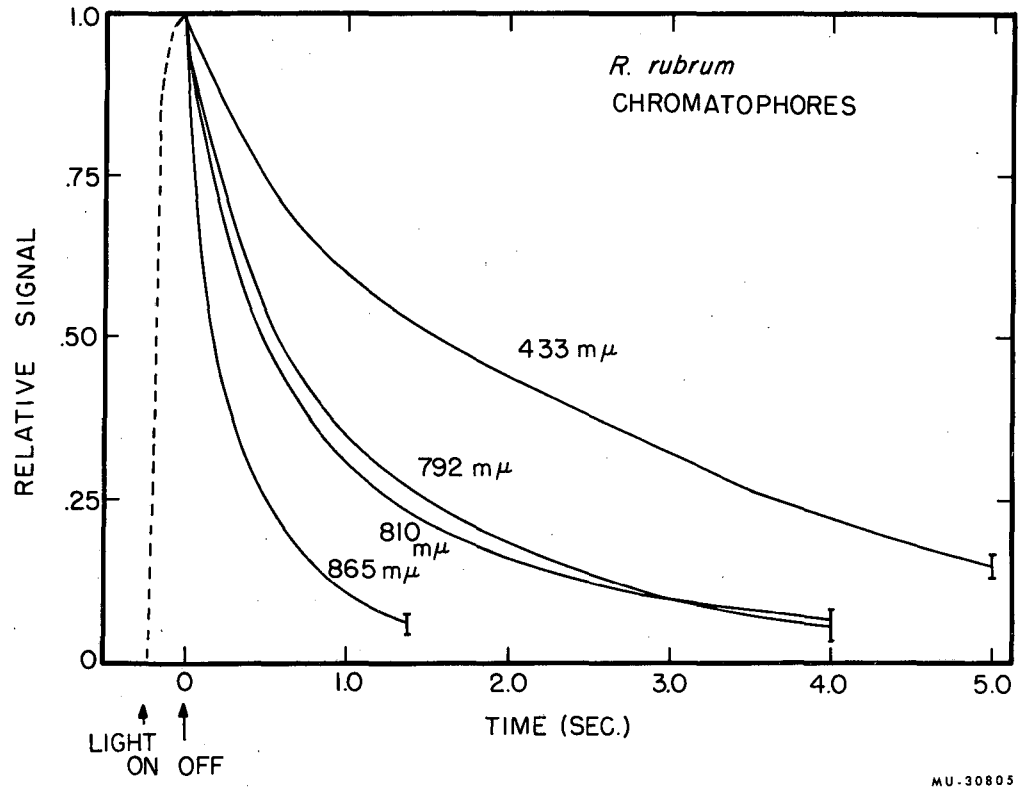

Fig. IV-9. Variation with wavelength in the decay kinetics of the light-induced absorption changes at 433, 792, 810, and 865 mμ in R. rubrum chromatophores. Conditions as in Fig. IV-8. The bars represent the total estimated uncertainties including base line drift and sample variability. The actinic lamp was on 0.5 sec. and off 7.5 sec.

occurred in the decay kinetics. The rise and decay kinetics are complex. The simplest interpretation of the data is a first-order (or pseudo first-order) forward reaction and two parallel first-order (or pseudo first-order) decay (or back) reactions (Figures IV-10 and IV-11). Rate constants for the first-order reactions are compared in Table VII.

Table VII

Rate Constants for Photoabsorption Changes*

[assuming a first-order forward reaction (K_f) and two parallel first-order back reactions (K_{B1}, K_{B2})]

Wavelength (mμ)	K_f (sec.$^{-1}$)	K_{B1} (sec.$^{-1}$)	K_{B2})sec.$^{-1}$)
433	16.3 ± 0.3	0.9 ± 0.2	0.2 ± 0.06
792	15.9 ± 0.3	1.7 ± 0.3	0.4 ± 0.1
810	16.1 ± 0.3	1.9 ± 0.3	0.4 ± 0.1
865	16.3 ± 0.3	4.8 ± 0.6	0.9 ± 0.2

*Deaerated samples, $E_h \sim +0.35$ v

These different decay kinetics at different wavelengths indicate that the absorption changes studied belong to at least three different pigments (Figure IV-9).*

Variation of kinetics with light intensity. A further study of the kinetic order of the decay reactions involves changing the steady-state level of photoproducts by variation of the incident light intensity.

*This conclusion is only rigorous if we keep to our assumptions that the various redox couples have only two forms.

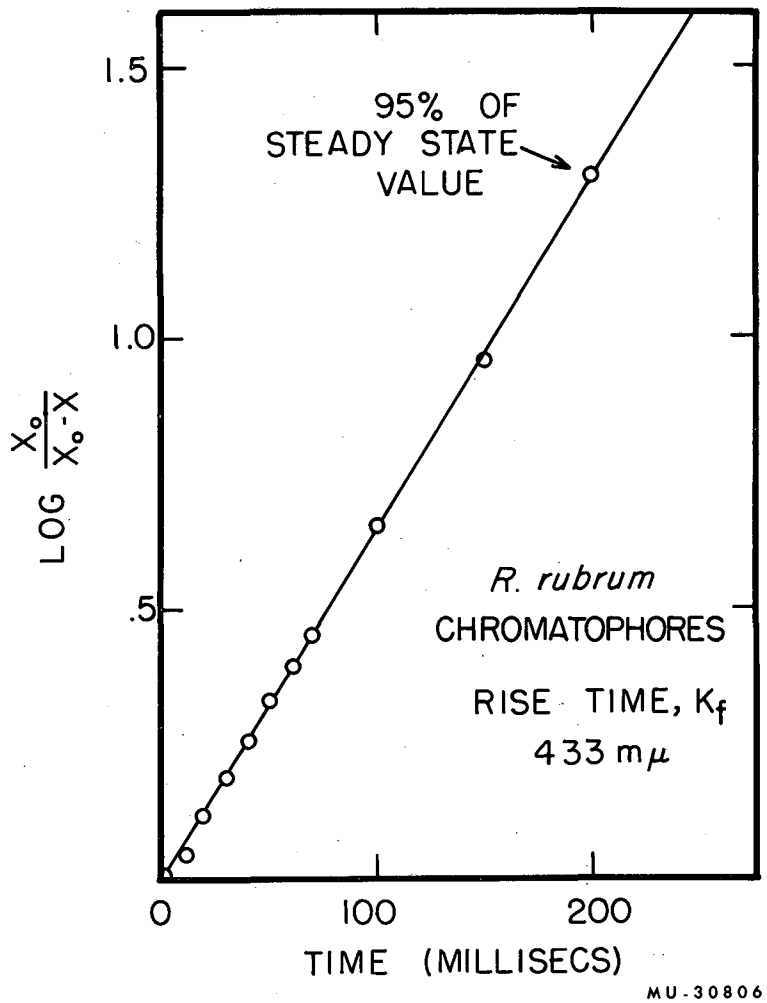

Fig. IV-10. Analysis of rise kinetics for 433 mμ as shown in Fig. IV-8. X_o = maximum observed steady-state absorption change, X = absorption change at any given time. The solid line is the theoretical plot for a first-order reaction with K_f = 16 sec^{-1}. Other wavelengths show similar behavior.

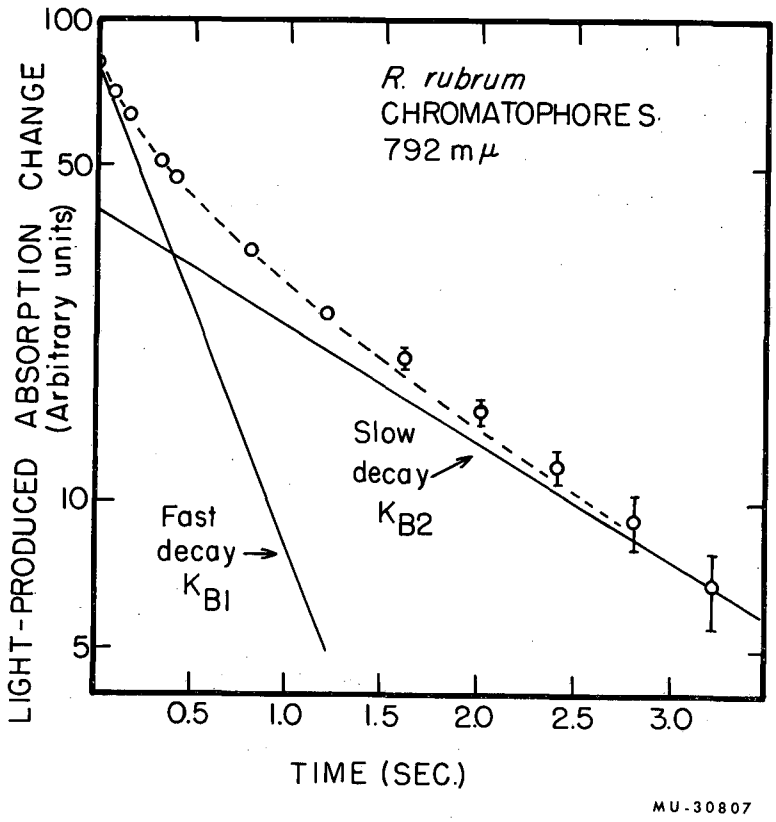

Fig. IV-11. Analysis of decay kinetics of the light-induced absorption changes at 792 mμ in R. rubrum chromatophores shown in Fig. IV-9. The vertical scale is logarithmic. Two decay processes are shown by solid lines (K_{B1} and K_{B2}). The computed decay pattern (dotted line) was obtained from

$$X_{caln} = \alpha \exp(-K_{B1}t) + \beta \exp(-K_{B2}t)$$

where X = concentration of photoproduced species, K_{B1} and K_{B2} are first-order decay constants 2.0 and 0.46 sec^{-1}, respectively. β is the extrapolated Y intercept for the slow decay process. α = total initial signal minus β. t is time measured from when the lamp went off.

A fourfold change in the steady-state level produced less than a 20 percent change in the time for half decay. This observation strongly supports the assignment of one or more first-order or pseudo first-order decay reactions to each of the three different pigments.

Variation of kinetics with potential. While the rate constant for the forward reaction, K_f, is nearly independent of potential in the regions studied, the decay constant, K_{B1}, is a function of redox potential. Figure IV-12 shows the variation of the first-order decay constant K_{B1} for the changes in the 865 mμ band in the potential range of -0.15 to +0.5 v. The rate constant for the 792 mμ band showed similar behavior. The rapid change in half times in the vicinity of -0.05 v suggests the reduction of a pigment which can then interact with the photo-oxidized materials.

The decay rates never become rapid enough to explain the loss in signals at low potential (or, for that matter, at high potential). For the reactions described here the steady-state concentration of the photo-oxidized species is given by

$$\frac{P^+}{P_o - P^+} = \frac{K_f}{K_B} \quad \text{or} \quad P^+ = \frac{K_f/K_B}{1 + K_f K_B} P_o$$

where P_o is the initial concentration of the oxidizable species, P^+ is the concentration of the oxidized material, K_f is the first-order forward rate constant, K_B is the fast back reaction first-order rate constant. K_f = 16 sec.$^{-1}$, K_B varies from 2 to 14 sec.$^{-1}$ Experimentally the steady-state value of P^+ would fall from 89 percent of P_o to 53 percent of P_o because of the increase in decay constant from 2 to 14 sec.$^{-1}$. Experimentally the steady-state level of P^+ fell to lower than 2 percent for K_B = 14 sec.$^{-1}$ (at E_h = -0.12 v). These findings support the assignment

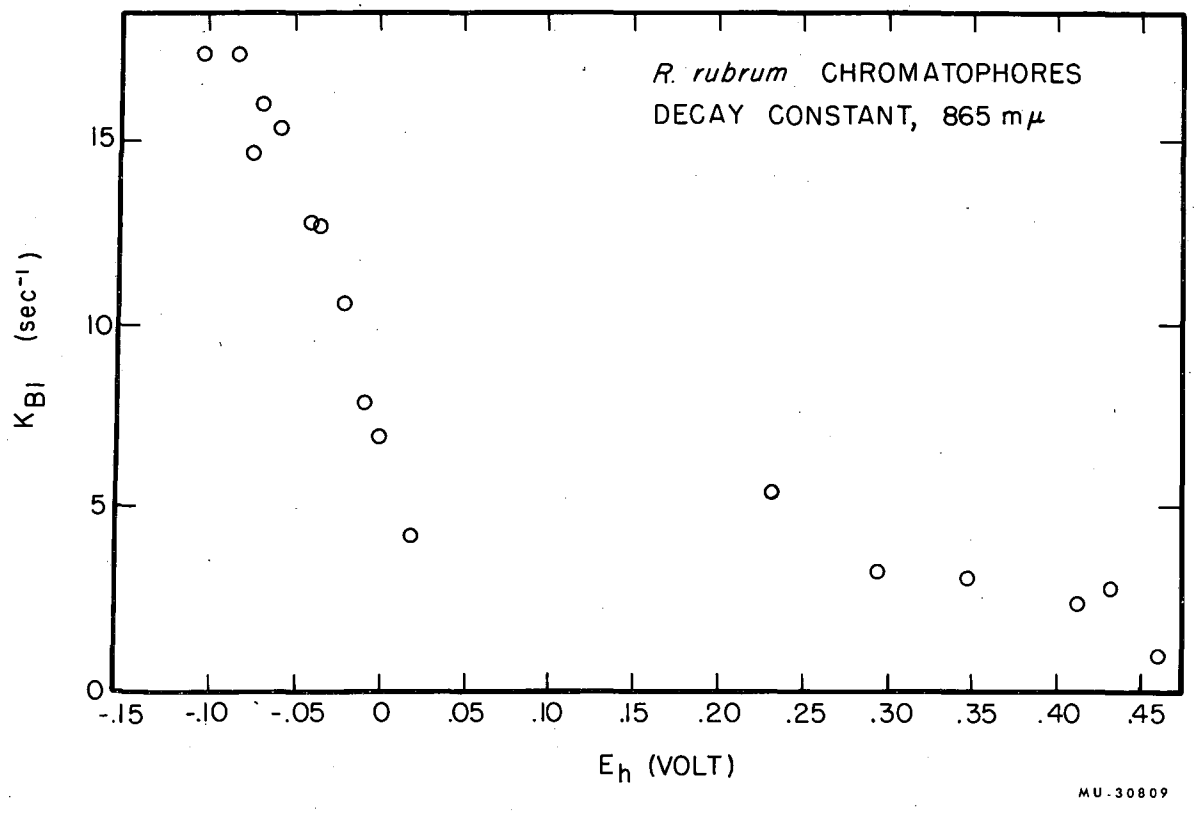

Fig. IV-12. Variation with potential of the decay rate constant (K_{Bl}) of light-induced absorption changes in R. rubrum chromatophores. Experimental conditions as given in Figs. IV-2, 3.

of the losses in the steady-state signal to the titration of pigments required for the appearance of the light signal rather than those hastening its disappearance.

It is of interest to note that the decay rates tend to approach the same high value ($K_B \approx 14$ sec.$^{-1}$) for each of the three wavelengths studied at high concentrations of $K_4Fe(CN)_6$ (> 0.1 M). (Figure IV-13).

Discussion of kinetic findings

The discovery of different decay times for different absorption changes was one of the most striking features of our studies on chromatophores. These results can be documented by the finding of Olson and Kok that, in chromatophores treated with phenylmercuric acetate the behavior of the 433 mμ band was consistent with very slow decay, while the chlorophyll bands were more rapidly reversible.[113] However, kinetics were not measured directly in this work. The difference in decay times we have been considering suggests many other experiments. One extension of this work is discussed in the next section.

The exponential rise and decay curves require further consideration because our theories are certainly predicated upon bimolecular reaction. A model based on the concept of a reaction unit containing very few active molecules is our current favorite. The development is outlined in Chapter V.

II. Kinetic Comparison with Electron Paramagnetic Resonance Signals*

Before leaving the experimental discussion of photosynthesis in chromatophores, we should examine our only major attempt to relate the

---

*In collaboration with Dr. R. Ruby, present address: Department of Biology, MIT, Cambridge, Mass. This material was published in Ref. 114.

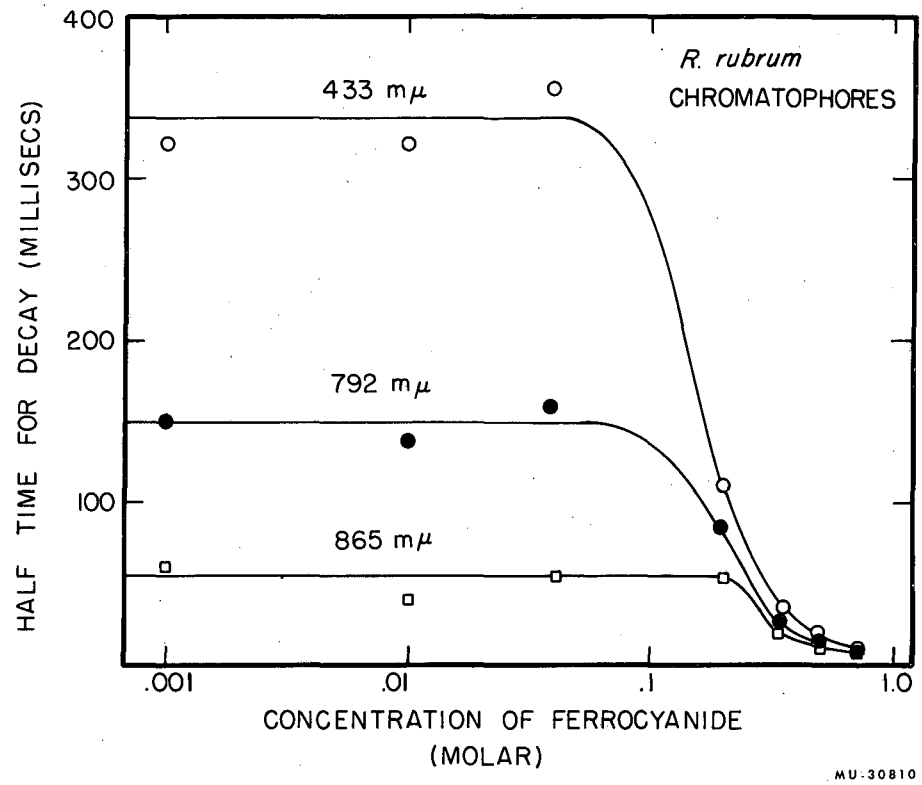

Fig. IV-13. Effect of ferrocyanide concentration on decay kinetics. Potential was held nearly constant with added ferricyanide. Other conditions as in Figs. IV-2, 3.

absorption changes in these systems to other aspects of photosynthesis.

Light-induced electron paramagnetic resonance (EPR) signals have been observed in photosynthetic systems for many years.[115,116] A positive identification of the signal with a definite molecular species has proved difficult on the basis of EPR properties alone. Thus, correlations of these properties with other physical measurements have been sought. Independent studies of absorbance changes in photosynthetic bacteria[30,31,117] have led to the tentative detection of bacteriochlorophyll positive ion, thereby leading to the working hypothesis that the EPR signal might be $BChl^{+}$.[115] This view was strengthened by recent work showing that the bacterial spin signal could be produced by chemical oxidation.[107] Parallel kinetic studies with both spectroscopic methods offered evidence which was not consistent with this hypothesis.

Experimental

The optical spectrometer was the one just outlined above. The EPR spectrometer has been described in earlier publications.[115] Chromatophores from 5-day growth of R. rubrum were prepared in the usual fashion. They were suspended in glycylglycine buffer. The EPR aqueous sample cell (0.4 mm optical path) was used for both spectrometers. Typical experimental conditions were: redox potential +0.30 v; pH 7.5; temperature 22^{+} 2° C; incident light intensities 10^{16} hν/cm^2/sec; absorbance approximately 1-1.5 optical density units.

The EPR signal, $S_{(t)}$, was measured at the point of maximum slope of the absorption curve, and is proportional to the number of observable unpaired electrons. The response of this signal to the light pulse is shown in Figure IV-14. Also shown is an example of the growth of the signal when the light is turned on (when an expanded time scale is used).

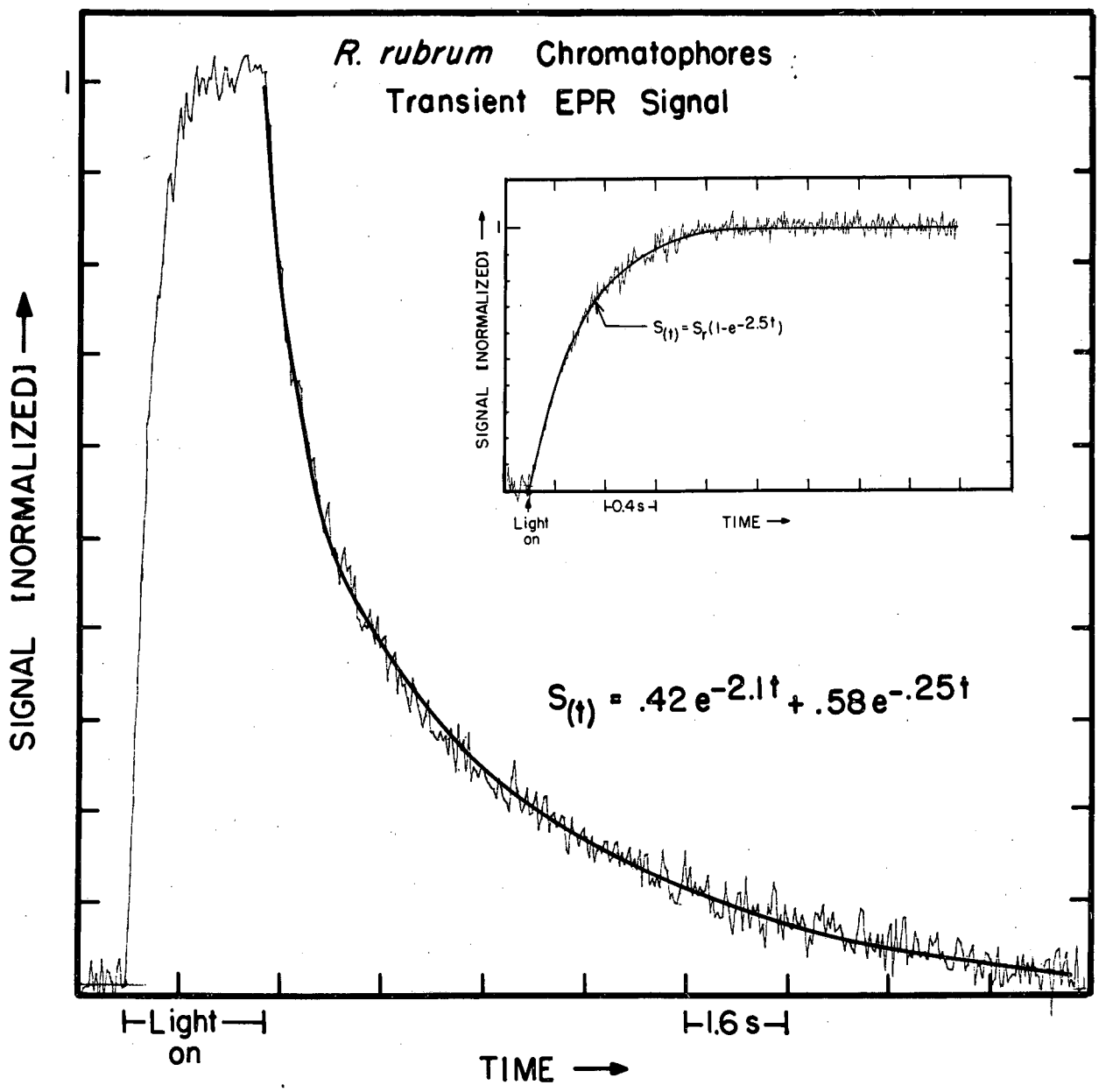

Fig. IV-14. Time response of the electron paramagnetic resonance (EPR) signal to light. The insert is the growth of the EPR on an expanded time scale. Also shown are exponential curves fitting the data. S_r is the normalized steady-state value of the signal.

The growth may be described by the expression

$$S_t = S_r (1 - e^{k_r t}) \qquad \text{(IV-5)}$$

and the decay curve by the expression

$$S_{(t)} = S_d e^{-k_d t} + S_d' e^{-k_d' t}, \text{ with } S_r = S_d + S_d'. \qquad \text{(IV-6)}$$

S_r is proportional to the steady-state of photoproduced spins, S_d and S_d' are proportional to the fraction of photoproduced spins decaying by parallel paths with unimolecular rate constants k_d and k_d'. k_r is approximately the unimolecular rate constant for spin production.

As we have seen, the changes in absorption show similar kinetic responses although the time constants varied through the major bands in the light-dark difference spectra. We compared the time course of the EPR and optical signals, with the results shown in Figure IV-15.

Conclusions

The following conclusions may be drawn from this evidence: (1) The rise and decay kinetics of the spin signal are the same as the kinetics of the 433 mμ absorbance changes, within experimental error. Of the major absorbance changes, only the one at 433 mμ shows this close agreement. We thus assign the observed EPR signal to the molecular species which produces the 433 mμ optical change. (2) The molecules responsible for the absorbance change at 433 mμ are not the same as those molecules responsible for the absorbance change at 865 mμ because of the much slower decay rate of the 433 mμ band.

Unfortunately, we have little information about the nature of the 433 mμ pigment. The difference band is most often found as a large signal in damaged cells (heat-treated) or in chromatophore preparations. Even is we assume that it is the source of the EPR signal in chromatophores, there is no guarantee that this compound plays an important role in photosynthesis.

NEUTRALIZING EFFECT OF RABBIT ANTI-HUMAN URINARY ERYTHROPOIETIN ON ERYTHROPOIETIN EXTRACTS

Extracts	PERCENT RADIOIRON INCORPORATION INTO RBC OF POLYCYTHEMIC MICE	
	Normal rabbit serum	Anti-E serum
Phenylhydrazine anemic sheep plasma	13.51±1.36*	3.91±0.50
Human urinary erythropoietin	11.88±1.11	0.28±0.07
Saline control	0.18±0.04	

* Standard error of the mean

MU-32311

Fig. IV-15. Comparison of EPR and OD signals from the same sample of R. rubrum chromatophores. Experimental conditions are given in the text.

III. Kinetic Studies of Oxygen-evolving Systems

In contrast to the bacterial studies, most of the work on "green plants" has been done with whole cells, and particularly with the unicellular algae, Porphyridium cruentum, Chlorella, and Scenedesmus. Some general remarks are in order.

Almost all systems—including the photosynthetic bacteria—show two broad ranges of decay time constants for the light-minus-dark transients. The fast reactions in Porphyridium or Chlorella have times for half decay of about 0.02 seconds. Chloroplasts or chromatophores have normal decay times of a second, but the reactions in these samples are extremely sensitive to previous treatment and environmental conditions. However, there are also a class of reactions with time constants of several minutes or longer. For example, the cytochromes in some chromatophore or chloroplast preparations oxidize when first exposed to light and are not reduced in the dark for extremely long times (many minutes or hours).[110,118] Similarly, some of the difference bands shown in Figure III-1 for Chlorella display different kinetics on the first flash of light as opposed to later flashes (Figure IV-16). It takes two or three minutes in the dark before the system reverts to its original behavior. These slowly reversing reactions could well be of great importance to the proper operation of the photosynthetic mechanism. However, they have been relatively little studied, in part because of considerable technical difficulties involved in very slow measurements. Also there is a strong presumption that the basic quantum conversion steps and reactions closely associated with them will show the rapid decay kinetics which imply rapid turnover.

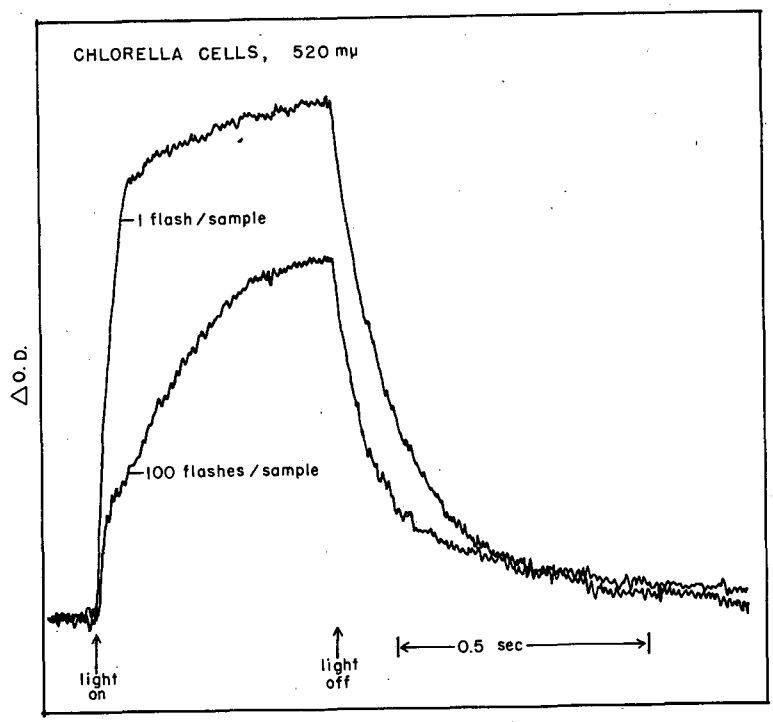

Fig. IV-16. Kinetic curves for the 520 mμ band of Chlorella, showing the difference between the response to light after a very long dark time and the normal repetitive experiment. 1 flash/sample: obtained in a stop-flow apparatus, about 10 minute dark time. 100 flashes/sample: obtained under normal conditions of .25 seconds light/.75 dark.

Ordinarily, the whole cell responses show many similarities to those of the bacterial chromatophores discussed in the last section. The signals are almost always lacking induction periods.* This is true even for the signals produced by the first flash of light after a long dark time. Rise times were very sensitive to light intensities, varying approximately linearly over the intensity range available to us. Decay times, but not initial decay rates, were much less sensitive. The decay kinetics usually display the two exponential functions found for the bacterial kinetics. Unlike the chromatophores, one customarily observed differences in rise times in looking at the various intermediates. Figure IV-17 indicates some of these differences for Chlorella. The whole-cell decay patterns show relatively little difference from one compound to another, probably indicating that the whole cell reactions are closely coupled to each other. Representative absorption change kinetics obtained from normal, healthy cells are shown in later figures (IV-18, 19).

Electron flow experiments

The great wealth of kinetic data has proved relatively unenlightening upon close scrutiny. One would hope, of course, for clear indications of reaction sequences along the electron transport pathway. In fact, the almost complete absence of induction periods under normal conditions makes it very difficult to assign detailed reaction mechanisms.

We have chosen to approach the problem from a different standpoint. As mentioned earlier, it is possible to measure electron flow rates by measuring the initial decay rates from an illuminated steady state. If we make such measurements under conditions which are known (independently) to influence the overall rates of reaction from CO_2 to O_2 we can look for coordinated differences in the kinetics of the (presumed) intermediates. Experiments of this type are described below.

*The minimum induction period that could be determined is limited by the on and off times of the flash (a few milliseconds).

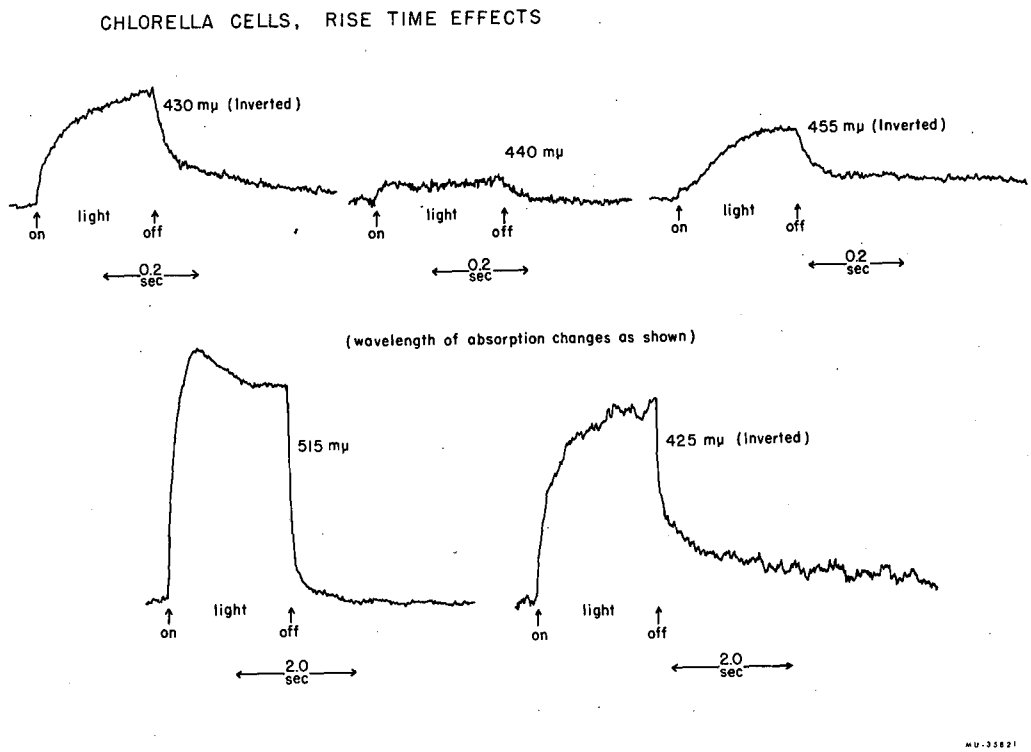

Fig. IV-17.

Rise time effects in Chlorella. Notice the differences in the half-rise time for the 430 and 440 mμ bands. Excitation wavelength: 660-670 mμ. Aerated Chlorella cells, 0.0. 1.0 at 678 mμ, suspended in phosphate buffer at pH 5.0.

One of the simplest starting points for an examination of electron flow was suggested by the Emerson "red-drop" and "enhancement" experiments (Chapter III). These showed that one could influence electron flow rates (steady-state rates of O_2 evolution) by varying the wavelength of the exciting light. It was to be expected, then, that the decay kinetics of the spectroscopic intermediates would also display a sensitivity to excitation wavelength. Several workers had reported that the steady-state level of chlorophyll,[51] cytochromes,[66,119,120] and quinone[79,82] is closely associated with the color of the actinic light employed. In general, alterations in the concentrations of reactive species would be expected to result from differences in the rise and/or decay kinetics associated with the photo-reactions.

Experimental

Materials. Chlorella pyrenoidosa was grown in continuous culture as described in Ref. 1, Chlorella ellipsoidea, Scenedesmus obliquus, and Porphyridium cruentum were grown in cotton-plugged 125 ml flasks. Chlorella was grown on modified Meyers' medium,[121] Scenedesmus on Lynch's medium,[122] and Porphyridium on artificial sea water. Cultures were normally used resuspended in growth medium to an optical density of 1.0-1.5 in the 680 mμ chlorophyll band.

Chloroplasts were prepared by standard techniques.[123] Dichlorophenyldimethylurea (DCMU) was purchased from dePont de Nemours, Wilmington, Delaware. 2,6-Dichlorophenol-indophenol (DCPIP) was purchased from K and K Laboratories, Jamaica, N. Y.

We used the digital memory spectrometer for these studies. The actinic source was the 500 mm Bausch and Lomb monochromator described earlier, used in conjunction with the stepping motor shutter. For some

of these experiments we used a 150 W tungsten lamp as a second actinic source. In some experiments it provided a continuous "background" light which was focused on the same face of the sample cuvette as the first actinic beam. Narrow band interference filters (Baird-Atomic) and suitable Corning color glasses were used to select the desired wavelengths. Typical filter half-band widths were 5-10 mμ. The photomultiplier tube was protected from the actinic light with complementary filters.

Relative light intensities were measured with a silicon cell (Hoffman Type 120 CG). Maximum incident intensities were of the order of 10^{16} quanta/sec/cm^2.

Errors

The reproducibility of the data in these experiments is limited by coherent noise, low frequency noise, and changes in the biological material. In practice, proper triggering and the use of stable power supplies place the electronic noise level well below the "biological noise". Typical limits on the day-to-day reproducibility of magnitude and rate data were ± 10 percent and ± 30 percent respectively for samples of comparable preparation and treatment. Undoubtedly, variations in the physiological state of the organisms are principal components producing these fluctuations and will ultimately require specific investigation. There is the presumption that these fluctuations do not reflect day-to-day alterations in the basic quantum conversion apparatus. This presumption is, of course, open to experimental test.

Results

1. Decay kinetics as a function of excitation wavelength

Our first experiments were designed to measure the rise and decay

times of the major absorbance change bands as a function of the wavelength of the actinic light. Typical absorption spectra and light-dark spectra for Chlorella and Porphyridium cruentum were shown in Figures III-1, 3. No background illumination (except for that provided by the weak analyzing beam) was used. Actinic flashes were bright enough to saturate the absorption changes at each actinic wavelength up to 710 mμ. We found that, in general, the rise kinetics were insensitive to exciting wavelength. On the other hand, the decay kinetics of the absorbance changes showed a pronounced and uniform dependence on the color of the actinic beam, quite apart from any effects of intensity. Excitation with light of wavelengths longer than 700 mμ, which we will henceforth call $h\nu_1$, produces much slower decay kinetics than does short-wavelength actinic light, $h\nu_2$ (550-630 mμ for Porphyridium; 600-800 mμ for Chlorella and Scenedesmus). Some typical examples of these kinetic effects are shown in Figure IV-18. "Action spectra" which plot reciprocal half life or initial decay rate as a function of exciting wavelength are given in Figures IV-19 and IV-20. In the case of Porphyridium (Figure IV-20) the action spectrum indicates that light absorbed by the chlorophyll a and that absorbed by the phycobilins participate to different degrees in the reaction studied, an observation well documented by other types of experiments.[124] Table VIII summarizes the time for half-decay for the absorbance changes we have studied to date. We conclude that the initial decay rates of the absorbance changes are a strong function of exciting wavelength; the rates fall sharply in the region of 700 mμ.

2. Effect of background illumination on decay kinetics

In view of the relatively slow decay rates produced by $h\nu_1$, an obvious experiment is the effect of a background of $h\nu_2$ on the kinetics

KINETIC DEPENDENCE ON EXCITATION WAVELENGTH

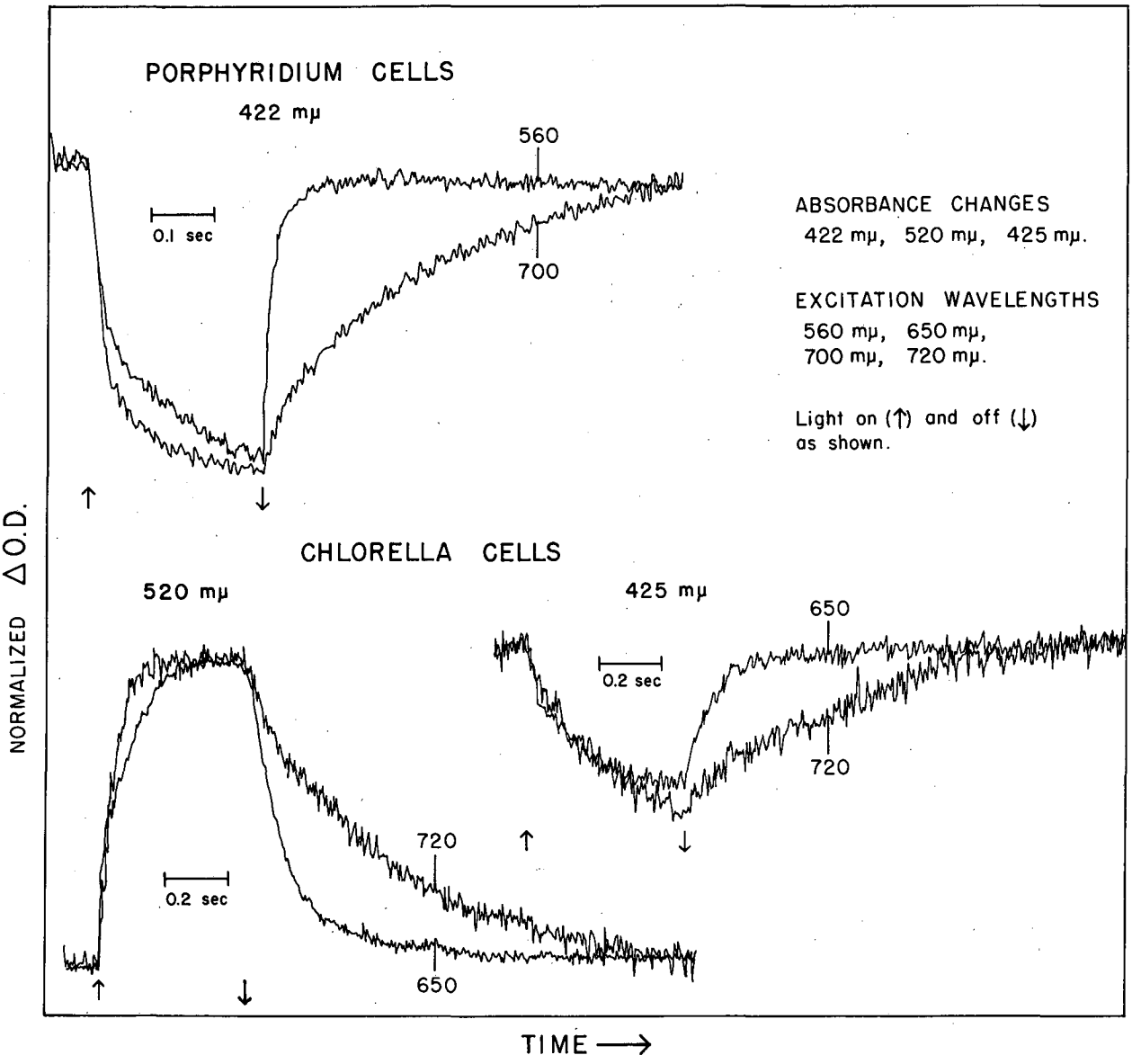

Fig. IV-18. Representative decay kinetics induced by different actinic wavelengths. Experimental conditions given in text.

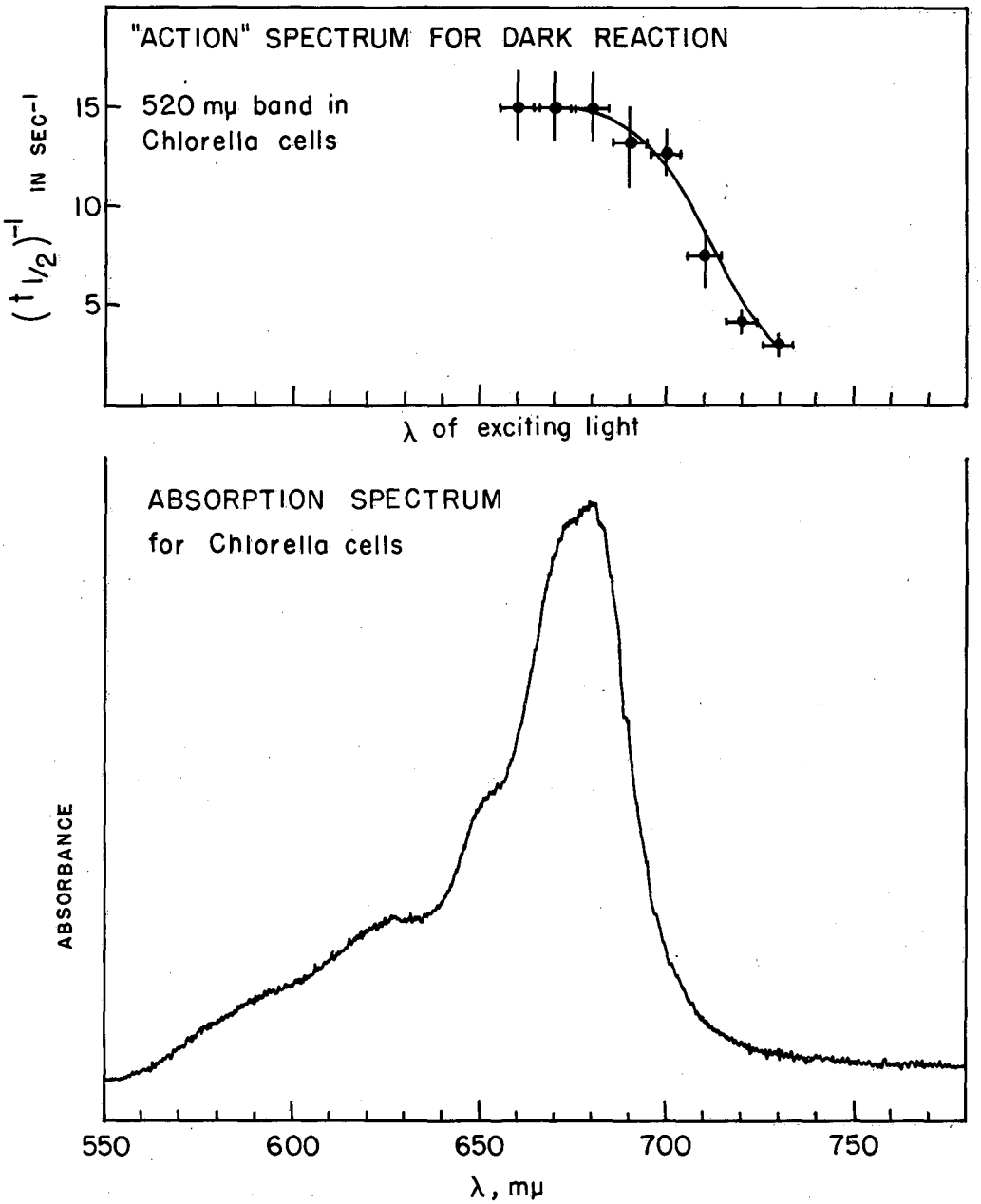

Fig. IV-19. Reciprocal times for half-decay as a function of actinic wavelength. 520 mμ absorption change in Chlorella. Part of the absorption spectrum is shown for reference. Maximum value about 15 sec^{-1}.

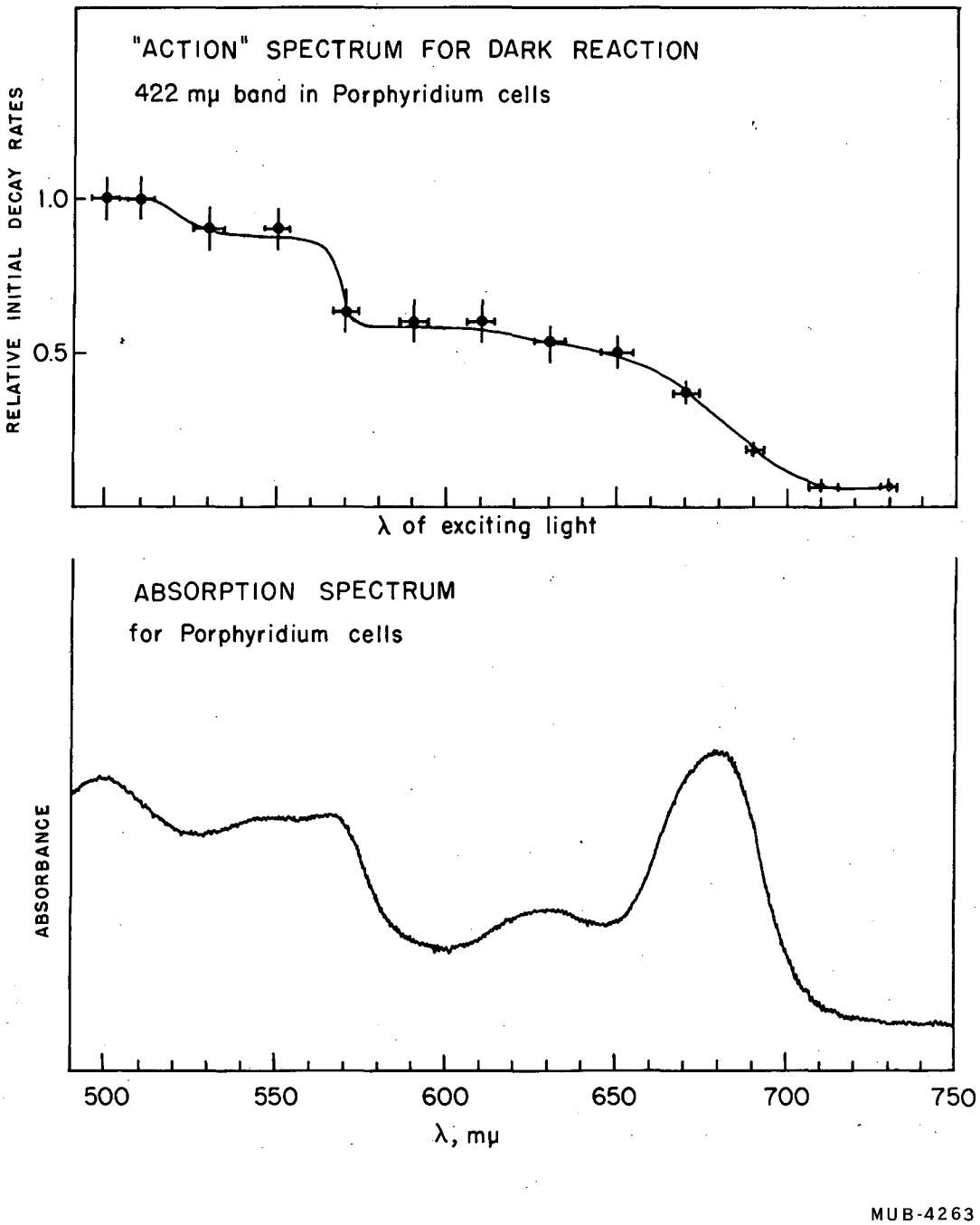

Fig. IV-20. Relative initial decay rates as a function of actinic wavelength. 422 mμ absorption change in Porphyridium. Part of the absorption spectrum is shown for reference.

Table VIII

Decay Kinetics as a Function of Excitation by $h\nu_2$ or $h\nu_1$

Organism	Detecting wavelength (mμ)	Assignment of Absorbance change*	Time for half decay (sec) $h\nu_2$ excitation	$h\nu_1$ excitation
Porphyridium	340	Reduced PN	0.2	(0.3-0.7)
	405	Oxidized cytochrome(f?)	0.01_5	0.26
	422	Reduced cytochrome(f?)	0.01	0.16
Chlorella elp.	405	Depends on excitation wavelength**	(0.05)**	(0.28)**
	425	Chlorophyll, cytochrome(?) (see Ref. 125)	0.02	0.21
	430	Chlorophyll	0.02	0.21
	620	?(see Ref. 126)	0.07	0.28
Chlorella pyr.	340	Reduced PN	0.07	0.30
	425	Chlorophyll, cytochrome(?) (see Ref. 125)	0.07	0.36
	432	Chlorophyll	0.09	0.24
	475	Quinone complex;[127] carotenoid[76] chlorophyll b(??)	0.08	0.25
	520	"	0.07	0.28
	560	Cytochrome(?)		
	650	Chlorophyll b(??) (see Refs. 51,126)	0.05	0.16
Scenedesmus	520	Quinone complex;[127] carotenoid[76]	0.05	0.16

*This list reflects the current literature and the assignments made by the various authors. Aside from the specific works cited, the reader is referred to Chapter III for general discussion.

**The signal polarity is a function of excitation wavelength (see Refs. 51,125). Hence these time constants may derive from different compounds and may not be directly comparable.

produced by a flash of $h\nu_1$. This experiment is a logical analog to the Emerson "Enhancement" experiments.[99] We find, as Emerson did with O_2 evolution, that the slow decays associated with $h\nu_1$ excitation are speeded up in the presence of a continuous background illumination of $h\nu_2$. The most pronounced effect was seen with the cytochrome bands in Porphyridium (Figure IV-21). Our preliminary experiments suggest that the time for half decay for the 405 and 422 mμ bands is inversely proportional to the background intensity. A similar but smaller effect was observed for the 520 mμ band in Chlorella and Scenedesmus. De Kouchousky and Fork have recently reported qualitatively similar results for the 590 mμ absorbance change in Chlorella and in Ulva.[91] Rumberg has also reported systems in which decay rates were enhanced by using a second flash of light in place of a continuous background.[80]

General Remarks

Effects of DCMU

Excitation with either $h\nu_1$ (710 mμ) or $h\nu_2$ (660 mμ) in the presence of 10^{-5} M DCMU yields similar kinetics and signal magnitudes to those produced by $h\nu_1$ in the unpoisoned system (Figure IV-22).

Chloroplast and quantasome preparations

Spinach chloroplasts and quantasomes[6] were studied under a variety of reaction conditions. These included untreated fresh chloroplasts and leaf homogenate, chloroplasts in Hill reaction mixtures (ferricyanide or DCPIP) and triphosphopyridine nucleotide (TPN) reduction systems, using either H_2O or DCPIP-ascorbate as electron donor.[123] None of the broken leaf fractions showed rise or decay kinetics that were influenced by the color of the actinic light (Figure IV-23), although sections of

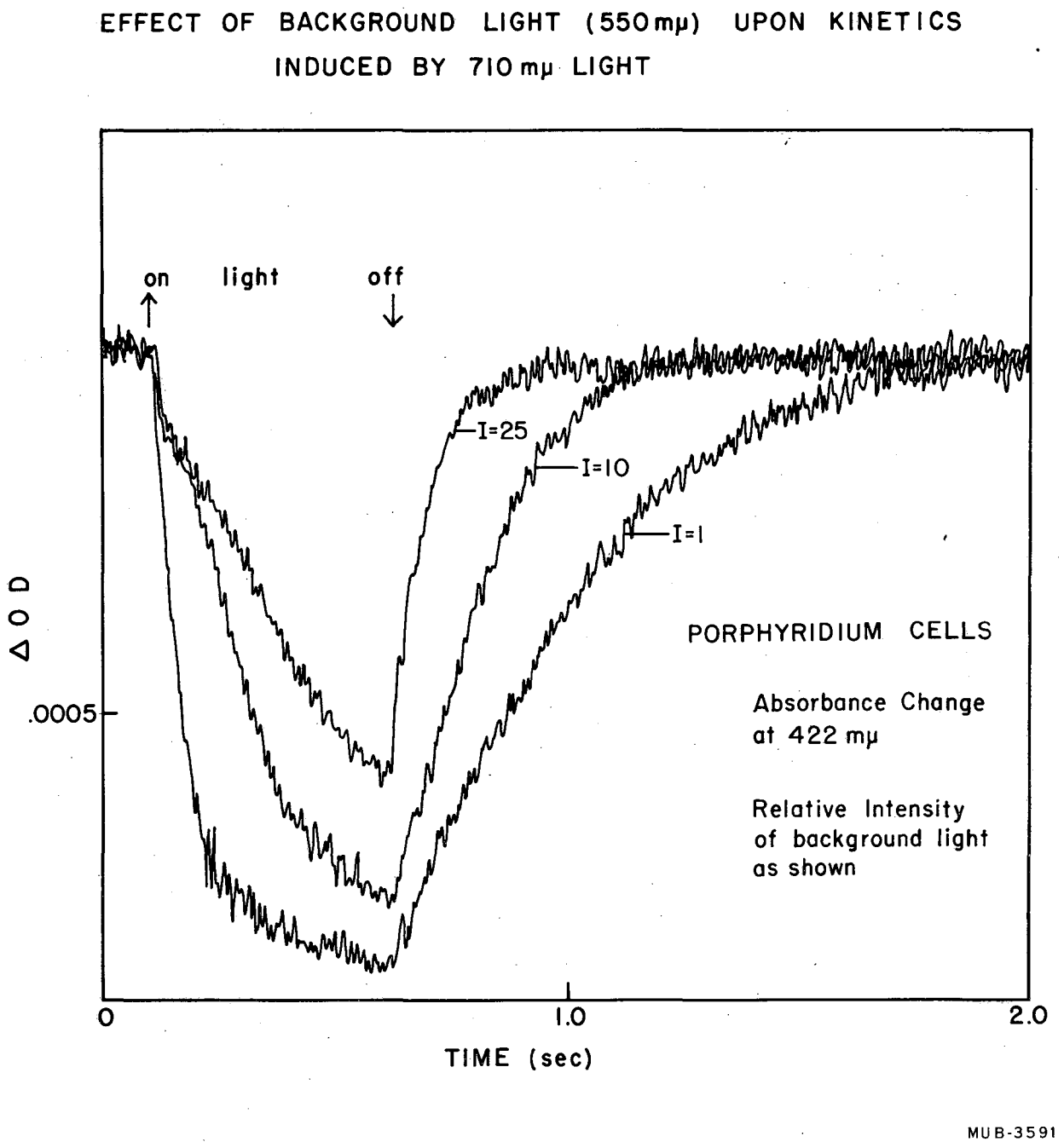

Fig. IV-21. "Enhancement experiment". Flash 710 mμ, background 560 mμ. 422 mμ band in Porphyridium.

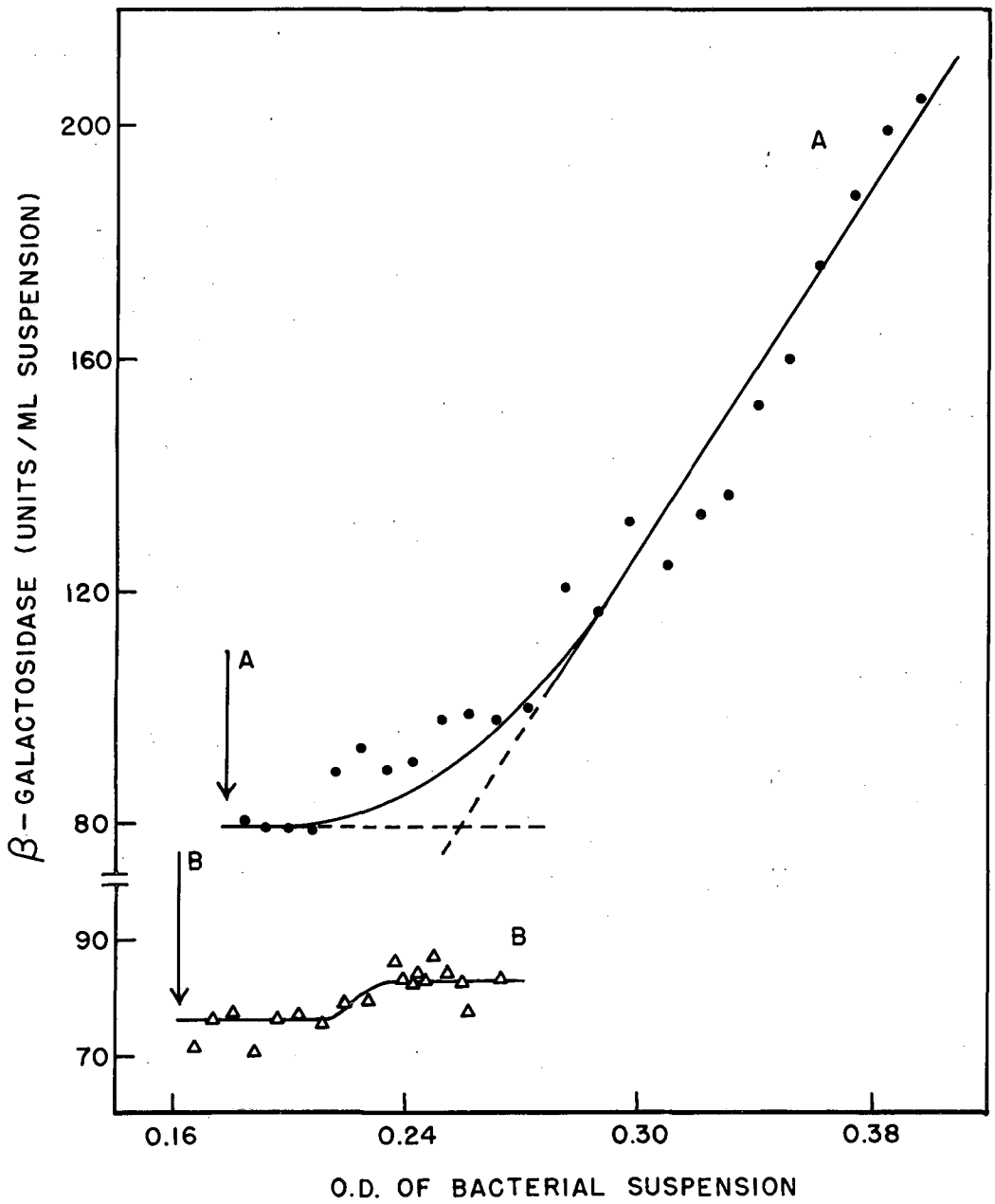

Fig. IV-22. Effect of 10^{-5} M DCMU on 430 mμ absorbance change in Chlorella. Two actinic wavelengths were used, as shown.

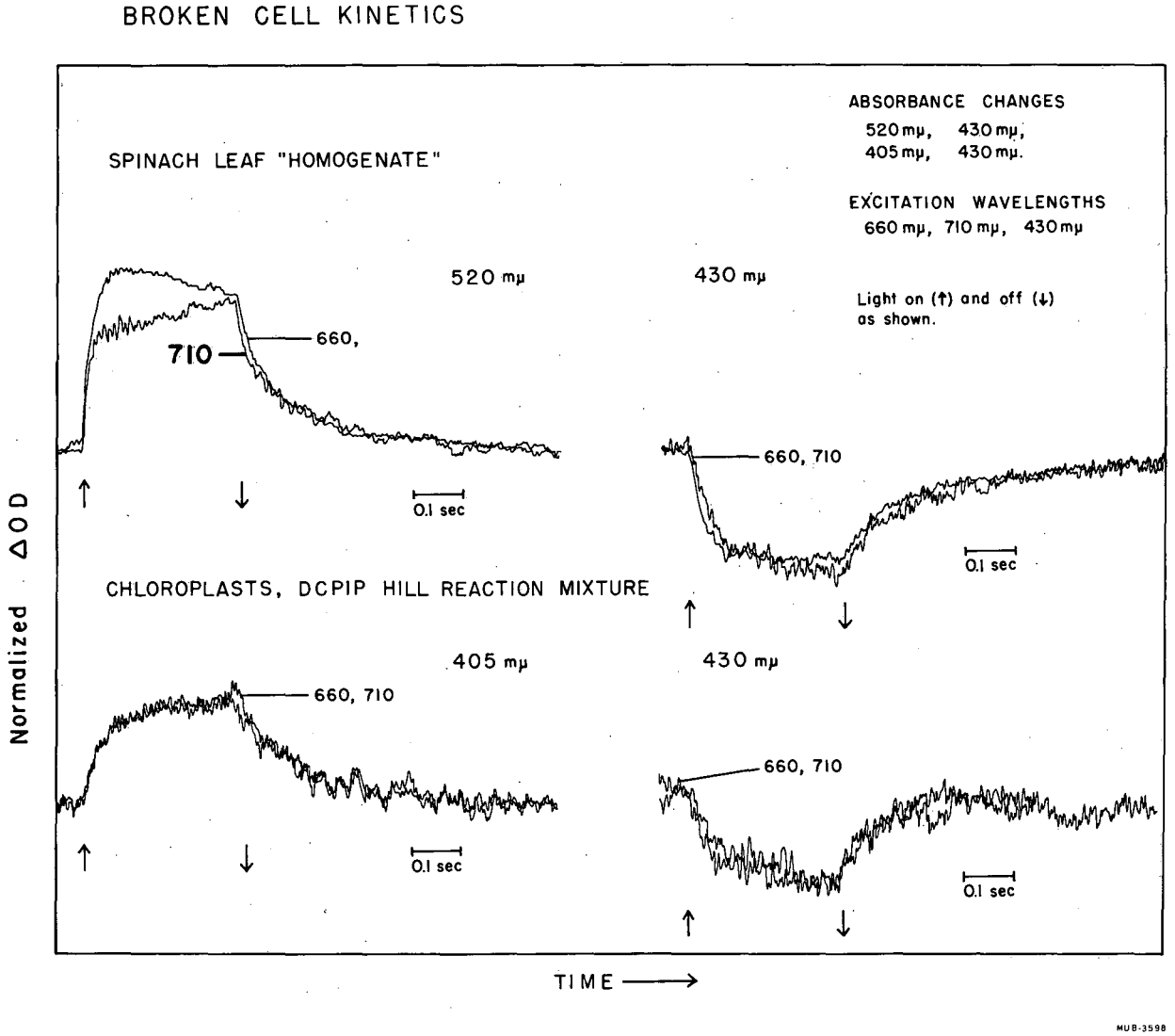

Fig. IV-23. Absorbance change kinetics in various broken cell reaction mixtures. Preparation of materials and reaction conditions are described in Ref. 123.

the whole leaves from which they were made showed the general behavior reported for green algae.

Anaerobioses

Low oxygen tension can also materially affect some of the rise and decay rates. We feel these effects are not sufficient to explain the large changes in rate observed on changing wavelengths because the decay rates were "stable" for some time (many minutes at these low cell concentrations) before the cuvette went anaerobic. Aeration could never make the $h\nu_1$-induced decay commensurate with those found with shorter wavelengths.

Intensity dependence

A preliminary study of the light intensity dependence of the absorbance change kinetics was undertaken. The results of interest here are: (1) rise and decay kinetics in these green and red algae show some intensity dependence, the initial rise rates are directly related to intensity; (2) the effects described in this paper are most pronounced at high actinic intensities; (3) taken as a whole, these intensity effects are not sufficient to explain the results ascribed to actinic wavelength.

Discussion

It is interesting to note that, regardless of the detailed mechanism involved, much of the data presented in this paper can be conveniently summarized in terms of the Emerson "red-drop" and "enhancement" experiments on O_2 evolution. To make this comparison, we need only assume that the rate of O_2 evolution is directly related to the steady-state rate of electron flow through a series of reversible redox reactions. We can convert our kinetic data into rates of electron flow if we measure the

initial rates of the dark reactions. A detailed discussion of the assumptions required to relate rates of O_2 evolution to the reaction rates of electron transport intermediates is given in the next chapter. These assumptions are not particularly restrictive, and would be consistent with most proposed mechanisms for photosynthesis.

Thus, we interpret the drop in initial decay rates observed at long excitation wavelengths (Figures IV-18, 19, 20; Table VIII) as reflecting the same phenomenon that Emerson observed when he found that the rate of O_2 evolution in far-red light was much slower than in light of shorter wavelength. Furthermore, we feel the increase in the "far-red" initial decay rates when a short wavelength background light is added (Figure IV-21) is closely related to the "enhancement" of O_2 evolution rates in similar experiments. Finally, the slow decay rates observed for DCMU-treated algae (Figure IV-22) are consistent with the marked inhibition of O_2 evolution in these cases. We feel that the changes in decay rates involved are large enough to explain the alterations in the steady-state concentrations of photoactive intermediates mentioned in the introduction (Refs. 51,66,82,119,120,128). This is particularly true of Porphyridium where the "enhancement" in decay rates can be quite striking.

From the fact that most or all of the light-dark difference bands show the same qualitative effects, we can draw some general conclusions. First, following the logic used by Emerson for the oxygen results, we find:

(1) Two or more light-driven reactions have been demonstrated at the spectroscopic level in terms of kinetic behavior of the optical density changes absorbance.

(2) These light reactions can interact with one another.

Our study can also point to the mode of the interaction between the two light reactions:

(3) Generally speaking, the products of the light reaction interact with each other at the level of "dark" recovery reactions. This follows from our primary observation that the major difference between $h\nu_1$ and $h\nu_2$ excitation is a difference in decay rates rather than rise rates. An even more direct demonstration of the type of interaction arises from the "two-light" experiments where there was a speed-up in the decay reactions produced by $h\nu_1$ when $h\nu_2$ was added as background light.

(4) The whole cell environment seems to be required for the efficient interaction of the two-light systems because chloroplast preparations which were physiologically active for $TPNH_2$ formation or Hill reactions did not show any of the whole cell effects described above.*

The conclusions reached here concerning the photosynthetic mechanism have, for the most part, been reached independently by other workers using many different techniques. Observations of these types are most frequently used to support the broad outlines of the Hill-Bendall mechanism discussed in Chapter III, which postulates two light reactions cooperating in series with each other. Rather than developing this point of view further, we will discuss briefly two aspects of this work which require some effort to fit into the Hill-Bendall picture.

First, in connection with the enhancement experiment shown in Figure IV-21, it should be pointed out that the fastest decay time observed

---

*Rumberg has reported a specially treated chloroplast system which does show spectroscopic interactions of two light reactions.[80] The reasons for the difference between his system and ours are not clear.

in the double irradiation experiment (40 msec) is considerably longer than the 10-20 msec decay produced by 560 mμ excitation along (Figure IV-18). Furthermore, the absorbed intensity of 560 mμ light used as background illumination in this experiment was fifty times that of the 700 mμ flash. Thus, there does not seem to be a simple quantum-for-quantum interaction between red and green light. The simplest explanation consonant with the series mechanism is that $h\nu_2$ drives both light reactions approximately equally, thus leaving very few excess quanta to couple with the flash of $h\nu_1$. An alternative explanation is that the coupling of the two light reactions represented by this enhancement of decay rate is, in fact, an inefficient process.

Second, to pursue this latter argument a bit further, the chloroplast preparations described in the test showed good quantum yields for, say, $TPNH_2$ reduction with H_2O. But they showed none of the kinetic effects ascribed to the presence of two cooperating light reactions, nor did they show significant "enhancement" effects as measured by $TPNH_2$ reduction rates.[129] These observations might lead us to conclude that efficient photosynthesis could well require only one photochemical reaction.

In conclusion, although the correspondence described in this paper between the spectroscopic results and the oxygen evolution experiments is quite encouraging, both as a tool for further study and as evidence that the absorbance changes are rather directly related to the photosynthetic processes, it should be remembered that the molecular basis for, and the importance of, the Emerson enhancement effects is still unknown.

The experiments on the effects of the color of the actinic beam on reaction kinetics led naturally to an investigation of the interactions

between the photochemical steps when two actinic beams of different color were applied together. We used a flash of one color and a steady background or, in some cases, a long flash of the other color. Some of these results were considered (p.179) when the enhancement experiments were presented.

Double excitation experiments

The prominent difference bands in Porphyridium (the 405-425 cytochrome signals and the 700 mμ change associated with chlorophyll) provide strong evidence for the presence of two light-driven reactions. There are four basic experiments to consider:

(1) A flash of $h\nu_1$ on a background of $h\nu_2$

(2) A flash of $h\nu_1$ on a long flash of $h\nu_2$

(3) A flash of $h\nu_2$ on a background of $h\nu_1$

(4) A flash of $h\nu_2$ on a long flash of $h\nu_1$

The experimental conditions were very similar to those of the experiments just described. The second light source was also equipped with a stepping motor shutter for some of the double flash experiments.

Results

The first experiment is just the enhancement study already referred to (Figure IV-21). It will be remembered that the very slow decay kinetics induced by far-red excitation were speeded up considerably when a background of short wavelength light was also presented. The interpretation offered was that the 560 mμ excitation actually drives both photoreactions, thus leading to the net oxidation of the cytochrome and to the build-up of an undefined source of reducing agent. This view is confirmed by the double flash work. Because of problems with filtering

the actinic and detecting beams, these experiments could not be successfully performed for the chlorophyll band.

The complimentary study using flashes of $h\nu_2$ and background light or long flashes of $h\nu_1$ provided additional information. Figure IV-24 shows the cytochrome bands at 405 mμ (positive signal indicates cytochrome oxidation) when the actinic beam was 560 mμ. It also indicates the results obtained when a strong background light of 710 mμ was added. The double flash experiment strongly supports the observation that a net reduction of the cytochrome occurs when a suitable oxidation level has been achieved by means of background light (Figure IV-25; detecting wavelength 425 mμ, a positive deflection indicates cytochrome reduction). Some of the interesting aspects of the reactions can be brought out more strongly by varying the intensity of the background light. See Figure IV-24 again for the single flash result at 405 mμ; Figure IV-26 shows the double flash result for 425 mμ. Notice, first, that bipolar rise and decay patterns were obtained. It appears that, kinetically speaking, the initial photo-oxidation and photoreduction reactions, as well as the dark reduction and photo re-oxidation by the background light, proceed independently of one another. Second, the photoreduction reaction and in some cases the re-oxidation by background light are quite slow steps.

The interpretation of these results in Hill-Bendall terms is relatively straightforward. The part of the mechanism which concerns us here can be written:

$$X \xrightarrow{h\nu 2} X^- \qquad \text{(IV-7)}$$

$$X^- + Cyt^+ \xrightarrow{K} X + Cyt \qquad \text{(IV-8)}$$

$$Cyt \xrightarrow{h\nu 1} Cyt^+ \qquad \text{(IV-9)}$$

where the light reactions are summary forms, rather than the elementary reactions themselves. Thus, the action of the two photo-steps is predicted

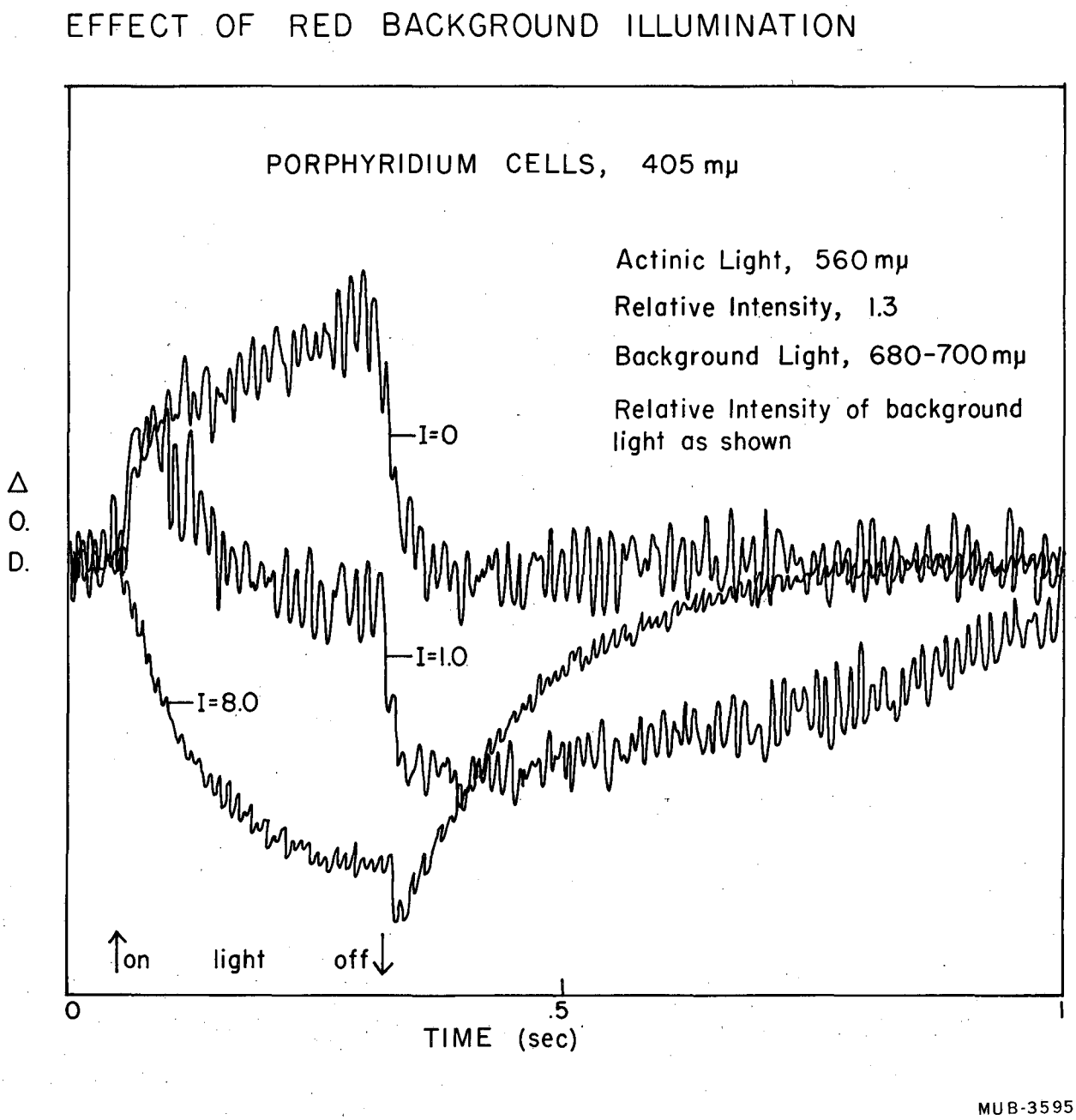

Fig. IV-24. Effect of red background ($h\nu_1$) on kinetics induced by green ($h\nu_2$) flash. Intensity effects are also indicated.

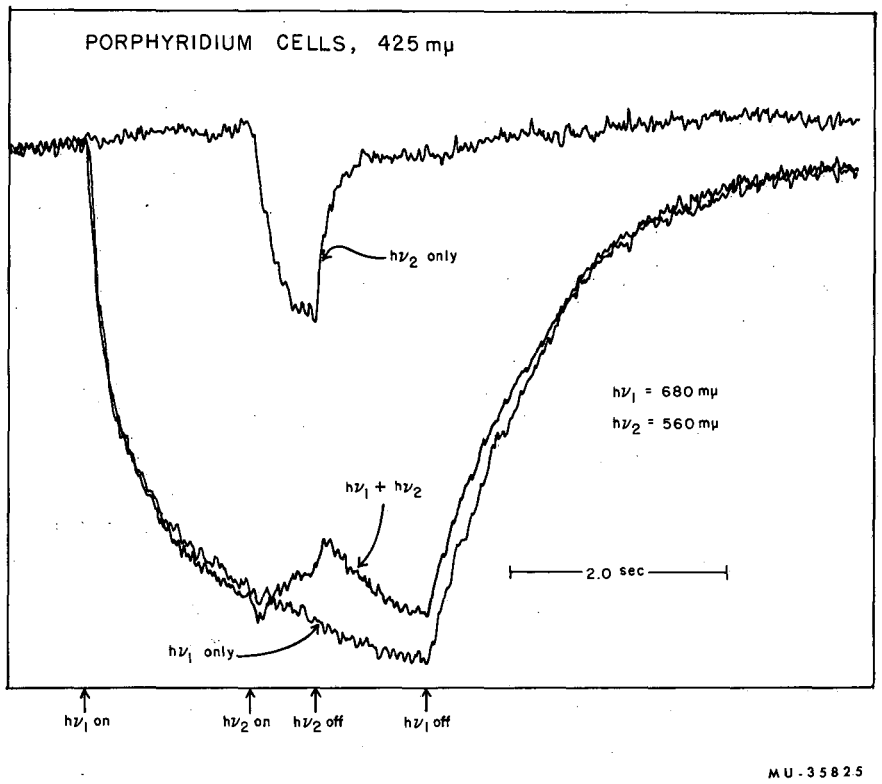

Fig. IV-25. Porphyridium double flash experiment. Detecting beams, 425 mμ. Actinic beams: $h\nu_1$ (680 mμ) on for 4 seconds, $h\nu_2$ (560 mμ) on for 0.4 seconds. Dark time: 4 seconds. The absorbed intensities of $h\nu_1$ and $h\nu_2$ were comparable.

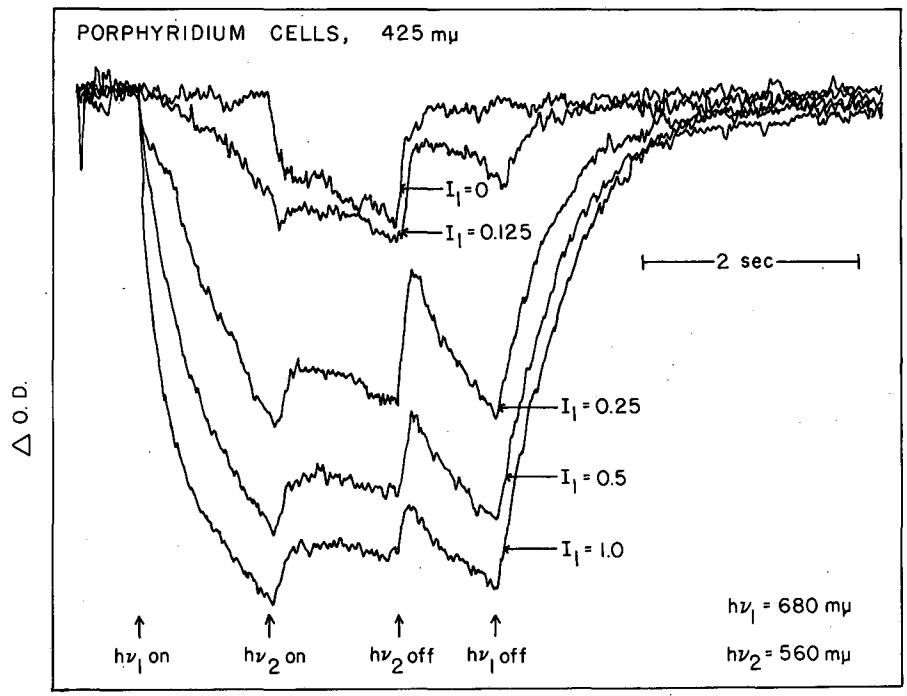

Fig. IV-26. Double flash kinetic curves as a function of $h\nu_1$ intensity. Other conditions as in Fig. IV-25.

to be antagonistic--one driving the cytochrome more oxidized, the second driving the cytochrome more reduced. Remember that the 560 mμ photons can excite both reactions--presumably the rate constants and concentrations being sufficient to produce a net oxidation. 700 mμ quanta are used in the $h\nu_1$ step much more readily than in $h\nu_2$. Both the high steady-state level of Cyt^+ and the slow dark reduction of Cyt^+ after exposure to 700 mμ light confirm the prediction that an amount of X^- would be formed in far-red light. For the photo-oxidation and photo-reduction--as well as the back reactions--to appear together, we must postulate some method of "weak coupling" in the system. There are four general ways of explaining the apparent kinetic independence of coupled reactions. A large pool of the $X\text{-}X^-$ couple would have this effect. A small amount of $X\text{-}X^-$, or even $Cyt\text{-}Cyt^+$, could suffice if we postulate steps which allow these compounds to interact with the environment, such as

$$X + S \rightleftharpoons X^- + S^+ \qquad \text{(IV-10)}$$

where S, S^+ are substrate materials. These methods work by making the concentrations of one or another of the intermediates approximately independent of the reaction conditions. A third possibility is that the time constants for the opposing reaction are so very different that the fast reaction can proceed nearly to completion before the slow step is "felt". Lastly, we could be dealing with strictly independent parallel reactions, involving non-equilibrating pools of cytochromes.

Each of these alternatives has certain advantages and certain difficulties. The first three are consistent with the Hill-Bendall picture. A very slow step is perhaps undesirable in that it places a slow rate-limiting step on the overall process, lowering the quantum yield. Too

much interaction with the environment would permit the partial reactions (oxygen evolution using a substrate electron acceptor, CO_2 uptake using a substrate electron donor) to proceed independently of one another, in conflict with the well-known stoichiometry of normal photosynthesis. Certainly these possibilities are not mutually exclusive, and they may all be in part responsible for the kinetics we have seen. Independent reactions involving only a small amount of interaction is the only way suggested that runs counter to the Hill-Bendall picture of series-linked photochemical steps.

The slowness of the photoreduction and photo re-oxidation can be explained by the mechanism suggested above. If we write out the rate equations associated with Eqns. IV-7, 8, 9, we have for the flash effect

$$\Delta\, dX/dt = -\Delta I_2 X/X_o + K[X^-][Cyt^+] \qquad \text{(IV-11)}$$

$$\Delta\, dCyt/dt = -\Delta I_1 C/C_o + K[X^-][Cyt^+] \qquad \text{(IV-12)}$$

where the ΔI's symbolize the change in absorbed intensities due to the flash of 560 mμ light. The initial rate of cytochrome reduction, dCyt/dt, is seen to be a balance of two opposed processes and measurement of it does not tell us how efficiently electrons are being transferred. Again we must rely on the initial decay rate when the flash is extinguished. The rapid reduction at this point would be interpreted as the "enhancement" phenomenon we have seen before. The slow re-oxidation or recovery from this reductive "spike" is a bit more puzzling since it can be much slower than the original 700 mμ produced oxidation prior to the 560 mμ flash (Figure IV-26). Again one could postulate a balance of opposing rates so that the true re-oxidation rate is never observed.

We have spoken mainly of the Porphyridium cytochrome(s). Interestingly enough, P700 shows essentially the same feature of photoreduction by $h\nu_2$

if $h\nu_1$ is present as a background light. Although our experiments were limited to single flash experiments, Figure IV-27 indicates the bipolar reactions observed with a flash of relatively weak 560 mμ light. The 700 mμ detecting beam served as the $h\nu_1$ background excitation. We see the same qualitative results: a fast photo-oxidation, a slower photo-reduction; then when the flash is over, a very rapid reduction is followed by a slow oxidation.

Without tying ourselves too closely to a particular mechanism these results suggest, at least for photosynthesis in Porphyridium, that:

(1) Two or more light reactions are present.

(2) These reactions work, at least in part, in opposition—that is, one supplying oxidizing power, the other reducing power.

(3) The reactions are, at least in part, cooperative in that they act to an unknown but finite extent on the same intermediates.

(4) The coupling between the photoreactions is relatively weak, but the implications of this coupling for overall rates or quantum efficiencies are difficult to determine.

Chlorella and the other green algae studied did not show these pronounced effects involving bipolar kinetics. Whether this reflects a difference in rate constants or in mechanism is not known.

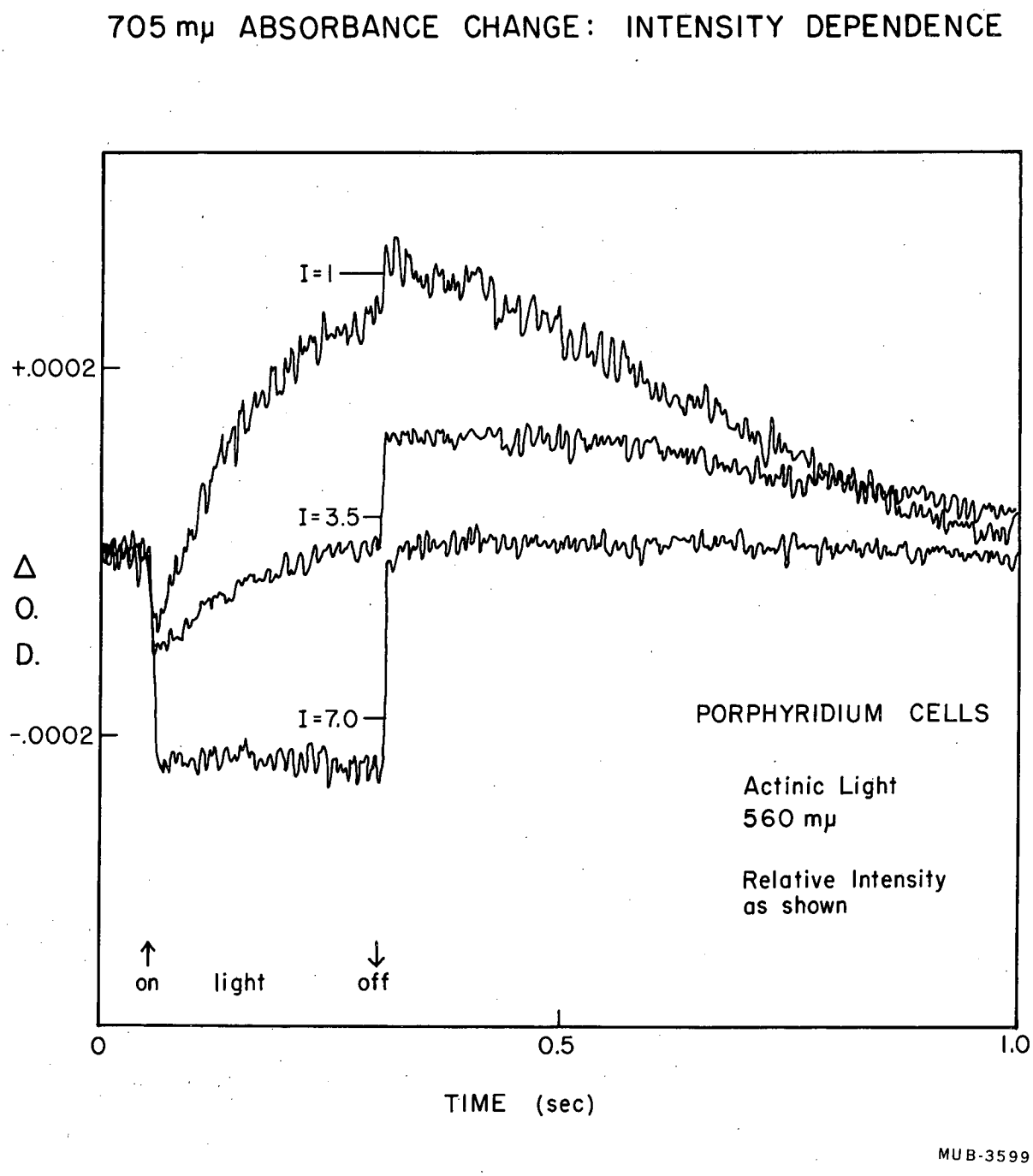

Fig. IV-27. 705 mμ absorbance change in Porphyridium: 560 mμ actinic flash, the detecting beam serves as $h\nu_1$ background actinic light.

Chapter V. THE KINETICS OF ELECTRON TRANSPORT SYSTEMS

Earlier we examined in summary form the ways in which the kinetics of photosynthetic systems might vary from the problems of interest in simpler cases. Two major points were made: First, we wish rate laws in terms of intermediate concentrations (instead of reactant concentrations); second, we need a formalism to deal with independent reactive units which contain very few active molecules per unit. We will explore these two problems in a more quantitative fashion in this chapter.

The reactions we have been considering can be treated as a set of consecutive bimolecular reactions of the type:

$$A + B \xrightarrow{K_1} C + D \qquad (V\text{-}1)$$

$$C + E \xrightarrow{K_2} A + F \qquad (V\text{-}2)$$

where A, B, C, etc. are intermediates and the K's are rate constants which may include light dependent terms. The rate expressions for a set of such reactions consists of a set of simultaneous non-linear differential equations. In the general case, these equations can only be solved numerically or by analog computers. Several approximate methods can be made to yield useful information.[130]

We are basically interested in how much the kinetics can tell us about the photosynthetic mechanism. In the absence of a fairly good guess at the detailed elementary equations and rate constants, it would be hopeless to attempt to find some method of plotting the observed kinetics against a derived function of concentrations of reactants to "prove" or "disprove" a proposed mechanism, even given the high-speed

computer facilities now available. We have decided to use a less satisfactory but more manageable approach--namely, to use a few very simple model systems. Even these are generally not soluble in closed form, so that we have resorted to various approximation methods to achieve some "feel" for the important parameters in the kinetics of such reactions. As a starting point we have selected several characteristic features of the experimental concentration-versus-time curves and studied the way in which comparable features in the model system kinetics were derived from the rate equations. For these purposes, shorter versions of the Hill-Bendall mechanism served as a good place to begin. We found that some parameters were fairly easy to estimate. These included (1) initial concentrations, (2) initial rates of reaction, (3) maximal rise rates, (4) steady-state concentrations, (5) terminal induction periods, and (6) initial decay rates. Quantities that were much more difficult to calculate were (1) maximal rates of reaction if they were not the initial rates, (2) apparent rate constants or half-times for rise and decay, and (3) the points of inflection for the complicated kinetic patterns sometimes observed.

Reactions

The mechanism we propose to study is given below. The column on the right indicates how the reactions are related to the Hill-Bendall mechanism.

Net reaction:

$$M^- + N \xrightarrow{h\nu} N^- + M \qquad (V\text{-}3)$$

Elementary reactions:

$$A + X \xrightarrow{K_{L2}} A^+ + X^- \qquad \text{Photoreaction 2} \qquad (V\text{-}4)$$

$$A^+ + M^- \xrightarrow{K_1'} A + M \qquad \text{Terminal oxidation} \qquad (V\text{-}5)$$

$$X^- + Q \xrightarrow{K_2} Q^- + X \qquad \text{Electron transport} \qquad (V\text{-}6)$$

$$N + C \xrightarrow{K_{L1}} C^+ + N^- \qquad \text{Photoreaction 1} \qquad (V\text{-}7)$$

$$C^+ + S \xrightarrow{K_3} C + Q \qquad \text{Coupling of system 1 and 2} \qquad (V\text{-}8)$$

$$Q + S \underset{K_5'}{\overset{K_4'}{\rightleftharpoons}} Q^- + S^+ \qquad \text{Interaction with potential setting substrates} \qquad (V\text{-}9)$$

where $K_{L2} \equiv \phi_2 I_2 (A/A_o \cdot X/X_o)$,* and $K_{L1} \equiv \phi_1 I_1 (C/C_o)$* (V-10)

Assume that $\underline{M}^-$, $\underline{N}$, $\underline{S}$, $\underline{S}^+$ are in very high and hence constant concentration compared to the intermediates, $\underline{A}$, $\underline{A}^+$, $\underline{X}$, $\underline{X}^-$, $\underline{Q}$, $\underline{Q}^-$, $\underline{C}$, $\underline{C}^+$.

Then define:

$$K_1 \equiv K_1' [M], \quad K_4 \equiv K_4' [S], \quad K_5 \equiv K_5' [S^+] \qquad (V\text{-}11)$$

---

*I_1 is the light intensity absorbed by photosystem 1. This quantity is not dependent on the concentration of $\underline{C}$ because the reactive centers are present in very small amounts compared to the absorbing pigments. However, the reaction rate does depend on the concentration of $\underline{C}$ since the absorbed quanta can only be used if $\underline{C}$ is present. Thus, the dimensionless quantity (C/C_o) is simply the reaction probability for a given intensity. A similar treatment is needed for the other photo reaction. It should be noted that throughout this chapter we have used the steady-state approximation for all of the electronically excited species which are involved in the energy transfer reactions discussed in Chapter I.

Rate Equations

We next write out the differential equations for the concentrations of the reactants, products, and intermediates as a function of time when the system is illuminated.

$$dM^-/dt = -K_1[A^+] \qquad (V\text{-}12)$$

$$dN^-/dt = \phi_1 I_1 (C/C_o) \qquad (V\text{-}13)$$

$$dA/dt = -\phi_2 I_2 (A/A_o \cdot X/X_o) + K_1[A^+] = -dA^+/dt \qquad (V\text{-}14)$$

$$dX/dt = -\phi_2 I_2 (A/A_o \cdot X/X_o) + K_2[X^-][Q] = -dX^-/dt \qquad (V\text{-}15)$$

$$dQ/dt = -K_2[X^-][Q] + K_3[C^+][Q^-] - K_4 Q + K_5 Q^- = -dQ^-/dt \qquad (V\text{-}16)$$

$$dC/dt = -\phi_1 I_1 (C/C_o) + K_3[C^+][Q^-] = -dC^+/dt \qquad (V\text{-}17)$$

The ϕ's are quantum efficiencies, the I's are absorbed moles of quanta/cm^2/second.

Initial Conditions and Rate Constants

Aside from the order of magnitude assumptions we made above to pick out pseudo-first-order reactions, it is difficult to "guess" relative concentrations of the active pools of the intermediates. For simplicity we shall assume that all the pools are of equal size: $A_o = X_o = Q_o = C_o$. Let us assume that in the dark the concentration of the reactive species A^+, X^-, and C^+ are zero. Assume that Q has a redox potential in the range of normal cell potentials and hence the dark concentration is not zero. We chose Q to be largely oxidized in the dark by setting the ratio of K_5/K_4 as 9.00.

It is also difficult to make a priori assignments for the values of the various rate constants. Let us assume that $K_1 = K_2 = K_3 = 1$ and that K_4 and K_5 are much smaller. We need this last assumption because a reaction such as (V-9) really represents an uncoupling of the oxidation

of $\underline{M}^-$ and the reduction of $\underline{N}$, with $\underline{S}$ and $\underline{S}^+$ substituting for the normal electron donor and acceptor. Such reactions are known but are much slower than normal photosynthetic reactions. We also assume that $\phi_1 = \phi_2 = 1$.

Initial Rates of Reaction

Using the dark stationary-state concentrations and the differential rate equations we can obtain the limiting initial rise rates for the various compounds.

$$(dM^-/dt)_i = 0 \qquad \text{(V-18)}$$

$$(dN^-/dt)_i = I_1 \qquad \text{(V-19)}$$

$$(dA/dt)_i = -I_2 = -(dA^+/dt)_i \qquad \text{(V-20)}$$

$$(dX/dt)_i = -I_2 = -(dX^-/dt)_i \qquad \text{(V-21)}$$

$$(dQ/dt)_i = 0 = -(dQ^-/dt)_i \qquad \text{(V-22)}$$

$$(dC/dt)_i = 0 = -(dC^+/dt)_i \qquad \text{(V-23)}$$

Thus, all compounds which are directly associated with the photochemical steps show intensity-determined initial rates. Other intermediates have zero initial rates. This generalization would also hold for any number of electron transfer intermediates in reactions of the type:

$$Q^- + P \xrightarrow{K} P^- + Q \qquad \text{(V-24)}$$

Of course, it is assumed that the time scale on which these measurements are being made is long compared to the rise time of the actinic flash and also long compared to the time it takes for the electronically excited species to come to their stationary-state concentrations.

Induction Periods

Exact calculations of induction periods are very difficult. However, good approximations to the first portion of the rise curves can be obtained by use of the initial rise rates.

$$\text{If } (dA/dt) \cong -I_2 \tag{V-20}$$

then the initial behavior of [A] is available by integration:

$$[A] \cong A_o - I_2 t \tag{V-25}$$

$$\text{and } [A^+] \cong I_2 t \tag{V-26}$$

Similarly,

$$[X] \cong X_o - I_2 t \tag{V-27}$$

$$[X^-] \cong I_2 t \tag{V-28}$$

$$[C] \cong C_o - I_1 t \tag{V-29}$$

$$[C^+] \cong I_1 t \tag{V-30}$$

$$N \cong N_o - I_1 t \tag{V-31}$$

Using these functions we can estimate Q(t).

$$(dQ/dt)_i = -K_2[X^-][Q] + K_3[C^+][Q^-] \tag{V-32}$$

$$= -K_2[I_2 t][Q]_i + K_3[I_1 t][Q^-]_i \tag{V-33}$$

Assume that the terms in K_4Q and K_5Q^- are negligible. Initially [Q] and $[Q^-]$ do not change much from their dark steady-state values, so that we can integrate in this simple form:

$$Q(t) = Q_i - K_2 I_2 t^2/2\, Q_i + K_3 I_1 t^2/2\, (Q_o - Q_i) \tag{V-34}$$

Rearranging:

$$Q(t)/Q_o = Q_i/Q_o\, [1 - K_2 I_2 t^2/2 - K_3 I_1 t^2/2] + K_3 I_1 t^2/2 \tag{V-35}$$

Since the first time-dependent term is quadratic, some lag or "induction" phase is always to be expected. Of course the lag period, to be observable, must extend for a sufficient period of time so that it can be distinguished from the linear rise rates of the primary intermediates.

We can attempt to place the "observability" of the induction period on a quantitative basis by calculating the time it takes for $\underline{Q}$ to react a certain amount. If we choose, arbitrarily, to define the "induction time" as the time it takes for $\underline{Q}$ to change by 10% of Q_o, and if we substitute in values for Q_i and $(Q^-)_i$, we find that

$$(t)_{10\% \text{ reaction}} \equiv (t_{.1})_Q = (0.1/(.05\ I_2) - 0.45\ I_2)^{1/2} \qquad \text{(V-36)}$$

$(Q_i = 9.00,\ Q_i^- = 1.00,\ K_3 = 1,\ K_2 = 1)$.

We next need to estimate the time it takes for $\underline{A}^+$ or $\underline{C}^+$ to undergo a change of similar magnitude. This is obtained from Eqns. V-26 and V-30.

$$(t_{.1})_{A^+} = 0.1/I_2 \qquad \text{(V-37)}$$

$$\text{and } (t_{.1})_{C^+} = 0.1/I_1 \qquad \text{(V-38)}$$

A plot of the "induction time", as defined in Eqn. V-36, is given in Figure V-1. The heavy straight lines mark the regions where

$$(t_{.1})_{A^+} \text{ or } (t_{.1})_{C^+} \geq (t_{.1})_Q \qquad \text{(V-39)}$$

The following interpretations are, perhaps, intuitively correct:

if $(t_{.1})_Q > (t_{.1})_{A^+}$ AND $(t_{.1})_{C^+}$ (V-40a)

then $\underline{Q}$ will show noticeable quadratic character.

if $(t_{.1})_Q \leq (t_{.1})_{A^+}$ OR $(t_{.1})_{C^+}$ (V-40b)

then the rise of $\underline{Q}$ will look linear. In effect, these cases are just those of the light reactions being rate-limiting steps for the formation of $\underline{Q}$. Under these conditions $\underline{Q}$ can change no faster than its precursors.

Notice that although this treatment has assumed particular values for the constants, changing the values of $\underline{K}_2$, $\underline{K}_3$ or the initial values of $\underline{Q}$, $\underline{Q}^-$ would be equivalent to displacing the entire family of curves vertically or horizontally.

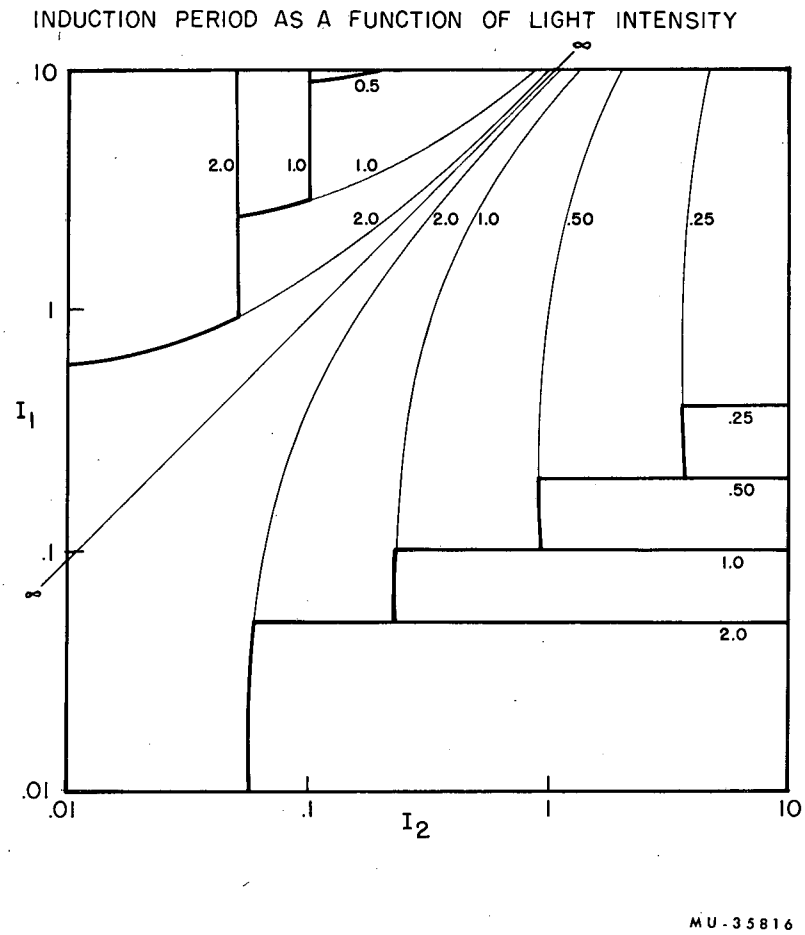

Fig. V-1. Induction period as a function of light intensity. $(t_{.1})_Q$ plotted as a function of I_1 and I_2 as given by Eqn. V-36. The heavy lines mark off regions where $(t_{.1})_{A^+}$ or $(t_{.1})_{C^+}$ are greater than $(t_{.1})_Q$ (Eqns. V-37, 38). No induction period would be observed for Q in these regions.

Three factors limit the observation of the quadratic portions of the rise curves in an actual experiment. First, signal/noise ratios may be poor enough to preclude seeing such effects. Second, the light flash has a finite rise time (1-2 milliseconds in our experiments). During this period induction phenomena will be observed even for the direct photochemical reactions. Third, these calculations are approximations, based on certain assumptions. If these assumptions are not met by the particular case in point, the quadratic portion of the curve might not noticeably arise. The detection of a zero initial slope, in response to light, is sufficient evidence for that compound being an intermediate rather than a direct photoreactant or product.

We can explore further the conditions under which an induction period would be most pronounced. First, inspection of Eqn. V-36 and Figure V-1 indicates that for any values of $\underline{I_1}$ and $\underline{I_2}$ such that $.05\ K_3I_1 = .45\ K_2I_2$ a very long delay phase is expected. We can calculate the relative $t_{10\%}$ time for $\underline{Q}$ and for either $\underline{C}^+$ or $\underline{A}^+$, whichever is the faster in reacting for two limiting cases:

a) $I_2 \gg I_1$

$$\frac{(t_{.1})_Q}{(t_{.1})_{A^+}} \propto \frac{I_2}{(K_3I_1 - K_2I_2)^{1/2}} \qquad \text{(V-41)}$$

b) $I_1 \gg I_2$

$$\frac{(t_{.1})_Q}{(t_{.1})_{C^+}} \propto \frac{I_1}{(K_3I_1 - K_2I_2)^{1/2}} \qquad \text{(V-42)}$$

Because of the rather complicated dependence on two light steps, the only simple predication generated by Eqns. V-41, 42 is that appropriate variation of I_1 and I_2 might well reduce the denominator sufficiently to produce a long relative rise time.

If we calculate the duration of the induction period rather than its relative value, we find:

$$t_{induction} \equiv (t_{.1})_Q - (t_{.1})_{A^+ \text{ or } C^+} \qquad (V-43)$$

Since $t_i \geq 0$, we find on substituting Eqns. V-36 or V-37, 38 into Eqn. V-43,

$$t_i = \frac{0.1}{.05\, I_1 - 0.45\, I_2}^{1/2} - \frac{0.01}{I_2} \text{ (or } I_1) \qquad (V-44)$$

Assume that the I_1 term is small, then t_i has the form

$$t_i = \frac{\alpha}{I_2^{1/2}} - \frac{\beta}{I_2} \qquad (V-45)$$

This equation leads to Figure V-2 which plots

$$\frac{t_i}{\alpha} \equiv \frac{1}{I_2^{1/2}} - \frac{\beta/\alpha}{I_2} \qquad (V-46)$$

for $\beta/\alpha = 0.01$

t_{max} and I for t_{max} can easily be found:

$$t_{max} = \beta/\alpha \qquad (V-47)$$

$$I(t_{max}) = \frac{4\beta^2}{\alpha^2} \qquad (V-48)$$

Thus, as long as the initial assumptions remain true, we find the various constants do not change the shape of the curve, but only act as scale factors. Similar considerations would hold for the alternative assumption that $K_3 I_1 >> K_2 I_2$.

We can now make some qualitative predictions for the observation of induction phenomena in light-driven electron transport systems:

(1) The duration of the induction period should increase at low light intensities, but at very low intensities the photochemical reactions will become rate-limiting and the effect will disappear.

(2) The relative duration of the induction period compared to a similar portion of the rise curve of the photochemical steps will increase

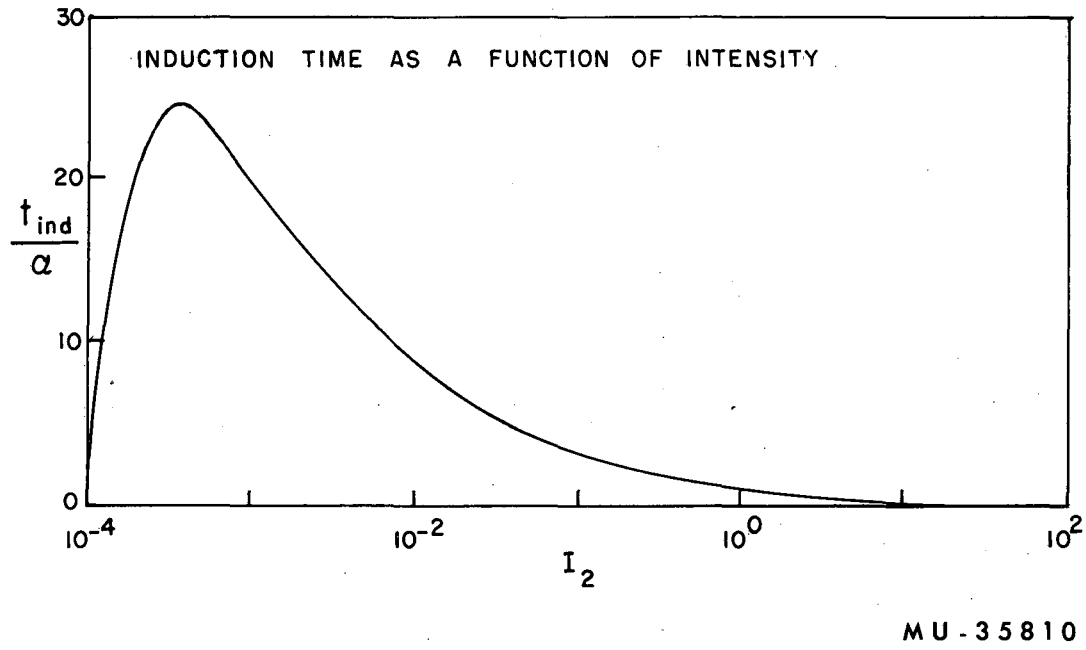

Fig. V-2.

Induction time as a function of I_2. See Eqn. V-46 and discussion in text.

at high light intensities. This effect can increase without limit, but instrumental parameters will place an upper limit on the time resolution.

(3) For intermediates which lie between two light reactions (such as Q in our mechanism) induction phenomenon will be observed for intermediate values of light intensity. Such induction periods should be sensitive to either an increase or a decrease in either I_1 or I_2.

We can extend this general line of analysis to mechanisms with more electron transport steps both between the two light reactions or at either end.

First, consider a series of electron transport reactions at one end of the overall mechanism. The general form of these reactions is:

$$B_i + A_{i+1} \xrightarrow{K_i} A_i + B_{i+1} \qquad \text{(V-49)}$$

where the B's are the reduced forms of the i^{th} redox couple and the A's are the oxidized forms.

The first step is given by

$$e^- + A_1 \longrightarrow B_1 \qquad \text{(V-50)}$$

where e^- represents the light-produced reductant. The assumptions we have previously invoked are (1) we are still in the linear portion of the rise of e^- so that

$$e^- \alpha (e^-)_i \pm It \qquad \text{(V-51)}$$

and (2) the dark steady-state conditions were achieved before the light was turned on. Then, if we calculate the initial rise behavior we find that

$$-\frac{dA_1}{dt} \alpha It \qquad \text{(V-52)}$$

so

$$-\Delta A_1 \alpha It^2 \qquad \text{(V-53)}$$

Similarly,

$$-\frac{dA_i}{dt} \propto It^i \qquad \text{(V-54)}$$

so that

$$-\Delta A_i \propto It^{i+1} \qquad \text{(V-55)}$$

If we next consider intermediates which lie between the two light reactions we can characterize a step by how far it lies from the light steps. Thus A_{ij} is the i^{th} redox couple from light reaction 1 and the j^{th} couple from light reaction 2. By the same arguments given above,

$$\Delta A_{ij} = \alpha t^{i+1} - \beta t^{j+1} \qquad \text{(V-56)}$$

As a check we can note that the Q, Q^- couple in this notation would have $i = j = 1$. Then

$$Q(t) = (\alpha - \beta)t^2, \text{ as we saw before} \qquad \text{(V-57)}$$

Induction periods can be calculated as we did earlier.

Maximum Rise Rates

We will not be able to calculate the maximum rise rates for a general electron transfer step, even using approximate methods. However, the maximum possible rates can be calculated in a very simple fashion from the initial concentrations. The maximum rise rates for our mechanism are derived from the differential equations (V-12 through V-17).

$$(dA/dt)_{max} = -I_2 \qquad \text{(V-58)}$$

$$(dX/dt)_{max} = -I_2 \qquad \text{(V-59)}$$

$$(dC/dt)_{max} = -I_1 \qquad \text{(V-60)}$$

$$(dQ/dt)_{max} = -K_2X_oQ_o \text{ or } -K_3C_oQ_o, \text{ whichever is greater} \qquad \text{(V-61)}$$

$$(dM/dt)_{max} = -K_1A_o \qquad \text{(V-62)}$$

$$(dN^-/dt)_{max} = +I_1 \qquad \text{(V-63)}$$

There is one very important conclusion available from these equations. The compounds which are direct participants in the light reactions have maximum rates which CAN INCREASE WITHOUT LIMIT as the light intensity is increased.* On the other hand, (dQ/dt) can never exceed a certain maximum value, regardless of how much higher the light intensity is raised. This result can be expressed in another way. In any mechanism of the type we are considering the light-driven steps can always be made much faster than the other steps.

Thus we have a general test for distinguishing light-driven reactions from dark reactions by measuring the maximum rise rates as a function of light intensity. Such a test should work even if no induction period is readily observable or if the signal has a complex time course. The actual experiment is limited by the rise time of the actinic lamp and the possibility that very high light intensities would be required.

Steady-state Concentrations

If we solve the differential rate expressions (V-14 through V-17) for the steady-state (by setting all the reaction rates of the intermediates equal to zero) we find:

$$I_2 (A/A_o)(X/X_o) = K_1[A^+] \qquad (V\text{-}64)$$

$$I_2 (A/A_o)(X/X_o) = K_2[X^-][Q] \qquad (V\text{-}65)$$

$$I_2 (A/A_o)(X/X_o) = K_3[C^+][Q^-] \text{ **} \qquad (V\text{-}66)$$

$$I_2 (A/A_o)(X/X_o) = I_1 (C/C_o) \qquad (V\text{-}67)$$

*For any light intensity presently obtainable with high intensity flashes. At extreme intensities we could no longer assume the steady-state approximation for the excited states.

**We have neglected, for the moment, the K_4Q, K_5Q^- terms.

We have four equations in four unknowns (remembering that the sum of the concentrations of the oxidized and reduced forms of each couple equals a time-independent constant. Though we can solve these equations explicitly, the resulting expressions contain roots of a fourth power polynomial and are cumbersome, to say the least. A much simpler approach employs the following equations which are derived from the steady-state solutions and the stoichiometry:

$$[X]_s = K_1/I_2\ (A_o)(X_o)\ [A^+]_s/[A]_s \qquad (V\text{-}68)$$

$$[X^-]_s = X_o - [X]_s \qquad (V\text{-}69)$$

$$[Q]_s = K_1K_2\ [A^+]_s/[X^-]_s \qquad (V\text{-}70)$$

$$[Q^-]_s = Q_o - [Q]_s \qquad (V\text{-}71)$$

$$[C^+]_s = K_1\ [A^+]_s/K_3\ [Q^-]_s \qquad (V\text{-}72)$$

$$[C] = C_o - [C^+]_s \qquad (V\text{-}73)$$

$$I_1 = K_1\ [A^+]_s/[C]_s \qquad (V\text{-}74)$$

We can solve these equations by selecting values of any ratio of concentrations and a light intensity and then solving for the other concentrations and light intensity. Typical solutions are given in Figures V-3, V-4, and V-5, showing the steady-state concentrations as a function of I_1 and I_2. The constants K_1, K_2, and K_3 were set equal to 1; $A_o = X_o = Q_o = C_o = 1$; $K_4 = K_5 = 0$. Several features of these plots are of interest to us. First, the "push-pull" effect of the two photoreactions means that most of the redox couples cannot be completely oxidized or reduced by light, no matter how intense. Second, the light saturation curves of the intermediates are somewhat different from one another (Figure V-4). It should be possible, with careful and accurate saturation data, to gain some information about the sequence of reactions.

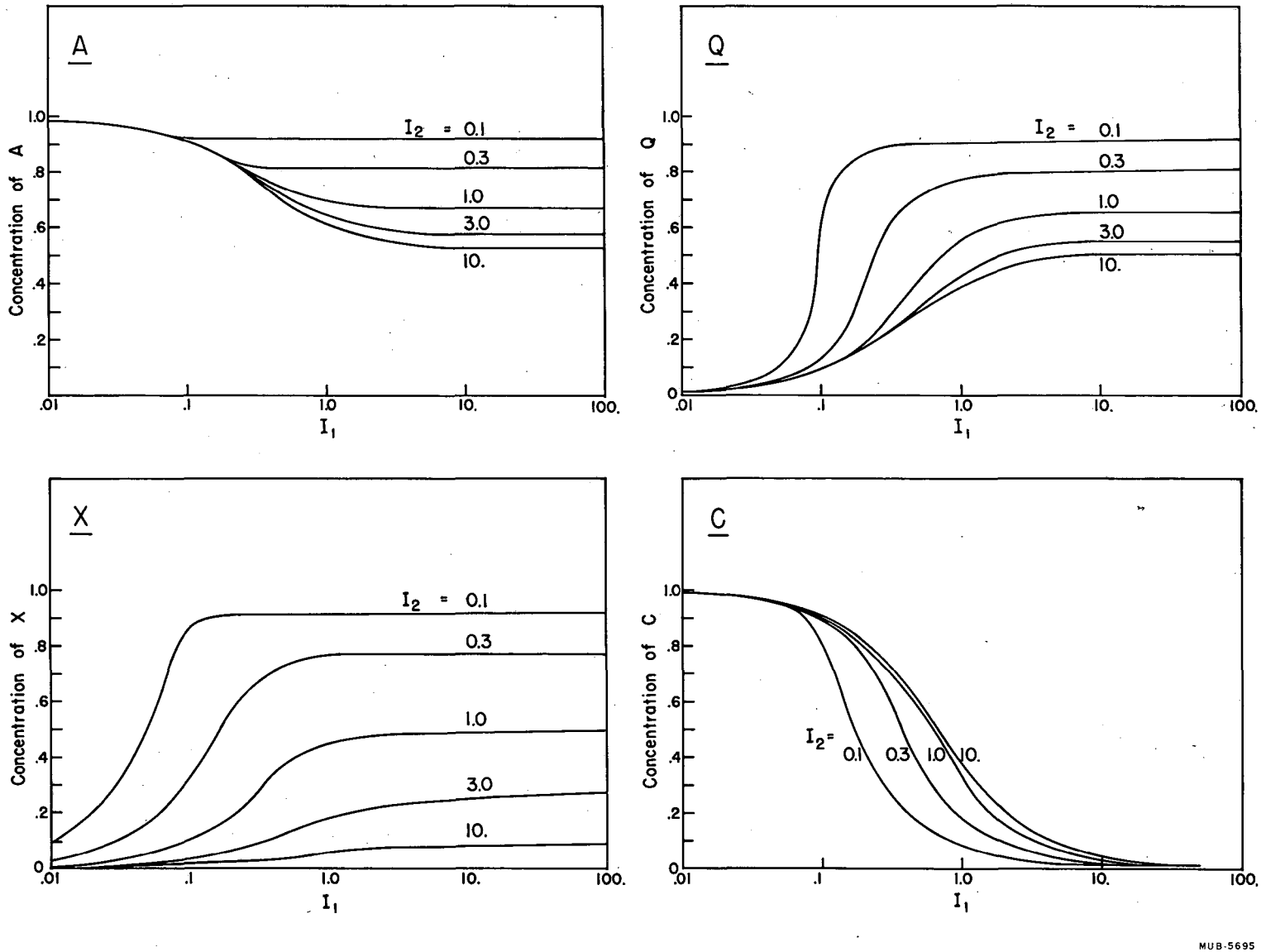

Fig. V-3. Steady-state concentrations of intermediates in the mechanism given on page 198' as a function of I_1 and I_2. Detailed equations and conditions are given in Eqns. V-68 to V-74 and page 210.

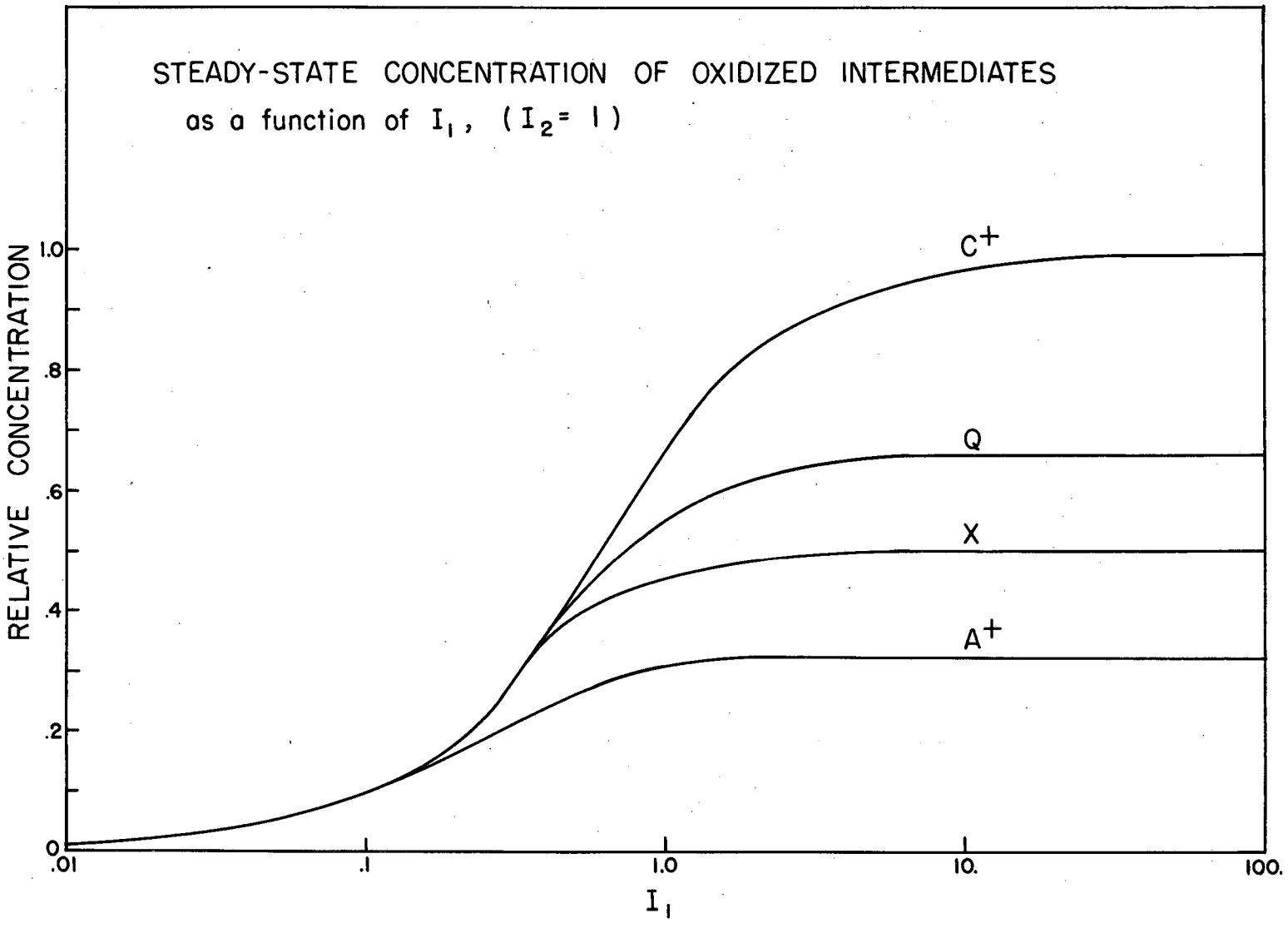

Fig. V-4. Comparison of "saturation curves" of the intermediates. I_2 is held constant as I_1 varies from .01 to 100. Conditions as in Fig. V-3.

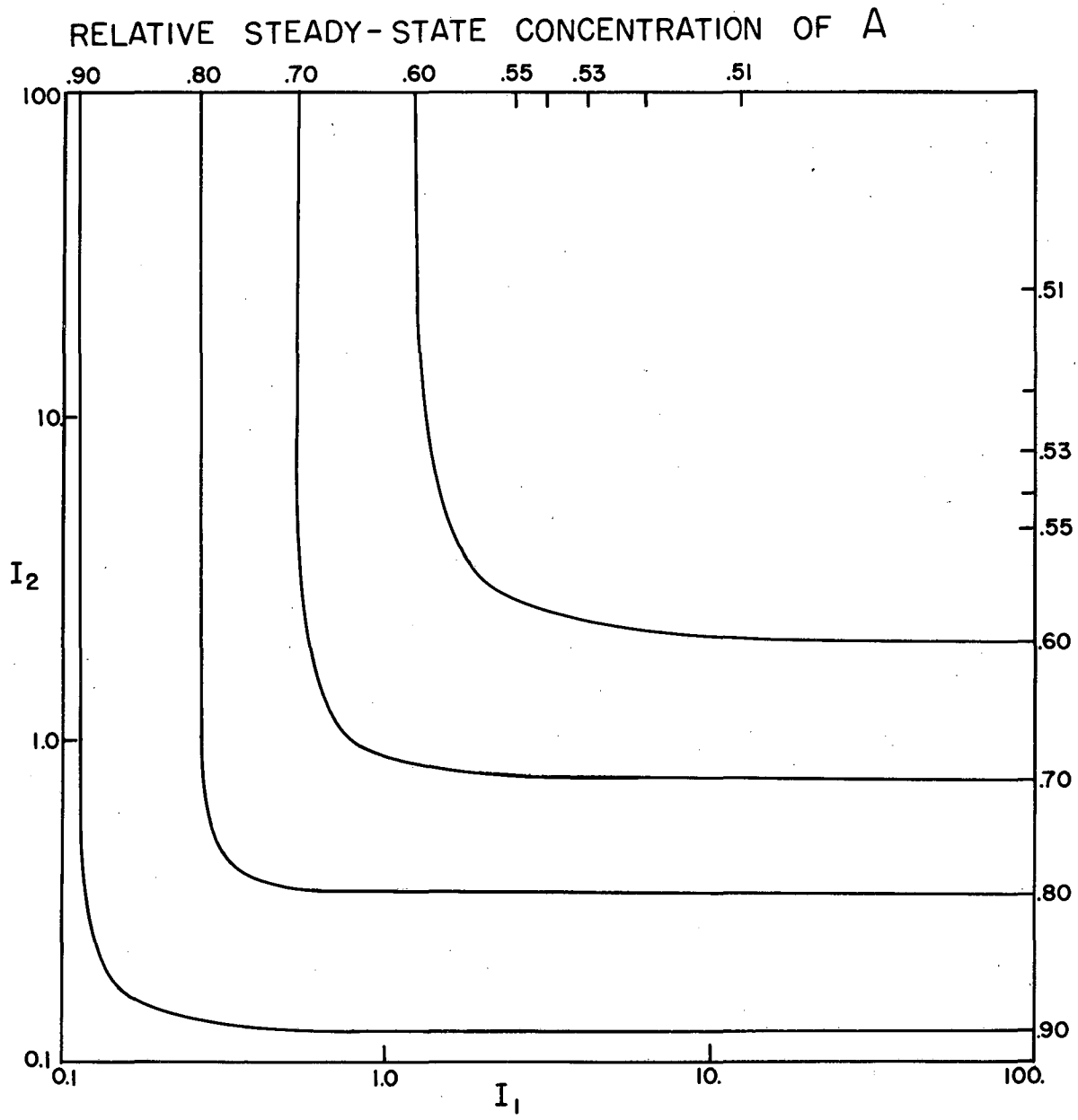

Fig. V-5. Steady-state concentration of A as a function of I_1 and I_2. Lines connect equal concentrations of A. Conditions as in Fig. V-3.

Steady-state Rates

Knowing the elementary reactions and the steady-state concentrations, it is an easy matter to calculate the steady-state rate of the overall reaction. For the particular case we have been treating,

$$-dM/dt = +dN^-/dt = [A^+]_s \qquad (V\text{-}75)$$

Since $[A^+]$ is present in some finite concentration, it is clear that this model displays "light-saturation" of the overall rate. At high intensities the rate becomes independent of intensity.

This model also contains the enhancement phenomenon we have spoken of previously. Figure V-5 is replotted in somewhat different form from Figure V-3. It shows the steady-state concentration of $\underline{A}^+$ as a function of the two light intensities; the lines connect equal concentrations of $\underline{A}^+$. To measure the overall rate of reaction we need only this one number. To show the enhancement effect let us do the following thought experiment. Calculate the rate of the reaction using "far-red" light (say, $I_1 = 10$, $I_2 = 0.1$, since pure excitation is not practicable). The rate is approximately 0.08. Now use just "red" light ($I_1 = 0.1$, $I_2 = 10$). The rate is 0.09. The sum of the two independent flashes is 0.17. However, if the two lights had been given simultaneously, the combined illumination would have the composition $I_1 = 10.1$, $I_2 = 10.1$, which would produce a rate of 0.47, an almost threefold greater value than the previous "experiment".

The effect is based on the fact that the overall steady-state rate of the reactions driving electrons in series must be no faster than the slower rate of quantum input. Hence most of "I_1" is wasted in the "far-red" light, most of the "I_2" is wasted in the "red" light, since the rate-limiting step in both cases is very slow. The combined lights

raise this slow rate from 0.1 to 10.1, a value sufficiently high so that other reactions become limiting (i.e., the combined rate is not 100-fold greater than that of the individual beams, as would be expected if the system was responding in a linear fashion).

Before leaving the topic of steady-state rates, let us return to the question of the effect of "uncoupling" reactions such as:

$$Q \rightleftharpoons Q^- \qquad \text{(V-9)}$$

We rearrange the steady-state equations as shown:

$$(dM/dt)_s = K_1[A^+]_s = K_2[X^-]_s\,[Q]_s \qquad \text{(V-76)}$$

By substitution,

$$(dM/dt)_s = K_3[C^+]_s\,[Q^-]_s + K_5[Q^-]_s - K_4[Q]_s \qquad \text{(V-77)}$$

but

$$K_3[C^+]_s\,[Q^-]_s = I_1[C]_s = (dN^-/dt)_s \qquad \text{(V-78)}$$

Thus

$$(dM/dt)_s - (dN^-/dt)_s = K_5\,Q_o - (K_4 + K_5)[Q]_s \qquad \text{(V-79)}$$

Depending on the values of the constants and the concentration terms the photo-reactions can thus proceed at different rates. The effect will be strongest at low intensities since the consumption of $\underline{M}$ and the production of $\underline{N}^-$ are sensitive to the light intensity whereas the $K_5\,Q_o$ term is not.

Thus, the "decoupling" effect of this type of reaction is readily apparent. As mentioned previously, it is thought that this sort of process is not too important in steady-state photosynthesis where the rates of oxygen evolution and carbon dioxide uptake agree to $\pm$ 10%.

Steady-state Quantum Yields

Unlike the steady-state rates, the quantum yields diminish with increasing light intensity. If we select an efficient combination of I_1 and I_2 (say, $I_1 = I_2$), the relative quantum yields drop as shown in Table IX.

Table IX

Quantum Yield as a Function of Light Intensity

Intensity of either light ($I_1 = I_2$)	Quantum yield $\phi = \frac{\text{Rate}}{I_1 + I_2}$
.01	0.5
.1	0.4
1	0.15
10	0.023
∞	0

The quantum yields generated by this mechanism have the form

$$\phi = \phi_o - \alpha I \qquad \text{for low intensities} \qquad \text{(V-80)}$$

$$\phi = \frac{\beta\phi_o}{I} \qquad \text{for high intensities} \qquad \text{(V-81)}$$

ϕ_o = quantum yield at zero intensity.

Decay Reactions

The rate equations for the decay reactions are:

$$dM^-/dt = -K_1[A^+] \qquad \text{(V-82)}$$

$$dN^-/dt = 0 \qquad \text{(V-83)}$$

$$dA/dt = K_1[A^+] = -dA^+/dt \qquad \text{(V-84)}$$

$$dX/dt = K_2[X^-][Q] = -dX^-/dt \quad \text{(V-85)}$$

$$dQ/dt = -K_2[X^-][Q] + K_3[C^+][Q^-] + K_5 Q^- - K_4 Q = -dQ^-/dt \quad \text{(V-86)}$$

$$dC/dt = K_3[C^+][Q^-] = -dC^+/dt \quad \text{(V-87)}$$

Although this is a simpler set of equations than the complete set, the non-linear terms make it too difficult to solve in closed form.* Thus, we will turn to the type of approximations used in the earlier parts of this chapter.

Initial Decay Rates

Assume that the illuminated steady-state was achieved. If we examine the system rapidly enough after the light is extinguished, the concentrations of the intermediates will have changed only a negligible amount from their steady-state values. The initial decay rates are thus:

$$(dA/dt)_{initial} = K_1[A^+]_s = -(dA^+/dt)_i \quad \text{(V-88)}$$

$$(dX/dt)_i = K_2[X^-]_s[Q]_s = -(dX^-/dt)_i \quad \text{(V-89)}$$

$$(dQ/dt)_i = 0 = -(dQ^-/dt)_i \quad \text{(V-90)}$$

$$(dC/dt)_i = K_3[C^+]_s[Q^-]_s = -(dC^+/dt)_i \quad \text{(V-91)}$$

We then expect that Q, the one compound which does not interact directly with the light, will show a zero initial-decay rate and the attendant induction period. The other intermediates show their maximum decay rates as the light is extinguished.

Another important observation is the expected relationship between the initial decay rates of the photo-reactants and products and the

---

*Aside from noting that $A^+ = (A^+)_d\, e^{-K_2 t}$ where $(A^+)_d$ is the concentration of A^+ at the time the actinic beam is shut off.

steady-state rate of electron flow. For the closely coupled case, where K_4 and K_5 are zero,

$$(dM/dt)_s = (dN^-/dt)_s = K_1[A^+]_s \qquad (V-92)$$

Reference to Eqns. V-64 to V-67 and V-88 to V-91 indicates that the initial decay rates for A, X, and C are just equal to the steady-state electron flow rate as postulated earlier (page 151). If the two photosteps are partially uncoupled (K_4, $K_5 \neq 0$), each photo-reaction achieves its own steady-state condition. Then

$$(dM/dt)_s \neq (dN^-/dt)_s \qquad (V-93)$$

However, those intermediates involved directly with the reaction of M will show initial decay rates equal to $|(dM/dt)_s|$ while those involved with the formation of N^- will show initial decay rates of $|(dN^-/dt)_s|$. It must be emphasized that these relationships are only valid if a steady-state was reached during illumination, and if the compounds involved have an intensity-dependent term in their rate expressions which accounts for all of the net reaction in that direction. A very fast reaction with a direct photoproduct could approximate these requirements. It may appear that the initial decay rate calculations are of the same type and importance as the calculation of the steady-state rates (page 214). This is not so. The latter results are only available if the mechanism is known, whereas the relationship between the initial decay rates and the steady-state rates is quite general within the limits set by the assumptions just discussed. As we have seen, initial decay rates are, in practice, a very useful tool in comparing experimental results with the (unknown) mechanism under study.

Induction Period for Decay Reactions

We can proceed exactly as we did for the induction period associated with the rise curve. As before, $\underline{X^-}$ and $\underline{C^+}$ vary linearly during the first phases of the dark reaction. Thus,

$$[X^-] \simeq [X^-]_s - K_2't \qquad \text{(V-94)}$$

where $K_2' = K_2[X^-]_s[Q]_s$

$$\text{and } [C^+] \simeq [C^+]_s - K_3't \qquad \text{(V-95)}$$

where $K_3' = K_3[C^+]_s[Q^-]_s$

$K_2' = K_3'$ for a closely coupled system.

Substituting these values into the rate expression for $\underline{Q}$ yields:

$$Q \simeq (Q)_s + K_2't^2/2 \{(K_2 + K_3)(Q)_s - K_3Q_o\} . \qquad \text{(V-96)}$$

$\underline{Q}$ can increase or decrease quadratically or stay essentially constant. This expression does not contain light intensity as an explicit variable. We could work out in detail the same type of relationship that we derived earlier for the duration and relative magnitude of the induction period associated with the decay curve, but in the absence of accurately known constants it will suffice to say that the qualitative behavior is rather similar to Figure V-1. It is possible, at least in principle, to perform the same type of experiment suggested earlier where one varies the light intensity and hence the steady-state level of $\underline{Q}$, hoping to find that critical region where the induction phase is extended greatly for a small change in light intensity.

Maximum Decay Rates

These rates can also be estimated in the manner used for the maximum rise rates, which yields the values:

$$(dM/dt)_{max} = -K_1A_o \qquad (V\text{-}97)$$

$$(dN^-/dt)_{max} = 0 \qquad (V\text{-}98)$$

$$(dA/dt)_{max} = K_1A_o = -(dA^+/dt)_{max} \qquad (V\text{-}99)$$

$$(dX/dt)_{max} = K_2X_oQ_o = -(dX^-/dt)_{max} \qquad (V\text{-}100)$$

$$(dQ/dt)_{max} = -K_2X_oQ_o - K_4Q_o = -(dQ^-/dt)_{max} \qquad (V\text{-}101a)$$

$$\text{or} = +K_3C_oQ_o + K_5Q_o \qquad (V\text{-}101b)$$

$$(dC/dt)_{max} = K_3C_oQ_o = -(dC^+/dt)_{max} \qquad (V\text{-}102)$$

These calculations support the conclusions drawn previously about the value of measuring rise and decay rates as a function of light intensity.

This completes the detailed calculations we will perform for this type of model system. The next section explores in a more qualitative fashion the complex rise and decay curves that have been observed experimentally. Analog computer methods will be briefly considered as an attractive way to gain further insight into these complex patterns.

Complex Rise and Decay Kinetics

We have been focusing our attention on the various aspects of the kinetic curves which were readily accessible to a quantitative or semi-quantitative study. However, we have really only dealt with a small part of the information contained in such curves and, in fact, we have said almost nothing of the more striking features of the time courses obtained experimentally--namely, the "overshoots", "two-phase rise" and "bipolar rise" curves which were illustrated schematically in Figure IV-7. Actual kinetic curves have been presented at various points in our discussion (see Figures IV-17, 21, 24, 25, 26, 27).

Two conditions need to be met before a system of coupled reactions can show kinetic effects of these types. First, three or more intermediates

are required. Second, there must be one or more relatively slow steps which determine the overall approach of the system to the illuminated or dark steady-state. One or more relatively fast steps will then be be sufficient to produce complex kinetics of these types.

Some qualitative calculations can be predicated on these conditions. The kinetic curves in which we are interested have the property of a point with zero slope after the induction period and before reaching steady-state. The rate-limiting step has only the steady-state as a point of zero slope (except for the induction period). Thus, we can solve the differential equations for these points of extrema by setting the various rate expressions to zero INDEPENDENTLY of one another (if they are all equal to zero simultaneously, we have, of course, the steady-state condition). If it is possible to make reasonable approximations for some of the non-linear terms (such as A = X for the initial phases of the reaction), we can calculate the concentration at which the particular intermediate has a point of zero slope. To decide whether this point is a maximum, minimum, or inflection point we need to know the steady-state concentrations. Such an approach is actually more quantitative than might be thought at first glance. However, it is only really applicable to cases where there is a well defined rate-limiting step.

Analog Computation

A modern analog computer provides a rapid and accurate method for graphical solution of the sets of linear and non-linear differential equations that we have been considering. This approach has been used relatively little for chemical kinetic problems, but a copious literature

is available on the principles and use of commercial instrumentation,[131,132] and no difficulty was experienced in setting up mechanisms of widely varying complexity. A sample circuit diagram for the mechanism we have been analyzing is shown in Figure V-6. It takes approximately two to four hours to draw out and "patch" a problem of this size. Systematic variation of four and even five rate constants is feasible, requiring about eight to sixteen hours of running time. Obviously, a considerable "feel" for the nature of the solutions can be developed if one explores kinetic problems in this manner. We used a large 100 amplifier unit (Electronic Associates, Inc., Long Branch, N. J.) at the Lawrence Radiation Laboratory in Livermore. Only a few of the results obtained will be summarized in Figure V-7. Notice how closely the experimental curves (Figures IV-17, 21) can be simulated by a model such as we have been using. It should be realized, however, that the transient behavior patterns are not severe tests of the overall mechanism. For example, any more complicated system and some less complicated sets of reactions will also account for these transients. In fact, the reactions do not even have to be bimolecular. A closed cycle of first-order reactions will also have sufficient complexity to generate curves of these types. The computer analysis, coupled with the qualitative calculations already alluded to, is more revealing for the explanations it provides for the complex reaction patterns. These explanations can probably be taken over to a rather general form which could, of course, be very useful in determining reaction sequence. For example, the "overshoot" pattern arises because a relatively fast step is followed at some later point in the electron transport chain with a relatively slow step. During the initial phases of the reaction the fast step may

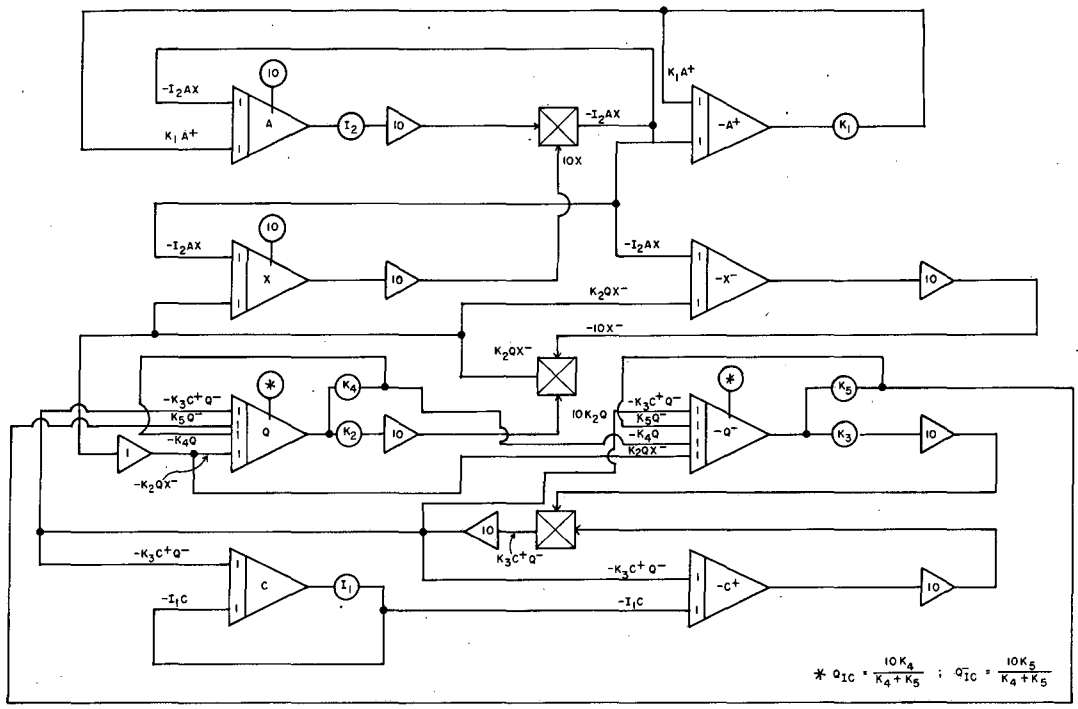

Fig. V-6.

Analog computer circuit for basic mechanism (Eqns. V-3 to V-9). Standard symbols are used[131] and initial conditions are indicated.

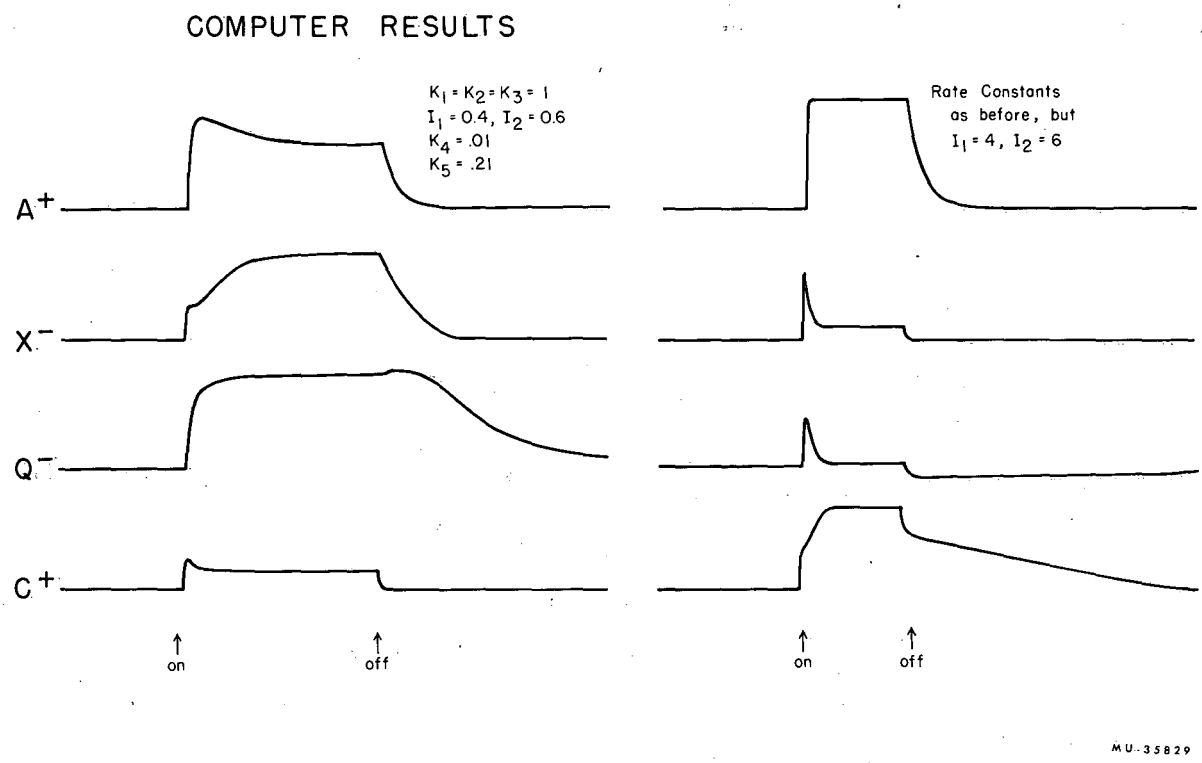

Fig. V-7.

Analog computer results from circuit shown in Figure V-6. The initial conditions are shown in Fig. V-6. The values of the constants are given.

proceed relatively unaware of the slow one. However, sooner or later the overall rate will be set by the slow step, and thus the steady-state level of the fast reacting component will undergo either a transient overshoot or undershoot. This point of a "slow" follow reaction is well taken for the 520 mμ absorption change shown in Figure IV-17. The overshoot is normally seen at very high light intensities. However, when DCMU, an inhibitor of electron flow, is added, the overshoot transient appears at very low intensities. This indicates that some step following the photoproduction of the 520 mμ band is the one primarily affected by DCMU. Similarly, the two-phase rise curve develops in those situations where one intermediate takes a relatively long time to make a major change in concentration. Then intermediates that are "downstream" and which can react rapidly will reach a pseudo steady-state early in the reaction from which they will shift as the slowly changing compound assumes its final steady-state value. Of course, the magnitudes of these effects cannot be predicted from such crude considerations. But even the qualitative information is valuable in studies of complex reactions.

We have seen that a simple Hill-Bendall type mechanism provides a suitable mathematical model to describe most of the qualitative kinetic patterns that have been measured experimentally. It has been possible to deduce many of the properties of electron transport chain kinetics, even if complete solutions of the differential rate equations were not feasible. Some of our predictions are quite suitable for experimental tests, particularly those involving light intensity experiments. Finally, we point out once again that the agreement between theory and experiment at this stage of our discussion is suggestive that reaction systems of this general kind are involved in photosynthesis, but the actual

verification of the proposed mechanisms on strictly mathematical grounds is still beyond our reach.

Derivation of First-order Kinetics

The most significant feature of the kinetics of the photosynthetic reactions that is not explained by the model considered above is the first-order rise and decay curves which we and other workers have reported.[31,105] First-order kinetics do not arise easily from a set of bimolecular reactions under the normal conditions of solution or solid state chemistry, unless one of the compounds in each of the coupled reactions is present in large excess. This assumption would be inconsistent with the known concentrations of active species in the photosynthetic reactions and with the concentrations as measured directly by light-dark or oxidized-reduced difference spectroscopy. To pursue this matter more quantitatively we need two pieces of information: (1) what is the smallest independent unit which can perform the photochemical steps of photosynthesis and (2) what are the reagent concentrations within such a unit. There is fairly widespread agreement that the small subcellular fragments we have called "quantasomes" and "chromatophores" are the physical containers which enclose the "photosynthetic unit". These units are certainly independent of one another in the isolated preparations. Only linear dependencies of rate upon particle concentration have been reported.* Recent measurements of the concentrations of transition metals within quantasomes strongly

*At very high concentrations of particles less than linear relationships have been noted, but these arise from the very strong absorption of light under such conditions.

suggest that the actual number of active molecules of any one type per quantasome is very small indeed (Table X),[133,134,135] approaching one or two active molecules of each species per quantasome.

Table X

Approximate Numbers of Active* Molecules per Photosynthetic Unit

Intermediate or Metal Ion		Number of molecules or equivalents per unit (mw = 1,000,000)
Chlorophyll		1
Quinones:	total	20
	active (ca. 10%)	2
Phosphate:	total	150
	active	?
Fe:	total	6
	cytochrome f	1
	cytochrome b_6	1
Cu:	total	3
	plastocyanin	1-2**
Mn		1

*Estimated from data in References 133, 134.

**Reference 135.

Thus we are faced with kinetic analysis of a rather unusual reaction system—namely, we must predict the behavior of a very large number of independent reactions, each reaction being able to influence only a very small number of molecules. Recent formulations of chemical kinetics in terms of the theory of stochastic processes[136,137] provide, in principle,

the most satisfactory method of analysis of such a problem. The detailed procedures involved in this approach become rather complex, even for very simple cases such as 2A = B.[137]

We have developed a different method which is considerably less elegant, provides less information (dispersion terms are not calculated), and is much easier to manipulate and relate to the chemistry.

Consider a system of $\underline{N}$ independent reaction cells each containing no more than $\underline{X}$ reacting molecules. If $\underline{X}$ is a very small number ($\underline{X} < 10$) the observed kinetics of the total system of $\underline{N}$ cells can be quite different from those obtained if the total number of particles (NX) were allowed to react under normal solution chemistry conditions. This difference in kinetics is not due to any change in the elementary reactions which the molecules undergo because of their relative isolation. The behavior of the total system can be predicted in a straightforward manner. The critical factors are the mechanism of the reaction occurring in the cell and the number of reacting molecules within the cell.

Let $n_{\underline{xy}\ldots}$ be the concentration of cells which contain $\underline{x}$ reacting molecules of type $\underline{A}$, $\underline{y}$ reacting molecules of type $\underline{B}$, etc. $\underline{x,y,\ldots}$ are small integers with any value between 0 and $\underline{X,Y,\ldots}$. Then, in general,

$$A = \sum_{x=0}^{x=x} x n_{xy\ldots}; \quad B = \sum_{y=0}^{y=y} y n_{xy}; \quad \ldots\ldots \qquad (V\text{-}103)$$

where $\underline{A}$, $\underline{B}$,... are the concentrations of reactants in the total solution.

Our problem is to calculate the concentrations of the various types of cells ($n_{00\ldots}$, $n_{10\ldots}$, etc.) as a function of time. As the chemical reaction proceeds one type of cell is converted to another. Explicit calculations thus require a knowledge of the mechanism so that we know

what interconversions are possible, and a knowledge of the rate constants for these "cell reactions" which we can obtain from the concentrations of reagents within each cell and the intrinsic rate constants of the chemical reactions. Our assumption that the reactions within a cell proceed independently of reactions in adjoining cells requires that the conversion of one type of cell into another type is a first-order process, thus yielding for our cell reactions a set of coupled first-order rate equations. It is well known that such a system yields exact solutions in closed form.[138] These solutions are in fact expressible as a series of exponential terms with various coefficients and time constants:

$$\begin{aligned} n_{xy\ldots}(t) = {} & (C_{0y\ldots})e^{-(K_{0y\ldots})t} \\ & + (C_{1y\ldots})e^{-(K_{1y\ldots})t} \\ & + (C_{2y\ldots})e^{-(K_{2y\ldots})t} \end{aligned} \qquad \text{(V-104)}$$

The C's and K's will be related to the explicit mechanism for the chemical reactions. The connection with the macroscopic observables such as the concentration of A, B, etc., is given below:

For a generalized elementary chemical reaction,

$$aA + bB + \ldots \xrightarrow{k} cC + dD + \ldots \qquad \text{(V-105)}$$

we have:

$$n_{xy\ldots} \xrightarrow{K_{xy\ldots}} n_{(x-a)(y-b)\ldots} \xrightarrow{K_{(x-a)(y-b)}} n_{(x-2a)(y-2b)} \longrightarrow \ldots \qquad \text{(V-106)}$$

where $K_{xy} = kx^a y^b$ (V-107)

Knowing how the n_{xy}'s can react and knowing the K_{xy}'s permits us to write out the rate equations for cells of various types:

$$\frac{dn_{xy}}{dt} = -K_{xy}\, n_{xy} \qquad \text{(V-108)}$$

$$\frac{dn_{(x-a)(y-b)}}{dt} = +K_{xy}\, n_{xy} - K_{(x-a)(y-b)}\, n_{(x-a)(y-b)} \cdots \qquad \text{(V-109)}$$

etc.

As remarked above, these sets of equations, being linear in the variables n_{xy}'s, can always be solved in closed form.* These solutions plus the initial conditions allow one to calculate the "C's" of Eqn. V-106.

Thus we expect any general chemical reaction to yield sums of first-order kinetic curves. By way of example, consider the simple bimolecular reaction:

$$A + B \xrightarrow{k} C \qquad \text{(V-110)}$$

Assume that we initially have in all of the cells 2 molecules of A, 2 molecules of B, and 0 molecules of C. The possible cells are then

$$n_{220}, n_{111}, n_{002},$$

no other combinations of A, B, C molecules/cell being available under the mechanism and initial conditions.

How are these three types of cells related to one another? The flow diagram is also determined simply from the mechanism.

$$n_{220} \xrightarrow{K_{220}} n_{111} \xrightarrow{K_{111}} n_{002} . \qquad \text{(V-111)}$$

The cell rate constants K_{40}, K_{21} are calculated from Eqn. V-107.

$$K_{220} = k(2)(2) = 4k \qquad \text{(V-112a)}$$

$$K_{111} = k(1)(1) = k \qquad \text{(V-112b)}$$

The rate equations for the cell reactions are:

$$\frac{dn_{220}}{dt} = -K_{220}\, n_{220} = -4k\, n_{220} \qquad \text{(V-113a)}$$

$$\frac{dn_{111}}{dt} = +K_{220}\, n_{220} - K_{111}\, n_{111} = 4kn_{220} - kn_{111} \qquad \text{(V-113b)}$$

$$\frac{dn_{002}}{dt} = K_{111}\, n_{111} = kn_{111} . \qquad \text{(V-113c)}$$

Let k = 1.

---

*Although a computer may be required to manipulate the high order secular equations which are generated.

These equations are readily integrated.

$$n_{220} = Ne^{-4t} \quad \text{(V-114a)}$$

$$n_{111} = 4/3\ Ne^{-4t} + 4/3\ Ne^{-t} \quad \text{(V-114b)}$$

$$n_{002} = +\ 1/3\ Ne^{-4t} - 4/3\ Ne^{-t} \quad \text{(V-114c)}$$

Now

$$A = 2n_{220} + 1n_{111} = 2Ne^{-4t} - 4/3\ Ne^{-4t} + 4/3\ Ne^{-t} \quad \text{(V-115)}$$

$$A = 2/3\ N\ \{e^{-4t} + 2e^{-t}\} \quad \text{(V-116)}$$

Since $A_o = 2N$, (V-117)

$$A = 1/3\ A_o\ \{e^{-4t} + 2\ e^{-t}\} \quad \text{(V-118)}$$

So, instead of a second-order reaction, as we would have expected for A in solution, we find two exponentials.

A more complicated example was set up as an analog computer problem to investigate the complex kinetic patterns that a simple Hill-Bendall scheme might yield when recast into terms suitable for very small photosynthetic reaction units.

The computer program (Figure V-8) used the following mechanism:

$$A \xrightarrow{I_2} A^- \quad \text{(V-119)}$$

$$A^- + B \xrightarrow{K_2} A + B^- \quad \text{(V-120)}$$

$$C \xrightarrow{I_1} C^+ \quad \text{(V-121)}$$

$$C^+ + B^- \xrightarrow{K_1} C + B \quad \text{(V-122)}$$

This will be recognized as a simple version of the Hill-Bendall scheme. It was selected to see if the B, B^- couple would reproduce the two-light experiments shown in Figure IV-26. We used this mechanism to check the "small cell" ideas just discussed. The possible reactions for the case of 1 molecule each of the couples A, A^-; B, B^-; C, C^- per reaction cell are:

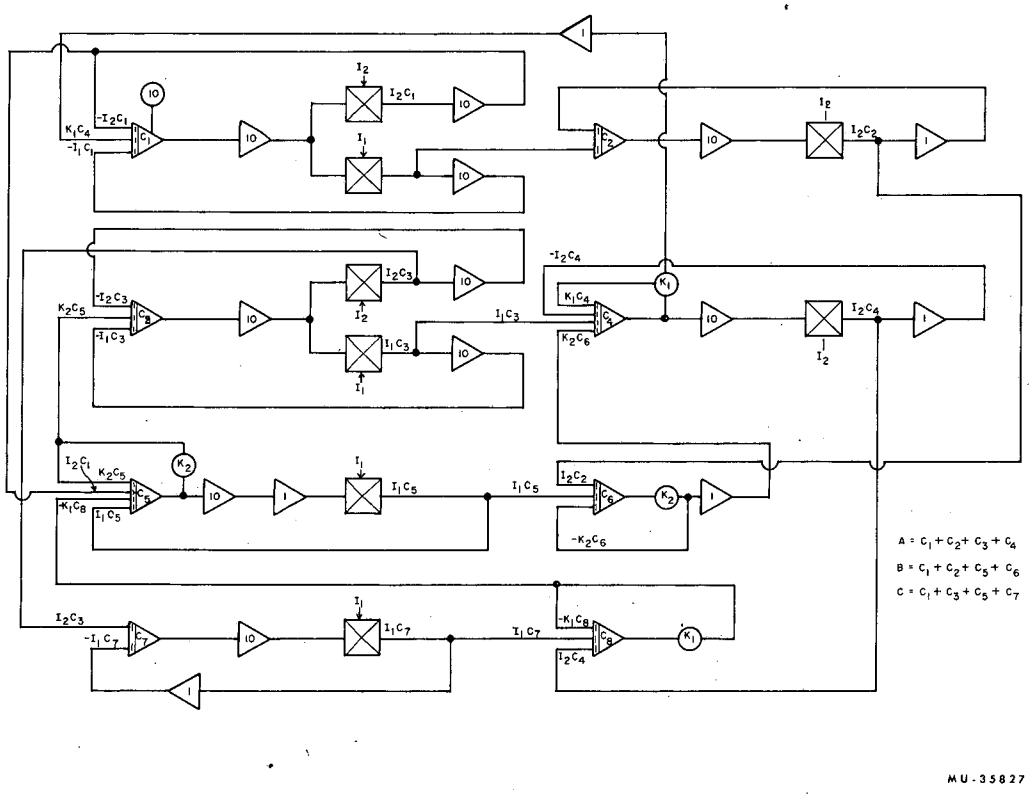

Fig. V-8. Analog computer circuit for small reaction cells. Set up for the differential Eqns. V-127 to V-136. Initial conditions as indicated.

$$C_{AXX} \xrightarrow{I_2} C_{A-XX} \qquad \text{(V-123)}$$

$$C_{XXC} \xrightarrow{I_1} C_{XXC^+} \qquad \text{(V-124)}$$

$$C_{A-BX} \xrightarrow{K_2} C_{AB-X} \qquad \text{(V-125)}$$

$$C_{XB-C^+} \xrightarrow{K_1} C_{XBC} \qquad \text{(V-126)}$$

The C's represent the concentrations of cells having the composition shown in subscript. The X's indicate that the state of those particular couples is not important to the reaction indicated (i.e., the four cells C_{ABC}, C_{ABC^+}, C_{AB-C}, and C_{AB-C^+} will all react by Eqn. V-119 to give C_{A-XX}).

A simple "flow" diagram can be set up for the eight possible cell types:

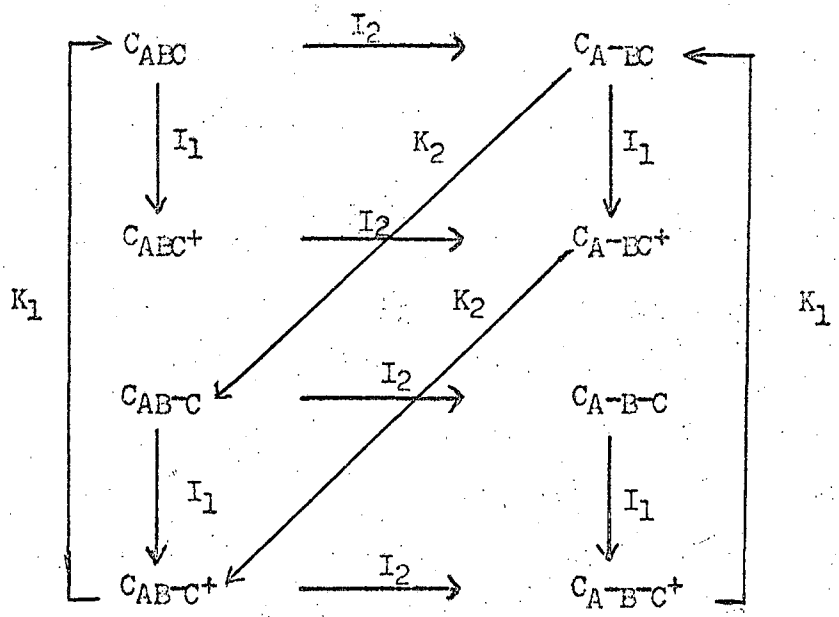

The differential equations are readily available from this diagram. We introduce the shorthand notation:

$C_{ABC} \equiv C_1$		$C_{A-BC} \equiv C_5$	
$C_{ABC^+} \equiv C_2$		$C_{A-BC^+} \equiv C_6$	
$C_{AB-C} \equiv C_3$		$C_{A-B-C} \equiv C_7$	
$C_{AB-C^+} \equiv C_4$		$C_{A-B-C^+} \equiv C_8$	

$$\dot{C}_1 = -(I_1 + I_2)\, C_1 + K_1 C_4 \qquad \text{(V-127)}$$

$$\dot{C}_2 = -I_2 C_2 + I_1 C_1 \qquad \text{(V-128)}$$

$$\dot{C}_3 = -(I_1 + I_2)\, C_3 + K_2 C_5 \qquad \text{(V-129)}$$

$$\dot{C}_4 = -(K_1 + I_2)\, C_4 + I_1 C_3 + K_2 C_6 \qquad \text{(V-130)}$$

$$\dot{C}_5 = -(I_1 + K_2)\, C_5 + I_2 C_1 + K_1 C_8 \qquad \text{(V-131)}$$

$$\dot{C}_6 = -K_2 C_6 + I_1 C_5 + I_2 C_2 \qquad \text{(V-132)}$$

$$\dot{C}_7 = -I_1 C_7 + I_2 C_3 \qquad \text{(V-133)}$$

$$\dot{C}_8 = -I_1 C_7 + I_2 C_4 - K_1 C_8 \qquad \text{(V-134)}$$

As can be seen from Figure V-9, the general kinetic features of Figure IV-26 can be duplicated by this type of mechanism.

All in all, the "cell reaction" model is worth pursuing over a very limited set of experimental conditions. It becomes important when only one or two molecules of reactant are present per cell. Since these are precisely the conditions that we expect for the photosynthetic mechanism, it would seem that any detailed mathematical model of photosynthesis should take into account these differences from normal solution kinetics.

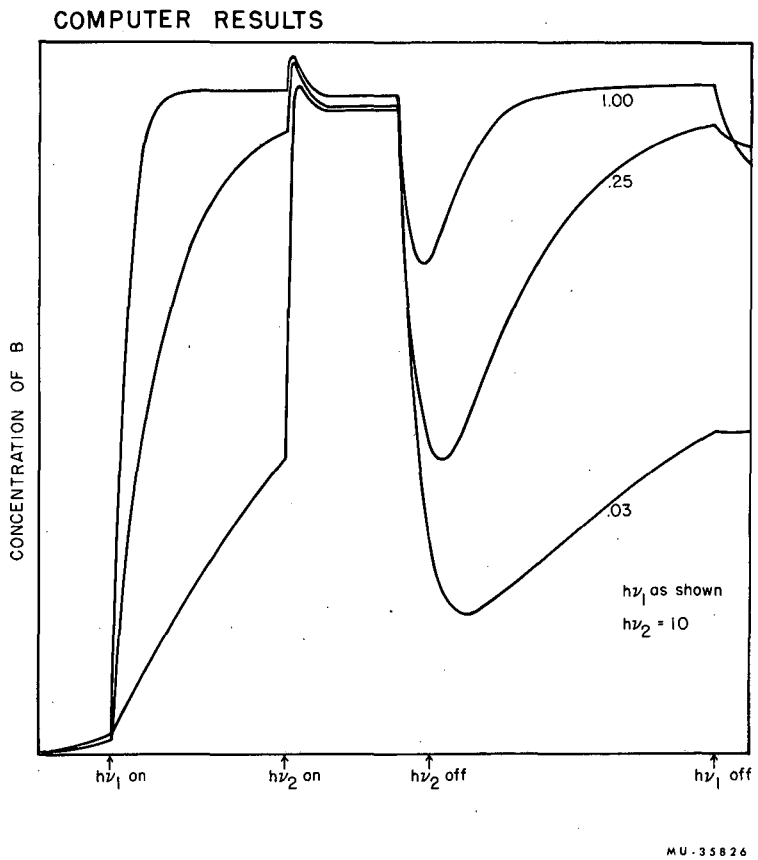

Fig. V-9. Analog computer results for circuit of Figure V-8 for "two-light" experiment. All K's = 1; $h\nu_1$ and $h\nu_2$ as

Chapter VI. CONCLUSIONS

Most of our time has been spent in discussion of various parts of the photosynthetic apparatus. Detailed conclusions were taken up as they arose in the earlier chapters rather than saved for a major "synthesis" here.

At this point I would like to explore a question that motivated much of the thinking behind these studies: which (or how many) of the reactions we have discussed are responsible for the high quantum yield and good free energy storage displayed by overall photosynthesis. Of course, in a multi-step process of this kind each reaction has some effect on the total result, and, obviously, the overall yields can be no better than the worst step.

We first considered those reactions which involved the absorption of light and the transfer of the absorbed energy to a reactive site. If we accept the proposed mechanisms for these steps, our major concern is with the efficiency that accompanies such reactions. The obvious quanta losses are (1) non-radiative degradation of quanta and (2) radiative emissions. Both of these loss processes appear to be rather inefficient. The former, estimated from fluorescence data, accounts for 10-30% of the input quanta; the latter, including all forms of radiative emission, cannot exceed 1-3% of the input quanta.

Such small losses must be attributed to very large rate constants in the forward direction, approaching 10^{11} $sec.^{-1}$. This is not an improbable situation. After all, the type of energy transfer that we have been considering involves exothermic reactions as quanta from the blue end of the spectrum are degraded into 650-700 mμ quanta.

Several papers have pointed out that a rather large loss in the ΔF takes place during the absorption of light. This loss can be treated as a Carnot efficiency problem, or it can be thought of as arising from the very small concentrations of excited states that are produced during illumination at normal light intensities. Roughly 30% of the calories present in the light of these intensities is not available as free energy.

Neither the quantal nor the ΔF losses in these steps is particularly surprising when one considers the behavior of concentrated solutions (liquid or solid) of pigments. Such systems, say, 0.01 M chlorophyll in methanol, show strongly quenched fluorescence which indicates efficient energy transfer. ΔF terms of the type described above must also be present in the solution. Furthermore, the random orientations of the pigment molecules in solution are in keeping with the random orientation of the bulk of the pigment molecules within the photosynthetic apparatus. The major difference between the chlorophyll solution and the in vivo system is that the latter has a pathway for further reaction, whereas the solution rapidly degrades all of its photo-energy.

Let us turn then to another examination of the trapping system. As we have just seen, the forward reaction must be quite fast to prevent competition with energy losses from the electronically excited states. Furthermore, the back reaction

$$P + T^* \longrightarrow P^* + T \qquad \text{(VI-1)}$$

must be relatively unimportant. We are reasonably certain that the trap itself is a very shallow one. Its performance is made even more difficult by the degeneracy factor which must favor the 100 or so chlorophyll molecules which are thought to be associated with each trap site. Thus,

as we concluded in Chapter I, the efficient performance of the trap must be based on kinetic considerations. In fact, we wish the quantum conversion reaction to proceed rapidly compared with that shown in Eqn. VI-1 and to proceed in such a manner as to minimize back reactions:

$$T^* \underset{\text{slow rate}}{\overset{\text{fast rate}}{\rightleftharpoons}} T^+ + e^- \qquad \text{(VI-2)}$$

If Eqn. VI-2 goes through a triplet intermediate or if a direct photoionization reaction is involved, it is quite feasible that a large forward rate constant could exist. ($K_f \sim 10^{11}$ sec.$^{-1}$ or 10^{15} liters/mole-sec.*). Before we dismiss the question of the forward reaction, note that a bimolecular mechanism forces us to a high <u>local</u> concentration of active intermediates so that the rate will be fast enough to compete with the (essentially) unimolecular emissive and nonradiative decay processes. If we postulate that $K_{2nd\ order}$ has a "normal" value of 10^{11} liter/mole-sec., then such a process can only compete effectively with the first order processes if one of the reactants' concentrations approaches one molar. A limiting case of this model envisions the molecules which are involved in the bimolecular reactions as having essentially fixed positions in space. This picture indicates the manner in which very high, <u>local</u> concentrations can be established even when the overall concentration of reactant, distributed throughout the solution, is quite small. In effect, one can treat the fixed position case as a unimolecular reaction with a rate constant approaching that for molecular vibrations

*Based on uniform distribution throughout solution.

(10^{13} sec.$^{-1}$). This first order behavior is, of course, implicit in the kinetic analysis at the end of Chapter V.

To prevent an important back reaction there must be one or more essentially irreversible steps. These can arise by forming an energy barrier to a back reaction or to the rapid depletion of the compounds needed for the back reaction. A straightforward barrier to back reaction has never been a popular proposal because of the high efficiency of the overall process. However, only 30% of the input energy is actually stored as free energy. The early steps of the reaction probably run at less than twice this value (say 50%). Thus, a quite large barrier to back reaction could be constructed without cutting into the efficiency of the system. A few tenths of an electron volt would, after all, be worth several powers of ten in the relative concentrations of high and low energy levels.*

Rather similar results can be obtained by a suitable selection of time constants. Consider the mechanism below:

$$A + X \underset{K_B}{\overset{I}{\rightleftharpoons}} A^+ + X^- \qquad \text{(VI-3)}$$

$$A^+ + Y \underset{}{\overset{K_1}{\rightleftharpoons}} Y^+ + A \qquad \text{(VI-4)}$$

$$X^- + Z \underset{}{\overset{K_2}{\rightleftharpoons}} X + Z^- \qquad \text{(VI-5)}$$

In such a situation if $K_1 > K_2$ (or $K_2 > K_1$) then K_B can be quite large ($\sim K_1$ and $>> I$) without altering the quantum yield or free energy storage

*Some very stimulating experiments by Arnold and Clayton[139] have indicated that reversible absorption changes can be observed at 1° K (in bacterial chromophores). This result can be interpreted as evidence for a small back reaction barrier. However, this argument doesn't help if the photochemical process and the dark reversal reaction proceed by different mechanisms.

appreciably (Table XI). It is encouraging that a range of relatively simple mechanisms suffice to greatly reduce the significance of direct back reactions.

Table XI

Effect of K_B on Quantum Yields for Reactions VI-3, 4, 5

Light intensity	K_B	ϕ Relative
Weak, 0.1	0	.9
	0.1	.9
	1.0	.9
	10.	.9
	∞	0
Moderate, 1.0	0	.50
	0.1	.50
	1.0	.48
	10.	.41
	∞	0
Strong, 10.	0	.09
	0.1	.09
	1.0	.09
	10.	.08
	∞	0

We have considered many electron transport reactions which, at least, seem to serve as suitable models for similar steps within the photosynthetic apparatus. In sum, those reactions contained within the photosynthetic systems probably proceed with efficiencies similar to those of the electron transport reactions of respiration. Although such efficiencies may well be high, it would seem that most of the "hard work" has been done by this point, and that no features unique to the photosynthetic mechanism need to be involved.

The central result of the speculations is not unexpected. Namely, it is the high degree of organization at the quantum conversion site which permits a rapid bimolecular reaction to compete effectively with the unimolecular losses associated with all photochemical processes. Thus, this organization is essential to the efficiency of the entire photosynthetic mechanism.

REFERENCES

1. J. A. Bassham and M. Calvin, "Path of Carbon in Photosynthesis," Prentice-Hall, Inc., Englewood Cliffs, N. J., 1957.

2. J. A. Bassham, A. A. Benson, L. D. Kay, A. Z. Harris, A. T. Wilson, and M. Calvin, J. Am. Chem. Soc. 76, 1760 (1954).

3. R. Emerson and C. M. Lewis, Am. J. Bot. 30, 165 (1943).

4. D. I. Arnon, F. R. Whatley, and M. B. Allen, J. Am. Chem. Soc. 76, 6324 (1954).

5. A. V. Trebst, H. Y. Tsujimoto, and D. I. Arnon, Nature 182, 351 (1958).

6. R. B. Park and N. G. Pon, J. Mol. Biol. 3, 1 (1961).

7. Th. Förster, Ann. Physik. 2, 55 (1948).

8. G. W. Robinson, Ann. Revs. Phys. Chem. 15, 328 ff. (1964).

9. H. Linschitz and K. Sarkanen, J. Am. Chem. Soc. 80, 4826 (1958).

10. L.M.N. Duysens, Thesis, Utrecht, 1952.

11. W. Arnold and E. Meek, Arch. Biochem. Biophys. 60, 82 (1956).

12. J. A. Bassham, Advances in Enzymol. 25, 39 (1963).

13. P. Latimer, T. T. Bannister, and E. I. Rabinowitch, in "Research in Photosynthesis," H. Gaffron (Ed.), Interscience, New York, 1957.

14. P. Latimer, T. T. Bannister, and E. I. Rabinowitch, Science 124, 585 (1956).

15. B. L. Strehler and W. Arnold, J. Gen. Physiol. 34, 809 (1951).

16. W. Arnold and J. B. Davidson, in "Photosynthetic Mechanisms in Green Plants," B. Kok and A. T. Jagendorf (Eds.), National Academy of Sciences-National Research Council Publication 1145, 1963.

17. G. W. Robinson, op. cit., p. 325 ff.

18. W. Arnold, in "Photosynthesis in Plants," J. Franck and W. E. Loomis (Eds.), Iowa State College Press, Ames, Iowa, 1949.

19. G. Weber, in "Comparative Biochemistry of Photoreactive Systems," M. B. Allen (Ed.), Academic Press, New York, 1960.

20. S. S. Brody, Z. Electrochem. 64, 187 (1960).

21. R. Emerson and W. Arnold, J. Gen. Physiol. 15, 191 (1932).

22. B. Kok and J. A. Businger, in Ref. 13, p. 357.

23. W. H. Butler and N. I. Bishop, in Ref. 16, p. 98.

24. K. Sauer and M. Calvin, J. Mol. Biol. 4, 451 (1962).

25. R. A. Olson, W. L. Butler, and W. H. Jennings, Biochim. Biophys. Acta 58, 144 (1962).

26. K. Sauer, Biophys. J. 5, 337 (1965).

27. R. A. Olson, W. L. Butler, and W. H. Jennings, Biochim. Biophys. Acta 54, 615 (1961).

28. B. Kok, Biochim. Biophys. Acta 48, 527 (1961).

29. H. T. Witt, A. Müller, and B. Rumberg, Nature 192, 967 (1961).

30. R. K. Clayton, Photochem. Photobiol. 1, 201 (1962).

31. I. D. Kuntz, Jr., P. A. Loach, and M. Calvin, Biophys. J. 4, 227 (1964).

32. R. H. Ruby, I. D. Kuntz, Jr., and M. Calvin, Cinquantenaire de la Société de Chimie Biologique, Paris, 1964, p. 75.

33. G. S. Hammond and N. J. Turro, Science 142, 1541 (1963).

34. A. A. Krasnovsky and G. P. Brin, Doklady 67, 325 (1949).

35. E. I. Rabinowitch, "Photosynthesis," Interscience, New York, 1956, Chap. 35, p. 1487 ff.

36. E. I. Rabinowitch, in Ref. 16, p. 112.

37. A. L. Lehninger and C. L. Wadkins, Ann. Rev. Biochem. 31, 47 (1962).

38. E. Racker, Advances in Enzymol. 23, 323. (1961).

39. J. S. Fruton and S. Simmonds, "General Biochemistry," John Wiley & Sons, Inc. (1959), 2nd edition.

40. M. P. Klein and G. M. Barton, Rev. Sci. Inst. 34, 754 (1963).

41. P. Pringsheim, "Fluorescence and Phosphorescence," Interscience, New York (1949), p. 319.

42. R. J. Blume, Rev. Sci. Inst. 32, 1016 (1961).

43. B. Chance, Rev. Sci. Inst. 22, 634 (1951).

44. H. T. Witt, in Ref. 13, p. 75.

45. B. Kok, Plant Physiol. 34, 184 (1959).

46. B. Ke, R. W. Treharne, and C. McKibben, Rev. Sci. Inst. 41, 296 (1964).

47. B. Ke, private communication.

48. I. D. Kuntz, Jr. and M. Calvin, Photochem. Photobiol., in press.

49. K. Shibata, A. A. Benson, and M. Calvin, Biochim. Biophys. Acta 15, 461 (1954).

50. B. Kok, Acta. Bot. Neer. 6, 316 (1957).

51. B. Kok and G. Hoch, in "A Symposium on Light and Life," W. D. McElroy and B. Glass (Eds.), Johns Hopkins Press, Baltimore, 1961, p. 403.

52. B. Ke, Biochim. Biophys. Acta 88, 1 (1964).

53. I. D. Kuntz, Jr., unpublished results.

53a. K. Sauer and R. B. Park, Biochim. Biophys. Acta 79, 476 (1964).

54. W. Vredenberg, J. Amesz, and L.N.M. Duysens, Information Exchange Group 1, #261 (1964).

55. S. Morita, J. M. Olson, and S. F. Conti, Arch. Biochem. Biophys. 104, 346 (1965).

56. J. S. Fruton and S. Simmonds, op. cit., p. 352.

57. D. Keilin and E. C. Slater, Brit. Med. Bull. 9, 89 (1953).

58. R. Hill and W. D. Bonner, Jr., in Ref. 51, p. 424.

59. W. D. Bonner, Jr. and R. Hill, in Ref. 16, p. 82.

60. M. Nozaki, M. Ogata, and D. I. Arnon, in Ref. 51, p. 516.

61. F. Perini, in Ref. 16, p. 291.

62. R. Goldberger, A. L. Smith, H. D. Tisdale, and R. Bomstein, J. Biol. Chem. 236, 2788 (1961).

63. T. Yonetani, J. Biol. Chem. 236, 1680 (1961).

64. M. D. Kamen, in Ref. 51, p. 483.

65. M. D. Kamen, "Primary Processes in Photosynthesis," Academic Press, New York, 1963, p. 174.

66. J. M. Olson and R. M. Smillie, in Ref. 16, p. 56.

67. M. Nishimura, S. B. Roy, H. Schleyer, and B. Chance, Biochim. Biophys. Acta 88, 251 (1964).

68. J.H.C. Smith and A. Benitez,"Modern Methods of Plant Analysis," Vol. IV, p. 164 (1955), Springer-Verlag, Berlin.

69. A.F.H. Anderson, Thesis, University of California, Berkeley, 1962.

70. A. Takamiya, H. Obata, and E. Yakushiji, in Ref. 16, p. 479.

71. E. I. Rabinowitch and J. Weiss, Proc. Roy. Soc, London, A 162, 251 (1937).

72. A. A. Krasnovsky, Doklady 61, 91 (1948).

73. P. Loach and I. D. Kuntz, Jr., unpublished results.

74. J. C. Goedheer, Brookhaven Symp. Biol. 11, 325 (1958).

75. K. Sauer and M. Calvin, Biochim. Biophys. Acta 64, 324 (1962).

76. B. Chance and B. Strehler, Plant Physiol. 32, 536 (1957).

77. J. W. Coleman, A. S. Holt, and E. I. Rabinowitch, in Ref. 13, p. 68.

78. H. T. Witt, Naturwiss. 3, 72 (1955).

79. B. Rumberg, P. Schmidt-Mende, J. Weikard, and H. T. Witt, in Ref. 16, p. 9.

80. B. Rumberg, Nature 204, 860 (1964).

81. J. S. Fruton and S. Simmonds, op. cit., p. 311.

82. J. Amesz, Biochim. Biophys. Acta 66, 22 (1963).

83. L.N.M. Duysens and J. Amesz, Biochim. Biophys. Acta 24, 19 (1957).

84. H. Beinert, J. Am. Chem. Soc. 78, 5323 (1956).

85. H. Beinert, in Ref. 51, p. 163.

86. I. D. Kuntz, Jr., and R. Hiller, in preparation.

87. L.N.M. Duysens, in Ref. 16, p. 10.

88. M. Klingenberg, A. Müller, P. Schmidt-Mende, and H. T. Witt, Nature 194, 379 (1962).

89. J. Amesz, Biochim. Biophys. Acta 79, 257 (1964).

90. R. K. Clayton, Biochem. Biophys. Res. Commun. 9, 49 (1962).

91. Y. de Kouchousky and D. C. Fork, Proc. Nat. Acad. Sci. U.S. 52, 232 (1964).

92. S. Katoh, I. Shiratori, and A. Takamiya, J. Biol. Chem. 51, 31 (1962).

93. C. B. van Niel, in Ref. 18, p. 437.

94. A. W. Frenkel, in Ref. 51, p. 587.

95. R. K. Clayton, Bact. Rev. 26, 151 (1962).

96. R. Hill and F. Bendall, Nature 186, 136 (1960).

97. B. Kok, in "Encyclopedia of Plant Physiology," No. 1, W. Ruhland (Ed.), Springer-Verlag, Berlin (1960), p. 566.

98. J. A. Bassham, Advances in Enzymol. 25, 39 (1963).

99. R. Emerson, C. V. Chalmers, and C. Cederstrand, Proc. Nat. Acad. Sci. U.S. 43, 133 (1957).

100. K. Sauer and R. Park, in preparation.

101. A. San Pietro, Brookhaven Symp. Biol. 11, 262 (1958).

102. T. Horio and M. D. Kamen, Biochim. Biophys. Acta 48, 226 (1961).

103. B. Chance and A. San Pietro, Proc. Nat. Acad. Sci. U.S. 49, 633 (1963).

104. T. Horio and T. Yamashita, Biochem. Biophys. Res. Commun. 9, 142 (1962).

105. B. Chance and W. D. Bonner, Jr., in Ref. 16, p. 66.

106. L. R. Blinks and C. B. van Niel, "Microalgae and Photosynthetic Bacteria," Plant and Cell Physiol., p. 297 (1963).

107. P. A. Loach, G. M. Androes, A. F. Maksim, and M. Calvin, Photochem. Photobiol. 2, 443 (1963).

108. H. A. Harbury, J. Biol. Chem. 225, 1009 (1957).

109. W. M. Clark, "Oxidation-Reduction Potentials of Organic Systems," Williams and Wilkins Co., Baltimore (1960).

110. R. K. Clayton, Photochem. Photobiol. 1, 313 (1962).

111. M. D. Kamen and R. G. Bartsch, Internat. Union Biochem. Symp. Haematin Enzymes, Canberra, 1959, p. 419.

112. E. S. Gould, I. D. Kuntz, Jr., and M. Calvin, Photochem. Photobiol., in press.

113. J. M. Olson and B. Kok, Biochim. Biophys. Acta 32, 278 (1959).

114. R. H. Ruby, I. D. Kuntz, Jr., and M. Calvin, Proc. Nat. Acad. Sci. U.S. 51, 515 (1964).

115. M. Calvin and G. M. Androes, Science 138, 867 (1962).

116. B. Commoner, in Ref. 51, p. 356.

117. L.N.M. Duysens, Brookhaven Symp. Biol. 11, 325 (1958).

118. M. Avron, private communication.

119. L.N.M. Duysens, in "Progress in Photobiology," B. C. Christensen and B. Buchman (Eds.), Elsevier Publishing Co., Amsterdam (1961), p. 135.

120. H. T. Witt, A. Müller, and B. Rumberg, Nature 191, 194 (1961).

121. J. S. Burlew (Ed.), "Algae Culture from Laboratory to Pilot Plant," Carnegie Institute of Washington, 1953, p. 94.

122. D. F. Bradley and M. Calvin, Proc. Nat. Acad. Sci. U.S. 41, 563 (1955).

123. J. Biggins and K. Sauer, Biochim. Biophys. Acta 88, 655 (1964).

124. L.N.M. Duysens and J. Amesz, Biochim. Biophys. Acta 64, 243 (1962).

125. L.N.M. Duysens, in Ref. 16, p. 1.

126. B. Kok, B. Cooper, and L. Yang, in Ref. 106, p. 373.

127. J. Weikard, A. Müller, and H. T. Witt, Z. Naturforsch. 18b, 139 (1963).

128. B. Kok and H. Beinert, Biochem. Biophys. Res. Commun. 9, 349 (1962).

129. K. Sauer, private communication.

130. R. M. Noyes, Prog. in Reaction Kinetics 2, 337 (1964).

131. N. R. Scott, "Analog and Digital Computer Technology," McGraw-Hill, New York (1960).

132. G. A. Korn and T. M. Korn, "Electronic Analog Computers," McGraw-Hill, New York (1956), 2nd edition.

133. R. B. Park and N. G. Pon, J. Mol. Biol. 6, 105 (1963).

134. H. K. Lichtenthaler and R. B. Park, Nature 198, 1070 (1963).

135. D. Fork, private communication.

136. A. T. Bharucha-Reid, "Elements of the Theory of Markov Processes and Their Applications," McGraw-Hill, New York, 1960, Chapter 8.

137. K. Ishida, J. Chem. Phys. 41, 2472 (1964).

138. A. A. Frost and R. G. Pearson, "Kinetics and Mechanism," John Wiley & Sons, Inc. (1961), 2nd edition, p. 173 ff.

139. W. Arnold and R. Clayton, Proc. Nat. Acad. Sci. U.S. 46, 769 (1960).